1,3-Butadiene-Induced DNA Damage: Ethnic Differences and Sources of Formation

A Dissertation
SUBMITTED TO THE FACULTY OF THE
UNIVERSITY OF MINNESOTA
BY

Caitlin C. Jokipii Krueger

IN PARTIAL FULFILLMENT OF THE REQUIREMENTS
FOR THE DEGREE OF
DOCTOR OF PHILOSOPHY

Dr. Natalia Tretyakova, Adviser

July 2022

Acknowledgements

The following dissertation is a work that could not have been completed alone. First, I would like to express my gratitude to my advisor, Dr. Natalia Tretyakova, for her guidance, support, and advice over the last five years. I am very thankful to Dr. Daniel Harki for being my mentor throughout my undergraduate research, my graduate school applications, and my graduate studies as the chair of my committee. I am also thankful for Dr. Carston Wagner and Dr. Stephen Hecht for serving on my committee, always taking the time to discuss my work, and giving their feedback, guidance, and support. This work would also not be possible without the valuable contributions of our collaborators. I am grateful to Dr. Loic Le Marchand and Dr. Lani Park (University of Hawaii) and Dr. Daniel Stram and Yesha Patel (University of Southern California). I would also like to thank the NIH, NCI, and University of Minnesota Department of Medicinal Chemistry for funding this research.

I would also like to express my gratitude to Dr. Peter Villalta, Dr. Yingchun Zhao, and Xun Ming for their frequent assistance with LCMS training and troubleshooting. I want to thank Dr. Christopher Seiler and Amanda Degner for their training in how to use and maintain the mass spectrometers in the lab. I am grateful to Dr. Suresh Pujari, Dr. Guru Madugundu, Dr. Luke Erber, Amanda Degner, Alexander Hurben, Erik Moran, Dominic Najjar, Ashley Rensted, Spencer Hutchins, and Danielle Chew-Martinez for their contributions to the research in this dissertation. I would additionally like to extend my thanks to all the members of the Tretyakova group for their frequent feedback and support and Bob Carlson for preparing figures and references for this thesis and many other presentations and publication.

Finally, I would like to extend my gratitude to my family and friends. A very special thanks to my husband, David Jokipii Krueger, for being my everyday support and encouragement. I am

grateful for my parents, Matt and Bonnie Puro, for their encouragement to keep learning and always do my best. I am additionally thankful for my sister Hope Puro and my in-laws Joel and Brenda Krueger. I could not have accomplished this without your support.

Dedication

This work is dedicated to my great-grandfather Jonas Erickson (1919-2022).

Abstract

In the United States, lung cancer is the leading cause of cancer-related deaths. Cigarette smoking is a major risk factor for lung cancer development, with approximately 80% of lung cancer cases directly related to smoking. Up to 1 in 4 smokers will develop lung cancer over the course of their lifetime. This risk varies by racial/ethnic group, with African Americans and Native Hawaiians at greater risk as compared to whites, and Japanese and Latinos at a relatively lower risk than whites. This racial/ethnic difference in risk is not explained by differences in smoking dose, diet, occupation, or socioeconomic status. Cigarette smoke is comprised of over 7000 chemical compounds, more than 70 of which are known human carcinogens. These carcinogens undergo metabolic activation to reactive species which can form adducts with DNA, leading to mutations and eventually lung cancer development. Polymorphisms in metabolic genes responsible for the bioactivation and detoxification of tobacco smoke carcinogens have been hypothesized to play a role in the racial/ethnic differences in lung cancer risk.

Among tobacco smoke carcinogens, 1,3-butadiene (butadiene, BD) is one of the most abundant and has the highest cancer risk index. BD is metabolically activated to reactive epoxides 3,4-epoxy-1-butene (EB), 1,2-dihydroxy-3,4-epoxybutane (EBD), and 1,2,3,4-diepoxybutane (DEB) by CYP2E1 and 2A6. These epoxides can be detoxified through glutathione conjugation by GSTT1 to form 2-(N-acetyl-L-cystein-S-yl)-1-hydroxybut-3-ene and 1-(N-acetyl-L-cystein-S-yl)-2-hydroxybut-3-ene (MHBMA) from EB, N-acetyl-S-(3,4-dihydroxybutyl)-L-cysteine (DHBMA) from EB-derived hydroxymethylvinyl ketone (HMVK), 4-(N-acetyl-L-cystein-S-yl)-1,2,3-trihydroxybutane (THBMA) from EBD, and *bis*-butanediol mercapturic acid (*bis*-BDMA) from DEB. If not detoxified, these epoxide species can form covalent adducts with DNA such as N7-(1-

hydroxy-3-buten-2-yl) guanine (EB-GII) from EB, N7-(2,3,4-trihydroxybut-1-yl) guanine (N7-THBG) from EBD, and 1,4-*bis*-(guan7-yl)-2,3-butanediol (*bis*-N7G-BD) from DEB.

The first goal of this thesis work was to investigate urinary levels of EB-GII as a biomarker of lung cancer risk in smokers. In Chapter 2 of this thesis, we report the temporal stability and association with smoking of urinary EB-GII. Urinary EB-GII levels were stable over time in smokers, indicating that single adduct measurements provide reliable levels of EB-GII. Additionally, we observed a 34% decrease in the levels of urinary EB-GII upon smoking cessation, indicating that it is associated with smoking status but may also have other sources of formation. In Chapter 3 we quantified urinary EB-GII adducts in smokers and non-smokers belonging to three racial/ethnic groups with differing risks of lung cancer development: Native Hawaiian, white, and Japanese American. We observed higher levels of urinary EB-GII excretion in Japanese Americans as compared to whites and Native Hawaiians and these differences could not be explained by *GSTT1* gene deletion or CYP2A6 activity. In Chapter 4 we directly examined the association between urinary EB-GII and lung cancer incidence, revealing that EB-GII levels are elevated in lung cancer cases as compared to smokers without lung cancer (OR = 1.91).

In Chapters 2 and 3, we observed that there were low but detectable levels of urinary EB-GII in smokers following smoking cessation and in non-smokers, suggesting additional sources of EB-GII adduct formation. In Chapter 5, we utilized stable isotope tracing to investigate the formation of BD DNA adducts and metabolites from endogenous sources. Laboratory rats were treated with low ppm (0.3-3.0 ppm) concentrations of BD-d_6 to approximate occupational exposure to BD (~1 ppm). Levels of exogenous (deuterated) EB-GII, MHBMA, and DHBMA increased in a dose-dependent manner following BD exposure, while endogenous (unlabeled) adducts and metabolites were unaffected by BD dose. While urinary EB-GII and MHBMA were formed primarily by

exogenous exposure, significant amounts of endogenous DHBMA were observed. Additionally, urinary exogenous EB-GII was associated with butadiene-induced genomic EB-GII, suggesting that urinary EB-GII can be used as a non-invasive surrogate measurement for genomic BD-DNA damage.

In Chapter 6, formation of a novel BD-DNA adduct, N^6-[2-deoxy-D-*erythro*-pentofuranosyl]-2,6-diamino-3,4-dihydro-4-oxo-5-*N*-1-(oxiran-2-yl)propan-1-ol-formamidopyrimidine (DEB-FAPy-dG) was investigated. A sensitive isotope dilution nanoLC-ESI^+-HRMS/MS methodology was developed and applied to quantitation of DEB-FAPy-dG formation in DEB treated calf thymus DNA. DEB-FAPy-dG formation was dependent on DEB concentration and pH, with higher adduct levels observed at higher pH. Detection of DEB-FAPy-dG in mouse embryonic fibroblast cells and nuclei treated with DEB was unsuccessful, likely due to the adduct forming in low quantities at physiological conditions.

Table of Contents

List of Tables

List of Figures

List of Abbreviations

1,N^6-α-HMHP-dA	1,N^6-(1-hydroxymethyl-2-hydroxypropan-1,3-diyl)-2′-deoxyadenosine
1,N^6-γ-HMHP-dA	1,N^6-(2-hydroxy-3-hydroxymethylpropan-1,3-diyl)-2′-deoxyadenosine
2-oxo-dA	2-hydroxy-2′-deoxyadenosine
7-mG	7-methylguanine
8-oxo-dA	8-oxo-7,8-dihydro-2′-deoxyadenosine
8-oxo-dG	8-oxo-7,8-dihydro-2′-deoxyguanosine
A	adenine
α-OH-Acr-dGuo	(6*R/S*)-3-(2′-deoxyribos-1′-yl)-5,6,7,8-tetrahydro-6-hydroxypyrimido[1,2-*a*]purine-10(3*H*)one
BaP	benzo[*a*]pyrene
BD, butadiene	1,3-butadiene
BER	base excision repair
bis-BDMA	*bis*-butanediol mercapturic acid
bis-N7G-BD	1,4-*bis*-(guan7-yl)-2,3-butanediol
BMI	body mass index
BPDE-N^2-dG	10-(deoxyguanosin-N2-yl)-7,8,9-trihydroxy-7,8,9,10-tetrahydrobenzo[a]pyrene
C	cytosine
CE	collision energy
CI	confidence interval

CID	collision-induced dissociation
COPD	chronic obstructive pulmonary disease
CPD	cigarettes per day
CRI	cancer risk index
CT DNA	calf thymus DNA
CV	coefficient of variation
CYP 450	cytochrome P450 monooxygenase
Da	dalton
DEB	1,2,3,4-diepoxybutane
DEB-FAPy-dG	N^6-[2-deoxy-D-*erythro*-pentofuranosyl]-2,6-diamino-3,4-dihydro-4-oxo-5-*N*-1-(oxiran-2-yl)propan-1-ol-formamidopyrimidine
DHBMA	N-acetyl-S-(3,4-dihydroxybutyl)-L-cysteine
DNA	deoxyribonucleic acid
DSB	double strand break
dT	2′-deoxythymidine
EB	3,4-epoxy-1-butene
EB-Ade I	N1-(2-hydroxy-3-buten-1-yl) adenine
EB-Ade II	N1-(1-hydroxy-3-buten-2-yl) adenine
EB-Ade III	N3-(2-hydroxy-3-buten-1-yl) adenine
EB-Ade IV	N3-(1-hydroxy-3-buten-2-yl) adenine
EBD	1,2-dihydroxy-3,4-epoxybutane
EB-Diol	1-butane-3,4-diol

EB-FAPy-dG	N^6-(2-deoxy-d-*erythro*-pentofuranosyl)-2,6-diamino-3,4-dihydro-4-oxo-5-N-(2-hydroxybut-3-en-1-yl)formamidopyrimidine
EB-GI, EB-Guanine I	N7-(2-hydroxy-3-buten-1-yl) guanine
EB-GII, EB-Guanine II	N7-(1-hydroxy-3-buten-2-yl) guanine
EH	epoxide hydrolase
ESI	electrospray ionization
FAPy	formamidopyrimidine
G	guanine
γ-OH-Acr-dGuo	(8*R/S*)-3-(2′-deoxyribos-1′-yl)-5,6,7,8-tetrahydro-8-hydroxypyrimido[1,2-*a*]purine-10(3*H*)one
G-NOR-G	nornitrogen mustard guanine-guanine crosslink
GST	glutathione-S-transferase
GSTT1	glutathione-S-transferase theta 1
HB-Val	*N*-(2-hydroxy-3-buten-1-yl)-valine
HCD	higher-energy C-trap dissociation
HILIC	hydrophilic interaction liquid chromatography
HMVK	hydroxymethylvinyl ketone
HPLC	high performance liquid chromatography
HRMS	high resolution mass spectrometry
HRR	homologous recombination repair
LC-MS	liquid chromatography mass spectrometry
MEC	multiethnic cohort
MEF	mouse embryonic fibroblast

MHBMA-1	2-(N-acetyl-L-cystein-S-yl)-1-hydroxybut-3-ene
MHBMA-2	1-(N-acetyl-L-cystein-S-yl)-2-hydroxybut-3-ene
MHBMA-3	1-(N-acetyl-L-cystein-S-yl)-4-hydroxybut-2-ene
MMR	mismatch repair
MS	mass spectrometry
MS/MS	tandem mass spectrometry
m/z	mass to charge ratio
N1A-N7G-BD	1-(aden-1-yl)-4-(guan-7-yl)-2,3-butanediol
N-1-THB-Ade	N-1-(2,3,4-trihydroxybutyl) adenine
N3A-N7G-BD	1-(aden-3-yl)-4-(guan-7-yl)-2,3-butanediol
N3-THB-Ade	N3-(2,3,4-trihydroxybut-1-yl) adenine
N^6A-N7G-BD	1-(aden-6-yl)-4-(guan-7-yl)-2,3-butanediol
N^6-THB-Ade	N^6-(2,3,4-trihdyroxybut-1-yl) adenine
N7A-N7G-BD	1-(aden-7-yl)-4-(guan-7-yl)-2,3-butanediol
N7-THBG, THBG	N7-(2,3,4-trihydroxybut-1-yl) guanine
NaC	N-acetyl cysteine
NE	nicotine equivalents
NER	nucleotide excision repair
NHEJ	nonhomologous end-joining
O^6-mG	O^6-methylguanine
PhIP	2-amino-1-methyl-6-phenylimidazo[4,5-b]-pyridine
POB	pyridyloxobutyl
ppm	parts per million

Pt-GG	platinum guanine-guanine crosslink
pyr-Val	*N*,*N*-(2,3-dihydroxy-1,4-butadiyl)-valine
Q	quadrupole
QC	quality control
RF	radio frequency
RNA	ribonucleic acid
ROS	reactive oxygen species
SD	standard deviation
SPE	solid phase extraction
SRM	selected reaction monitoring
T	thymine
THB-FAPy-dG	N^6-(2-deoxy-d-*erythro*-pentofuranosyl)-2,6-diamino-3,4-dihydro-4-oxo-5-N-(2,3,4-trihydroxybutyl)formamidopyrimidine
THBMA	4-(N-acetyl-L-cystein-S-yl)-1,2,3-trihydroxybutane
THB-Val	1,2,3-trihydroxybutyl-valine
TLS polymerase	translesion synthesis polymerase
TNE	total nicotine equivalents
UV/Vis	ultraviolet/visible spectroscopy

1. Literature Review

1.1 Carcinogen-DNA adduct formation and their use as biomarkers of exposure and cancer risk

1.1.1 Chemical carcinogenesis: the role of DNA adducts

Human exposures to carcinogens occur through a variety of exogenous sources, such as air[1], water[2], and food[3]. Additionally, there are endogenous sources of carcinogen exposure, including metabolism, inflammation, lipid peroxidation, and oxidative stress[4]. These electrophilic carcinogens react with nucleophilic biomolecules, such as proteins, RNA, or DNA to form covalent adducts, leading to toxicity, mutations, and carcinogenesis[5-7].

Indirectly acting carcinogens require metabolic activation, usually through cytochrome P450s, to the electrophilic metabolite[7]. Cytochrome P450 monooxygenases are responsible for the oxidation of drugs and carcinogens as a part of Phase I metabolism[8]. In contrast, direct acting carcinogens already contain electrophilic functional groups, including aldehydes[9] and nitrogen mustards[10]. These reactive electrophiles can be detoxified by enzymes such as epoxide hydrolases and glutathione-S-transferases and excreted in the urine (Phase II metabolism)[11]. Detoxification products of carcinogens such as mercapturic acids can be utilized as biomarkers of exposure[12].

If not detoxified, these electrophiles interact with nucleophilic sites in DNA to form carcinogen-DNA adducts[6, 12]. Among the nucleophilic sites in DNA, the N7-position of guanine is the most reactive[13]. The N7 position does not participate in Watson-Crick base-pairing interactions and is located peripherally in the helix, making it the most accessible site for adduct formation[14]. DNA adducts can also form at other nucleophilic sites in DNA. DNA adducts are typically recognized by DNA repair mechanisms that will remove the adduct and restore the DNA[15]. If not repaired, the DNA adducts can interfere with DNA replication, resulting in mutations[16]. Some

mutations have no biological effects. Non-viable mutations result in apoptosis, while viable mutations located in tumor suppressor or protooncogenes lead to the development of cancer[17] (Figure 1.1).

Tobacco smoke is a major source of carcinogens and carcinogen-DNA adducts. Tobacco specific nitrosamines result in the formation of pyridyloxobutyl (POB) adducts such as O^6-POB-dG[18]. Polyaromatic hydrocarbon benzo[*a*]pyrene (BaP) forms bulky DNA adduct BPDE-N^2-dG[19]. Methylating agents result in 7-methylguanine (7-mG) and O^6-methylguanine (O^6-mG)[20]. 1,3-butadiene results in DNA adducts N7-(1-hydroxy-3-buten-2-yl) guanine (EB-GII), N7-(2,3,4-trihydroxybut-1-yl) guanine (N7-THBG), and 1,4-*bis*-(guan7-yl)-2,3-butanediol (*bis*-N7G-BD)[21-23]. (6*R/S*)-3-(2′-deoxyribos-1′-yl)-5,6,7,8-tetrahydro-6-hydroxypyrimido[1,2-*a*]purine-10(3*H*)one (α-OH-Acr-dGuo) and (8*R/S*)-3-(2′-deoxyribos-1′-yl)-5,6,7,8-tetrahydro-8-hydroxypyrimido[1,2-*a*]purine-10(3*H*)one (γ-OH-Acr-dGuo) form from acrolein[24] (Figure 1.2). Carcinogen-DNA adducts can be used as biomarkers of carcinogen exposure.

Endogenous exposures to reactive oxygen species (ROS) can also lead to the formation of DNA adducts. Oxidative metabolism in the mitochondria leads to the formation of superoxide anions, hydrogen peroxide, and hydroxide radicals, which can form adducts such as 8-oxo-7,8-dihydro-2′-deoxyguanosine (8-oxo-dG), 8-oxo-7,8-dihydro-2′-deoxyadenosine (8-oxo-dA), 2-hydroxy-2′-deoxyadenosine (2-oxo-dA), 4,6-diamino-4-hydroxy-5-formamidopyrimidine (Fapy-dG), and 4,6-diamino-5-formamidopyrimidine (Fapy-dA)[25] (Figure 1.2).

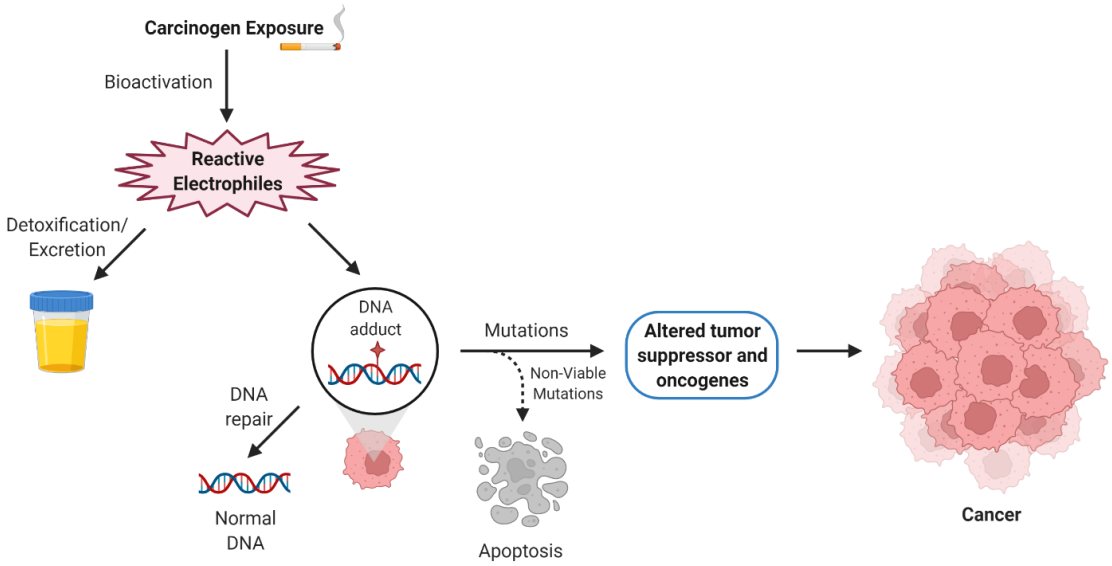

Figure 1.1. The role of DNA adducts in carcinogenesis.

Created with Biorender.com.

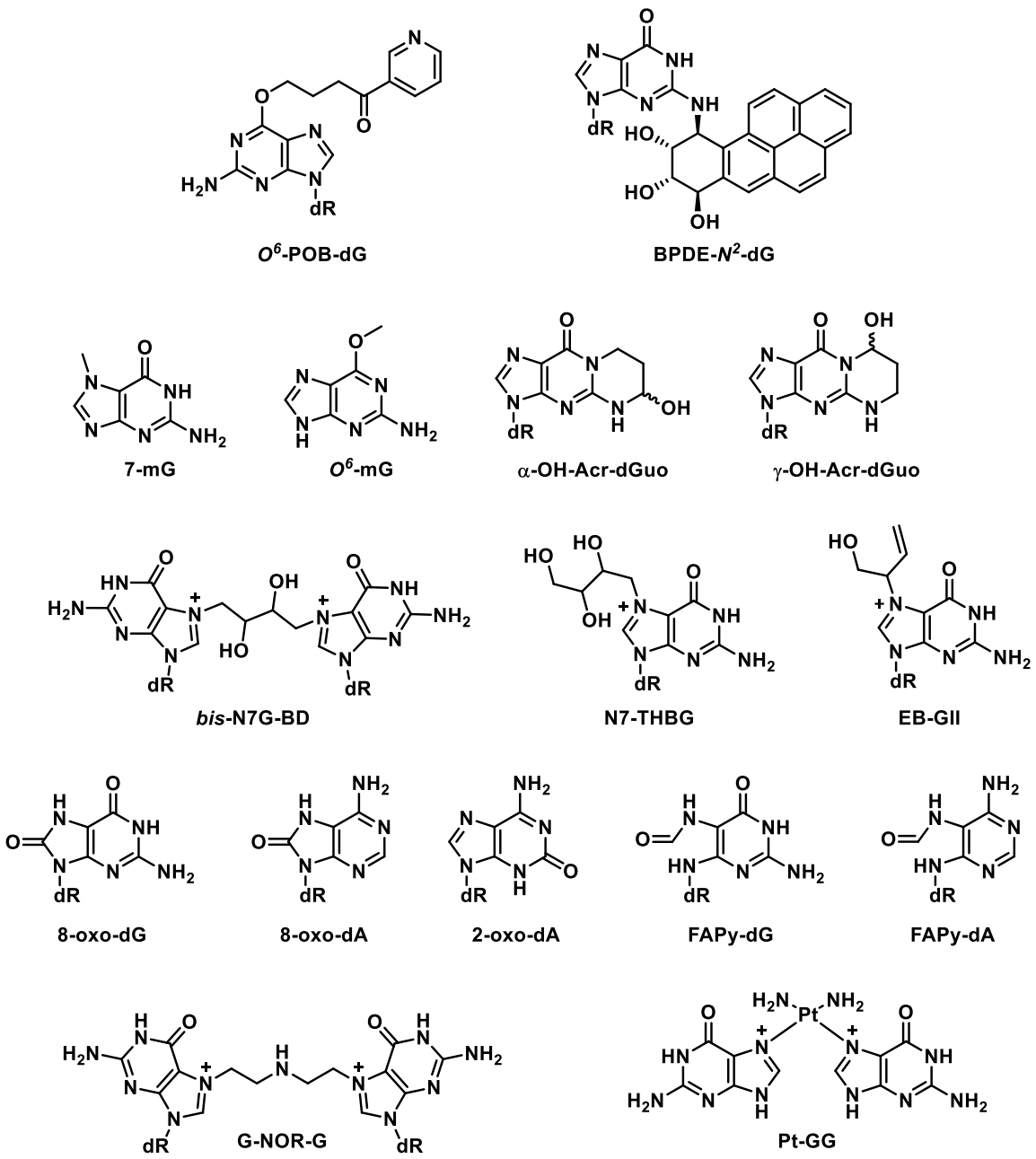

Figure 1.2. Representative DNA adducts formed by chemical carcinogens, reactive oxygen species, and anticancer agents.

Another source of DNA adducts is the intentional introduction of toxic DNA adducts through treatment with anti-cancer agents for the purpose of inducing cancer cell death. Cyclophosphamide induces the formation of interstrand guanine-guanine crosslinks (G-NOR-G)[26]. Cisplatin treatment results in intrastrand guanine-guanine crosslinks (Pt-GG)[27]. Treosulfan forms guanine-guanine crosslinks (*bis*-N7G-BD)[28] (Figure 1.2). These anti-cancer agent DNA adducts can be used as biomarkers of drug efficacy[29].

1.1.2 Repair of carcinogen-induced DNA adducts

Removal of DNA adducts is carried out through DNA repair pathways, restoring the DNA to its original state and preventing the toxicity or carcinogenesis that could result from mutations. There are five main repair pathways: direct repair, base excision repair (BER), nucleotide excision repair (NER), double strand break (DSB) repair, and mismatch repair (MMR)[30].

Direct repair of DNA in humans consists of enzymatic removal of alkyl groups from DNA adducts, restoring the normal DNA base. O^6-mG arises from exposure to endogenous and exogenous methylating agents and is a mutagenic and cytotoxic lesion[31]. O^6-methylguanine-DNA methyltransferase (MGMT) repairs O^6-alkylated guanine adducts by transferring the alkyl group to a cysteine located in the enzyme active site, thereby restoring the DNA and inactivating the enzyme[31, 32]. 1-methyladenine and 3-methylcytosine DNA adducts can also be directly repaired by oxidative methyl transferases hABH2 and hABH3. These enzymes utilize Fe^{2+} and α-ketoglutarate as cofactors and release the hydroxylated methyl group as formaldehyde[33-35].

BER is primarily responsible for the repair of small nucleobase adducts that do not result in distortion of the helix. Following recognition of the damaged base, DNA glycosylases cleave the glycosidic bond releasing the DNA adduct as a free base and resulting in the formation of an abasic site. The substrate specificity varies by DNA glycosylase. 8-oxo-dG is excised by 8-oxoguanine

DNA glycosylase (OGG1)[36] while the *E. coli* MutY homolog (MUTYH) repairs adenine incorrectly paired with 8-oxo-dG[37]. *E. coli* Nei-like DNA glycosylases (NEIL1, NEIL2, and NEIL3) remove oxidized pyrimidines such as formamidopyrimidines[38-40]. Cytosine that is deaminated to uracil is removed by uracil DNA glycosylase (UDG)[41]. In addition to nucleobase adduct removal by DNA glycosylases, abasic sites can be formed through spontaneous hydrolysis and loss of the nucleobase[42]. The abasic sites are then repaired by endonuclease cleavage of the backbone by AP-endonuclease 1 (APE1)[43], insertion of the correct nucleotide by DNA polymerase β (Polβ)[44], and ligation of the DNA strand by DNA ligases[45] in short patch BER. Alternatively, in long patch BER, the nicked strand generated by APE1 is displaced, DNA polymerase δ (Polδ) or Polβ polymerize as strand of 2-12 nucleotides, flap structure-specific endonuclease 1 (FEN1) removes the nicked strand, and the newly synthesized DNA is ligated to the original strand[46].

NER repairs helix-distorting, bulky nucleobase adducts, such as BPDE-N^2-dG. The bulky DNA damage recognition is carried out by enzymes including XPA, XPC-hHR23B, replication protein A (RPA), and centrin 2 (CENT2) in global genomic NER (GG-NER) and by stalled RNA polymerases in transcription coupled NER (TC-NER)[47, 48]. The DNA strand is cleaved on both sides of the DNA adduct, the oligonucleotide containing the damage is removed, the gap is filled by DNA polymerases δ, ε, or κ and ligated by DNA ligase I or IIIα to introduce the repaired strand into the original DNA[48, 49].

Recombinational repair occurs through homologous recombination repair (HRR) or nonhomologous end-joining (NHEJ), and repairs double strand breaks (DSBs) generated as a result of DNA crosslinks. In HRR 5′-3′ resection at the site of the damaged DNA strand results in a single stranded 3′ end. The sister chromatid is then utilized as a template for repair by polymerases[50]. NHEJ is utilized in cell cycle phases when a sister chromatid is not available as a repair template.

In the NHEJ pathway, the ends of the double strand break are directly ligated together without a template in an error prone manner. Damaged nucleotides at the site of the DSB are often removed prior to ligation, leading to deletions and mutations[51].

MMR is responsible for the repair of mispaired bases and insertion-deletion loops as a result of errors in DNA replication or homologous recombination. These lesions are recognized by MutSα or MutSβ, which recruit MutLα. EXO1 removes the mismatch, while RPA stabilizes the resulting single stranded DNA. Polδ replaces the removed nucleotides and the newly synthesized DNA is ligated to the original strand by DNA ligase I[52].

1.1.3 DNA adducts as biomarkers of carcinogen exposure

Interindividual differences in metabolism and detoxification of carcinogens results in discrepancies between the exposure level of a carcinogen and an individual's internal dose. Therefore, further understanding of the exposure risk can be measured through biomarkers of exposure. These carcinogen biomarkers consist of detoxification metabolites, protein adducts, and DNA adducts[12]. Detoxification metabolites such as mercapturic acids are excreted in the urine and can be quantified as biomarkers of exposure[53, 54]. While they are biomarkers of exposure, they do not necessarily represent cancer risk associated with exposure. These metabolites represent the amount of carcinogen that is metabolically detoxified and excreted. Protein adducts are popular choices for long-term exposure monitoring, due to their long half-life, high abundance, and absence of repair mechanisms[55]. Recent advances in untargeted adductomics have allowed for the use of carcinogen-protein adducts in biomonitoring[56, 57]. DNA adducts provide the most relevant biomarkers of risk, due to their role in chemical carcinogenesis (section 1.1.1)[17, 58]. While metabolites and protein adducts provide insight into the exposure and activation of carcinogens, DNA adducts represent the portion of carcinogen that is bioactivated and bound to DNA.

DNA adducts can be used as a measure of environmental exposure to carcinogens. DNA adducts of tobacco smoke carcinogens have been used as biomarkers of exposure and risk. BPDE-N^2-dG is used as a biomarker of exposure to BaP[19]. α-OH-Acr-dGuo and γ-OH-Acr-dGuo have been used as biomarkers of exposure to acrolein in oral cell DNA[59, 60]. Exposure to the cooked meat carcinogen 2-amino-1-methyl-6-phenylimidazo[4,5-b]-pyridine (PhIP) is quantified by the measurement of PhIP-DNA adducts in lymphocytes as biomarkers of exposure[61]. N7-glycidamide guanine (N7-GA-Gua) adducts are utilized as biomarkers of environmental and dietary exposure to acrylamide, a dietary carcinogen formed by cooking at high temperatures[62]. Carcinogen-DNA adducts provide insight into the dietary, lifestyle, and environmental factors influencing human disease.

Additionally, chemotherapy DNA adducts can be utilized as a measure of treatment efficiency. Antitumor effects of crosslinking agents such as cyclophosphamide and cisplatin are attributed to the efficient formation of DNA adducts[63, 64]. Cyclophosphamide is a prodrug that is activated by CYP 2B6 to phosphoramide mustard and nornitrogen mustard, both of which form G-NOR-G (Figure 1.2) DNA crosslinks[65, 66]. Interindividual differences in G-NOR-G crosslink formation have been observed[66, 67], in addition to increased G-NOR-G adduct levels and hypersensitivity to cyclophosphamide treatment in patients with DNA repair deficiencies[66]. Pt-GG (Figure 1.2) cisplatin DNA adducts quantified in patient xenografts or biopsies following *ex vivo* cisplatin treatment can be utilized to predict treatment efficacy prior to administration of the drug to the patient[64]. Monitoring the level of DNA adducts in precision medicine for cancer chemotherapy is an ongoing field of research[29, 68].

1.1.3.1 Urinary excretion of DNA adducts

As discussed previously (Chapter 1.1.2), BER removal of carcinogen-DNA adducts leads to the release of modified nucleobases. In addition to repair, some DNA adducts are removed from the backbone via spontaneous depurination. The positive charge at the N7 position of N7-guanine DNA adducts leads to destabilization of the glycoside bond, release of the modified nucleobase, and the formation of abasic sites in the DNA (Figure 1.3)[14, 69]. Depurination of N3-adenine adducts has also been reported[69-72]. These DNA adducts that are released from the backbone through repair or spontaneous hydrolysis can be excreted in the urine[69].

While many DNA adduct studies have quantified them in genomic DNA, the presence of DNA adducts in urine provides a unique opportunity for analysis. In large-scale epidemiological studies, tissue and blood samples are scarce, while urine is collected in a non-invasive manner and is therefore more readily available for analysis. Urinary excretion of carcinogen-DNA adducts have been observed, including adducts of aflatoxin B_1[73], 1,3-butadiene[23], styrene[74], and BaP[75] in exposed animals and humans.

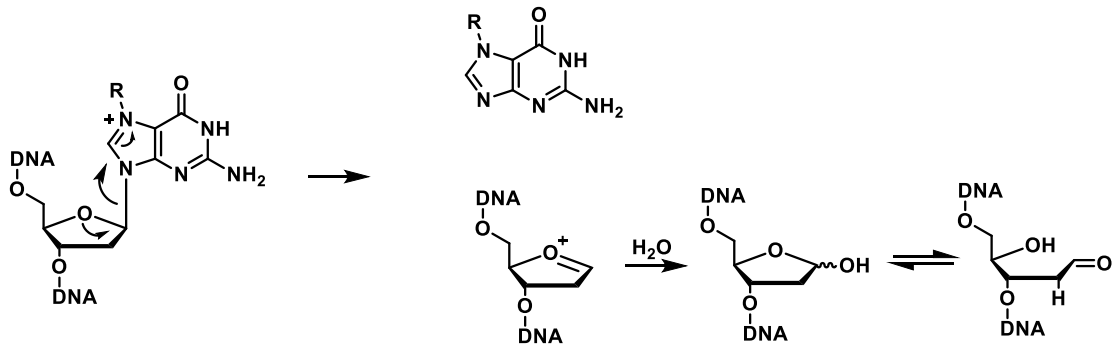

Figure 1.3. Depurination of N7-guanine adducts and abasic site formation

1.2 Mass spectrometry-based quantitation of DNA adducts

Traditional methodologies for the detection and quantitation of DNA adducts consist of ^{32}P-postlabeling and high performance liquid chromatography-ultraviolet visible light absorbance detection (HPLC-UV/Vis). Substantial improvements in the specific and accurate quantitation of DNA adducts can be attributed to the use of mass spectrometry (MS) based methodologies. Isotope dilution mass spectrometry is the gold standard for the absolute quantification of DNA adducts[76, 77]. In this approach, stable isotopes ^{13}C, ^{15}N, and ^{2}H are used to replace naturally occurring isotopes of carbon, nitrogen, and hydrogen in the adduct structure to generate isotopically labeled internal standards. These standards have the same structure and properties as the DNA adduct analyte of interest, with the exception of heavy stable isotopes in the structure resulting in a distinct molecular mass. A known amount of this internal standard added at the beginning of sample preparation interacts with all preparation steps in identical ways to the analyte, accounting for any sample loss throughout the process. Upon mass spectrometry analysis, the analyte and internal standards will have different mass to charge (*m/z*) ratios. The absolute quantitation of the analyte can be obtained through the ratio of analyte to internal standard area under the liquid chromatography-mass spectrometry (LC-MS) peak and the known amount of internal standard added to the samples (Figure 1.4)[77].

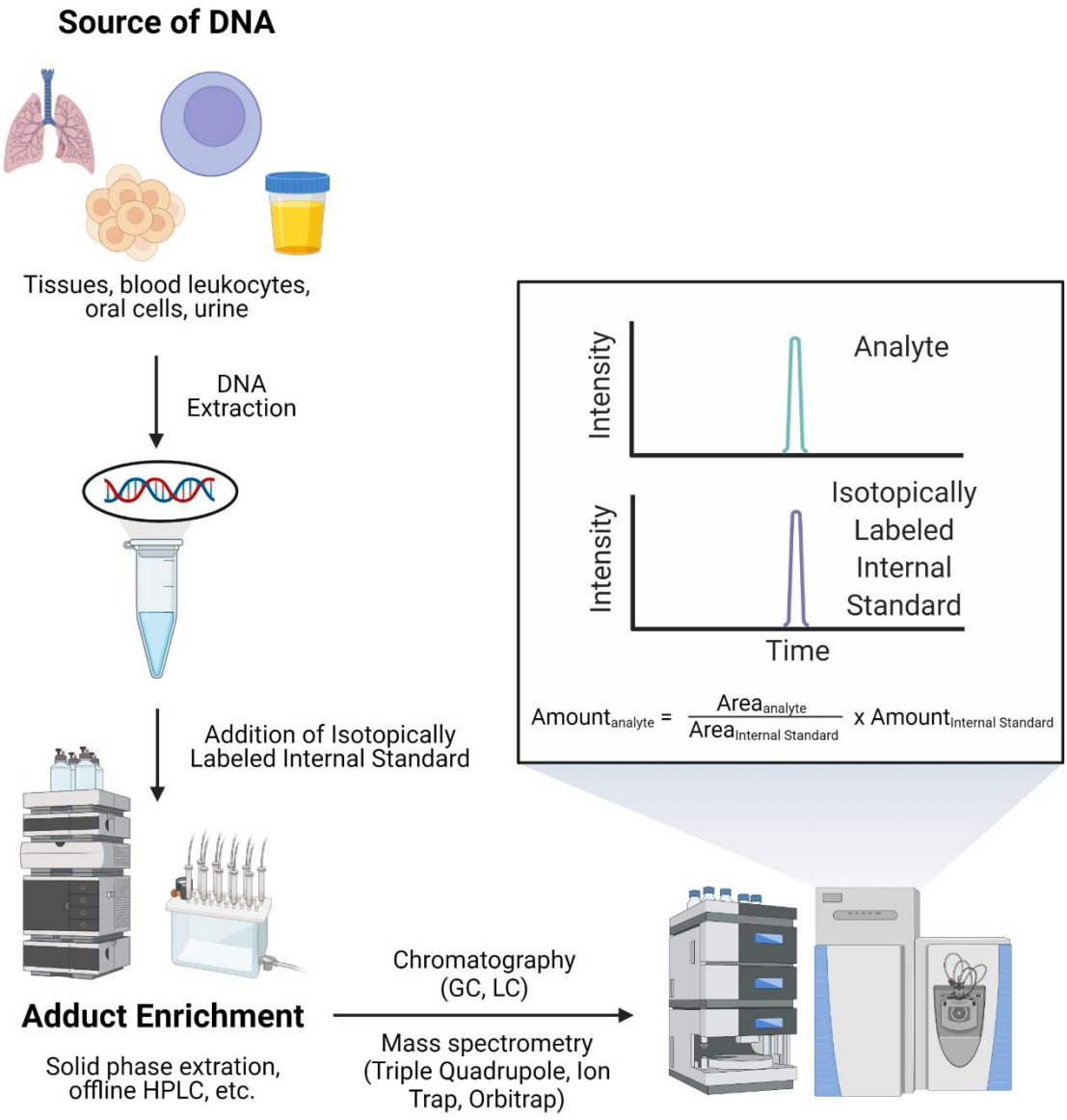

Figure 1.4. Isotope dilution mass spectrometry-based quantitation of DNA adducts. Created with Biorender.com

1.2.1 DNA adduct sample preparation for mass spectrometry analysis

Carcinogen-DNA adducts can be measured in DNA extracted from a variety of biological sources, such as tissues (liver, lung, kidney, brain, etc.)[78, 79], blood leukocytes[24], oral cells[59, 80], saliva[81-83], and exfoliated urothelial cells in urine[84, 85]. Once DNA has been isolated, the DNA adducts need to be released from the DNA prior to LC-MS analysis. Some strategies are non-selective, including enzymatic hydrolysis and acid hydrolysis. Complete enzymatic hydrolysis of DNA by enzymes such as phosphodiesterase I and II, DNase I and II, and nuclease P1 results in nucleotides, and alkaline phosphatase removes the phosphate groups to form nucleosides[86-88]. Mild acid hydrolysis can be used to release all purines as free bases from the DNA backbone[89, 90]. A more specific strategy is neutral thermal hydrolysis, where the DNA is heated to 70-90°C for 30-60 min, cleaving the glycosidic bond and releasing hydrolytically labile N7-guanine and N3-adenine adducts as free bases[89, 91]. As previously discussed in Chapter 1.1.3.1, hydrolytically labile DNA adducts can also be spontaneously released from DNA as free bases, excreted, and quantified in urine[69].

Following the release of DNA adducts and the addition of an isotopically labeled internal standard, the DNA adducts can be enriched. Due to the low abundance of DNA adducts as compared to native nucleosides or nucleobases, enrichment is necessary to reduce background noise or ion suppression upon analysis. Ultrafiltration can be utilized to remove high molecular weight compounds such as the DNA backbone remaining after neutral thermal or acid hydrolysis of DNA and proteins remaining after enzymatic digestion. The sample is loaded onto a filter with a molecular weight cutoff such as 3000, 10000, or 30000 Da and subjected to centrifugation. Small

molecules, such as nucleobase and nucleotide adducts pass through the filter, while higher molecular weight molecules remain above the filter.

Solid phase extraction (SPE) is then used to separate the DNA adduct of interest from other small molecule impurities. SPE cartridges can contain a variety of stationary phases, including normal phase, reversed phase, and ion exchange and are chosen based on the properties of the analyte of interest. Once the sample is loaded onto the single use cartridge and the DNA adduct is bound to the stationary phase, impurities such as salts and other small molecules can be washed from the cartridges. After the washing steps, the adduct of interest and its internal standard can be eluted with high aqueous (normal phase), organic (reverse phase), or acidic/basic (ion exchange) conditions. Mixed mode cartridges (reverse phase and ion exchange) can also be used. SPE has been utilized for the enrichment of many DNA adducts, including N7-THBG adducts in our laboratory[22].

An alternative to the single use SPE cartridges is offline HPLC enrichment of DNA adducts. The sample containing the DNA adduct of interest is injected onto a column containing the desired stationary phase, and a mobile phase gradient is utilized to remove impurities and elute the DNA adduct from the column. Fractions containing the adduct of interest are collected, concentrated under vacuum or nitrogen, and reconstituted for LC-MS analysis. The mobile phase gradient provides more complete separation of the DNA adduct from other sample impurities as compared to the stepwise addition of different solvents to an SPE cartridge. However, levels of DNA adducts are often lower than what can be detected by HPLC-UV/Vis, so a retention time marker such as 2′-deoxythymidine can be added to the sample to adjust fraction collection times. The use of the same instrument and column can lead to analyte carryover, which must be carefully monitored. Our

laboratory has utilized offline HPLC enrichment for DNA adducts such as EB-GII[92] and *bis*-N7G-BD[93].

Some sample matrices or DNA adducts require multiple purification steps (SPE and HPLC) to achieve sufficient DNA adduct purification. In our laboratory, SPE alone did not sufficiently clean up urine samples for the analysis of EB-GII, so offline HPLC was additionally utilized for sample clean up and enrichment prior to LC-MS analysis of urinary EB-GII[23].

1.2.2 Mass spectrometry methodologies for the quantification and identification of DNA adducts

Mass spectrometry provides structural information, sensitive detection, and specific quantitation of DNA adducts, making it the preferred method for DNA adduct analysis. Mass spectrometry based methodologies have been published for the quantitation of a number of DNA adducts. Many methods utilize LC-MS for DNA adduct detection and quantitation, while gas chromatography-mass spectrometry is useful in certain situations but less frequently employed for DNA adducts.

1.2.2.1 Liquid chromatography-mass spectrometry

Separation of the DNA adduct of interest from other components in the sample is essential for sensitivity. While mass spectrometers can detect an analyte based on its mass to charge ratio (*m/z*), the presence of other interfering compounds can result in signal suppression that reduces sensitivity. Removal of this signal suppression is of increased importance in the measurement of trace levels of DNA adducts. Separation of the DNA adducts of interest from interfering compounds can be achieved through the coupling of liquid chromatography and mass spectrometry (Figure 1.5).

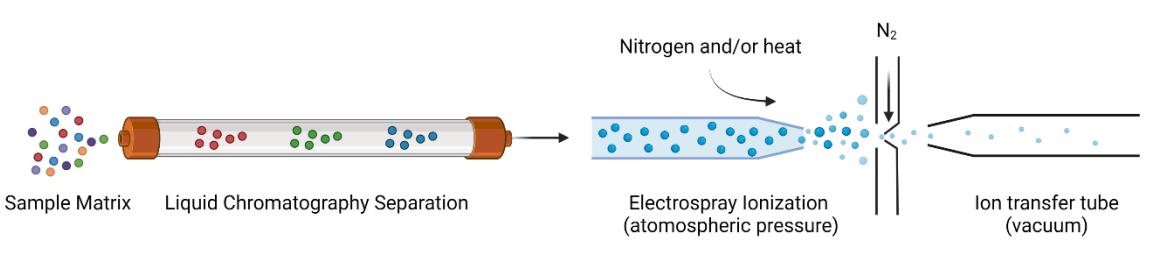

Figure 1.5. Liquid chromatography and electrospray ionization.
Created with Biorender.com

Commercially available stationary phases for liquid chromatography include reverse phase C18, C8, and polyphenyl, among many others. Polar endcapped C18 stationary phases such as Synergi Hydro RP result in excellent separation of many modified nucleobases and nucleosides. However, some extremely polar DNA adducts do not retain on reverse phase HPLC columns. For these analytes, hydrophilic interaction liquid chromatography (HILIC) has the potential to provide a chromatography solution. This method requires analyte solubility in nonpolar organic solvents, which can be limited for many polar DNA adducts. LCMS systems are compatible with multiple flow rates: analytical flow (>100 μL/min), micro flow (10-100 μL/min), capillary flow (1-10 μL/min) and nanoflow (<1 μL/min). Lower flow rates allow for more efficient ionization and greater sensitivity.

For mass spectrometry analysis, analytes must be ionized following chromatography. Electrospray ionization (ESI) allows for the application of high voltage (2-4 kV) to the solvent from the HPLC, resulting in the formation of a fine aerosol containing charged molecules. The application of nitrogen gas and heat as the droplets enter the ion transfer tube remove the remaining solvent from the droplets, allowing the charged ions to enter the mass spectrometer in the gas phase (Figure 1.5). This ionization can occur either by protonation (positive ion mode) or deprotonation (negative ion mode). DNA adducts are generally analyzed in positive ion mode due to their ease of protonation[77].

1.2.2.2 Mass analyzers

Quadrupole mass analyzers

Quadrupole mass analyzers (Q) consist of 4 parallel rods arranged in a square array. Alternating radio frequency (RF) voltages allow the quadrupole to select ions based on *m/z* to pass through the quadrupole, while ions without the selected *m/z* will have an unstable trajectory and be ejected from the quadrupole. For accurate quantitation of DNA adducts, a triple quadrupole MS in selected reaction monitoring (SRM) mode is frequently used. A triple quadrupole consists of the Q_1 quadrupole, the Q_2 collision cell, and the Q_3 quadrupole. In SRM mode, Q_1 filters for the precursor ion of interest. The selected ions then enter the Q_2 collision cell where collisions with inert gas (nitrogen or argon) induce fragmentation via collision-induced dissociation (CID). The resulting fragments enter Q_3 where the quadrupole filters for the fragment ion of interest to send to the detector. This MS/MS analysis allows for sensitive and specific detection and quantitation of DNA adducts, as only the ions with the correct precursor and fragment ions will reach the detector, reducing background noise and interference[77, 94].

Ion trap mass analyzers

In contrast to quadrupole mass analyzers which allow ions of a certain *m/z* to flow through, ion trap mass analyzers trap and store ions. Ions can be selected to remain in the trap based on their *m/z* while all others are ejected from the trap. The selected ions can be fragmented via CID followed by mass analysis of the resulting fragments. This allows for multistage tandem mass spectrometry experiments (MS^n), as the cycle of trapping and fragmenting ions can be repeated approximately 10 times. The higher degree of fragmentation available with the ion trap as compared to a triple quadrupole can be beneficial for structure elucidation experiments. The major MS/MS fragment observed with modified nucleosides is the loss of sugar, which does not provide structural

information regarding nucleobase adducts. Further fragmentation of the modified base can reveal structural details. Additionally, the MS^3 mode can result in greater selectivity and sensitivity for DNA adduct quantitation[77, 94].

Orbitrap mass analyzers

Orbitrap mass analyzers utilize an electrostatic field to trap ions between an outer barrel-like electrode and a central spindle-like electrode. There are three characteristic frequencies that categorize the ion trajectories around the central electrode: axial frequency (ω), radial frequency (ω_r), and rotational frequency (ω_ψ)[95]. Of these three, only axial frequency can be used for mass analysis as it does not rely on energy or position of ions, but on *m/z* and field curvature (k) as described by the following equation: $\omega = \sqrt{(z/m)k}$. Following ion injection between the two electrodes, ions move in orbit around the central electrode, and the axial frequency of the ions is detected as an image current and Fourier transformed into a mass spectra[95]. While the Orbitrap has primarily been utilized for proteomic applications, the high mass resolution (HRMS) capabilities have been successfully implemented for the improvement in sensitivity for DNA adduct quantitation by mass spectrometry[93, 96].

Hybrid mass spectrometers

The combination of multiple mass analyzers in a single instrument results in expanded instrumental capabilities. The combination of a linear ion trap and an Orbitrap in the LTQ Orbitrap Velos (Thermo Scientific, Waltham, MA, USA) allows for MS^n fragmentation of ions coupled with high resolution detection of the resulting fragments. Our laboratory has utilized this instrument for the sensitive and specific quantification of butadiene DNA adducts in urine and genomic DNA[22, 23, 92]. The Q Exactive (Thermo Scientific, Waltham, MA, USA) combines a quadrupole with an Orbitrap to allow for precursor ion filtering, followed by CID and HRMS detection of all generated

fragments. Our laboratory recently published the development of a quantitative nanoLC/NSI$^+$-HRMS methodology for the quantification of *bis*-N7G-BD in urine utilizing a Q Exactive Orbitrap[97]. Finally, the Orbitrap Fusion Lumos (Thermo Scientific, Waltham, MA, USA) is the combination of a quadrupole, linear ion trap, and orbitrap mass analyzers into a single instrument, providing high resolution detection of intact proteins, peptides, and small molecules with initial quadrupole mass filtering, optional MS^n in the linear ion trap, and high resolution detection in the Orbitrap.

1.3 Endogenous formation of DNA adducts

1.3.1 The exposome

While disease risk is often attributed to genetics, environmental factors represent a much larger contribution to disease development[98]. The exposome, a term first used in 2005 to describe the life-course environmental exposures[99], is discussed in three categories: general external exposures, specific external exposures, and internal exposures (Figure 1.6)[4]. General external exposures include socio-economic status, urban/rural environment, and climate. Specific external exposures include chemical contaminants, occupation, and lifestyle factors such as tobacco or alcohol. External exposures can be quantified through analysis of biomarkers of exposure, such as carcinogen-DNA adducts, carcinogen-protein adducts, and carcinogen metabolites. Biomarkers of specific external exposures are typically the focus of epidemiological studies and are used for risk assessment of disease.

External exposures are not the only sources of carcinogens, however. Internal exposures to endogenous molecules, such as those formed through metabolism, also play a role in DNA damage[100]. There are several known human carcinogens that, in addition to external exposures, are also produced endogenously by humans. Formaldehyde, acetaldehyde, vinyl chloride, and ethylene oxide are occupational and environmental carcinogens that are also produced endogenously[101-103]. The presence of endogenous adducts originating from internal exposures in humans complicates risk assessment using biomarkers of exposure and raises questions about the relative contributions of environmental and internal sources of DNA damage to cancer development.

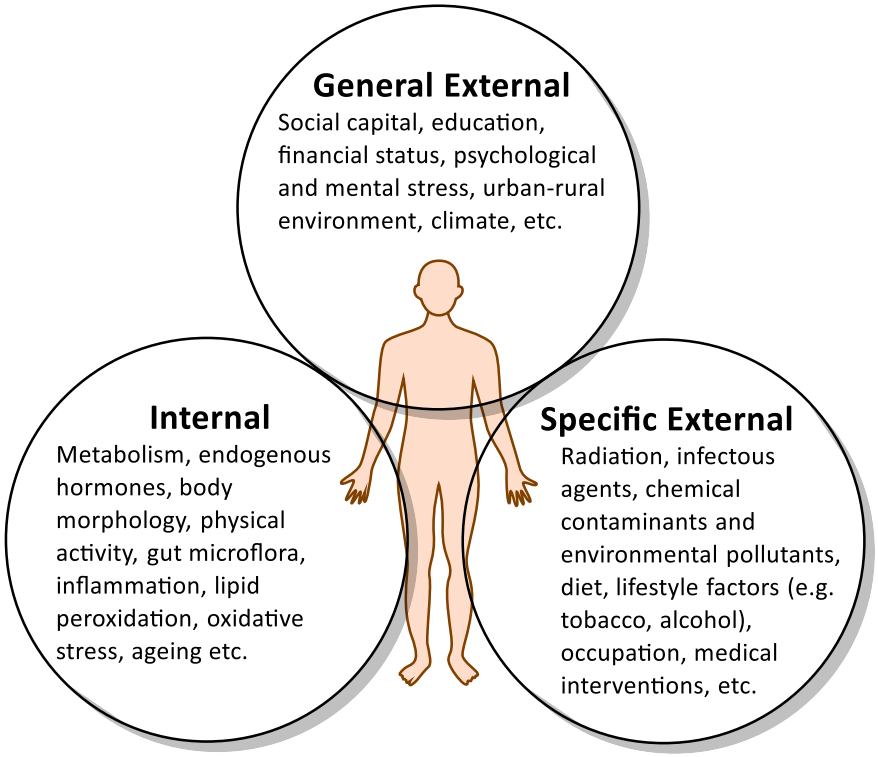

Figure 1.6. The exposome: categories of human sources of chemical carcinogens and examples[4].

1.3.2 Isotope-labeling studies to distinguish endogenous and exogenous DNA adducts

Exposures to external or internal sources of the same carcinogen leads to the formation of structurally identical DNA adducts. Stable isotope labeled carcinogens allow for the determination of relative contributions of exogenous and endogenous DNA adduct formation. Isotope-labeling studies to distinguish exogenous and endogenous DNA adducts have been conducted in cultured cells and laboratory animals.

1.3.2.1 Isotope-labeling studies in cells

Formaldehyde and acetaldehyde are highly used industrial chemicals. Formaldehyde is classified as carcinogenic to humans, while acetaldehyde is classified as possibly carcinogenic to humans[104, 105]. Exposure to these aldehydes additionally occurs through tobacco smoke, automobile exhaust, and endogenous production[106-108]. Utilizing isotope labeling studies, the Swenberg lab was able to distinguish between hydroxymethyl DNA adducts forming from endogenous and exogenous formaldehyde in Hela cells treated with [$^{13}CD_2$]-formaldehyde[107]. They additionally treated human lymphoblastoid cells with [$^{13}C_2$]-acetaldehyde and measured the formation of N^2-ethylidene-dG adducts as a biomarker of exposure[108]. They detected exogenous adducts at levels higher than the background of endogenous adduct formation at concentrations of [$^{13}C_2$]-acetaldehyde at 50 μM or higher, indicating that low level acetaldehyde exposures are unlikely to result in a significant increase from background endogenous DNA adducts. However, exposure to acetaldehyde via alcohol consumption leads to 100-fold increases in N^2-ethylidene-dG adduct levels as compared to baseline prior to alcohol consumption, indicating primarily exogenous formation of the DNA adduct upon alcohol exposures[109].

Alkylation of DNA is both common and potentially mutagenic[110]. Exposure to alkylating agents occurs endogenously, environmentally, through lifestyle choices such as diet, alcohol, and tobacco, and through their use as anti-cancer drugs[110]. *S*-adenosylmethionine is the primary source of endogenous methylation[100] and is additionally involved in DNA methylation as a mode of epigenetic regulation[111]. While there are many exogenous methylating agents, methylnitrosourea has been used to model low dose mutations upon DNA alkylation and investigate the relative contributions of endogenous and exogenous methylated DNA adducts[112]. In human lymphoblastoid cells treated with 0.0075-2.5 μM [D_3]-methylnitrosourea, levels of endogenous N7-methyl-guanine adducts were present in significantly higher concentrations than the exogenous adduct at concentrations ≤ 0.75 μM, and exogenous adducts only became more prevalent at 2.5 μM. In contrast, exogenous O^6-methyl-dG were more prevalent at all but the lowest treatment and became significantly higher at concentrations ≥ 0.025 μM[112]. This study indicates that endogenous methylation is responsible for a significant amount of N7-methyl-guanine adducts, while having a much lower effect on O^6-methyl-dG.

1.3.2.2 Isotope-labeling studies in animals

Isotope labeling studies have been most frequently employed in laboratory animals to quantify exogenous and endogenous DNA adducts. In rats exposed to ≤10 ppm levels of [$^{13}CD_2$]-formaldehyde, endogenous formaldehyde-DNA adducts are detected in each tissue type evaluated while exogenous adducts are detected only in the nose, at concentrations lower than those forming endogenously[79, 106, 113, 114]. At concentrations greater than 10 ppm, the exogenous adducts become more prevalent than the endogenous adducts in the nasal tissue[79, 113]. Studies conducted in non-human primates show similar results, with exogenous formaldehyde-DNA adducts forming only in the nasal tissue and at concentrations less than that of endogenous damage[79, 114, 115]. Methanol is

metabolized to formaldehyde by alcohol dehydrogenase and CYP2E1. In rats exposed to 500 or 2000 mg/kg/day of [$^{13}CD_4$]-methanol, exogenous formaldehyde-DNA adducts are observed, but in much lower levels than the endogenously forming DNA adducts[116]. These studies indicate that the risk of exogenous exposures to low ppm levels of formaldehyde are lower than previously thought, as endogenous formaldehyde is resulting in significantly higher levels of DNA damage. Additionally, exogenous formaldehyde does not appear to enter circulation, only forming adducts in the tissues at the source of exposure.

Vinyl chloride is metabolized to active metabolite chloroethylene oxide by CYP2E1[117]. Chloroethylene oxide reacts with guanine bases in DNA to form 7-(2-oxyethylguanine) and N^2,3-ethenoguanine DNA adducts[118]. 7-(2-oxyethylguanine) and N^2,3-ethenoguanine have been observed in unexposed humans and animals, leading to the hypothesis of endogenous formation[102, 119-121]. In rats exposed to 1100 ppm of isotopically labeled vinyl chloride ([$^{13}C_2$]-vinyl chloride), exogenous N^2,3-ethenoguanine adducts are higher than the endogenous adducts in the liver and formed in similar quantities to endogenous adducts in the lung and kidney[122]. In contrast, exogenous 7-(2-oxyethylguanine) was observed in the same tissues at levels over 40 times greater than endogenous 7-(2-oxyethylguanine), suggesting that it is a specific biomarker for VC exposure[102].

Ethylene is an endogenous and environmental chemical. Ethylene is metabolized through CYP2E1 oxidation to ethylene oxide, which is also a widely used intermediate in industrial settings and classified carcinogenic to humans[103, 123]. The primary DNA adduct of ethylene oxide is N7-(2-hydroxyethyl)guanine. In liver, spleen, and stomach tissue of rats treated with 0.0001-0.1 mg/kg of [14C]-ethylene oxide, levels of exogenous N7-(2-hydroxyethyl)guanine were insignificant as compared to the background levels of endogenous damage. This study suggests that, at low

exposures to ethylene oxide, there is no significant increase due to risk associated with background endogenous exposures[103].

In summary, endogenous adducts represent a significant amount of overall adducts at low dose exposures to carcinogens and need to be considered in risk assessment. In many of these studies, it was observed that low exogenous exposures did not significantly increase the level of adducts above the background endogenous adducts, suggesting that low exogenous exposures are not responsible for disease development. However, many carcinogen DNA adducts are not formed by endogenous agents and low exogenous exposures will have a significant impact on the overall DNA adduct levels and associated cancer risk. It is critical to understand if DNA adducts are affected by endogenous formation prior to their use as biomarkers of external carcinogen exposures and risk.

1.4 Overview of 1,3-butadiene as a human and animal carcinogen

1.4.1 1,3-Butadiene sources of exposure and toxicity

Occupational exposure to 1,3-butadiene (BD) occurs in the synthetic polymer industry, where BD monomers are used as building blocks for polymer formation[124]. Workers occupationally exposed to BD have an elevated risk of developing lymphoma and leukemia[125-130] and possibly lung cancer[128, 131-133], COPD[133], and bladder cancer[128, 133]. Environmental exposure to BD also occurs through tobacco smoke[134], wood burning smoke[135], automobile exhaust[136], surgical smoke[137], and urban air[138]. Exposure to environmental sources of BD during pregnancy and infancy results in an increased risk of childhood leukemia[139, 140], central nervous system primitive neuroectodermal tumors[141], and germ cell tumors[142]. Children exposed to environmental BD may be at higher risk of asthma[143]. Environmental exposures to BD as adults have been associated with hepatocellular carcinoma[144].

BD is a multi-site carcinogen in laboratory animals, inducing lymphoma, neoplasms of the heart, lung forestomach, liver, Harderian gland, mammary gland, and ovary in mice at concentrations of butadiene exposure greater than 200 ppm. Tumors in the lungs of mice were observed at concentrations as low as 6.25 ppm[145]. Laboratory rats are less susceptible to BD induced tumorigenesis, with tumor formation observed at BD concentrations of 1000 or 8000 ppm[146, 147]. BD is classified as a Group 1 carcinogen by the International Agency for Research on Cancer based on the evidence for increased occupational cancer risk in humans and carcinogenicity studies in laboratory animals[148].

1.4.2 1,3-Butadiene metabolism and mutagenicity

BD is metabolized to reactive epoxide 3,4-epoxy-1-butene (EB) by cytochrome P450 monooxygenases CYP 2E1 and CYP 2A6[149]. EB undergoes epoxide hydrolase (EH) mediated hydrolysis to form 1-butane-3,4-diol (EB-diol), which is epoxidized by CYP 2E1 or 2A6 to form 1,2-dihydroxy-3,4-epoxybutane (EBD)[150]. Alternatively, EB can be further oxidized by CYP 2E1 or 2A6 to form 1,2,3,4-diepoxybutane (DEB), which can additionally be hydrolyzed via EH to form EBD (Figure 1.7) [149, 151]. These three reactive epoxides (EB, EBD, and DEB) form covalent adducts at nucleophilic sites in DNA and proteins and are responsible for the toxicity and carcinogenicity of BD. EBD is the most abundant BD epoxide, followed by EB and DEB. Despite its low abundance, DEB is by far the most mutagenic epoxide, likely due to the ability to form interstrand DNA crosslinks and DNA-protein crosslinks.

In human TK6 lymphoblast cells treated with BD epoxides, DEB is the most potent mutagen, inducing mutations at concentrations as low as 1-4 μM[152, 153]. Mutagenicity by EB required concentrations of 100-150 μM, while EBD was the least mutagenic, at concentrations of 350-450 μM[153]. At 4 μM DEB for 24 hours, AT → TA transversions and partial deletions were significantly increased in the *hprt* gene in TK6 cells[152, 154], while EB concentrations required to induce significantly increased AT → TA transversions and GC → AT transitions were at least 100-fold higher (400 μM EB for 24 hours)[154, 155]. Similar results were also observed for *hprt* mutations in CHO-K1 cells exposed to EB and DEB[156].

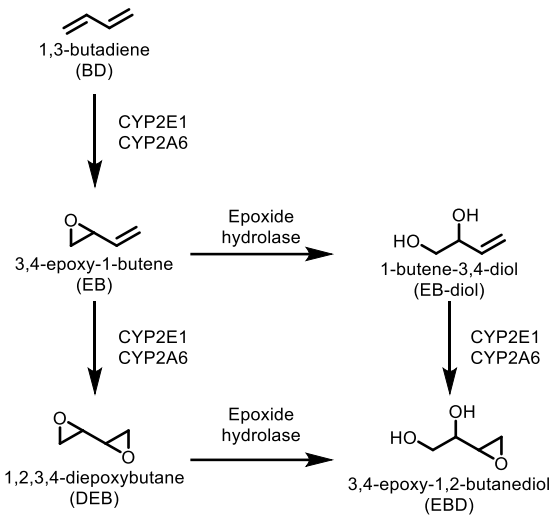

Figure 1.7. Metabolic activation of 1,3-butadiene

In B6C3F1 mice exposed to 625 ppm BD for 2 weeks via inhalation, 60-100 mg/kg EB (i.p.), or 7-21 mg/kg DEB (i.p.), *hprt*$^-$ mutation frequency in splenic T cells was increased compared to controls[157]. AT → GC transitions and AT → TA transversions are increased in the bone marrow and spleen of B6C3F1 *laci* transgenic mice upon exposure to BD (6.25-1250 ppm, 6 h/day, 5 days/week, 4 weeks)[154]. Exposure to EB (29.9 ppm) or DEB (3.8 ppm) did not increase *laci* mutation frequency in the bone marrow or spleen, but EB exposure did result in a 3-fold increase in *laci* mutations in the lung[154]. In BD exposed workers, an increase in *hprt* AT → TA transversions[158] and exon deletions have been observed[159]. However, other studies among occupationally exposed workers reported that no significant differences in *hprt* mutation frequency as compared to controls were observed[159-161].

1.4.3 1,3-Butadiene biomarkers of exposure

BD metabolic activation results in the generation of reactive epoxides. These epoxides are detoxified through glutathione conjugation or form covalent adducts with biomolecules such as DNA and proteins. The metabolites and adducts generated through each of those processes can be quantified and utilized as biomarkers of BD exposure, detoxification, and bioactivation.

1.4.3.1 Urinary mercapturic acids as biomarkers of 1,3-butadiene exposure

BD epoxides are detoxified through glutathione S transferase (GST) mediated conjugation to form glutathione conjugates[162, 163]. The conjugates are ultimately excreted as mercapturic acids in the urine. These mercapturic acid metabolites represent the dose of BD that is detoxified and have been used as biomarkers of BD exposure.

2-(N-acetyl-L-cystein-S-yl)-1-hydroxybut-3-ene (MHBMA-1), 1-(N-acetyl-L-cystein-S-yl)-2-hydroxybut-3-ene (MHBMA-2), and 1-(N-acetyl-L-cystein-S-yl)-4-hydroxybut-2-ene (MHBMA-3) are formed from EB[164, 165] (Figure 1.8). MHBMA-3 was originally identified as an impurity resulting from synthesis or storage in acidic conditions[166] but was detected in fresh urine samples and classified as a butadiene metabolite by Alwis et al. in 2012[165]. Many studies which quantified MHBMA only reported the sum of MHBMA-1 and MHBMA-2 due to the original report by Elfarra et al[166]. For the rest of this thesis MHBMA will refer to the sum of MHBMA-1 and MHBMA-2, while MHBMA-3 will be noted separately if quantified. N-acetyl-S-(3,4-dihydroxybutyl)-L-cysteine (DHBMA) is formed from EB-diol derived hydroxymethylvinyl ketone (HMVK)[164], 4-(N-acetyl-L-cystein-S-yl)-1,2,3-trihydroxybutane (THBMA) is formed from EBD[167], and *bis*-butanediol mercapturic acid (*bis*-BDMA) is formed from DEB[168] (Figure 1.8).

MHBMA and DHBMA have been detected and quantified in a variety of animal species. In F344 and Sprague-Dawley rats, B6C3F1 mice, Syrian hamsters, and cynomolgus monkeys treated with 8000 ppm ^{14}C-BD, MHBMA and DHBMA were the two most abundant metabolites detected in the urine. Levels of MHBMA were highest in the mice, followed by rats and hamsters, and lowest in monkeys. Levels of DHBMA followed the opposite trend, lowest in the mice, followed by hamsters and rats, and highest in the monkeys. The metabolic ratio DHBMA/MHBMA+DHBMA and epoxide hydrolase activity in these species were positively correlated, suggesting the importance of EB hydrolysis to EB-diol in the formation of DHBMA[169]. Additionally, this data revealed significant species differences in the metabolism of BD, suggesting that not all animal models of BD toxicity are relevant to humans.

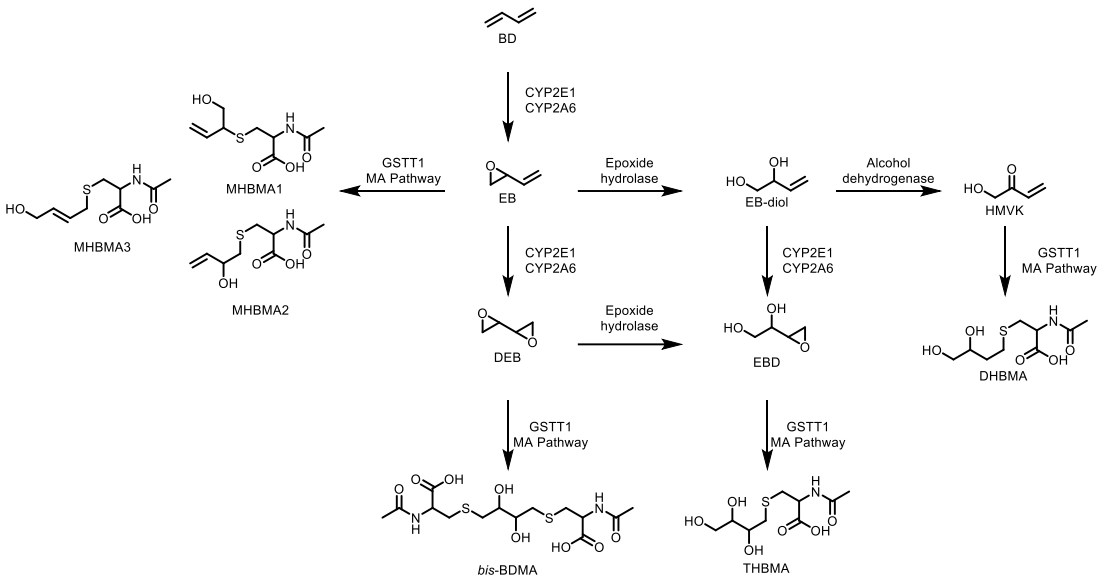

Figure 1.8. Detoxification of BD epoxides through glutathione conjugation

MHBMA and DHBMA have also been measured in monomer and polymer workers occupationally exposed to BD. Occupationally exposed workers excrete significantly higher levels of urinary MHBMA and DHBMA as compared to controls[164, 170-173]. Workers occupationally exposed to automobile exhaust, such as traffic policemen and gas station workers also excrete elevated levels of DHBMA, but not MHBMA as compared to non-occupationally exposed controls[174]. Among policemen, traffic policemen exposed to BD in automobile exhaust have significantly higher levels of DHBMA as compared to office policemen, while MHBMA levels are slightly, but not significantly elevated in traffic policemen[175, 176]. Coke oven workers exposed to BD excrete significantly higher levels of MHBMA, but not DHBMA, as compared to controls[177].

MHBMA has been shown to be associated with smoking status, with significantly higher levels of MHBMA in smokers as compared to non-smokers[178-180]. Levels of urinary MHBMA decrease by 80-96% as quickly as 3 days post-smoking cessation[181, 182]. In contrast, DHBMA levels remain unchanged upon smoking cessation, suggesting the presence of endogenous sources of DHBMA formation[181]. MHBMA levels are additionally associated with racial/ethnic groups[163, 183, 184] and lung cancer development[185]. A genome wide association study in 2017 revealed that *GSTT1* gene deletion is responsible for 7.3% of the variability in MHBMA levels in current smokers[163]. These results show MHBMA as a specific biomarker of BD exposure in humans, while DHBMA likely has additional sources of formation and is not specific to BD exposure.

MHBMA-3 was first quantified as a BD metabolite in humans in 2012, where levels of MHBMA-3 were reported significantly higher in smokers as compared to non-smokers[165]. Additionally, MHBMA-3 levels were 20-fold higher than levels of MHBMA-2, suggesting it as a major metabolite of BD[165]. No ethnic differences in MHBMA-3 excretion among African Americans and whites were observed[184]. Levels of MHBMA-3 in smokers were significantly higher

than in e-cigarette uses, smokeless tobacco users, and nontobacco users[186]. Additionally, levels of MHBMA-3 in smokers decreased to the level of nontobacco users within 48 hours of smoking cessation[186]. In non-smokers exposed to 1 hour of secondhand cigarette smoke, MHBMA-3 levels are significantly increased as compared to baseline before exposure[187].

THBMA was detected and quantified in rats and mice following treatment with 200 ppm [2,3-^{14}C]-BD. THBMA levels represented 4.1% of total butadiene dose in rats, and 6.7% in mice[188]. Initial attempts to detect THBMA in humans were unsuccessful, due to insufficient sensitivity of the GC-MS methodology[164]. Kotapati et al. reported the first quantification of THBMA in humans, showing that smokers excrete significantly higher levels of THBMA as compared to non-smokers, and that levels of THBMA decrease 25-50% post-smoking cessation[167]. These results indicate that BD exposure in tobacco smoke is a significant source of THBMA formation.

Bis-BDMA is a specific biomarker of BD activation to the most mutagenic epoxide DEB, as the diepoxide is required for the formation of *bis*-BDMA. In rats exposed to 62.5 and 200 ppm BD, a concentration-dependent increase in *bis*-BDMA was observed. *bis*-BDMA accounted for 1% of the total mercapturic acids detected in these animals[168]. A recent study quantifying *bis*-BDMA and other urinary BD biomarkers in mice treated with 590 ppm BD revealed *bis*-BDMA at levels of 8.09 ± 6.3 μg/mL urine[97]. Attempts to quantify *bis*-BDMA in human urine have been unsuccessful[168], likely due to the much lower BD exposures in humans (1 ppm for occupationally exposed workers)[189], more efficient hydrolysis of DEB in humans as compared to laboratory mice and rats[190], and low abundance of the metabolite as compared to MHBMA, DHBMA, and THBMA[168].

1.4.3.2 Protein adducts as biomarkers of 1,3-butadiene exposure

If not detoxified by glutathione conjugation, BD epoxides form covalent adducts with proteins. *N*-(2-hydroxy-3-buten-1-yl)-valine (HB-Val), 1,2,3-trihydroxybutyl-valine (THB-Val), and *N*,*N*-(2,3-dihydroxy-1,4-butadiyl)-valine (*pyr*-Val) are formed at the *N*-terminal valine of hemoglobin by EB, EBD, and DEB, respectively (Figure 1.9)[191]. Hemoglobin adducts provide a representation of long-term exposure, as they accumulate over time in red blood cells and there are no mechanisms for their repair.

HB-Val and THB-Val are detected through a modified Edman degradation protocol developed by Törnqvist et al[192]. HB-Val was first detected in Wistar rats treated with BD (0-1000 ppm, 6 h/day, 5 days/week) for two weeks. The levels of HB-Val increased linearly with increasing concentrations of BD exposure[193]. In laboratory animals treated with BD, HB-Val levels were 2-5-fold greater in mice than rats[194-196], with increased levels in females as compared to males[195, 196]. HB-Val adducts are increased in workers occupationally exposed to BD, as compared to controls[171, 172, 197-199]. After adjusting for BD dose, these levels were significantly lower than levels of HB-Val observed in rats and mice[197, 200].

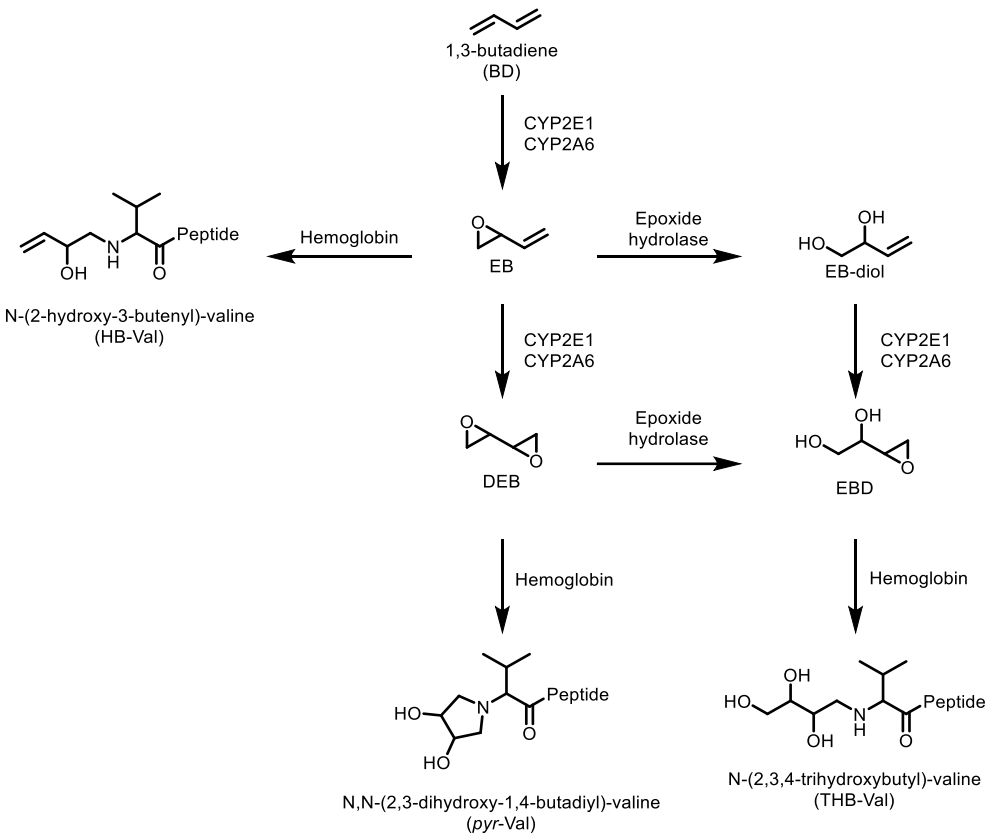

Figure 1.9. Protein adducts of 1,3-butadiene.

THB-Val adducts were initially detected in Sprague-Dawley rats exposed to EB, EBD, or DEB[200]. In Wistar rats treated with BD, it was identified that EBD resulting from oxidation of EB-Diol is the main precursor of THB-Val adducts, due to low levels of DEB in the blood upon BD treatment[200]. Similar to HB-Val, THB-Val adduct levels were higher (2-8 fold) in mice as compared to rats when treated with 1000 ppm (13 weeks, 5 days/week, 6 h/day)[196]. In workers occupationally exposed to BD, levels of THB-Val were elevated as compared to controls[171, 172, 200] and associated with individual mean BD exposures[171]. The THB-Val adduct levels in rats and humans are significantly higher than the HB-Val adduct levels, 70 and 321- to 431-fold greater, respectively[171, 200].

Pyr-Val is a specific biomarker of DEB formation, the most mutagenic BD derived epoxide. *Pyr*-Val adducts cannot be detected through the same protocol as HB-Val and THB-Val, as the tertiary amine formed upon cyclization to a pyrrolidine prevents derivatization by the Edman reagent. *Pyr*-Val adducts have been quantified via proteomics methodologies that quantify the N-terminal peptide of hemoglobin following trypsin digestion[201-204]. The 7-mer peptide containing *pyr*-Val was enriched via HPLC and detected by LC-MS/MS in mice and rats treated with DEB. Adduct levels increased upon increasing concentration of DEB[201, 202]. In mice and rats treated with 3 or 62.5 ppm BD for 10 days, digestion to the 11-mer N-terminal peptide followed by immunoaffinity chromatography and LC/MS-MS was utilized to quantify *pyr*-Val adducts[203, 204]. Concentrations of *pyr*-Val in mice and rats were similar to concentrations of HB-Val, with increased concentrations in mice as compared to rats[203]. THB-Val was formed in the highest concentrations in both species, indicating that EBD is more abundant than EB and DEB in both species[203]. Sensitive nanoLC-ESI$^+$-MS/MS methodologies allowed for the detection of *pyr*-Val adducts in mice and rats treated with sub-ppm levels of BD and revealed the rate of adduct

formation as decreasing with increasing concentrations of BD exposure, suggesting saturation at high concentrations[204]. Concentrations of *pyr*-Val are significantly elevated in polymer workers as compared to monomer workers and controls[205]. Formation of *pyr*-Val adducts per dose BD is lower in humans than in mice and rats, indicating that DEB is formed in smaller amounts in humans[205]. *Pyr*-Val and THB-Val are significantly associated with BD mercapturic acids MHBMA, DHBMA, and THBMA in occupationally exposed workers[206].

1.4.3.3 DNA adducts as biomarkers of 1,3-butadiene exposure

In addition to protein adducts, BD epoxides form covalent adducts at nucleophilic sites in DNA. DNA adducts are the ultimate carcinogenic species, as they lead to mutations and cancer. Among the BD-DNA adducts, N7-guanine adducts are the most prevalent. BD-DNA adducts have also been reported at other sites in adenine and guanine.

EB is known to form guanine adducts N7-(2-hydroxy-3-buten-1-yl) guanine (EB-GI) and N7-(1-hydroxy-3-buten-2-yl) guanine (EB-GII) adducts at the N7-position of guanine[195, 207-210]. EB-GII adducts undergo imidazole ring opening form the corresponding N^6-(2-deoxy-d-*erythro*-pentofuranosyl)-2,6-diamino-3,4-dihydro-4-oxo-5-N-(2-hydroxybut-3-en-1-yl)formamidopyrimidine (EB-FAPy-dG) adducts[86]. EB also reacts with adenine to form N1-(2-hydroxy-3-buten-1-yl) adenine (EB-Ade I), N1-(1-hydroxy-3-buten-2-yl) adenine (EB-Ade II), N3-(2-hydroxy-3-buten-1-yl) adenine (EB-Ade III) and N3-(1-hydroxy-3-buten-2-yl) adenine (EB-Ade IV)[195, 210-212] (Figure 1.10). EBD forms DNA adducts N7-(2,3,4-trihydroxybut-1-yl) guanine (N7-THBG), N^6-(2,3,4-trihdyroxybut-1-yl) adenine (N^6-THB-Ade), N3-(2,3,4-trihydroxybut-1-yl) adenine (N3-THB-Ade), and N-1-(2,3,4-trihydroxybutyl) adenine (N-1-THB-Ade)[195, 208, 213-215] (Figure 1.10). Due to its bifunctional nature, DEB forms exocyclic DNA adducts 1,N^6-(1-hydroxymethyl-2-hydroxypropan-1,3-diyl)-2′-deoxyadenosine (1,N^6-α-HMHP-dA) and

1,N^6-(2-hydroxy-3-hydroxymethylpropan-1,3-diyl)-2′-deoxyadenosine(1,N^6-γ-HMHP-dA)[216]. DEB can also form DNA-DNA crosslinks 1,4-*bis*-(guan7-yl)-2,3-butanediol (*bis*-N7G-BD), 1-(aden-1-yl)-4-(guan-7-yl)-2,3-butanediol (N1A-N7G-BD), 1-(aden-7-yl)-4-(guan-7-yl)-2,3-butanediol (N7A-N7G-BD), 1-(aden-3-yl)-4-(guan-7-yl)-2,3-butanediol (N3A-N7G-BD), and 1-(aden-6-yl)-4-(guan-7-yl)-2,3-butanediol (N^6A-N7G-BD)[217, 218] (Figure 1.10).

While BD metabolites and protein adducts serve as useful biomarkers of 1,3-butadiene exposure as discussed in the previous sections, they are not responsible for the carcinogenic effects of 1,3-butadiene exposure. DNA adducts are the ultimate carcinogenic species, as they can lead to mutations and cancer. BD-DNA adducts can also be used as biomarkers of exposure, metabolic activation, and risk.

Initial methods for the detection and quantification of BD-DNA adducts relied on HPLC and ^{32}P-postlabeling[219-225]. Using these methodologies, N^6 adenine and N7 guanine adducts of EB and EBD were shown to increase in in the lung and testes of rats and mice upon increasing exposure to BD[219, 226-229]. In mice treated with DEB, DNA adducts were detected in a dose-dependent manner in skin DNA[223, 224]. ^{32}P-Postlabeling methods were additionally extended to human subjects, where N1-THB-Ade was found in significantly higher levels among occupationally exposed workers as compared to controls[230]. N1-THB-Ade levels were also associated with GST genotype and individual BD exposure[231].

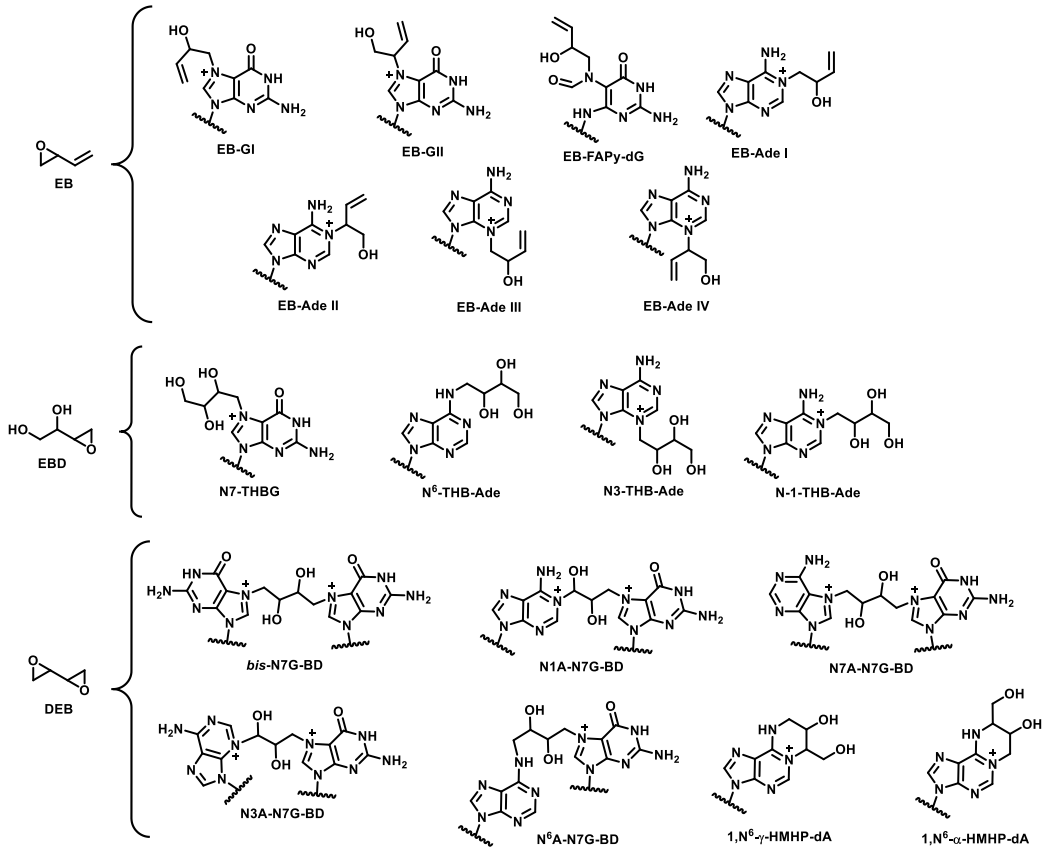

Figure 1.10. DNA adducts formed by BD epoxides EB, EBD, and DEB

The application of isotope dilution LC-ESI-MS/MS to the quantification of BD DNA adducts allowed for both greater sensitivity and accurate quantification. EB-GI, EB-GII, EB-Ade III, EB-Ade IV, N7-THBG, and N^6-THB-Ade were identified in the liver and lung of laboratory animals exposed to 1250 ppm BD for 2 weeks[213]. In F344 rats and B6C3F1 mice treated with 0-625 ppm BD, a linear dose response in levels of EB-GI and EB-GII was observed, while levels of N7-THBG were the most abundant but exhibited a nonlinear dose response[214]. Levels of the DNA adducts were significantly higher in liver DNA in mice as compared to rats at exposure levels ≥ 625 ppm[214, 232, 233]. THBG adduct levels in mouse liver were also more persistent than in rats, suggesting differences in repair efficiency[232, 233]. However, after exposure to 1250 ppm BD, urinary levels of EB-GI, EB-GII, and THBG were higher in rats as compared with mice[233]. Studies utilizing mice and rats subjected to inhalation exposure to 1-200 ppm 1,3-[2,3-^{14}C]-BD further confirm THBG as the major adduct, higher levels in mice compared to rats, the linear dose response in mice, and the non-linear dose response in rats[234, 235]. In mice exposed to BD, EB-GII and THBG adduct levels showed variation among sex and strain[236-239]. The higher levels of DNA adducts in BD exposed mice as compared to rats is consistent with the higher susceptibility of mice to BD induced carcinogenesis[146, 240].

Methodologies for the specific detection of DEB induced DNA adducts were also developed. In C57BL/6 mice exposed to 625 ppm BD, levels of guanine-guanine crosslink *bis*-N7G-BD were 3.2 ± 0.4 adducts/10^6 nucleotides in the liver and 1.8 ± 0.5 adducts/10^6 nucleotides in the lung, while *bis*-N7G-BD adducts were not detected in the control animals[21]. In B6C3F1 mice subjected to inhalation exposure to 635 ppm BD, levels of the guanine-adenine crosslink N7G-N1A-BD were 3.1 ± 0.6 adducts/10^8 nucleotides, while N7G-N3A-BD and N7G-N7A-BD were not detected[89]. Dose-dependent increases in both *bis*-N7G-BD and N7G-N1A-BD were observed in mice treated

with 0-625 ppm BD, while adduct levels in rats reached saturation at 62.5 ppm BD[78]. Sex, strain, and tissue specific differences in *bis*-N7G-BD in mice have also been reported[241]. In mice exposed to 590 ppm BD, urinary levels *bis*-N7G-BD levels are associated with DEB derived mercapturic acid metabolite *bis*-BDMA, but not with EB derived adduct EB-GII or metabolites MHBMA and DHBMA[97].

HPLC-ESI-MS/MS analysis revealed the presence of exocyclic DEB-DNA adducts 1,N^6-α-HMHP-dA and 1,N^6-γ-HMHP-dA in the liver of B6C3F1 mice exposed to 625 ppm BD[216]. At BD exposure levels of 0-200 ppm, a curvilinear dose-response in 1,N^6-HMHP-dA was observed[242]. 1,N^6-HMHP-dA and N7G-N1A-BD adducts were persistent in mice and rats, with half-lives estimated at 36-42 days. In contrast, *bis*-N7G-BD was more abundant than N7G-N1A-BD and 1,N^6-HMHP-dA, but exhibited a much shorter half-life of 2.3-5.7 days[243]. The use of nanoLC substantially increased the method sensitivity and allowed for the quantification of *bis*-N7G-BD adduct levels at much lower BD exposures (0-1.5 ppm). *Bis*-N7G-BD adducts formed in a linear dose-dependent manner at low- and sub-ppm exposure levels[93], in contrast to the saturation previously observed at higher BD exposure levels[78].

The use of high-resolution mass spectrometry (HRMS) allowed for the detection of low levels of BD DNA adducts in humans. Sangaraju et al developed a capillary HPLC-ESI^+-HRMS/MS method for the detection and quantitation of THBG in human leukocyte DNA. Occupationally exposed workers had significantly increased levels of THBG (N = 10, 9.72 ± 3.8 adducts/10^9 nucleotides) as compared to controls (N = 10, 3.08 ± 2.15 adducts/10^9 nucleotides). However, THBG levels did not decrease upon smoking cessation and were not significantly different between smokers and non-smokers, suggesting endogenous sources of formation[22].

Due to background THBG levels that may not reflect accurate human exposures to BD, a nanoLC-ESI^{+}-HRMS^{3} method was developed for the quantitation of EB-GII in human leukocyte DNA. While the EB-GII adducts were detected in blood leukocyte DNA (75 μg) from smokers, they were below the method's limit of quantitation[92]. Increasing the amount of DNA to obtain higher adduct levels in each sample was not possible due to low availability of human blood samples[92]. The method was adapted for more readily available urine samples, and levels of urinary EB-GII were shown to be significantly increased in occupationally exposed workers as compared to controls. No significant differences were observed between smokers and non-smokers (N = 29 and 28, respectively), while white smokers excreted increased levels of urinary EB-GII as compared to African American smokers[23].

These initial studies quantifying N7 guanine BD-DNA adducts in humans were low-throughput methods conducted on relatively small sizes of samples, which could contribute to the lack of difference in BD-DNA adduct levels between smokers and non-smokers. Development of high-throughput methodologies for the quantitation of BD-DNA adducts in humans will allow for the quantitation of these adducts in larger sample sizes with greater power to identify any differences between smokers and non-smokers.

In summary, BD DNA adducts, protein adducts, and detoxification metabolites can be utilized as biomarkers of exposure to BD. The elevated levels of many of these biomarkers among smokers or occupationally exposed workers suggests their use as biomarkers of BD exposure. However, studies investigating these biomarkers and lung cancer incidence are limited. Investigating the associations of these biomarkers with cancer incidence is critical for understanding and predicting BD induced carcinogenesis.

1.4.4 Variances in 1,3-Butadiene metabolism by species and gender

The animal models utilized to study the toxicity and carcinogenicity of BD revealed a higher sensitivity to BD among mice as compared to rats. In B6C3F1 mice exposed to BD for 2 years, lung tumors developed at concentrations as low at 6.25 ppm[240]. In contrast, tumor formation in rats were observed in small numbers at BD concentrations of 1000 or 8000 ppm[146, 147]. Gender differences in mice were also observed, with female mice developing lung and liver tumors at 10-fold lower concentrations than were required for the same tumor formation in male mice[240].

Studies with liver and lung microsomes from B6C3F1 mice, Sprague-Dawley rats, and humans showed a greater ratio of activation by oxidation to detoxification by hydrolysis or glutathione conjugation in mice (72), as compared to rats (5.8) and humans (5.9). Additionally, rates of oxidation from EB to DEB were 3-60 fold higher in mouse lung microsomes as compared to rats and humans[190, 244], while detoxification rates by epoxide hydrolase were highest in human liver microsomes[150, 245]. Levels of EB and DEB quantified in the blood were 4-8 times higher in mice as compared to rats[246-248]. Additionally, levels of DEB in the blood were 4.5 fold greater in female rats as compared to males[248].

The metabolic ratio DHBMA/MHBMA+DHBMA, a measure of detoxification through epoxide hydrolase or glutathione conjugation, is higher in humans (0.97) as compared to rats (0.52) and mice (0.20)[164, 170]. Additionally, DHBMA represents 93% of the BD mercapturic acids formed in humans, but only 47% in rats. MHBMA, THBMA, and *bis*-BDMA all make up a greater portion of the overall mercapturic acids in rats as compared to in humans[168]. DHBMA levels are not associated with cigarette smoking exposure to BD, suggesting additional sources of DHBMA formation[181].

Female mice excrete significantly higher levels of MHBMA and DHBMA, but there are no significant gender differences in the excretion of *bis*-BDMA[97]. While female occupationally exposed workers excrete lower levels of MHBMA, DHBMA, and THBMA the metabolic ratio was similar, suggesting the relative usage of metabolic pathways of BD detoxification does not differ between genders[206, 249]. However, significantly higher levels of DHBMA have been observed in female smokers (547.5 [95% CI: 508.5-589.4] ng/mg creatinine) vs male smokers (485.2 [95% CI: 449.8-523.5] ng/mg creatinine)[183].

In mice and rats treated with 100-1300 ppm BD, HB-Val adducts are 4-5 times greater in mice as compared to rats[194, 195, 250, 251]. At lower concentrations of BD (0.5-62.5 ppm) the differences are even more pronounced, with 4-20 fold greater concentrations in mice as compared to rats[191, 203]. *Pyr*-Val adduct levels are increased 10-60 fold in mice as compared to rats[191, 203, 204, 251]. THB-Val adducts are also elevated in mice as compared to rats, and the differences are more pronounced at lower exposure levels, with an 18-fold increase at 1 ppm and an 2.4-fold increase at 62.5 ppm[118]. 1.7-2.1 fold greater levels of THB-Val are observed in mice treated with EB-diol (0-36 ppm) as compared to rats[252]. All three hemoglobin adducts show increased sensitivity to BD in the mouse as compared to the rat. HB-Val and *pyr*-Val adducts have also been shown to be higher in female mice and rats as compared to males[195, 203]. In contrast to the gender differences observed in animals, with females showing higher sensitivity to BD, levels of THB-Val are significantly elevated in both occupationally exposed and control males as compared to female exposed workers and controls[253].

Species and gender differences in BD-DNA adducts have also been reported. Levels of EB-GI, EB-GII, and THBG are higher in mice treated with 625-1250 ppm as compared to rats[213, 214, 232], but were similar between the two species at lower exposure levels (20-62.5 ppm)[214]. THBG has also been reported in higher concentrations in mice as compared to rats after exposures to 0-36 ppm

EB-Diol[252]. EB-GII and THBG adduct levels are also strain specific in mice, exhibiting significant interstrain variability[237-239, 241]. The concentration of the DEB specific *bis*-N7G-BD crosslink is 4-10 fold greater in mice as compared to rats and 2-2.5 fold greater in females than in males[78].

Hprt mutations are significantly increased above background levels in mice exposed to 3 ppm BD and in rats exposed to 6.25 ppm BD, providing further evidence of increased sensitivity to BD in mice[191, 254, 255]. Additionally, in both species *hprt* mutation frequency was increased in females over males[255].

In summary, there are significant differences in BD metabolism between species and genders. Mice are more susceptible to the toxic and carcinogenic effects of BD, due to more efficient metabolism of BD to DEB as compared to rats and humans. Additionally, levels of metabolites, protein adducts, and DNA adducts differ by gender, with increased levels in female laboratory animals. Interestingly, this trend was not consistent in humans, with higher levels of protein adducts in males. These species and gender differences in BD biomarkers can complicate their use in risk assessment.

1.4.5 1,3-Butadiene exposure in cigarette smoke and lung cancer risk

Lung cancer is the leading cause of cancer related deaths in the United States, with lung cancer representing 21% of cancer deaths estimated in 2022[256]. 82% of lung cancer cases are directly attributable to smoking[257]. Among smokers, 11-24% will develop lung cancer over the course of a lifetime[258]. Tobacco smoke contains over 70 known carcinogens, including polycyclic aromatic hydrocarbons, nitrosamines, aromatic amines, aldehydes, phenols, volatile hydrocarbons, nitro compounds, and metals[17, 134]. Among these, 1,3-butadiene is one of the most abundant and has the highest cancer risk index (CRI) per cigarette/day[259].

In the United States, the risk of lung cancer development also varies by race/ethnicity. Among 2,356 (740 lung cancer cases) subjects in Hawaii, lung cancer incidence was found to differ by race/ethnicity in males, with the order Hawaiian > Caucasian > Chinese > Japanese > Filipino[260]. In females a similar trend was observed, in the order Hawaiian > Caucasian > Chinese > Filipino > Japanese[260]. Another Hawaii based case-control study of 2779 female subjects (375 cases) revealed the racial/ethnic differences in lung cancer risk to be Hawaiian > Japanese > Chinese[261]. Racial/ethnic differences in lung cancer risk among African Americans and whites in metropolitan Detroit were investigated by Schwartz et al[262]. Among the younger men (age 40-54 years) African American smokers were 2-4 times more likely to develop lung cancer[262]. The differences in risk were not explained by smoking habits, suggesting dietary or genetic risk factors influence the ethnic differences[260].

Among 180,000 subjects in the Multiethnic Cohort Study (MEC)[263], 1979 cases of lung cancer were identified. In this population (≤ 10 cigarettes per day (CPD)), lung cancer risk was highest in African Americans and Native Hawaiians, followed by whites, Japanese Americans, and Latinos (Relative Risk: 1.00, 0.88, 0.45, 0.25, 0.21, respectively). However, at smoking levels greater than

30 CPD, there were no significant differences in lung cancer risk between the racial/ethnic groups (Relative Risk: 1.00, 0.95, 0.82, 0.75, 0.79)[264]. In this population, risk factors such as smoking amount, diet, occupation, and socioeconomic status could not explain the racial/ethnic disparities in lung cancer risk, and the authors hypothesized that differences in metabolism of nicotine and tobacco smoke carcinogens may play a role in the differences in risk[264]. A follow up study increased the number of lung cancer cases from 1979 to 4993 and confirmed the results shown in the initial study; the risk of lung cancer at low CPD for Native Hawaiians and African Americans is 2-3 fold greater than Japanese Americans and Latinos and these differences diminish at high CPD[265]. Ethnic differences in the bioactivation and detoxification of BD could explain part of the observed racial/ethnic differences in observed lung cancer risk.

1.5 Summary and thesis goals

BD is an occupational and environmental carcinogen. Common human exposures to BD occur in the polymer industry, tobacco smoke, and automobile exhaust. BD is classified as a known human carcinogen based on carcinogenesis in laboratory animals and increased cancer incidence in occupationally exposed workers. BD is metabolically activated to three reactive epoxides, EB, EBD, and DEB. If not detoxified and excreted as mercapturic acids, these epoxides form covalent adducts at nucleophilic sites in DNA. BD metabolites MHBMA and DHBMA have been previously quantified in large scale epidemiological studies to examine the racial/ethnic differences in BD metabolism. However, in contrast to BD metabolites which are detoxification products, BD DNA adducts represent the biologically relevant dose of BD that is activated and available for DNA binding. Methods for the detection and quantitation of BD-DNA adducts EB-GII and THBG have been used to compare the BD-DNA adduct levels between occupationally exposed workers, smokers, and non-smoker controls. However, BD-DNA adducts have not been evaluated in large scale epidemiological studies to understand the racial/ethnic differences in BD bioactivation and cancer risk. Therefore, the initial goals of this thesis work were to validate urinary EB-GII as a biomarker of smoking exposure to BD, identify racial/ethnic differences in the excretion of urinary EB-GII in smokers, and examine associations between excretion of urinary EB-GII and lung cancer incidence in smokers.

Additionally, significant levels of BD-DNA adducts have been previously detected in non-smokers, unexposed laboratory animals, and untreated cultured cells, suggesting the formation of these adducts from sources other than BD exposure. The second goal of this thesis work was to quantify the relative contributions of endogenous and exogenous BD-DNA adducts and metabolites in animals. To accomplish this, an animal model in which laboratory rats were exposed to stable

isotope labeled BD [BD-d_6] was utilized. Biomarkers arising from BD-d_6 exposure contained the deuterium isotope label, while endogenously forming biomarkers were unlabeled and distinguishable by mass spectrometry.

While the N7-guanine adducts discussed throughout most of this work are useful biomarkers of BD exposure and risk, they are not expected to be mutagenic. Previous work has identified a ring opened formamidopyrimide adduct that forms from EB-GII, EB-FAPy-dG, and quantified the formation of this potentially mutagenetic BD-DNA adduct in mouse embryonic fibroblasts. The final goal of this thesis work was to develop a sensitive nanoLC-ESI$^+$-HRMS/MS methodology for the detection and quantification of the novel formamidopyrimidine DNA adducts of EBD and DEB, THB-FAPy-dG and DEB-FAPy-dG, and investigate their formation in DNA.

2. Urinary N7-(1-hydroxy-3-buten-2-yl) guanine adducts in humans: temporal stability and association with smoking

Reprinted with permission from:

Caitlin C. Jokipii Krueger, Guru Madugundu, Amanda Degner, Yesha Patel, Daniel Stram, Timothy Church, Natalia Tretyakova. Mutagenesis 2020, 35, 19-26.

Dr. Timothy Church provided samples for the temporal stability study. Dr. Guru Madugundu and Amanda Degner developed and validated the high-throughput 96-well plate method. Yesha Patel conducted statistical analyses under the direction of Dr. Daniel Stram. Dr. Guru Madugundu and Caitlin C. Jokipii Krueger quantified adduct levels in human urine samples by mass spectrometry.

2.1 Introduction

Lung cancer is the leading cause of cancer-related deaths [266]. While cigarette smoking is a major factor in lung cancer development, the risk differs greatly among smokers, with approximately 15% of smokers developing lung cancer [267]. It is important to identify smokers at highest risk, so that they can be targeted for smoking cessation and chemopreventive intervention. Carcinogen-DNA adducts can provide important information regarding carcinogen exposure and potentially lung cancer risk [181, 268].

1,3-butadiene (BD) is among the most abundant carcinogens in tobacco smoke [134]. BD concentrations in tobacco smoke (20-75 µg per cigarette in mainstream smoke and 205-361 µg per cigarette in side stream smoke) are several orders of magnitude higher than of other tobacco smoke carcinogens such as tobacco specific nitrosamines and polycyclic aromatic hydrocarbons [259, 269]. BD is also found in urban air, automobile emissions, smoke from wood burning, and in the synthetic polymer industries [124, 135, 136, 138]. BD is a multi-site carcinogen in laboratory animals, inducing lymphocytic lymphoma, neoplasms of the heart, forestomach, Harderian gland, mammary gland, ovary, liver, and the lung [270]. Malignant lung tumors were observed following inhalation exposure of laboratory mice to as low as 6.25 ppm BD [240]. Furthermore, BD causes chromosomal abnormalities and increases incidence of lymphatic and hematopoietic cancer in occupationally exposed workers [125-127]. The International Agency for Research on Cancer classifies BD as a "known human carcinogen" based on the evidence for increased occupational cancer risk in humans and carcinogenicity studies in laboratory animals [148].

The high prevalence of BD in tobacco smoke and urban environments and the significant potential for BD-mediated health effects warrant investigations into genetic factors that govern an individual's susceptibility to butadiene-induced cancer [163, 183, 259, 269]. BD is metabolized to reactive

epoxides 3,4-epoxy-1-butene (EB), 1,2,3,4-diepoxybutane (DEB), and 1,2-dihydroxy-3,4-epoxybutane (EBD) by cytochrome P450 monooxygenases (Figure 1.7) [149, 151, 271]. BD epoxides are detoxified by glutathione S transferases to form monohydroxybutenyl mercapturic acid (MHBMA) and dihydroxybutyl mercapturic acid (DHMBA) from EB and trihydroxylbutyl mercapturic acid (THBMA) from EBD, which are excreted in urine (Figure 1.8) [164, 167, 272]. BD-mercapturic acids have previously been investigated as urinary biomarkers of exposure to BD [162-164, 167, 168, 170, 173, 179-181, 206, 272-276]. Urinary MHBMA levels decreased 80-90% upon smoking cessation, confirming its association with smoking status [167, 181]. In contrast, DHBMA was unaffected by smoking status, suggesting that it is not associated with smoking [167, 181].

Unlike BD-mercapturic acids, which represent the metabolically inactivated dose of butadiene [183], BD-DNA adducts can be considered as mechanism-based biomarkers of exposure to BD. They can serve as useful indicators of a biologically relevant dose since they reflect the formation of reactive intermediates available for binding to DNA and other biomolecules [157, 277]. EB reacts with the N7 position of guanine to form N7-(2-hydroxy-3-buten-1-yl)guanine (EB-GI) and N-7-(1-hydroxy-3-buten-2-yl)guanine (EB-GII) adducts (Figure 1.10) [195, 214]. BD-DNA adducts such as EB-GI and EB-GII represent the biologically relevant carcinogen dose which is available for binding to DNA. DNA-DNA cross-links such as 1,4-*bis*-(guan-7-yl)-2,3-butanediol (*bis*-N7G-BD) and 1-(guan-7-yl)-4-(aden-1-yl)-2,3-butanediol (N7G-N1A-BD) and stable adducts such as *1,N*^{6}-(2-hydroxy-3-hydroxymethylpropan-1,3-diyl)-2′-deoxyadenosine are thought to be responsible for the carcinogenicity of BD, as they can lead to DNA polymerase errors during replication [278, 279]. In contrast, the highly abundant N7-(2-hydroxy-3-buten-1-yl)guanine (EB-GI) and N7-(1-hydroxy-3-buten-2-yl)guanine (EB-GII) adducts are not expected to be mutagenic, but can used biomarkers of risk associated with BD exposure [13, 23, 214, 280]. These adducts are hydrolytically labile and are

excreted in urine and have been previously detected in current smokers belonging to several ethnic groups [23].

Many large-scale epidemiological studies in smokers, for practical reasons, utilize a single urine sample from each individual. It is therefore important to characterize any variability in urinary EB-GII levels in the same smoker over time. We have previously developed a nanoLC-isotope dilution accurate mass spectrometry-based method for EB-GII in human urine [23]. In the present study, we quantified EB-GII in 19 smokers who provided urine samples every 2 months over the course of one year in order to evaluate the use of a single measurement as typical butadiene adduct load in a given individual. Furthermore, EB-GII adduct levels were quantified in urine samples from 17 subjects participating in a smoking cessation study to examine the association of urinary EB-GII adducts with smoking and to determine its endogenous concentrations in humans.

2.2 Materials and Methods

Materials

LC-MS grade water, methanol and acetonitrile were purchased from Fisher Scientific (Pittsburgh, PA). Strata X polymeric reversed phase SPE cartridges (30 mg/1 mL) were purchased from Phenomenex (Torrance, CA). EB-GII and $^{15}N_5$-EB-GII standards were prepared as previously reported [211, 281]. 96 well plates were purchased from Analytical Sales and Services Inc. (Ledgewood, New Jersey). All other chemicals and solvents were obtained from Sigma-Aldrich (Milwaukee, WI; St. Louis, MO) unless otherwise specified.

Human Urine Samples

Urine samples for the temporal stability study were obtained as described elsewhere [268]. Subjects (N = 19) were asked to collect their first void of the morning before each clinic visit.

60.9% were Caucasian, 31.9% African American, 1.5% Asian, and 5.8% other ethnicity. They reported smoking 24.1 ± 10.5 (range 10-50) cigarettes per day.

Human urine samples for the smoking cessation study were obtained from the previously described study [181]. Baseline 24 h urine samples were collected 14 and 7 days before smoking cessation. The urine collection started with the second void on the morning of their visit and continued through the first void of the next day. 24 h urine samples were also collected on 3, 7, 28, and 56 days after smoking cessation at clinic visits on each of those days. Seventeen (11 female) subjects participated in the study. Sixteen subjects were Caucasian, one was African American. Their mean age was 43.9 ± 11.0 years (range: 23-58). Subjects had been smoking an average of 17.3 ± 12.3 years and smoked 21.8 ± 6.7 cigarettes per day.

Urine Sample Processing and EB-GII Adduct Enrichment

Urine (200 μL) was centrifuged at 10 000*g* for 15 min to remove any particulate matter. The supernatants were spiked with $^{15}N_5$-EB-GII (5 fmol, internal standard for mass spectrometry) and subjected to solid phase extraction (SPE) on Strata X cartridges (30 mg/1 mL; Phenomenex, Torrance, CA). SPE 96-well plate was conditioned with 2 mL of methanol, followed by 2 mL of Milli-Q water. Urine samples (200 μL) were loaded onto prepared 96-well plates, and each well was washed with 1 mL of water followed by 1 mL of 10% methanol in water. EB-GII and its internal standard were eluted with 60% methanol in water, dried under vacuum, and reconstituted with 102 μL of 0.4% formic acid in water containing a 2′-deoxythymidine (dT) as an HPLC retention time marker (2.1 nmol).

Offline HPLC purification of SPE-enriched EB-GII and its internal standard was achieved on an Agilent 1100 series HPLC system equipped with a UV detector and an automated fraction collector (Agilent Technologies, Santa Clara, CA). A Zorbax Eclipse XDB-C18 column (4.6 × 150

mm, 5 μm; Agilent Technologies, Santa Clara, CA) was eluted at a flow rate of 1 mL/min with a gradient of 0.4% formic acid in Milli-Q water (A) and HPLC-grade acetonitrile (B). Solvent composition was maintained at 0% B for 5 min and then linearly increased to 3% B in 15 min and further to 40% B in 5 min. Solvent composition was returned to 0% acetonitrile in 5 min and held at 0% for 15 min for column equilibration. UV absorbance was monitored at 254 nm. dT was used as a retention time marker. Under these conditions, dT eluted at ∼17.4 min, and the retention time of EB-GII was ∼15.6 min. HPLC fractions containing EB-GII and its internal standard (14.1−16.1 min) were collected into 2 mL 96-well plate (Analytical Sales and Services Inc., Ledgewood, New Jersey), concentrated under vacuum, and redissolved in LC/MS grade water containing 0.01% acetic acid (30 μL) for nanoHPLC/nanoESI$^+$-HRMS^3 analysis. The injection volume was 5 μL. HPLC blanks were injected in the beginning of each sequence and after every 20 runs to detect any analyte carryover.

NanoLC/ESI$^+$-HRMS^3 Analysis of Urinary EB-GII

All nanoLC/ ESI$^+$-HRMS^3 analyses were conducted on a Dionex UltiMate 3000 RSLCnano HPLC system (Thermo Fisher Scientific Corp., Waltham, MA) fitted with a 5 μL injection loop and interfaced to an LTQ Orbitrap Velos instrument equipped with a nanospray source (Thermo Fisher Scientific Corp., Waltham, MA) using a method previously reported by our laboratory [23]. Gradient elution was achieved using LC/MS-grade water containing 0.01% acetic acid (A) and LC/MS-grade acetonitrile containing 0.02% acetic acid (B). Samples were loaded onto a nanoLC column (0.075 × 200 mm) manually packed with Synergi Hydro-RP 80 Å (4 μm) chromatographic packing (Phenomenex, Torrance, CA). The initial flow rate was maintained at 1 μL/min (with 2% B) for 5 min, followed by a flow rate decrease to 300 nL/min at 2% B for 1 min. The percentage of solvent B was linearly increased to 25% B in 9 min and further to 50% B in 10 min at a flow rate

of 300 nL/min. The flow rate was increased to 1 μL/min, and solvent B was returned to 2% in 1 min, followed by 5 min column equilibration. Under these conditions, EB-GII eluted as a sharp peak at 13 min. Tandem mass spectrometry analysis was performed by fragmenting $[M + H]^+$ ions of EB-GII (*m/z* 222.1) via collision induced dissociation (CID) in the linear ion trap portion of the instrument using the collision energy (CE) of 25 and an isolation width (IW) of 1.0 amu. MS/MS fragment ions at *m/z* 152.1 $[Gua + H]^+$ were subjected to further fragmentation in the high collision dissociation (HCD) cell of the instrument using nitrogen as a collision gas (CE = 75 units, IW = 1.0 amu). The resulting MS^3 fragment ions at *m/z* 135.0301 ($[Gua - NH_3]^+$) and *m/z* 153.0411 ($[Gua - NH_3 + H_2O]^+$) were detected in the mass range of *m/z* 50−270 using the Orbitrap mass analyzer (HRMS) at a mass resolution of 25,000. The $^{15}N_5$ labeled internal standard ($[^{15}N_5]$-EB-GII) was detected using an analogous MS^3 scan event consisting of fragmentation of *m/z* 227.1 ($[M + H]^+$) to *m/z* 157.1 ($[^{15}N_5$-Gua + H$]^+$) and further to *m/z* 139.0183 ($[^{15}N_5$-Gua - $NH_3]^+$) and *m/z* 157.0283 ($[^{15}N_5$-Gua - $NH_3 + H_2O]^+$). Neutral gain of water has been previously shown to occur in the MS collision cell due to the presence of residual water [282]. Extracted ion chromatograms corresponding to the sum of *m/z* 135.0301 ($[Gua - NH_3]^+$) and *m/z* 153.0411 ($[Gua - NH_3 + H_2O]^+$) were used for quantitation of EB-GII, whereas fragment ions at *m/z* 139.0183 ($[^{15}N_5$-Gua − $NH_3]^+$) and *m/z* 157.0283 ($[^{15}N_5$-Gua − $NH_3 + H_2O]^+$) at 5 ppm were used for quantitation of $[^{15}N_5]$-EB-GII. A full scan event was also performed over the mass range of *m/z* 100−500 at a resolution of 15,000 to monitor for any co-eluting matrix components. EB-GII amounts were determined by comparing the areas of the nanoLC/ESI^+-$HRMS^3$ peaks corresponding to the analyte and its internal standard using standard curves generated by analyzing known analyte amounts. The final EB-GII urine concentrations were normalized to urinary creatinine levels (determined separately, data not shown) to account for interindividual variability in urine flow rate and dilution.

Quality Control

Internal QC samples (pooled smoker urine) were included after every 10 samples onto 96 well plates. Statistical analyses were conducted to determine coefficient of variation, and data from plates exhibiting variation above 20% were discarded.

Statistical Analyses

For the cessation study, a paired *t*-test were used to compare the initial change from baseline to day 3. The repeated measures analysis of variance evaluated the rate of change during follow-up, starting from day 3 to day 56. A *p*-value <0.05 was considered statistically significant.

For the stability study, EB-GII measurements for each subject were plotted against time to examine the data for variability over time. Means, medians, standard deviations, and coefficients of variation (CV) were computed for each time point across individuals, CV were computed for each individual over time. To examine the reliability of individual measurements of EB-GII over time, we estimated the intraclass correlation coefficient (ρ_1) for the logarithm of the measurements, where σ_w^2 is the within-subject variance and σ_b^2 is the between-subject variance:

$$\rho_1 = \frac{\sigma_b^2}{\sigma_b^2 + \sigma_w^2}$$

It is estimated by

$$\widehat{\rho_1} = \frac{MS_b - MS_w}{MS_b + (k-1)MS_w},$$

Where MS_b = mean-square between subjects, MS_w = mean-square within subjects, and k = number of measurements per subject.

2.3 Results

2.3.1 High throughput 96-well plate method development and validation

Our previous nanoLC-ESI-MS/MS methodology [23] had a relatively low throughput (< 20 samples at a time) due to the use of traditional solid phase extraction as the first step in sample processing. Since the current study includes a large number of samples, we have developed a high throughput 96 well SPE (Strata™-X 33µm polymeric reversed phase, 30 mg/well, 96-well plates) methodology using True-taper 96-well, 2ml Polypropylene Square Tapered 100 µL Tear-Bottom plate. This new method is illustrated in Figure 2.1.

For initial method validation, 200 µL aliquots of water or synthetic urine (in triplicate) were spiked with 5 fmol of EB-GII and 5 fmol of $^{15}N_5$-EB-GII (isotopically labeled internal standard) either before or after performing SPE. These samples were then dried, HPLC purified, and analyzed by nanoLC-ESI-MS/MS on a Thermo LTQ Quantiva to determine the analyte recovery. SPE recovery was determined by comparing the observed and theoretical $^{15}N_5$-EB-GII:EB-GII peak area ratios. The analyte recovery from 96 well SPE plates was determined to be 83% in water and 75% in synthetic urine.

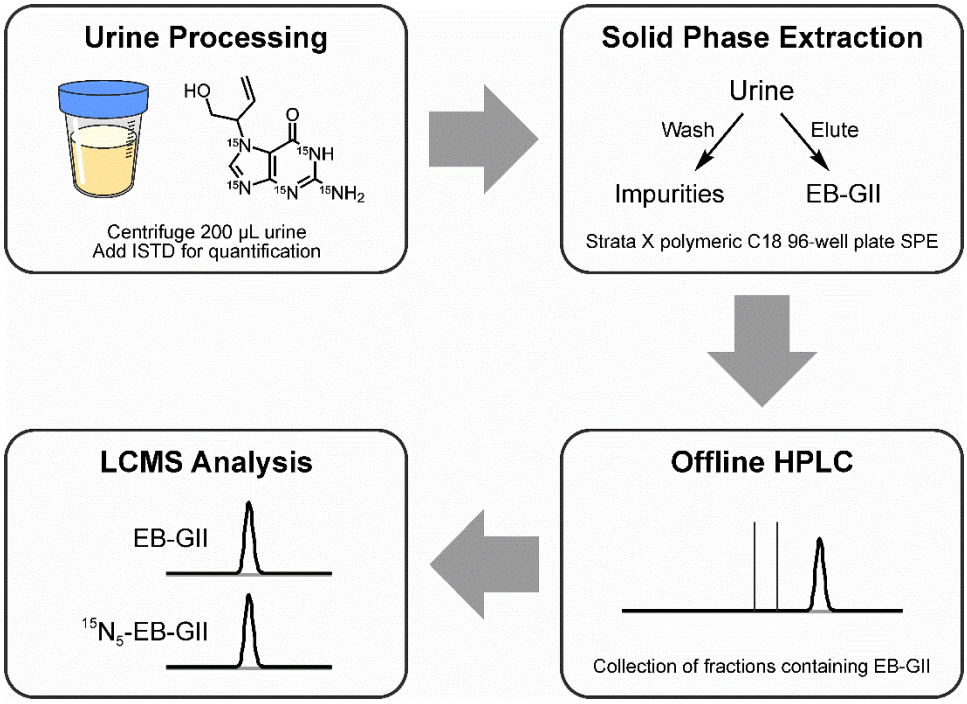

Figure 2.1. Sample preparation procedure for high-throughput nanoLC/ESI^{+}-HRMS^{3} analysis of EB-GII

Method standard curves were constructed by analyzing aqueous solutions containing $^{15}N_5$-EB-GII (5 fmol) and EB-GII (0.5-10.0 fmol) in triplicate. Method validation curves were constructed by analyzing synthetic urine spiked with $^{15}N_5$-EB-GII (5 fmol) and EB-GII (0.5-7.5 fmol) in triplicate, followed by the sample preparation steps described above. The observed EB-GII values were plotted against the actual values. Standard curves in water produced linear curves ($y = 0.859x$, $R^2 = 0.997$) (Figure 2.2). A linear correlation was also observed between the actual and observed EB-GII amounts in the synthetic urine matrix ($y = 0.8791x$, $R^2 = 0.9968$) (Figure 2.3). A representative nanoLC/ESI$^+$HRMS^3 chromatogram of EB-GII quantitation in a smoker sample is shown in Figure 2.4.

90%-110% accuracy was observed with internal QC samples analyzed in the cessation sample batch. The coefficient of variation among internal QC samples analyzed in the stability batch was 7.3%.

2.3.2 Determination of urinary EB-GII biomarker stability and intra-individual variation

To evaluate temporal biomarker stability, sensitive and specific isotope dilution nanoLC/ESI$^+$-HRMS^3 methodology was utilized to quantify EB-GII concentrations in urine of 19 smokers over time. Urine was sampled bimonthly over a period of a year for each smoker. The median, mean, SD, 95% confidence levels, and range of EB-GII levels at each time point in the study are shown in Table 2.1. Overall, urinary EB-GII concentrations ranged between 0.02 – 7.08 pg/mg creatinine among individuals and time points across the study. This illustrates the typical range of values for urinary EB-GII [23], as well as the inter-individual variation in urinary EB-GII levels.

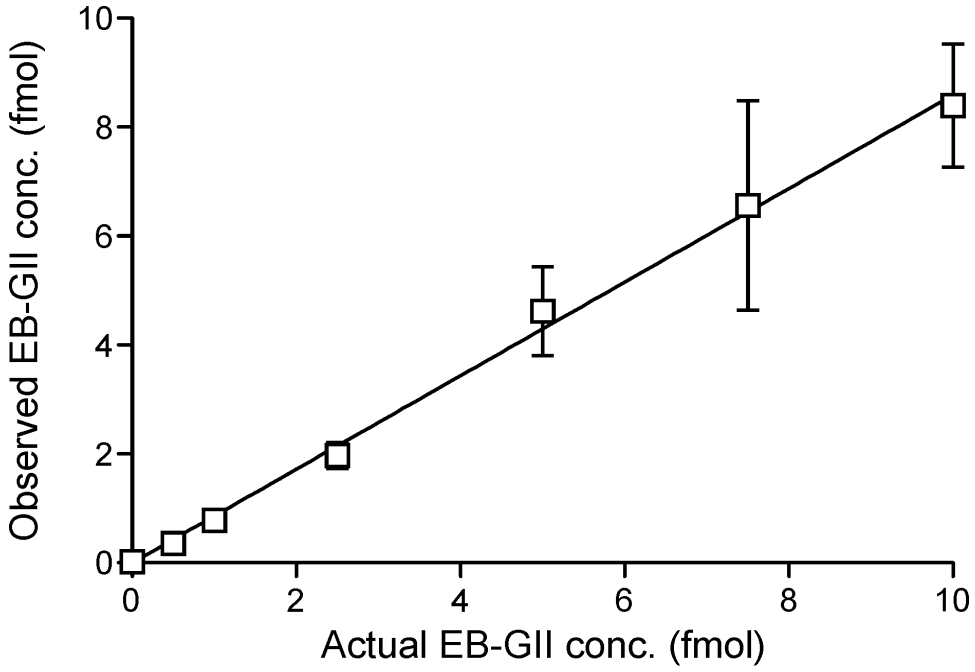

Figure 2.2. NanoLC/ESI$^+$-HRMS^3 method validation: correlation between the added and observed amounts of EB-GII spiked into 30 μL water.

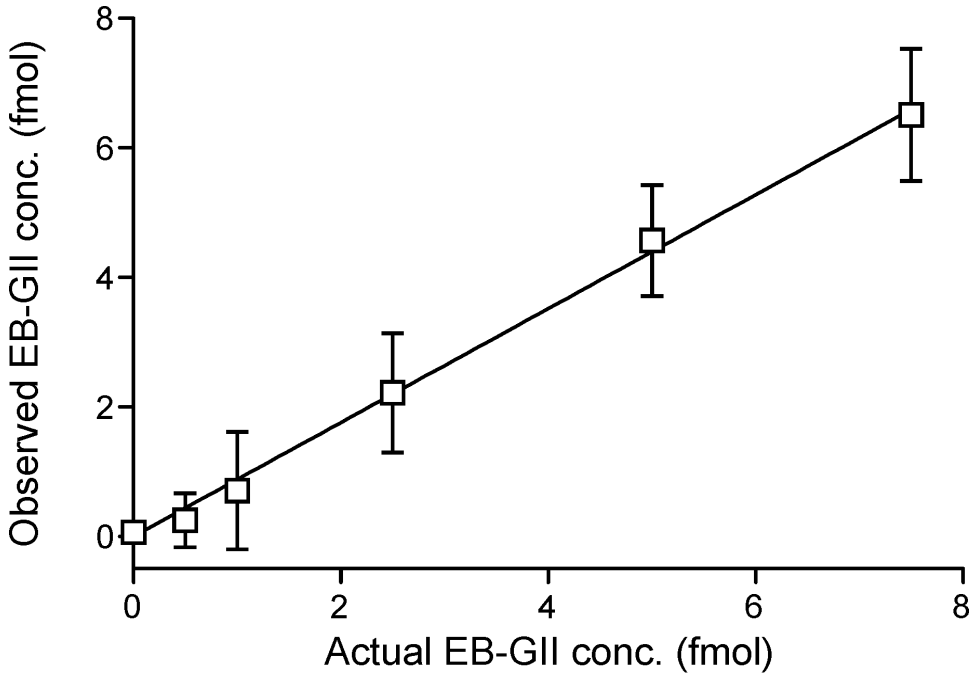

Figure 2.3. NanoLC/ESI^{+}-HRMS^{3} method validation: correlation between the added and observed amounts of EB-GII spiked into 200 μL synthetic urine.

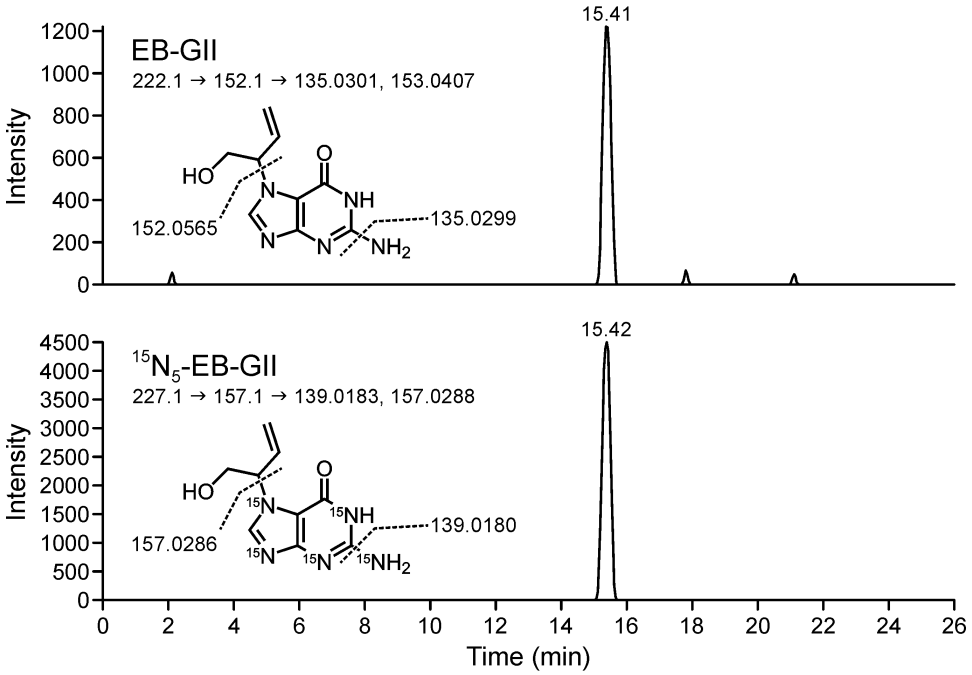

Figure 2.4. Representative nanoLC/ESI$^+$-HRMS^3 detection of EB-GII in urine of a smoker. Top and bottom panels show extracted ion chromatogram MS^3 spectra from EB-GII and $^{15}N_5$-EB-GII (internal standard), respectively.

Table 2.1. Urinary EB-GII levels (pg/mg creatinine) over the course of the study

Sampling Month	*N*	Median	Mean	SD	95% LCL	95% UCL	Minimum	Maximum
0	18	0.19	0.64	1.33	-0.02	1.3	0.03	5.67
2	19	0.21	0.81	1.73	-0.03	1.64	0.06	7.08
4	17	0.19	0.37	0.59	0.07	0.68	0.02	2.52
6	15	0.19	0.3	0.32	0.12	0.47	0.06	1.37
8	13	0.37	0.63	0.97	0.05	1.22	0.09	3.62
10	13	0.43	0.9	1.36	0.08	1.73	0.05	4.86
12	11	0.57	1.25	1.83	0.02	2.47	0.02	6.19

The results for intra-individual variation in urinary EB-GII levels are presented in Table 2.2. The coefficient of variation was calculated and averaged for each subject's urinary EB-GII levels to obtain the overall mean coefficient of variation. The mean coefficient of variation for EB-GII was 79% when normalized to urinary creatinine levels and 82% for urinary EB-GII described as fmol/mL urine. The intraclass correlation coefficient for urinary EB-GII as 68% when normalized to creatinine and 59% if expressed as fmol/mL urine.

2.3.3 Association of EB-GII with smoking status

To examine the association of urinary EB-GII adducts with smoking, they were quantified in urine samples from seventeen subjects participating in a smoking cessation study at the University of Minnesota [181]. These subjects had been smoking an average of 17.3 ± 12.3 years and smoked 21.8 ± 6.7 cigarettes per day. Urinary metabolites of butadiene were quantified in samples before smoking cessation and 3, 7, 28, and 56 days after smoking cessation using the nanoLC/ESI^+-$HRMS^3$ methodology described above. Abstinence from smoking was confirmed by total NNAL analyses[181].

Smoking cessation data are summarized in Figure 2.5. Baseline urinary EB-GII adduct load in smokers was 1.63 ± 0.64 pg/mL urine. Following smoking cessation, urinary EB-GII levels rapidly dropped to 1.073 ± 0.558 pg/mL at day 3 (p = 0.006). After the initial decline at 3 days, further decrease on days 7, 28, and 56 was not statistically significant.

Table 2.2. Average coefficient of variation (CV) within subjects and within- and between-subject variance and intraclass correlation coefficient for log-transformed urinary EB-GII

Urinary EB-GII in log scale	N	Average CV within subjects (CV x 100%)	Between subject variance	Within subject variance	Intraclass correlation coefficient
ln(fmol/mL)	19	82%	0.6834	0.4818	59%
ln(pg/mg creatinine)	19	79%	0.9482	0.4555	68%

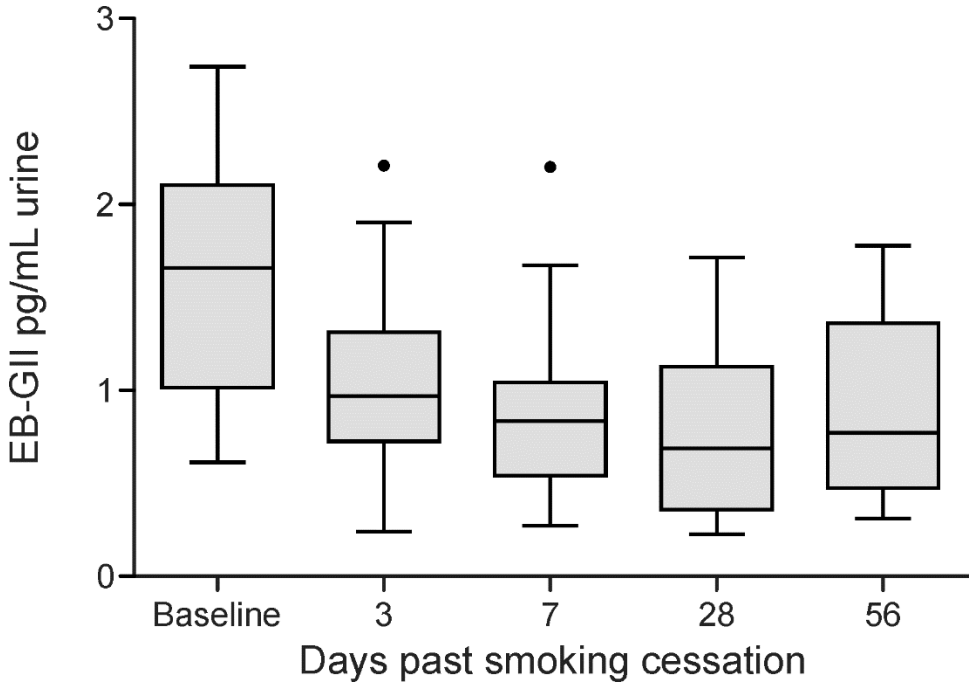

Figure 2.5. Urinary EB-GII levels (pg/mL urine) in subjects participating in a smoking cessation program. EB-GII levels decrease significantly from baseline to Day 3. Further decreases are not statistically significant.

2.4 Discussion

Smokers are exposed to a wide range of toxins and carcinogens in cigarette smoke. Exposure to tobacco smoke results in the increased risk of lung cancer development [134, 181, 267, 268]. Reliable measurements of carcinogen-DNA adducts in smokers are vital for the understanding of their exposure and cancer risk.

Toxicological risk assessments have identified BD as having a relatively high cancer risk index among all chemicals present in tobacco smoke [259]. This rating is a result of high abundance of BD in cigarette smoke, its ability to induce malignant lung tumors in laboratory mice at concentrations as low as 6.25 ppm, and increased cancer incidence in occupationally exposed workers [125-127, 240, 270].

We have previously quantified mercapturic acid metabolites of BD in urine of current smokers belonging to four different ethnic groups from the Multiethnic Cohort [163, 183]. These studies had revealed that White smokers excreted the highest amounts of MHBMA, followed by African American, Native Hawaiian, and Japanese smokers [163, 183]. These results are consistent with low susceptibility of Japanese individuals to smoking-induced lung cancer, but cannot explain high lung cancer incidence in African Americans and Native Hawaiians [163, 183, 264, 265].

Unlike urinary mercapturic acids, which represent metabolically inactivated butadiene, nucleobase adducts such as N7-(2-hydroxy-3,4-epoxybut-1-yl)guanine (EB-GII) can be used as true biomarkers of risk associated with exposure to BD as they reflect the amount of carcinogen bound to cellular DNA. N7-(2-hydroxy-3,4-epoxybut-1-yl)guanine (EB-GII) adducts are formed when 3,4-epoxy-1-butene (EB) alkylates the N7 position of guanine in DNA. EB-GII adducts undergo spontaneous hydrolysis (depurination) under physiological conditions, followed by their excretion in urine as free base adducts. We have developed ultra-sensitive analytical methodologies

for quantitation of butadiene-DNA adducts in human urine and have shown that White smokers excrete 3-fold higher levels of EB-GII than African Americans [23].

The main focus of the present study was to validate EB-GII as a non-invasive biomarker of exposure to BD and to examine its association with smoking. In order to achieve this goal, our previous mass spectrometry method for urinary EB-GII [23] was updated to include high-throughput sample processing utilizing 96-well plate solid phase extraction. EB-GII adducts were quantified in urine of 19 smokers over a period of a year. The intraclass correlation coefficient quantifies the amount of total variability that is caused by variability within subjects; the smaller the variance of measurements within subjects relative to between subjects will have an intraclass correlation coefficient closer to 100% [268]. We found that the intraclass correlation coefficient for EB-GII was greater than 50%, indicating that EB-GII adducts are less variable within an individual than between individuals. These results for the first time validate the use of single point measurements of urinary EB-GII as representative of an individual's overall EB-GII adduct load. We also found that while EB-GII is stable when described as fmol/mL urine (intraclass correlation coefficient = 59%), the variability in urinary EB-GII further decreases upon normalization to creatinine values (intraclass correlation coefficient = 68%).

To establish their association with smoking status, urinary EB-GII adducts were quantified in 17 smokers participating in a smoking cessation study. A significant reduction in EB-GII levels was observed three days after smoking cessation (Figure 2.5). These results indicate that smoking is a significant source of exposure to 1,3-butadiene and a significant factor in EB-GII DNA adduct formation. However, they also reveal the presence of endogenous, environmental, or dietary sources of EB-GII in humans. Our ongoing studies will evaluate the contributions of these other sources to BD-DNA adduct formation by exploring potential dietary/endogenous sources of THBG

and EB-GII adducts following the incorporation of stable isotope labeled butadiene-d_6 in animals and the incorporation of ^{13}C-labeled cellular metabolites into human cells. These experiments will elucidate the quantity of endogenous (unlabeled) and exogenous (labeled) BD-DNA adducts and identify their metabolic/dietary sources.

In summary, our results described here show that urinary EB-GII adducts are associated with smoking and are stable in human subjects over time, validating their use as a biomarker of cigarette smoke induced DNA damage. Urinary EB-GII levels can be reliably measured from point urine samples and are associated with smoking status. Therefore, studies measuring EB-GII levels from point urine samples can provide reliable estimates of the associations between urinary EB-GII with lung cancer risk. Future studies are required to investigate the associations between EB-GII adduct levels and lung cancer development.

3. Ethnic differences in excretion of butadiene-DNA adducts by current smokers

Reprinted with permission from:

Caitlin C. Jokipii Krueger, S. Lani Park, Guru Madugundu, Yesha Patel, Loic Le Marchand, Daniel Stram, Natalia Tretyakova. Carcinogenesis 2021, 42(5), 694-704.

Samples were provided by Dr. S. Lani Park and Dr. Loic Le Marchand. Statistical analyses were conducted by Yesha Patel under the guidance of Dr. Daniel Stram. Dr. Guru Madugundu and Caitlin C. Jokipii Krueger analyzed adduct levels in urine samples.

3.1 Introduction

Butadiene (1,3-butadiene, BD) is classified as a known carcinogen in humans [283] and is among the most potent and abundant carcinogens in tobacco smoke. There are 20-75 µg of BD per cigarette in mainstream smoke and 205-361 µg per cigarette in side stream smoke [259, 269]. In addition to tobacco smoke, BD is found in urban air, automobile emissions, smoke from wood burning, and in the synthetic polymer industries [124, 135, 136, 138]. BD is a known carcinogen in laboratory animals, inducing neoplasms of the lung in mice at exposures as low as 6.25 ppm [270]. Occupational exposure to BD has been associated with leukemia and possibly lung cancer [131, 132]. In the U.S., risk of many smoking-related cancers differs by racial/ethnic group [284]. Studies in the Multiethnic Cohort (MEC) have shown that, when accounting for risk factors including smoking, Native Hawaiians have a higher risk of lung cancer than whites and Japanese Americans [285]. It is possible that these disparities, at least in part, are attributed to population differences in the metabolic activation and detoxification of tobacco smoke carcinogens such as BD, which leads to higher load of mutagenic DNA adducts in susceptible populations.

BD is metabolized to DNA-reactive epoxides 3,4-epoxy-1-butene (EB), 1,2,3,4-diepoxybutane (DEB), and 1,2-dihydroxy-3,4-epoxybutane (EBD) by cytochrome P450 monooxygenases (Figure 1.7) [149, 245, 271]. BD epoxides are detoxified by glutathione S transferases (particularly glutathione S-transferase theta 1, GSTT1) to form monohydroxybutenyl mercapturic acid (MHBMA) and dihydroxybutyl mercapturic acid (DHMBA) from EB, trihydroxylbutyl mercapturic acid (THBMA) from EBD, and *bis*-butanediol mercapturic acid (*bis*-BDMA) from DEB, which are excreted in urine (Figure 1.8) [164, 167, 168, 272].

BD-mercapturic acids have previously been investigated as potential urinary biomarkers of tobacco smoke exposure to BD [162-164, 167, 168, 170, 173, 179-181, 206, 272-276]. Urinary MHBMA levels

decreased 80-90% upon smoking cessation, confirming its association with smoking status [167, 181]. In contrast, DHBMA levels were unchanged upon smoking cessation, suggesting that it was not associated with smoking status [167, 181]. We previously reported that, after controlling for internal smoking dose as measured by nicotine equivalents (NE, the sum of total urinary nicotine (free + nicotine N-glucuronide), cotinine (free + nicotine N-glucuronide), and trans-3′-hydroxycotinine (3-HC + its glucuronide)), MHBMA levels in Japanese American smokers were significantly lower than in Native Hawaiians and whites [183]. These differences are consistent with the direction of lower smoking-related lung cancer risk and are primarily a result of the higher frequency of *GSTT1* gene deletion in Japanese Americans [183].

The epoxide metabolites of BD, if not detoxified, can react with nucleophilic DNA bases to form covalent BD-DNA adducts. Specifically, EB alkylates the N7 position of guanine in DNA to form N7-(1-hydroxy-3-buten-2-yl)guanine (EB-GII) adducts (Figure 1.10) [195, 214]. Unlike BD-mercapturic acids, which represent the metabolically inactivated dose of butadiene [183], BD-DNA adducts can be considered as mechanism-based biomarkers of exposure. They can serve as useful indicators of the biologically relevant dose of carcinogens as they represent the dose of carcinogen which is available for binding to DNA [157, 277]. BD-DNA adducts are thought to be responsible for the carcinogenicity of BD, as they can lead to DNA polymerase errors during replication [278, 279]. In addition, N7-guanine lesions are hydrolytically labile and are excreted in urine as free nucleobases, making them potential biomarkers of risk associated with BD exposure [13, 23, 214, 280]. Workers occupationally exposed to BD (0.1-2.2 ppm of BD) excrete significantly higher concentrations of urinary EB-GII (1.25 ± 0.51 pg/mg creatinine) as compared to administrative controls (<0.01 ppm BD, 0.22 ± 0.08 pg/mg creatinine) [23].

In Chapter 2 of this Thesis, we described a high throughput, accurate quantitative nanoLC/ESI$^+$-HRMS^3 method for urinary EB-GII adducts in humans and validated their use as a biomarker of smoking-related exposure to BD. We showed that urinary EB-GII adducts are stable over time in human subjects [286]. Additionally, we quantified urinary EB-GII in 17 individuals participating in a smoking cessation program [286]. We found that EB-GII levels decrease by 34% from baseline (1.63 ± 0.64 pg/mL urine) to 1.07 ± 0.56 pg/m by day 3 following smoking cessation [286]. Low levels of EB-GII adducts were observed in unexposed animals and in non-smokers, indicating the presence of endogenous sources of EB-GII [23]. In the present study, urinary EB-GII adducts were quantified in Native Hawaiian, Japanese American, and white smokers and non-smokers (N = 205-210 per ethnic group) in an attempt to identify any ethnic differences in excretion of a mechanism-based biomarker of 1,3-butadiene-induced DNA damage.

3.2 Materials and Methods

Study population

Our study population included current cigarette smokers and nonsmokers at the time of urine collections from three racial/ethnic groups. The study details for the smokers and non-smokers [183, 287, 288] have been previously reported. In brief, all participants were from the state of Hawaii. For the smokers, the participants were selected at random from the Hawaii component of the Multiethnic Cohort study (MEC) or from the control groups of population-based case-control studies conducted in Hawaii [183, 287, 288]. The non-smokers were selected at random from the Hawaii component of the Multiethnic Cohort study (MEC). Approximately 100 subjects in each racial/ethnic and smoking status group were selected. A total of 623 samples were analyzed for urinary EB-GII DNA adducts (207 Native Hawaiians, 205 Japanese Americans, and 211 whites).

Materials

LC-MS grade water, methanol and acetonitrile were purchased from Fisher Scientific (Pittsburgh, PA). Strata X polymeric reversed phase SPE cartridges (30 mg/1 mL) were purchased from Phenomenex (Torrance, CA). EB-GII and $^{15}N_5$-EB-GII standards were prepared as previously reported [211, 281]. 96 well plates were purchased from Analytical Sales and Services Inc. (Ledgewood, New Jersey). All other chemicals and solvents were obtained from Sigma-Aldrich (Milwaukee, WI; St. Louis, MO) unless otherwise specified.

Nicotine equivalents

Nicotine equivalents (NE) were measured in the previous analysis of these subjects [288]. In that study, total urinary nicotine (free + nicotine N-glucuronide), cotinine (free + nicotine N-glucuronide) and trans-3′-hydroxycotinine (3-HC + its glucuronide), were measured by gas chromatography/mass spectrometry [289, 290]. The sum of these metabolites (nicotine equivalents, NE) was used as a measure of total nicotine uptake as it accounts for over 80% of nicotine and its metabolites [291]. The phenotypic measure of cytochrome P450 2A6 (CYP2A6) activity (the primary enzyme in nicotine metabolism) was quantified as total trans-3′-hydroxycotinine (nmol/mL)/total cotinine (nmol/mL) [292].

Urine sample processing and EB-GII adduct enrichment

Urinary EB-GII concentrations were determined using the high-throughput nanoLC/ESI$^+$-HRMS^3 method previously developed in the Tretyakova laboratory[23, 286]. In brief, urine samples (200 μL) were centrifuged at 10,000g for 15 min to remove any particulate matter. The supernatants were spiked with $^{15}N_5$-EB-GII (5 fmol, internal standard for mass spectrometry) and subjected to solid phase extraction (SPE) on Strata X cartridges (30 mg/1 mL; Phenomenex, Torrance, CA). SPE 96-well plates were conditioned with 2 mL of methanol, followed by 2 mL of Milli-Q water.

Urine samples were loaded onto prepared 96-well plates, and each well was washed with 1 mL of water, followed by 1 mL of 10% methanol in water. EB-GII and its internal standard were eluted with 60% methanol in water, dried under vacuum, and reconstituted with 102 μL of 0.4% formic acid in water containing 2′-deoxythymidine (dT) as an HPLC retention time marker (2.1 nmol).

Offline HPLC purification of SPE-enriched EB-GII and its internal standard was achieved on an Agilent 1100 series HPLC system equipped with a UV detector and an automated fraction collector (Agilent Technologies, Santa Clara, CA). A Zorbax Eclipse XDB-C18 column (4.6 × 150 mm, 5 μm; Agilent Technologies, Santa Clara, CA) was eluted at a flow rate of 1 mL/min with a gradient of 0.4% formic acid in Milli-Q water (A) and HPLC-grade acetonitrile (B). Solvent composition was maintained at 0% B for 5 min and then linearly increased to 3% B in 15 min and further to 40% B in 5 min. The solvent composition was returned to 0% acetonitrile in 5 min and held at 0% for 15 min for column equilibration. UV absorbance was monitored at 254 nm. dT was used as a retention time marker. Under these conditions, dT eluted at ∼17.4 min, and the retention time of EB-GII was ∼15.6 min. HPLC fractions containing EB-GII and its internal standard (14.1−16.1 min) were collected into 2 mL 96-well plates (Analytical Sales and Services Inc., Ledgewood, New Jersey), concentrated under vacuum, and reconstituted in LC/MS grade water containing 0.01% acetic acid (30 μL) for nanoHPLC/nanoESI$^+$-HRMS^3 analysis. The injection volume was 5 μL.

NanoLC/ESI$^+$-HRMS^3 analysis of urinary EB-GII

All nanoLC/ ESI$^+$-HRMS^3 analyses were conducted on an LTQ Orbitrap Velos instrument equipped with a nanospray source (Thermo Fisher Scientific Corp., Waltham, MA) interfaced with a Dionex UltiMate 3000 RSLCnano HPLC system (Thermo Fisher Scientific Corp., Waltham, MA) using previously described methodology [23, 286]. Gradient elution was achieved using LC/MS-grade

water containing 0.01% acetic acid (A) and LC/MS-grade acetonitrile containing 0.02% acetic acid (B). Samples were loaded onto a nanoLC column (0.075 × 200 mm) manually packed with Synergi Hydro-RP 80 Å (4 μm) chromatographic packing (Phenomenex, Torrance, CA). Initial HPLC flow rate was maintained at 1 μL/min at 2% B for 5 min to enable sample loading onto the nano column, followed by a flow rate decrease to 300 nL/min at 2% B for 1 min. The percentage of solvent B was linearly increased to 25% B in 9 min and further to 50% B in 10 min at a flow rate of 300 nL/min. The HPLC flow rate was increased to 1 μL/min, and solvent composition was returned to 2% B in 1 min, followed by 5 min column equilibration. Under these conditions, EB-GII eluted as a sharp peak at 13 min.

Tandem mass spectrometry analysis was performed by fragmenting the $[M + H]^+$ ions of EB-GII (*m/z* 222.1) via collision-induced dissociation (CID) in the linear ion trap portion of the instrument using the collision energy (CE) at 25 and an isolation width (IW) of 1.0 amu. MS/MS fragment ions at *m/z* 152.1 $[Gua + H]^+$ were subjected to further fragmentation in the high collision dissociation (HCD) cell of the instrument using nitrogen as a collision gas (CE = 75 units, IW = 1.0 amu). The resulting MS^3 fragment ions at *m/z* 135.0301 ($[Gua - NH_3]^+$) and *m/z* 153.0411 ($[Gua - NH_3 + H_2O]^+$) were detected in the mass range of *m/z* 50−270 using the Orbitrap mass analyzer (HRMS) at a resolution of 25,000. The $^{15}N_5$ labeled internal standard ($[^{15}N_5]$-EB-GII) was detected using an analogous MS^3 scan event consisting of fragmentation of *m/z* 227.1 ($[M + H]^+$) to *m/z* 157.1 ($[^{15}N_5$-Gua + H$]^+$) and further to *m/z* 139.0183 ($[^{15}N_5$-Gua - $NH_3]^+$) and *m/z* 157.0283 ($[^{15}N_5$-Gua - $NH_3 + H_2O]^+$). Extracted ion chromatograms corresponding to the sum of *m/z* 135.0301 ($[Gua - NH_3]^+$) and *m/z* 153.0411 ($[Gua - NH_3 + H_2O]^+$) were used for quantitation of EB-GII, whereas *m/z* 139.0183 ($[^{15}N_5$-Gua $- NH_3]^+$) and *m/z* 157.0283 ($[^{15}N_5$-Gua $- NH_3 + H_2O]^+$) were used for quantitation of $[^{15}N_5]$-EB-GII. Mass accuracy was 5 ppm. A full scan event was also performed

over the mass range of *m/z* 100−500 at a resolution of 15,000 to monitor for any co-eluting matrix components. EB-GII amounts were determined by comparing the areas of the nanoLC/ESI^+-$HRMS^3$ peaks corresponding to the analyte and its internal standard using standard curves generated by analyzing known analyte amounts. Method LOD and LOQ values were determined from the analysis of spiked non-smoker urine samples to be 0.25 fmol/mL and 0.5 fmol/mL urine, respectively. Intra- and interday precision was 13.1 and 10.6%, respectively. Method accuracy was between 83.9-115.4% for quantification of EB-GII through the dynamic range of the assay (0.1-10 fmol) [23, 286].

Genotyping

Genotyping methods for *GSTT1* gene deletion was achieved using the TaqMan copy number assay as previously reported [183]. In brief, DNA was extracted from blood leukocytes using a QiaAmp DNA Blood extraction kit (Qiagen, Germantown MD). The samples were genotyped using a predesigned TaqMan GSTT1 copy number assay (Hs00010004_cn) and run on the 7900HT Fast Real-Time System (Life Technologies, Foster City, CA). Copy number counts were calculated using Life Technologies CopyCaller v2.0 software. Approximately 5% of blind duplicates were included for quality control. Test for Hardy Weinberg Equilibrium was met for all three populations ($p > >0.05$).

Statistical methods

EB-GII adduct levels were expressed as fmol/mL urine. Spearman's partial correlation coefficients, adjusting for age, sex and race/ethnicity (for overall), were computed to examine the correlation between EB adducts, NE, monohydroxybutyl mercapturic acid (MHBMA), dihydroxybutyl mercapturic acid (DHBMA), and BD metabolite ratio MHBMA/[MHBMA+DHBMA], which were previously measured using an HPLC-ESI^--MS/MS

method developed in the Tretyakova laboratory [183]. Multivariable linear models regressed the urinary levels of EB-GII adducts on the following predictors: age at time of urine collection (continuous), race/ethnicity (when results were not stratified by race/ethnicity), smoking status (when results were not stratified by smoking status), BMI, batch and NE (natural log). To better meet model assumptions, all metabolite concentrations were transformed by taking the natural log. If large numbers of EB-GII values were at a detection limit (0.125 fmol/mL) in a given analysis, so that approximate lognormality was not achieved by transformation, we performed two supplementary analyses. The first was a logistic regression of a yes/no variable indicating whether the recorded EB-GII values were above or below the detection limit and the second a (log) linear regression model restricted to those with detectable levels. Both analyses used the same set of predictor variables as above. Consistency between these three analyses was assessed by checking that regression parameter estimates were in the same direction and whether they were statistically significant ($p < 0.05$).

To examine ethnic/racial differences of EB-GII adducts in smokers, covariate-adjusted geometric means were computed for each ethnic/racial group at the mean covariate vector using the LS means procedure in SAS. We also examined whether the geometric means of BD adducts differed according to nicotine metabolism or *GSTT1* gene deletion. Here, nicotine metabolism was quantified by the urinary CYP2A6 enzymatic activity ratio (measured by total trans-3′-hydroxycotinine (nmol/mL)/total cotinine (nmol/mL)). This biomarker was stratified by tertile based on the overall population. *GSTT1* gene deletion was modeled by the number of gene copies (2, 1, or 0), where 0 was the equivalent to no copies of the gene (i.e. gene deletion resulting in no enzymatic activity).

3.3 Results

3.3.1 Study population

Baseline demographic characteristics of the study population are presented in Table 3.1. Among 623 participants, 292 were non-smokers and 331 were current smokers at time of urine collection. The three racial/ethnic groups included were Native Hawaiian, white, and Japanese American. Racial/ethnic groups were approximately evenly distributed across each smoking status group. For smokers, additional measures including smoking frequency and measures of BD metabolites are also included.

Native Hawaiian smokers (n=110) were the heaviest (median BMI=28.04 ± 5.87 kg/m^2), followed by whites and Japanese Americans (26.92 ± 5.78 kg/m^2 and 24.81 ± 4.14 kg/m^2, respectively). Native Hawaiians and Japanese Americans reported smoking fewer cigarettes per day (mean cigarettes per day [CPD]=19.36 ± 9.26 and 20.02 ± 7.06, respectively) than whites (CPD=25.8 ± 11.41). Japanese Americans had the lowest CYP2A6 activity enzymatic ratio (0.86 ± 1.8) as compared to Native Hawaiians and whites (1.02 ± 0.84 and 1.32 ± 1.30, respectively). As previously reported for a larger group of smokers, half of whom were included in this current study [183], urinary MHBMA levels were higher in whites and Native Hawaiians (6.7 [95%CI: 5.8-7.8] ng/mg Cr and 5.3 [95%CI: 4.6-6.2] ng/mg Cr, respectively), as compared to Japanese Americans (4.4 [95%CI: 3.8-5.1] ng/mg Cr) (Table 3.1) after adjusting for age, sex, BMI, and nicotine equivalents (NE). DHBMA levels did not differ between the three ethnic groups (p>0.15). The Pearson's partial correlation (in smokers) between NE and MHBMA was statistically significant (r = 0.532, p <0.001).

Table 3.1. Demographic characteristics of study participants

	Japanese Americans	**Native Hawaiians**	**Whites**
N	205	207	211
Age, mean (SD)	63.30 (7.26)	60.32 (9.85)	62.74 (7.36)
Gender			
Males (%)	106 (51.71)	94 (45.41)	100 (47.39)
Females (%)	99 (48.29)	113 (54.59)	111 (52.61)
Smoking Status			
Smokers (%)	108 (52.68)	110 (53.14)	113 (53.55)
Non-Smokers (%)	97 (47.32)	97 (46.86)	98 (46.45)
EB-GII DNA Adducts (fmol/mL), mean (SD)	1.61 (3.20)	0.98 (1.50)	1.17 (2.19)
BMI, mean (SD) (kg/m^2)	24.81 (4.14)	28.04 (5.87)	26.92 (5.78)
NE, mean (SD) (nmol/mL), *Smokers only*	30.65 (22.02)	47.91 (34.18)	54.97 (49.24)
CPD, mean (SD), *Smokers only*	20.02 (7.06)	19.36 (9.26)	25.80 (11.41)
CYP2A6 Activity, mean (SD), *Smokers only*	0.86 (1.80)	1.02 (0.84)	1.32 (1.30)
MHBMA, mean (SD) (ng/mL), *Smokers only*[a]	3.45 (3.12)	7.22 (7.56)	7.13 (8.68)
DHBMA, mean (SD) (ng/mL), *Smokers only*[a]	342.68 (268.84)	448.49 (405.41)	437.25 (455.13)
Metabolic Ratio: MHBMA /[MHBMA + DHBMA][a]	0.012 (0.010)	0.017 (0.012)	0.018 (0.015)

[a.] Urinary MHBMA and DHBMA data was reported in our previous study [183]).

3.3.2 Urinary excretion of EB-GII adducts of 1,3-butadiene

To compare BD-DNA adduct load among the three ethnic groups, EB-GII levels were quantified in urine of Native Hawaiian, white, and Japanese American smokers and non-smokers. We found that when adjusting for sex, age, BMI, batch, and race/ethnicity, smokers excreted significantly higher levels of EB-GII adducts (0.98 [95%CI: 0.84-1.12] fmol/mL) than non-smokers (0.19 [95%CI: 0.15-0.22] fmol/mL) ($p = 5.8 \times 10^{-34}$) (Table 3.2). This is consistent with our earlier study revealing a strong association of urinary EB-GII with smoking and a decline in urinary adduct levels upon smoking cessation [286].

Among smokers, the highest concentration of urinary EB-GII adducts was found in Japanese Americans (1.35 [95%CI: 1.04-1.72] fmol/mL), with significantly lower levels in Native Hawaiians (0.68 [95%CI: 0.52-0.86] fmol/mL) and whites (0.73 [95%CI: 0.56-0.91] fmol/mL), after adjusting for sex, age, BMI, batch, and nicotine equivalents (Table 3.2). Urinary EB-GII adduct concentrations were significantly higher in Japanese American smokers than in white smokers ($p = 4.8 \times 10^{-5}$), while the amounts of urinary EB-GII in Native Hawaiian smokers were not significantly different from white smokers ($p = 0.938$). This pattern was not observed in non-smokers, instead, urinary EB-GII adduct levels were fairly consistent across the racial/ethnic groups (ranging from 0.19-0.21 fmol/mL). These results reveal ethic differences in EB-GII adducts in current smokers, but not in non-smokers.

Table 3.2. Geometric means (95% confidence limits) for EB-GII (fmol/mL) by race/ethnicity and smoking status

	N	Geometric Mean (95% CI)	Beta[d]	P-value	*N*[g]	Geometric Mean (95% CI)[g]	Beta[d,g]	P-value[g]
Non-smokers[a]								
Overall	290	0.19 (0.15 – 0.22) [e]			122	0.37 (0.28 – 0.46) [h]		
Native Hawaiians	97	0.21 (0.17 – 0.24)	0.098	0.355	42	0.44 (0.34 – 0.56)	0.047	0.789
Japanese Americans	96	0.21 (0.17 – 0.23)	0.084	0.435	45	0.35 (0.26 – 0.43)	-0.203	0.271
Whites	97	0.19 (0.16 – 0.22)	*Reference*		35	0.42 (0.32 – 0.54)	*Reference*	
Smokers[b]								
Overall	331	0.98 (0.84 – 1.12)[e]			266	1.66 (1.39 – 1.95)[h]		
Native Hawaiians	110	0.68 (0.52 – 0.86)	-0.071	0.664	79	1.39 (1.08 – 1.78)	0.066	0.664
Japanese Americans	108	1.35 (1.04 – 1.72)	0.618	**7.8×10^{-4}**	95	2.10 (1.65 – 2.65)	0.477	**0.0034**
Whites	113	0.73 (0.56 – 0.91)	*Reference*		92	1.31 (1.02 – 1.65)	*Reference*	
Smokers[c]								
Overall	331	0.90 (0.76 – 1.03) [f]			266	1.60 (1.34 – 1.89) [i]		
Native Hawaiians	110	0.67 (0.51 – 0.84)	-0.013	0.938	79	1.39 (1.07 – 1.76)	0.108	0.481
Japanese Americans	108	1.45 (1.12 – 1.87)	0.766	**4.8×10^{-5}**	95	2.22 (1.74 – 2.80)	0.578	**6.8×10^{-4}**
Whites	113	0.68 (0.52 – 0.85)	*Reference*		92	1.24 (0.97 – 1.57)	*Reference*	

[a.] The non-smoker analyses have been adjusted for sex, age, BMI, and batch

[b.] The smoker analyses have been adjusted for sex, age, BMI, and batch

[c.] The smoker analyses have been adjusted for sex, age, BMI, batch, and NE

[d.] Estimated difference in geometric means compared to whites.

[e.] P-value comparing smokers to non-smokers overall = 5.8×10^{-34}

[f.] For this analysis, it was assumed the non-smokers had NE = 0 nmol/mL. P-value comparing smokers to non-smokers overall = 1.9×10^{-22}

[g.] These analyses have been filtered to samples with EG-GII levels >0.125 fmol/mL (which is the limit of detection)

[h.] P-value comparing smokers to non-smokers overall = 5.12×10^{-18}

[i.] For this analysis, it was assumed the non-smokers had NE = 0 nmol/mL. P-value comparing smokers to non-smokers overall = 6.0×10^{-14}

3.3.3 Variation in urinary EB-GII by GSTT1 gene deletion or CYP2A6 enzymatic activity ratio

We next investigated whether population's variation of urinary EB-GII levels can be explained by metabolic enzymes involved in BD biotransformation. As GSTT1-catalyzed glutathione conjugation is the major metabolic detoxification pathway for butadiene epoxides including EB [164, 167, 272], we first investigated the relationship for *GSTT1* gene deletion status with urinary EB-GII adduct levels overall and by racial/ethnic groups. The geometric means of urinary EB-GII adduct levels did not differ by *GSTT1* genotype (p =0.2689, Table 3.3). This is different from our previous results for MHBMA, which was strongly correlated with GSTT1 copy number [183].

As CYP2A6 monooxygenase along with CYP2E1 is involved in epoxidation of butadiene to form 3,4-epoxy-1-butene (EB) [149, 245, 271], we additionally investigated the association of CYP2A6 enzymatic activity ratio with urinary EB-GII adduct levels overall and within each race/ethnicity. EB-GII adduct levels were not affected by CYP2A6 activity, although there was a suggestive positive increase of EB-GII adduct levels among Japanese Americans with higher CYP2A6 enzymatic activity (Table 3.4). This could be explained by CYP2E1 compensating for any deficiency of CYP2A6 activity.

Table 3.3. Geometric means (95% confidence limits) for EB-GII (fmol/mL) stratified by *GSTT1* CNV and race/ethnicity among smokers

***GSTT1* gene deletion genotype**[a]	***N***	**Geometric Mean (95% CI)**	**P-value**
All[b]	323		
1/1	70	0.92 (0.68 – 1.22)	
1/0	157	0.80 (0.65 – 0.96)	0.2689
0/0	96	1.02 (0.79 – 1.30)	
Whites[c]	109		
1/1	32	0.81 (0.52 – 1.22)	
1/0	46	0.67 (0.45 – 0.97)	0.2385
0/0	31	1.09 (0.68 – 1.70)	
Native Hawaiians[c]	109		
1/1	27	0.96 (0.59 – 1.54)	
1/0	59	0.66 (0.47 – 0.88)	0.1537
0/0	23	1.06 (0.63 – 1.77)	
Japanese Americans[c]	105		
1/1	11	1.28 (0.55 – 2.90)	
1/0	52	1.42 (0.93 – 2.15)	0.9537
0/0	42	1.33 (0.84 – 2.07)	

[a.] The GSTT1 genotypes are coded as: 1/1 = 2 copies of gene; 1/0 = 1 copy of the gene; 0/0 = gene deletion

[b.] The overall analyses have been adjusted for sex, age, BMI, NE, batch and race

[c.] The race/ethnic specific analyses have been adjusted for sex, age, BMI, NE and batch

Table 3.4. Geometric means (95% confidence limits) for EB-GII (fmol/mL) stratified by tertiles of CYP2A6 activity and race/ethnicity among smokers

Values of *CYP2A6* by tertiles[e]	*N*	Geometric Mean (95% CI)[a,b]	Beta[a,b]	P-value[a,b]	P-trend[a,b,c]	Geometric Mean (95% CI)[d]	Beta[d]	P-value[d]	P-trend[d]
All[a]	331								
Tertile 1	110	0.71 (0.55 – 0.90)	*Reference*			0.75 (0.57 – 0.95)	*Reference*		
Tertile 2	111	1.00 (0.78 – 1.26)	0.340	**0.056**	0.081	1.00 (0.78 – 1.25)	0.290	0.101	0.245
Tertile 3	110	0.99 (0.76 – 1.25)	0.327	0.073		0.93 (0.72 – 1.18)	0.223	0.227	
Whites[b]	113								
Tertile 1	16	0.74 (0.37 – 1.42)	*Reference*			0.87 (0.44 – 1.67)	*Reference*		
Tertile 2	44	0.85 (0.56 – 1.25)	0.140	0.722	0.856	0.88 (0.58 – 1.28)	0.009	0.981	0.616
Tertile 3	53	0.82 (0.37 – 1.42)	0.108	0.776		0.75 (0.51 – 1.08)	-0.140	0.718	
Native Hawaiians[b]	110								
Tertile 1	36	0.58 (0.38 – 0.86)	*Reference*			0.61 (0.40 – 0.91)	*Reference*		
Tertile 2	39	0.71 (0.47 – 1.04)	0.201	0.481	0.281	0.70 (0.46 – 1.02)	0.135	0.640	0.465
Tertile 3	35	0.79 (0.51 – 1.18)	0.312	0.284		0.76 (0.49 – 1.14)	0.216	0.467	
Japanese Americans[b]	108								
Tertile 1	58	0.98 (0.69 – 1.37)	*Reference*			0.99 (0.70 – 1.38)	*Reference*		
Tertile 2	28	1.80 (1.10 – 2.90)	0.601	**0.048**	0.084	1.79 (1.09 – 2.89)	0.589	**0.054**	0.100
Tertile 3	22	1.56 (0.90 – 2.68)	0.464	0.156		1.54(0.89 – 2.65)	0.443	0.178	

[a.] The overall analyses have been adjusted for sex, age, BMI, batch, and race/ethnicity. Beta values corresponds to the difference in EB-GII adducts (fmol/mL) for the second and third tertiles compared to the first.

[b.] The race/ethnic specific analyses have been adjusted for sex, age, BMI, and batch

[c.] A p-value for trend was calculated to determine if the noted shift from tertiles 1 to 3 is statistically significant

[d.] In addition to the model adjustments from a & b above, these analyses have been further adjusted for NE for both the overall and race/ethnic specific results. Beta values corresponds to the difference in EB-GII adducts (fmol/mL) per change in tertile.

[e.] CYP2A6 tertile range are as follows: Tertile 1 (0.0412 - 0.495), N=110 | Tertile 2 (0.496 - 1.195), N=111 | Tertile 3 (1.200 - 18.148), N=110

3.3.4 Relationship between urinary EB-GII and 1,3 butadiene metabolites

To compare the results for EB-derived urinary metabolites and DNA adducts in smokers, we evaluated the relationship between urinary EB-GII adducts quantified in this study and BD-mercapturic acids (MHBMA and DHBMA) among the subjects with the available data previously reported by our group [183] (Table 3.5). After adjusting for age, sex, BMI, and batch, urinary MHBMA and DHBMA levels were significantly associated with EB-GII adduct concentrations. Specifically, for MHBMA, a 1 log-unit increase (approximately a 2.7-fold increase) was associated with a 0.20 log unit increase (approximately a 1.2-fold increase) of EB-GII adduct levels (p = $4.1x10^{-3}$). This association was statistically significant in Native Hawaiians (p = 0.03) and whites (p = 0.02), but not in Japanese Americans (p = 0.28). For DHBMA, a 1 log-unit increase (approximately a 2.7-fold increase) was associated with a 0.68 log-unit increase (approximately a 2.0-fold increase) of EB-GII adduct levels (p = $8.4x10^{-12}$), and this association was statistically significant in all three populations. When adjusting for internal smoking dose, measured by NE, the association was found no longer statistically significant for MHBMA (r = 0.07, p = 0.22), but remained for DHBMA, overall (p = $7.2x10^{-10}$). By race/ethnicity, this relationship was most significant in whites, followed by Native Hawaiians and Japanese Americans (p = $5.4x10^{-6}$, $3.6x10^{-4}$, and $7.2x10^{-3}$, respectively, Table 3.5). These results indicate that urinary levels of BD-mercapturic acids are not predictive of the extent of BD-DNA damage. We also examined the potential association between urinary adducts and NE. For all smokers as a whole, urinary EB-GII adducts were not correlated with NE (r=0.09, p = 0.10). By race/ethnicity, EB-GII adducts were found to be correlated with NE only in whites (r = 0.25, p = 0.009) and not the other racial/ethnic groups (p's > 0.14). This indicates that in addition to smoking amounts, the levels of urinary EB-

GII adducts could be affected by other biological factors such as DNA repair, adduct excretion, and further metabolism [69].

Table 3.5. Association between urinary BD adducts (EB-GII, fmol/mL) and BD metabolites (MHBMA and DHBMA), overall and by race/ethnicity among smokers

	Overall[a]			Native Hawaiians[b]			Japanese Americans[b]			Whites[b]			
	n	**Beta**	**P-value**	***n***	**Beta**	**P-value**	***n***	**Beta**	**P-value**	***n***	**Beta**	**P-value**	**P-het[d]**
MHBMA (ng/mL)	330	0.200	**4.12E-03**	110	0.265	**0.03**	108	0.124	0.284	113	0.311	**0.022**	0.199
DHBMA (ng/mL)	329	0.682	**8.44E-12**	110	0.659	**1.03E-04**	108	0.489	**9.28E-03**	112	0.853	**3.22E-07**	0.200
Metabolic Ratio: MHBMA /[MHBMA + DHBMA]	323	-0.154	**0.049**	109	-0.062	0.645	105	-0.086	0.494	109	-0.311	**0.060**	0.511
MHBMA (ng/mL)[c]	330	0.126	0.112	110	0.227	0.127	108	0.104	0.397	113	0.179	0.290	0.449
DHBMA (ng/mL)[c]	329	0.749	**7.18E-10**	110	0.731	**3.64E-04**	108	0.654	**7.20E-03**	112	0.956	**5.37E-06**	0.108
Metabolic Ratio: MHBMA /[MHBMA + DHBMA][c]	323	-0.175	**0.024**	109	-0.113	0.413	105	-0.082	0.515	109	-0.348	**0.031**	0.496

[a.] The overall analyses have been adjusted for age, sex, BMI, batch and race. Beta values corresponds to the difference in EB-GII adducts (fmol/mL) per 1-log unit increase in BD metabolites.

[b.] The race/ethnic specific analyses have been adjusted for age, sex, BMI, and batch. Beta values corresponds to the difference in EB-GII adducts (fmol/mL) per 1-log unit increase in BD metabolites.

[c.] In addition to the model adjustments from a & b above, these analyses have been further adjusted for NE for both the overall and race/ethnic specific results

[d.] P-value for heterogeneity across the ethnic groups is reported

3.4 Discussion

1,3-Butadiene is one of the most abundant carcinogens in tobacco smoke [259, 269] and has a relatively high cancer risk index as compared to other tobacco smoke carcinogens [259]. Our laboratory has developed quantitative mass spectrometry methods for butadiene metabolites [167, 168, 206] and DNA adducts in humans [22, 23, 86, 92] . These advanced methodologies have been previously used to investigate interindividual differences in butadiene metabolism [293, 294], to establish the correlation of these biomarkers with smoking [286] and ethnicity/genetic polymorphisms [163, 183]. We found that GSTT1 copy number influenced BD metabolism and toxicity in human HAPMAP cells and could explain some of the ethnic differences in excretion of BD-mercapturic acid MHBMA [163, 293, 294]. Furthermore, the chemopreventive agent present in cruciferous vegetables (phenylethylisothiocyanate, PEITC) influenced the levels of BD-mercapturic acids in a nested study of current smokers by inducing glutathione-S-transferases [295].

The present study was focused on quantifying urinary EB-GII, a butadiene-DNA adduct formed from butadiene monoepoxide (EB), in a multiethnic group of smokers and nonsmokers. Unlike BD metabolites MHBMA and DHBMA, which can be considered as biomarkers of exposure to butadiene [162-164, 167, 168, 170, 173, 179-181, 206, 272-276], urinary DNA adducts represent the biologically relevant dose of butadiene bound to genomic DNA and subsequently released through DNA repair and/or spontaneous hydrolysis (Figure 1.3) [280, 296]. Therefore, BD-DNA adducts are considered a better biomarker of BD-associated cancer risk than previously employed BD-mercapturic acids (which represent detoxified butadiene). EB-GII adducts have a half-life of 2.20 ± 0.12 days, due to their spontaneous depurination [13, 280]. We previously reported the detection of urinary EB-GII adducts in laboratory animals treated with BD by inhalation and in current and former smokers, showing their association with smoking [23, 286].

Our new results reported here confirm the association of BD-DNA damage with smoking: EB-GII adducts levels were significantly higher in urine of smokers than non-smokers (0.98 [95%CI: 0.84-1.12] fmol/mL vs 0.19 [95%CI: 0.15-0.22] fmol/mL, $p = 5.8x10^{-34}$, Table 3.2). This is consistent with previous reports that suggest that smoking is an important source of butadiene exposure and BD-DNA adduct formation [23, 163, 167, 181, 183, 286]. We have previously shown that urinary EB-GII adduct levels decrease upon smoking cessation and are significantly higher in smokers as compared to non-smokers [23, 286]. Butadiene metabolites MHBMA and THBMA have also been shown to decrease upon smoking cessation [167, 181].

The main goal of our study was to investigate racial/ethnic differences in butadiene metabolism and DNA adduct formation in Japanese American, Native Hawaiian, and white smokers and non-smokers residing in Hawaii. While similar studies have been carried out in large multiethnic samples for butadiene metabolites [163, 183], this is the first attempt to quantify butadiene-DNA adducts among these racial/ethnic groups and to evaluate the relationship of these adducts with butadiene metabolites across populations. Among smokers, Japanese Americans had the highest levels of urinary BD-DNA adducts (EB-GII), compared to white and Native Hawaiians (Table 3.2). In contrast, our earlier study of urinary BD metabolites (MHBMA and DHBMA) using the same population found that white smokers excreted the highest concentrations of BD-mercapturic acids MHBMA, while Japanese American smokers excreted the lowest amounts of MHBMA [183]. However, it should be noted that while BD-mercapturic acids are a measure of carcinogen exposure, urinary EB-GII adduct levels represent the amount of butadiene metabolite bound to DNA and subsequently excreted due to spontaneous hydrolysis and active repair of the resulting DNA lesions. More efficient repair of genomic butadiene-DNA adducts by Japanese American smokers may help explain higher levels of EB-GII adducts in their urine, despite their

overall lower risk of lung cancer due to smoking. This possibility will be investigated in our future studies by correlating the levels of genomic and urinary EB-GII adducts and identifying DNA repair mechanisms involved in their removal.

Non-smokers from all three ethnic groups excreted low, but detectable levels of urinary EB-GII adducts (Table 3.2). These levels did not vary by racial/ethnic group. While tobacco smoke is one of the major sources of BD exposure, lower levels of BD are present in automobile exhaust, wood burning smoke, and urban air [124, 135, 136, 138]. Furthermore, in addition to DNA adducts forming from these environmental exposures to BD, EB-GII adducts may form endogenously. The contributions of endogenous EB-GII adducts to the overall adduct load are being examined in our ongoing laboratory animal studies utilizing stable isotope-labeling experiments to distinguish between endogenous and exogenous adducts. Additional analyses in cell culture are being conducted to identify potential metabolic and dietary sources of endogenous BD-DNA adducts.

Unlike EB-mercapturic acids (MHBMA) [183], urinary EB-GII levels in smokers were not associated with *GSTT1* gene deletion (Table 3.3). Conjugation of butadiene epoxides to glutathione through GSTT1 is a major metabolic detoxification pathway for EB, and previous studies reported that *GSTT1* gene deletion partially explains ethnic differences in butadiene metabolite excretion [163, 183]. In an earlier study of Japanese Americans, whites, and Native Hawaiian smokers, *GSTT1* gene deletion was significantly associated with MHBMA levels ($p < 0.0001$) [183]. Another study among African American, white, and Native Hawaiian smokers utilized a genome wide association study to identify genetic determinants of BD metabolism and found that *GSTT1* gene deletion explained 7.3% of the variability in MHBMA levels [163]. The observed lack of correlation between GSTT1 status and urinary EB-GII adduct excretion can be explained by the influences of other factors such as DNA repair and nucleotide metabolism (see below).

Additionally, urinary EB-GII levels in current smokers were not influenced by variation in CYP2A6 enzymatic activity (Table 3.4). CYP2A6 enzymatic activity is associated with lung cancer risk [297] and is partially responsible for the epoxidation of butadiene [149]. CYP2A6 enzymatic activity is highest among whites, followed by Native Hawaiians and lowest in Japanese Americans [298]. The observed lack of correlation between urinary EB-GII and *GSTT1* gene deletion or CYP2A6 enzymatic activity ratio is not surprising because CYP2E1 plays a much more important role in metabolism of BD, and polymorphisms in the *CYP2E1* gene are less common [149, 244]. Furthermore, other genetic factors such as polymorphisms in DNA repair genes might have a stronger influence on urinary EB-GII adduct levels. For example, our cell culture studies revealed that NEIL1 glycosylase plays a role in the removal of EB-GII adducts via the base excision repair pathway [86]. In mouse embryonic fibroblasts deficient in base excision repair protein NEIL1$^{-/-}$, EB-GII adduct levels were nearly 3-fold higher than in the isogenic strain (NEIL1$^{+/+}$) [86]. A genome wide association study for the three ethnic groups is now in progress to identify additional genes that may be contributing to the racial/ethnic differences observed in urinary EB-GII.

Urinary levels of butadiene metabolites and butadiene-DNA adducts represent total BD exposure and the biologically relevant dose of butadiene bound to DNA, respectively. We found that BD metabolite DHBMA levels were significantly associated with urinary EB-GII adduct levels, while MHBMA levels were not associated with urinary EB-GII adduct levels if values were adjusted to smoking levels as defined by nicotine equivalents (NE) (Table 3.5). Our earlier study observed no association between *GSTT1* gene deletion and DHBMA in Native Hawaiians, whites, and Japanese American smokers [183]. It should be noted that while DHBMA levels correlate with occupational exposure to BD [299], they do not decrease significantly upon smoking cessation [181] and are only 1.4 fold higher in smokers as compared to non-smokers [178]. Therefore, human exposure to

BD in cigarette smoke does not fully explain DHBMA levels, although the latter is significantly associated with urinary EB-GII adducts. Unlike DHBMA, MHBMA is strongly affected by smoking status as revealed in a smoking cessation study [181]. The observed lack of correlation between BD-mercapturic acids and urinary BD-DNA adducts indicates that they are influenced by different genetic factors and provide distinct information in population studies.

The main limitation of our study is the use of urinary adducts rather than adducts in genomic DNA to determine biologically relevant dose of BD bound to DNA. While our mass spectrometry methods for detection and quantitation of DNA adducts can be applied to either biological liquid, only human urine samples were available in the present study. Unlike genomic EB-GII adducts quantified in blood or oral DNA, urinary EB-GII adduct levels represent the amount of DNA lesions that are removed from the DNA backbone, either through active repair or via spontaneous hydrolysis. Therefore, urinary EB-GII adduct levels can be affected by the efficiency of EB-GII DNA adduct repair and their further metabolism, potentially leading to the lack of association between urinary EB-GII adduct levels and MHBMA, *GSTT1* gene deletion, and CYP2A6 activity. We are currently developing a method for the quantification of EB-GII in oral DNA to investigate genomic levels of EB-GII in smokers.

In conclusion, we found that urinary EB-GII adduct levels are greater in smokers than nonsmokers across all racial/ethnic groups and, among smokers, Japanese Americans had the highest urinary adduct levels. These findings warrant further investigation to quantify EB-GII adducts in genomic DNA and urine samples in the same smokers to investigate the relationship between excreted and persistent EB-GII adducts. Additional ongoing studies will utilize a genome wide association study to elucidate the role of DNA repair in EB-GII removal and to identify the

potential genetic polymorphisms in DNA repair genes that could affect urinary EB-GII adduct levels.

4. Association of urinary N7-(1-hydroxy-3-buten-2-yl) guanine adducts in current smokers with lung cancer development

This work was conducted in collaboration with S. Lani Park, Yesha Patel, and Daniel O. Stram under the guidance of Natalia Tretyakova. Yesha Patel conducted statistical analyses for urinary DNA adducts under the guidance of Dr. Daniel O. Stram. S. Lani Park conducted statistical analyses for urinary metabolites. Caitlin C. Jokipii Krueger quantified urinary DNA adducts and metabolites in urine of lung cancer cases and smoker controls.

4.1 Introduction

Lung cancer is the leading cause of cancer-related deaths in the United States[98], with the majority of cases (82%) attributable to cigarette smoking[257]. Approximately 11-24% of smokers develop lung cancer in their lifetime;[300] with risk being modified by genetic factors[298], ethnicity[265], gender[256], diet[301], and co-occurring lung inflammation. Smoking cessation prior to age 40 is associated with a 90% decrease in risk of smoking associated death as compared to continued smoking[302]. However, former smokers are still at increased risk, with a hazard ratio of excess risk of death of 1.2[302]. Identifying smokers at an increased risk is critical for early-stage lung cancer prevention efforts. This requires sensitive, specific, and non-invasive biomarkers that can be used in general populations.

Tobacco smoke is a complex mixture with over 7000 identified chemical compounds[258]. Of the 73 known human carcinogens in tobacco smoke, 1,3-butadiene (BD) is one of the most abundant (20-75 µg per cigarette in mainstream smoke and 205-361 µg per cigarette in side stream smoke)[134, 259, 269]. BD is classified as a Group 1 carcinogen by the International Agency for Research on Cancer based on the occupational risk and carcinogenicity in laboratory animals[148]. In addition to smoking, human exposure to BD occurs through automobile exhaust, wood burning smoke, and occupational exposures in the synthetic polymer industry[124, 135, 136, 138]. Workers occupationally exposed to BD (~1 ppm) are at an increased risk for lymphatic and hematopoietic cancers[125-127] and possibly lung cancer[131, 132]. In laboratory animals, BD induces neoplasms of the lung in mice at exposures as low as 6.25 ppm[240].

BD is metabolically activated by cytochrome P450 monooxygenases (CYP) 2E1 and 2A6 to 3,4-epoxy-1-butene (EB) (Figure 1.7)[149, 245, 271]. Cellular detoxification of EB occurs through GST-catalyzed glutathione conjugation to form N-acetyl-S-(1-hydroxymethyl-2-propenyl)-L-cysteine

(MHBMA-1) and N-acetyl-S-(2-hydroxy-3-butenyl)-L-cysteine (MHBMA-2) together known as MHBMA and N-acetyl-S-(3,4-dihydroxybutyl)-L-cysteine (DHBMA) (Figure 1.8)[164, 272]. N-acetyl-S-(4-hydroxy-2-buten-1-yl)-L-cysteine (MHBMA-3) was originally identified as an impurity resulting from synthesis or storage in acidic conditions[166] but was present in fresh urine samples and classified as a potential novel metabolite of BD by Alwis et al. in 2012[165]. Urinary MHBMA has been shown to be associated with occupational exposure to BD[206], smoking status[181], and ethnic differences in lung cancer risk[163, 183]. Urinary MHBMA-3 levels increased with tobacco smoke exposure[165, 186], but were not affected by race/ethnicity[184]. While not related to smoking status or ethnicity[163, 181, 183], the concentrations of DHBMA are significantly higher in urine of workers occupationally exposed to BD[206].

The carcinogenic activity of BD is attributed to its ability to alkylate genomic DNA to form DNA adducts. EB forms covalent adducts at multiple nucleophilic sites of DNA (Figure 1.10). Of the BD DNA adducts, hydrolytically stable adducts such as 1,N^6-(2-hydroxy-3-hydroxymethylpropan-1,3-diyl)-2′-deoxyadenosine are thought to result in DNA polymerase errors during replication,[157, 279, 303] while DNA-DNA crosslinks such as 1,4-*bis*-(guan-7-yl)-2,3-butane diol and 1-(guan-7-yl)-4-(aden-1-yl) -2,3-butane diol block DNA replication and induce error prone DNA repair[217, 218, 304]. Although N7-guanine monoadducts of BD such as EB-GII maintain base pairing with cytosine and are not expected to be mutagenic,[13] they have been shown to serve as useful biomarkers of BD exposure due to their relatively high abundance as compared to other BD lesions and their excretion in urine[23]. Unlike blood and tissue, urine collection is non-invasive, and urine samples are readily available from epidemiological studies.

In Chapters 2 and 3 of this Thesis, we reported that urinary EB-GII adducts (Figure 1.10) can be used as a biomarker of smoking-related BD exposure. Urinary EB-GII adducts demonstrated

good temporal stability in smokers, and their levels decreased immediately upon smoking cessation in Chapter 2[286]. In workers occupationally exposed to BD in a BD production facility, urinary EB-GII were over 5-fold more abundant than in administrative controls[23]. EB-GII adducts have been quantified in urine samples available from large epidemiological studies, exhibiting ethnic differences between groups with differing lung cancer risk (Chapter 3)[23, 305]. Urinary DNA adducts represent DNA lesions that are released from DNA backbone via spontaneous hydrolysis or active repair and thus reflect the number of promutagenic lesions formed in genomic DNA. However, the association between urinary EB-GII and lung cancer is not clearly established. In order to test the hypothesis that urinary EB-GII adduct load is higher in smokers who subsequently develop lung cancer, the present study accurately quantified EB-GII, MHBMA, and DHBMA in urine of smokers who subsequently lung cancer and the corresponding smoker controls (N = 519) using high-throughput, quantitative, LC-HRMS/MS methodologies established in our laboratory[206, 286].

4.2 Materials and Methods

Study Population

The study population included current cigarette smokers from two ethnic groups: African American and white. All participants were selected from the Southern Community Cohort Study (SCCS), which provides an epidemiological investigation of racial disparities in cancer risk.[306] In-person baseline interviews were used to establish baseline characteristics of the study population, followed by biospecimen collection A total of 519 samples were analyzed for urinary EB-GII, MHBMA, and DHBMA (N = 260 cases, N = 259 controls). Participants were selected using a nested case-control study design among those who were current smokers at time of cohort entry (and spot urine collection). Lung cancer cases were ascertained from linkage to the 12 state cancer registries in the study area. Among the current smokers with urine available 264 incident lung

cancer cases occurred during study follow-up (end of follow-up=December 31, 2015). For this study one control for every case were selected at random among a subcohort of SCCS current smoking participants with urine, matched on age, sex, race/ethnicity and recruitment site. Written informed consent was obtained from all study participants.

Materials

LC-MS grade water, methanol and acetonitrile were purchased from Fisher Scientific (Pittsburgh, PA, USA). Strata X polymeric reversed phase SPE cartridges (30 mg/1 mL) were purchased from Phenomenex (Torrance, CA, USA). EB-GII and $^{15}N_5$-EB-GII standards were prepared as previously reported [211, 281]. MHBMA, MHBMA-d_6, DHBMA, and DHBMA-d_7 were purchased from Toronto Research Chemicals (North York, ON, Canada). 96 well plates were purchased from Analytical Sales and Services Inc. (Ledgewood, New Jersey, USA). All other chemicals and solvents were obtained from Sigma-Aldrich (Milwaukee, WI; St. Louis, MO, USA) unless otherwise specified.

Urine sample processing and analyte enrichment

Urine samples were processed as described previously, with a modification to the SPE method to additionally collect MHBMA and DHBMA from the same urine sample[286]. In brief, urine samples (200 µL) were centrifuged at 10,000 x g for 15 min to remove particulate matter, spiked with 5 fmol of $^{15}N_5$-EB-GII, 37 ng of MHBMA1-d_6, 11 ng of MHBMA2-d_6, 25 ng of MHBMA3-d_6, and 60 ng of DHBMA-d_7 (internal standards for mass spectrometry), and subjected to solid-phase extraction (SPE) on Strata X 96-well plate cartridges (30 mg/mL; Phenomenex, Torrance, CA). The cartridges were conditioned with 2 mL of methanol, followed by 2 mL of water. Samples were loaded onto the cartridges, and MHBMA, DHBMA, and their internal standards were eluted with 1 mL of water. SPE eluates were collected into a 96 well plate, dried under nitrogen, and

stored at -20 °C until nanoLC/ESI$^+$-HRMS/MS analysis. SPE cartridges were washed with 1 mL of 10% methanol in water. EB-GII and its internal standard were eluted with 1 mL of 60% methanol in water. To determine mercapturic acid recovery from SPE, synthetic urine (200 μL, in triplicate) was spiked with unlabeled MHBMA and DHBMA. MHBMA-d_6 and DHBMA-d_7 internal standards were added prior or immediately following SPE. Samples were then quantified as described below. SPE recovery was determined by comparing the standard:internal standard peak area ratios when internal standard was added before or after SPE.

SPE eluates containing EB-GII and its internal standard were concentrated under nitrogen and subjected to offline high-performance liquid chromatography (HPLC) on an Agilent 1260 series HPLC system equipped with an automated fraction collector (Agilent Technologies, Santa Clara, CA) and a Zorbax Eclipse XDB-C18 column (4.6 x 150 mm, 5 μm; Agilent Technologies, Santa Clara, CA). Fractions containing EB-GII and its internal standard were collected, dried under nitrogen, and reconstituted in LC/MS-grade water containing 0.01% acetic acid (30 μL) for nanoLC/ESI$^+$-HRMS/MS analysis.

NanoLC/ESI$^+$-HRMS/MS analysis of urinary EB-GII

All nanoLC/ESI$^+$-HRMS/MS analyses were conducted on Q Exactive Orbitrap instrument equipped with a nanospray source interfaced with a Dionex UlitMate 3000 RSLC nano HPLC system (Thermo Fisher Scientific Corp., Waltham, MA). The LC gradient has been previously described[23, 286].

Tandem mass spectrometry analyses were performed in the parallel reaction monitoring (PRM) mode. $[M+H]^+$ ions of EB-GII (*m/z* = 222.0985) were fragmented using a normalized collision energy (NCE) of 30 and an isolation width of 1.0 amu. The resulting MS/MS fragment ions at *m/z* 152.0565 ($[Gua+H]^+$) were detected in the mass range of *m/z* 50-270 using an orbitrap

mass analyzer at a resolution of 70,000. The $^{15}N_5$-EB-GII internal standard was detected using an analogous MS/MS scan event consisting of fragmentation of *m/z* 227.0837 ($[M+H]^+$) to *m/z* 157.0418 ($[^{15}N_5\text{-Gua}+H]^+$). Extracted ion chromatograms corresponding to *m/z* 152.0565 and *m/z* 157.0418 were utilized for the quantification of EB-GII and $^{15}N_5$-EB-GII, respectively. EB-GII amounts were determined by comparing the areas of the peaks corresponding to the analyte and its internal standard.

Accuracy of the analytical method was determined by spiking synthetic urine with 0.2 fmol of EB-GII and 5 fmol of $^{15}N_5$-EB-GII, followed by sample processing and analysis as described above. This sample was analyzed on each plate of sample analysis, and the accuracy range was determined from (A_m/A_a*100%). Precision of the analytical method was determined by analyzing the same spiked synthetic urine samples and quality control samples (pooled smoker urine) included nine times on each plate and reported as percent coefficient of variation (% CV). Method LOD and LOQ were estimated as $3.3\sigma/S$ and $10\sigma/S$, where *S* is the slope of the validation curve in synthetic urine and σ is the standard deviation of the slope[307].

HPLC/ESI$^-$-HRMS/MS analysis of urinary MHBMA and DHBMA

SPE eluates containing MHBMA and DHBMA were reconstituted in LC/MS grade water containing 0.1% formic acid (30 µL) for nanoLC/ESI$^+$-HRMS/MS analysis on an Agilent Pursuit 3 Diphenyl (2.0x150 mm, 3µM) column equipped with an Agilent Metaguard Pursuit 3 Diphenyl guard column. The LC gradient has been previously described[206].

Tandem mass spectrometry analyses were conducted by fragmenting $[M-H]^-$ ions of MHBMA (*m/z* = 232.1) in the high collision dissociation (HCD) cell of the instrument using the normalized collision energy (NCE) of 25 and isolation width (IW) of 1.0 amu. The resulting fragment ion generated by the loss of N-acetyl cysteine (NaC) $[M\text{-NaC-H}]^-$ (*m/z* = 103.0223) was detected in the

mass range of *m/z* = 50-270 using the Orbitrap mass analyzer (HRMS) at a resolution of 70,000. MHBMA-d_6 was detected using an analogous scan event consisting of fragmentation of *m/z* = 238.1 to *m/z* = 109.0600. DHBMA was detected by fragmentation of *m/z* = 250.1 to *m/z* = 121.0329 with NCE of 35. DHBMA-d_7 was detected through an analogous scan event consisting of fragmentation of *m/z* = 257.1194 to *m/z* = 128.0768.

Accuracy of the analytical method was determined by spiking synthetic urine with 0.85 ng of MHBMA-1, 36 ng of MHBMA-1-d_6, 0.35 ng of MHBMA-2, 11 ng of MHBMA-2-d_6, 25 ng of DHBMA, and 60 ng of DHBMA-d_7, followed by sample processing and analysis as described above. This QC sample was analyzed on each plate of sample analysis, and the accuracy range was determined from (A_m/A_a*100%). Precision of the analytical method was determined by analyzing the same spiked synthetic urine samples and quality control samples (pooled smoker urine) included nine times on each plate and reported as percent coefficient of variation (%CV). Method LOD and LOQ were estimated as $3.3\sigma/S$ and $10\sigma/S$, where *S* is the slope of the validation curve in synthetic urine and σ is the standard deviation of the slope[307].

Statistical Methods

EB–GII adduct levels were expressed as fmol/ml urine. Pearson's partial correlation coefficients, adjusting for age, sex and race/ethnicity (for overall), were computed to examine the correlation between EB adducts, TNE, MHBMA, DHBMA (among those with complete data). To examine the difference of EB–GII adducts, MHMBA or DHBMA by lung cancer case status or by racial/ethnic groups, covariate-adjusted geometric means were computed for lung cancer status or ethnic/racial group at the mean covariate vector using the LS means procedure in SAS. Multivariable linear models regressed the urinary levels of EB–GII adducts on the following predictors: age at time of urine collection (continuous), race/ethnicity (when results were not

stratified by race/ethnicity). To assess effects independent of internal smoking dose another model with TNE (natural log, continuous) was also included. To better meet model assumptions, EB adducts, TNE, MHBMA, DHBMA were transformed by taking the natural log. To assess the association between EB-GII, MHBMA, DHBMA and lung cancer we used unconditional logistic regression, adjusting for age, sex, race/ethnicity and TNE.

4.3 Results

4.3.1 NanoLC/ESI$^+$-HRMS/MS and HPLC/ESI$^-$-HRMS/MS method validation

NanoLC/ESI$^+$-HRMS/MS analysis of standard solutions containing 0.05-10 fmol of EB-GII and 5 fmol of $^{15}N_5$-EB-GII in 30 µL of water ($y = 0.9269x$, $R^2 = 0.9997$) and synthetic urine ($y = 0.8929x$, $R^2 = 0.9999$) produced linear standard curves. Method accuracy was determined to be 88-123% for 0.2 fmol of EB-GII spiked in synthetic urine. Method precision (%CV) was determined to be 10% for 0.2 fmol of EB-GII spiked in synthetic urine and 20% for pooled smoker urine samples. Method LOD was 0.32 fmol/mL urine and method LOQ was 0.96 fmol/mL urine. SPE recovery for EB-GII has been previously reported as 75% in synthetic urine[286].

HPLC/ESI$^-$-HRMS/MS analysis of standard solutions containing 0.0009-3.14 ng MHBMA-1 and 36 ng of MHBMA-1-d_6 in synthetic urine ($y = 0.9724x - 0.0085$, $R^2 = 0.9995$) and 0.0003-1.27 ng of MHBMA-2 and 11 ng of MHBMA-2-d_6 in synthetic urine ($y = 0.9673x - 0.0031$, $R^2 = 0.9997$) produced linear standard curves. The same was true for DHBMA (0.025-100 ng, 60 ng DHBMA-d_7) in synthetic urine ($y = 0.9054x - 0.0296$), $R^2 = 0.9999$). Method accuracy was 99-118% for 0.85 ng of MHBMA-1, 98-116% for 0.35 ng of MHBMA-2, and 90-118% for 25 ng of DHBMA spiked in synthetic urine. Method precision (%CV) was determined to be 6% for 0.85 ng of MHBMA-1, 5% for 0.35 ng of MHBMA-2 and 9% for 25 ng of DHBMA spiked into synthetic urine and 14% for MHBMA-1 and 12% for DHBMA in pooled smoker urine samples. MHBMA-2 was not detected in pooled smoker urine samples. MHBMA-3 was not detected in pooled smoker samples or any subjects in this study. Method LOD was 0.11 ng/mL urine for MHBMA-1, 0.10 ng/mL urine for MHBMA-2, and 0.04 ng/mL urine for DHBMA. Method LOQ was 0.34 ng/mL urine for

MHBMA-1, 0.29 ng/mL urine MHBMA-2, and 0.13 ng/mL urine for DHBMA. SPE recovery in synthetic urine was 41%, 48%, and 27% for MHBMA-1, MHBMA-2, and DHBMA, respectively.

4.3.2 Study Population

The baseline demographic characteristics of the study population are presented in Table 4.1. Among the 519 participants, 260 were lung cancer cases and 259 were smoker controls. These smokers did not have lung cancer at the time of study enrollment and urine sample collection. The median age at enrollment was 53 for the controls and 54 for the lung cancer cases. The median age of lung cancer diagnosis among the cases was four years after study enrollment, at age 58. The two racial/ethnic groups included were African Americans and whites. The samples from 287 African Americans and 210 white smokers were approximately evenly distributed between cases and controls. For lung cancer cases, additional information regarding age at diagnosis is also included. Lung cancer cases reported smoking higher numbers of cigarettes per day (CPD) than controls [median CPD 20 (10-20) and 10 (6-20), respectively] and had higher levels of total nicotine equivalents (TNE) than controls [median TNE 82.9 (48.1-122.6) and 37.8 (24.7-65.2), respectively].

Table 4.1. Demographics for study participants

	Cases		Controls	
	Median	25-75th percentile	Median	25-75th percentile
N	260		259	
Age at Enrollment (years)	54	49-60	53	48-60
Age at Diagnosis (years)	58	54-65	-	-
Sex	N	%	N	%
Males	130	50.0	129	49.8
Females	130	50.0	130	50.2
Race/Ethnicity				
AA	144	55.4	143	55.2
Whites	105	40.4	105	40.5
Other	11	4.2	11	4.3
Menthol users, Y	127	48.8	148	57.1
	Median	25-75th percentile	Median	25-75th percentile
BMI (kg/m2)	25.2	22.2 - 29.1	27.2	23.3-31.4
TNE	82.9	48.1 - 122.6	37.8	24.7 - 65.2
Cigarettes per day	20	10 - 20	10	6 - 20
packyears	30	16.5 - 47.0	20	10 - 35
creatinine	101.1	50.5 - 162.07	93.99	47.55 - 144.91

4.3.3 Urinary excretion of EB-GII in lung cancer cases and controls

To examine possible association of urinary EB-GII adducts with cancer, they were quantified in smokers who subsequently developed lung cancer and the corresponding smoker controls who did not develop lung cancer (260 cases and 259 controls). Smokers included in the study belonged to two racial/ethnic groups with varying risks of lung cancer development: African American and white. We employed the isotope dilution nanoLC-ESI$^+$-HRMS/MS method described in Chapter 2 of this Thesis because it enables sensitive and accurate quantification of low levels of EB-GII in human urine (LOD = 0.25 fmol/mL urine)[305].

When adjusting for age and sex, there were no statistical differences in the levels of urinary EB-GII excreted by African American and white smokers (p = 0.259, Table 4.2). However, when the EB-GII values were adjusted for total nicotine equivalents (TNE) to account for smoking dose, African Americans excreted significantly lower levels of urinary EB-GII [1.84 (95% CI: 1.71-1.94) fmol/mL urine] than whites [2.08 (95% CI: 1.91-2.26) fmol/mL urine, p = 0.031] (Table 4.2). This is consistent with previous results from our laboratory showing higher levels of urinary EB-GII in whites as compared to African Americans[23].

Table 4.2. Geometric means for EB-GII (fmol/mL urine) by lung cancer incidence

Ethnicity	N	Geometric Mean	(95% CI)	*P*-value	N[d]	Geometric Mean[d]	(95% CI)[d]	*P*-value[d]
Overall[a]	519	2.07	(1.82 - 2.36)		519	2.04	(1.86 - 2.23)	
Cases	260	2.59	(2.24 - 3.00)	**1.22E-09**	260	1.93	(1.74 - 2.15)	0.071
Controls	259	1.65	(1.43 - 1.91)		259	2.14	(1.93 - 2.38)	
African Americans[b]	287	1.86[c]	(1.68 - 2.06)		287	1.84[e]	(1.71 - 1.97)	
Cases	144	2.54	(2.24 - 2.89)	**1.96E-09**	144	1.88	(1.70 - 2.08)	0.705
Controls	143	1.47	(1.30 - 1.67)		143	1.93	(1.75 - 2.14)	
Whites[b]	210	2.04[c]	(1.81 - 2.31)		210	2.08[e]	(1.91 - 2.26)	
Cases	105	2.50	(2.07 - 3.00)	**0.011**	105	1.89	(1.66 - 2.15)	**0.045**
Controls	105	1.80	(1.49 - 2.16)		105	2.28	(2.01- 2.59)	

Bold values denote statistical significance
[a]The analyses have been adjusted for age, sex, and race/ethnicity
[b]The analyses have been adjusted for age and sex
[c]*P*-value comparing African Americans to whites overall = 0.259
[d]These analyses have been additionally adjusted for TNE
[e]*P*-value comparing African Americans to whites overall = 0.031

Urinary EB-GII levels were quantified in the urine of smokers with lung cancer and matched controls (260 cases and 259 controls). When adjusting for age, sex, and race/ethnicity, lung cancer cases excreted significantly higher levels of urinary EB-GII [2.59 (95% CI: 2.24-3.00) fmol/mL urine] than matched controls [1.65 (95% CI: 1.43-1.91) fmol/mL urine, p = 1.22E-09] (Table 4.2). This trend was consistent within each racial/ethnic group when adjusting for age and sex, with levels of urinary EB-GII significantly higher in African American cases as compared to controls (p = 1.96E-09) and white lung cancer cases as compared to controls (p = 0.011). Upon further adjustment for total nicotine equivalents (TNE), there were no statistically significant differences in urinary EB-GII excretion between lung cancer cases and controls (p = 0.071, Table 4.2).

We further examined the associations of EB-GII with lung cancer incidence. When adjusting for age, sex, BMI, and race/ethnicity, the OR was 1.91 (95% CI: 1.52-2.40, p = 2.06E-08), indicating elevated cancer risk with higher excretion of urinary EB-GII adducts (Table 4.3). These results are consistent within each ethnic group (OR = 2.60 (1.81-3.73, p = 2.25E-07) for African Americans and 1.49 (1.10-2.03, p = 0.01) for whites), showing a stronger effect of butadiene exposure in African American smokers. Upon further adjustment for TNE, the OR (0.71 (0.50-1.01) was no longer statistically significant (p = 0.054) (Table 4.3). These results indicate that urinary EB-GII is a biomarker of lung cancer risk upon exposure to BD in tobacco smoke.

Table 4.3. Associations of log-transformed EB-GII with lung cancer incidence

Predictor	N_cases	N_controls	OR	(95% CI)	P-value	OR[c]	(95% CI)[c]	P-value[c]
Overall[a]								
Log-EBGII	260	259	1.91	(1.52 - 2.40)	**2.06E-08**	0.71	(0.50 - 1.01)	0.054
African Americans[b]								
Log-EBGII	144	143	2.60	(1.81 - 3.73)	**2.25E-07**	0.80	(0.48 - 1.34)	0.398
Whites[b]								
Log-EBGII	105	105	1.49	(1.10 - 2.03)	**0.010**	0.67	(0.41 - 1.11)	0.120

Bold values denote statistical significance

[a] The analyses have been adjusted for age, sex, log-BMI and race/ethnicity

[b] The analyses have been adjusted for age, sex, and log-BMI

[c] The analyses have been additionally adjusted for log-TNEyrs

4.3.4 Urinary excretion of BD metabolites in lung cancer cases and controls

To compare the abundance of urinary BD metabolites in lung cancer cases vs controls, urinary MHBMA-1, MHBMA-2, and DHBMA were quantified in the same subjects. Urinary MHBMA-3 was not detected in any subjects. 191 subjects had undetectable levels of MHBMA-1 and MHBMA-2. These subjects were randomly distributed by race/ethnicity and cancer status, so they were removed from analyses regarding MHBMA. Baseline characteristics of study participants among those with detectable MHBMA is presented in Table 4.4.

When adjusted for age, sex, log-BMI, and race/ethnicity, urinary MHBMA was significantly elevated in lung cancer cases [1.45 (95% CI: 1.22-1.71) ng/mL urine] as compared to smoking controls [0.84 (95% CI: 0.70-1.00) ng/mL urine, $P < 0.0001$, Table 4.5). This trend was consistent within each racial/ethnic group when adjusting for age, sex, and log-BMI, with African American lung cancer cases significantly elevated over controls (p =0.0006) and white lung cancer cases significantly elevated over controls (p = 0.006). Upon further adjustment for TNE, these differences were no longer statistically significant (Table 4.5).

When separately investigating the MHBMA isomers (Figure 1.8), we observe the same trends among overall lung cancer cases and smoker controls. Urinary levels of MHBMA-1 and MHBMA-2 are significantly higher in lung cancer cases as compared to smoking controls (p =0.0007, p = 0.0352 respectively, Table 4.5). Among ethnic groups, African American lung cancer cases have higher MHBMA-1 and MHBMA-2 as compared to controls (p = 0.0139, p = 0.0201 for MHBMA-1 and MHBMA-2, respectively), while only MHBMA-1 is elevated in white smokers as compared to controls (p = 0.0143, p = 0.4053 for MHBMA-2). Upon adjustment for TNE, neither of the two

MHBMA isomers are significantly associated with lung cancer incidence if analyzed separately (Table 4.5).

Urinary DHBMA (adjusted for age, sex, log-BMI, and race/ethnicity) is significantly elevated in lung cancer cases [117.62 (95% CI: 103.35-133.85) ng/mL urine] as compared to smoker controls [85.04 (95% CI: 74.69-96.82) ng/mL urine, $p = 0.0006$, Table 4.6). This difference is also significant in African American smokers ($p = 0.0011$) but not among white smokers ($p = 0.0774$). Further adjustment for TNE results in insignificant differences between lung cancer cases and controls overall and among each racial/ethnic group, indicating that tobacco smoke exposure to BD is associated with lung cancer incidence.

We further investigated the associations between lung cancer incidence and urinary BD metabolites. When adjusting for age, sex, BMI, and race/ethnicity, the OR was 1.32 (95% CI: 1.12-1.57, $p = 0.0015$) for MHBMA-1, 1.08 (95% CI: 1.02-1.14, $p = 0.0142$) for MHBMA-2, 1.63 (95% CI: 1.30-2.05, $p < 0.0001$) for MHBMA, and 1.37 (95% CI: 1.14-1.64, $p = 0.0007$) for DHBMA (Table 4.7). This indicates elevated cancer risk with increased levels of excreted BD metabolites. This trend is consistent within each ethnic group, with the exception of the association between MHBMA-2 and lung cancer incidence in white smokers ($p = 0.3464$). Upon adjustment for TNE, elevated levels of BD metabolites were no longer associated with elevated lung cancer risk.

Table 4.4. Demographics for study participants with detectable MHBMA.

	Controls				Cases			
	Mean	SE	Median	(25-75% interquartile range)	Mean	SE	Median	(25-75% interquartile range)
N	155				171			
				(25-75% interquartile range)				(25-75% interquartile range)
Age at Enrollment (years)	53.67	0.61	53.00	48.0 – 59.0	53.98	0.59	54.00	48.0 – 59.0
Age at Diagnosis (years)					58.73	0.59	58.00	53.0 – 65.0
Sex	N				N			
Males	71				89			
Females	84				82			
Race/Ethnicity								
AA	89				97			
Whites	62				69			
Other	4				5			
	Mean	SE	Median	(25-75% interquartile range)	Mean	SE	Median	(25-75% interquartile range)
BMI	28.45	0.52	27.65	23.65 – 31.62	25.85	0.43	25.24	22.31 – 28.72
Creatinine	108.84	5.91	97.06	56.63 – 142.64	117.45	6.31	104.28	54.32 – 159.75
EB-GII	2.13	0.13	1.59	1.05 – 2.64	3.22	0.19	2.77	1.61 – 3.92
MHBMA	1.43	0.14	0.85	0.45 – 1.83	2.63	0.31	1.53	0.7 – 3.07
MHBMA-1	1.23	0.12	0.73	0.37 – 1.46	2.28	0.29	1.24	0.59 – 2.67
MHBMA-2	0.20	0.03	0.06	0.0 – 0.28	0.35	0.04	0.18	0.0 – 0.46
DHBMA	145.21	9.47	116.62	65.24 – 180.43	193.27	14.30	149.28	60.81 – 251.67

TNE	50.36	2.72	39.87	28.84 – 61.08	97.30	5.05	84.76	48.41 – 122.58
CYP2A6	5.06	0.32	4.16	2.36 – 6.27	6.76	0.42	5.20	3.19 – 8.61
NNAL	1.73	0.12	1.37	0.79 – 2.13	2.98	0.22	2.18	1.45 – 3.59
3HPMA	4195.75	325.35	2918.83	1397.55 – 5392.48	7483.17	595.14	5075.62	2104.55 – 10304.64
2HPMA	472.14	69.74	301.36	159.09 – 469.56	589.06	53.49	379.11	184.13 – 709.56
CEMA	567.70	35.27	438.99	276.54 – 742.64	996.24	61.51	772.79	456.74 – 1238.98
8isoPGF2alpha	1.45	0.10	1.17	0.67 – 2.0	1.69	0.11	1.35	0.76 – 2.08

Table 4.5. Geometric means for MHBMA-1, MHBMA-2, MHBMA, and DHBMA (ng/mL urine) by lung cancer incidence

Ethnicity	N	Geometric Mean	(95% CI)	*P*-value	N[c]	Geometric Mean[c]	(95% CI)[c]	*P*-value[c]
MHBMA-1								
Overall[a]	323	0.808	0.67 – 0.98		323	0.825	0.69 – 0.98	
Cases	169	1.141	0.87 – 1.49	**0.0007**	169	0.865	0.67 – 1.12	0.6367
Controls	154	0.572	0.43 – 0.76		154	0.788	0.6 – 1.03	
African Americans[b]	186	0.758	0.59 – 0.98		186	0.744	0.59 – 0.94	
Cases	97	1.040	0.73 – 1.48	**0.0139**	97	0.701	0.5 – 0.98	0.6319
Controls	89	0.553	0.39 – 0.79		89	0.791	0.56 – 1.11	
Whites[b]	129	0.861	0.63 – 1.17		129	0.915	0.69 – 1.21	
Cases	68	1.251	0.83 – 1.89	**0.0143**	68	1.067	0.73 – 1.56	0.2762
Controls	61	0.592	0.38 – 0.92		61	0.784	0.52 – 1.18	
MHBMA-2								
Overall[a]	323	0.009	0.01 – 0.01		323	0.009	0.01 – 0.01	
Cases	169	0.015	0.01 – 0.03	**0.0352**	169	0.009	0 – 0.02	0.9306
Controls	154	0.006	0 – 0.01		154	0.010	0 – 0.02	
African Americans[b]	186	0.019	0.01 – 0.03		186	0.018	0.01 – 0.03	
Cases	97	0.037	0.02 – 0.08	**0.0201**	97	0.019	0.01 – 0.04	0.8847
Controls	89	0.009	0 – 0.02		89	0.017	0.01 – 0.04	
Whites[b]	129	0.004	0 – 0.01	0.4053	129	0.005	0 – 0.01	
Cases	68	0.006	0 – 0.02		68	0.004	0 – 0.01	0.8015
Controls	61	0.003	0 – 0.01		61	0.005	0 – 0.01	

MHBMA								
Overall[a]	323	1.103	0.98 – 1.24		323	1.126	1.03 – 1.24	
Cases	169	1.447	1.22 – 1.71	**<.0001**	169	1.110	0.97 – 1.27	
Controls	154	0.841	0.7 – 1		154	1.142	0.99 – 1.32	0.7912
African Americans[b]	186	1.127	0.96 – 1.32	**0.0006**	186	1.107	0.98 – 1.25	
Cases	97	1.490	1.2 – 1.86		97	1.022	0.85 – 1.22	0.2297
Controls	89	0.852	0.68 – 1.07		89	1.200	1 – 1.44	
Whites[b]	129	1.080	0.89 – 1.31	**0.006**	129	1.145	0.99 – 1.33	
Cases	68	1.405	1.09 – 1.82		68	1.207	0.99 – 1.48	0.4840
Controls	61	0.830	0.63 – 1.09		61	1.086	0.87 – 1.35	

Bold values denote statistical significance

[a]The analyses have been adjusted for age, sex, log-BMI, and race/ethnicity

[b]The analyses have been adjusted for age, sex, and log-BMI

[c]These analyses have been additionally adjusted for TNE

Table 4.6. Geometric means for DHBMA (ng/mL urine) by lung cancer incidence

Ethnicity	N	Geometric Mean	(95% CI)	*P*-value	N[c]	Geometric Mean[c]	(95% CI)[c]	*P*-value[c]
Overall[a]	510	100.009	91.34 – 109.5		510	100.255	92.73 – 108.39	
Cases	255	117.615	103.35 – 133.85	**0.0006**	255	94.389	84.04 – 106.01	0.1711
Controls	255	85.038	74.69 – 96.82		255	106.485	94.75 – 119.67	
African Americans[b]	283	136.693	121.1 – 154.29		283	134.856	121.5 – 149.68	
Cases	142	166.867	140.68 – 197.92	**0.0011**	142	125.558	107.74 – 146.33	0.2064
Controls	141	111.976	94.46 – 132.73		141	144.842	124.49 – 168.53	
Whites[b]	206	73.169	63.47 – 84.36		206	74.532	65.94 – 84.24	
Cases	103	82.899	67.98 – 101.09	0.0774	103	70.958	59.72 – 84.31	0.4298
Controls	103	64.581	52.93 – 78.79		103	78.285	65.81 – 93.13	

Bold values denote statistical significance

[a]The analyses have been adjusted for age, sex, log-BMI, and race/ethnicity

[b]The analyses have been adjusted for age, sex, and log-BMI

[c]These analyses have been additionally adjusted for TNE

Table 4.7. Associations of log-transformed MHBMA, MHBMA1, MHBMA2, and DHBMA with lung cancer incidence

	Model 1					Model 2				
Predictor	N_cases	N_controls	OR	(95% CI)	P-value	N_cases	N_controls	OR	(95% CI)	P-value
MHBMA-1										
Overall	169	154	1.32	1.112 – 1.568	**0.0015**	169	154	0.99	0.839 – 1.169	0.9078
African Americans	97	89	1.23	1.004 – 1.502	**0.0451**	97	89	0.98	0.79 – 1.213	0.8468
Whites	68	61	1.47	1.092 – 1.99	**0.0113**	68	61	1.08	0.797 – 1.464	0.6210
MHBMA-2										
Overall	169	154	1.08	1.015 – 1.141	**0.0142**	169	154	1.00	0.932 – 1.067	0.9347
African Americans	97	89	1.10	1.013 – 1.188	**0.0220**	97	89	1.02	0.927 – 1.114	0.7291
Whites	68	61	1.04	0.954 – 1.142	0.3464	68	61	0.97	0.878 – 1.08	0.6149
MHBMA										
Overall	169	154	1.63	1.305 – 2.047	**0.0000**	169	154	0.79	0.575 – 1.087	0.1485
African Americans	97	89	1.71	1.235 – 2.361	**0.0012**	97	89	0.71	0.45 – 1.131	0.1513
Whites	68	61	1.55	1.118 – 2.135	**0.0083**	68	61	0.94	0.598 – 1.489	0.8028
DHBMA										
Overall	255	255	1.37	1.144 – 1.645	**0.0007**	255	255	0.75	0.591 – 0.944	**0.0145**
African Americans	142	141	1.64	1.231 – 2.178	**0.0007**	142	141	0.84	0.592 – 1.202	0.3464
Whites	103	103	1.22	0.955 – 1.568	0.1104	103	103	0.72	0.515 – 0.998	**0.0488**

Bold values denote statistical significance
Model 1: adjusted for age, sex, log-BMI
Model 2: adjusted for age, sex, log-BMI, TNE

4.3.5 Associations between urinary BD-DNA adducts, metabolites, and other tobacco smoke biomarkers

We next evaluated the relationship between BD-induced DNA adducts (EB-GII) and BD metabolites MHBMA-1, MHBMA-2, and DHBMA. As MHBMA metabolites and EB-GII are formed from the same metabolite of BD (3,4-epoxy-1-butene (EB), Figures 1.8 and 1.10 in Chapter 1), we expected that their urinary levels would be correlated with each other. We found that urinary EB-GII, upon adjustment for age, sex, and log-BMI, and racial/ethnic group, was associated with MHBMA-1, MHBMA-2, MHBMA, and DHBMA ($p < 0.0001$ for each comparison, Table 4.8. Upon further adjustment for TNE, these associations remained statistically significant with the exception of MHBMA-2 (Table 4.8).

Additional biomarkers of smoking and CYP2A6 activity (TNE, CPD, NNAL, 3HPMA, 2HPMA, CEMA, and 8isoPGF2a) were quantified in these same subjects. We found that urinary EB-GII, when adjusted for age, sex, and race/ethnicity, was strongly associated with TNE (r = 0.65727, $p < 0.0001$), NNAL (r = 0.50095, $p < 0.0001$), CEMA (r = 0.58917, $p < 0.0001$), and 8isoPGF2a (r = 0.50011, $p < 0.0001$), moderately associated with CYP2A6 activity (r = 0.4233, $p < 0.0001$) and 2-HMPA (r = 0.47484, $p < 0.0001$), and weakly associated with 3-HPMA (r = 0.29288, $p < 0.0001$). We did not observe an association between urinary EB-GII and cigarettes per day.

Table 4.8. Associations of log-transformed MHBMA and DHBMA with urinary EB-GII

	Model 1				Model 2			
	N	Beta	SE	*P*-value	N	Beta	SE	*P*-value
log MHBMA (ng/mL urine)	323	0.45	0.03	**<0.0001**	323	0.27	0.04	**<0.0001**
log MHBMA-1 (ng/mL urine)	323	0.18	0.02	**<0.0001**	323	0.07	0.02	**0.001**
log MHBMA-2 (ng/mL urine)	323	0.05	0.01	**<0.0001**	323	0.00	0.01	0.673
log DHBMA (ng/mL urine)	510	0.37	0.03	**<0.0001**	510	0.14	0.03	**<0.0001**

Bold values denote statistical significance
Model 1: adjusted for age, sex, log-BMI
Model 2: adjusted for age, sex, log-BMI, TNE

Urinary DHBMA was additionally associated with TNE (r = 0.473, p <0.0001), CYP2A6 activity (r = 0.361, p < 0.0001), NNAL (r = 0.296, p < 0.0001), 3-HMPA (r = 0.773, p <0.0001), 2-HMPA (r = 0.642, p < 0.0001), CEMA (r = 0.586, p < 0.0001), and 8isoPGF2a (r = 0.475, p <0.0001). Similar results were observed for MHBMA, associated with TNE (r = 0.708, p <0.0001), NNAL (r = 0.412, p < 0.0001), 3-HMPA (r = 0.619, p <0.0001), 2-HMPA (r = 0.672, p < 0.0001), CEMA (r = 0.648, p < 0.0001), and 8isoPGF2a (r = 0.319, p <0.0001). These associations between BD biomarkers and additional biomarkers of tobacco smoke exposure confirm tobacco smoke as a major source of exposure to 1,3-butadiene in smokers.

4.4 Discussion

Smoking is the major risk factor for lung cancer development. Identifying smokers at an increased risk for lung cancer allows for early intervention by targeting high risk individuals to smoking cessation programs and chemoprevention therapy. Among tobacco smoke carcinogens, BD is one of the most abundant and has a high cancer risk index[259]. Our laboratory has previously utilized BD-DNA adducts and BD-mercapturic acids as biomarkers of BD exposure and cancer risk[23, 163, 183, 305] and to investigate inter-individual differences and ethnic differences in BD metabolite and adduct formation[293, 294]. MHBMA is associated with lung cancer incidence[185]. However, the association between urinary BD DNA adducts and lung cancer incidence has not been investigated.

Unlike BD metabolites MHBMA and DHBMA, which can be considered as biomarkers of exposure to and detoxification of butadiene, urinary DNA adducts are mechanism-based biomarkers, representing the biologically relevant dose of butadiene available for binding to genomic DNA. DNA lesions are directly involved in the etiology of cancer by causing mispairing during DNA replication[17]. Among BD-DNA lesions, N7-guanine adducts such as EB-GII are the

most abundant and are frequently used as representative biomarkers of total DNA damage[22, 23, 93, 195, 286]. EB-GII lesions are hydrolytically labile and are excreted in the urine following spontaneous hydrolysis or active repair (Figure 1.3), allowing for their use as non-invasive biomarkers of risk associated with BD exposures. We have previously quantified urinary EB-GII in a multiethnic cohort of smokers, demonstrating that adduct levels differ between ethnic groups with different lung cancer risk[305]. However, the association of EB-GII with lung cancer remained unknown.

The present study is the first to directly examine the relationship between urinary BD DNA adducts and lung cancer incidence. Adducts levels were determined in 260 smokers who subsequently developed lung cancer and 259 matched controls who did not develop the disease. Significantly higher levels of urinary EB-GII adducts were observed in lung cancer cases as compared to controls (Table 4.2). The OR per unit increase in log-EB-GII was 1.91, indicating an almost 2-fold increase in the risk of lung cancer incidence upon a 1 log unit increase in EB-GII levels. Importantly, the risk of cancer incidence with increasing urinary EB-GII differs by racial/ethnic group. Among African American smokers, the OR is 2.60 while the OR is 1.49 among white smokers per unit increase in log-EB-GII (Table 4.3), suggesting that the risk of lung cancer upon increasing exposure to BD is greater in African Americans as compared to whites. However, upon adjusting adduct values for smoking dose (total nicotine equivalents, TNE), the differences in EB-GII levels between lung cancer cases and controls were no longer significant, indicating that both biomarkers reflect the levels of tobacco smoke exposure.

We additionally observed significantly higher levels of urinary MHBMA and DHBMA in lung cancer cases as compared to controls. The OR for MHBMA was 1.32 and 1.37 for DHBMA (Table 4.7). The increased excretion of butadiene metabolites in lung cancer cases was consistent for each isomer of MHBMA (MHBMA-1 and MHBMA-2) and racial/ethnic group, with the exception of

MHBMA-2 in whites. Upon adjustment for smoking dose in the form of TNE, no associations were seen between butadiene metabolites and lung cancer incidence. This suggests that the increase in risk upon increasing butadiene metabolite levels can be explained by tobacco smoke exposure, as both the butadiene biomarkers and TNE are associated with cancer incidence. Therefore, butadiene metabolites MHBMA and DHBMA can be utilized as biomarkers of lung cancer risk in African American and white smokers.

One limitation of our study is that MHBMA 1 and 2 could not be quantified in a large number of smokers. This was due to the limited amounts of urine available, necessitating the use of the same urine sample (200 μL) for quantification of all four biomarkers. To quantify all four biomarkers, the urine samples were loaded onto SPE cartridges as described previously in Chapter 2 for EB-GII. MHBMA and DHBMA were eluted from the cartridges immediately following sample loading with 1 mL of H_2O. The cartridges were then washed with 10% MeOH and EB-GII was eluted with 60% MeOH. With this methodology, sample recovery of MHBMA through SPE was reduced to 41% for MHBMA-1 and 48% for MHBMA-2, as compared to our previously reported recovery of 92%[206]. When sufficient sample quantities are available, separate quantification of BD mercapturic acids and DNA adducts is recommended for optimal sensitivity.

MHBMA-3 (Figure 1.8) was not observed in smoker urine in this study population. Since the initial report of MHBMA-3 as a butadiene metabolite in 2012[165], MHBMA-3 has been quantified in several human studies[165, 186, 187]. The initial methodology identifying MHBMA-3 employed a rapid HPLC gradient and was used for the simultaneous quantification of 28 volatile organic compound (VOC) metabolites[165]. In contrast, the methodology reported in the present study was specifically focused on the metabolites of BD and utilized column cooling to 5 °C in order to achieve better retention and separation of the MHBMA isomers and impurities on the column. Our

experiments revealed three distinct peaks in smoker urine corresponding to the *m/z* = 232.1 → 103.0223 transition for the detection of MHBMA. The first two co-elute with the internal standards for MHBMA 1 and 2, while the third peak elutes over a minute later than the internal standard for MHBMA-3 and exhibits a distinct MS/MS fragment profile as compared to MHBMA 1 and 2. The primary fragment for MHBMA 1 and 2 in smoker urine is *m/z* = 103.0223, representing the loss of the N-acetyl cysteine group. However, for the third peak, the primary observed fragment is N-acetyl cysteine at *m/z* = 162.0230. It is likely that the peak identified by Alwis et al[165] as MHBMA3 is the same species as observed in this study. Based on the MS/MS fragmentation pattern we hypothesize that this species is a mercapturic acid metabolite in human urine. It is possible that this species arises from rearrangement of one of the MHBMA isomers. Further studies are warranted for structural identification of this unknown mercapturic acid.

Urinary levels of BD DNA adduct EB-GII were associated with BD metabolites MHBMA and DHBMA in this study population ($p < 0.0001$). Our previous work has shown moderate associations between EB-GII, MHBMA, and DHBMA in smokers[305]. The moderate strength of the association can be attributed to the fact that urinary butadiene metabolites and DNA adducts represent distinct information regarding biological effects of butadiene exposure. While the mercapturic acids represent the amount of butadiene dose that is detoxified and excreted, EB-GII adducts reflect the fraction of butadiene dose that is bioactivated and bound to genomic DNA (Figure 1.8, Figure 1.10). Urinary EB-GII, because it is representative of the extent of BD-DNA damage and has the highest OR (1.91), can be considered a superior biomarker of lung cancer risk.

We additionally found that urinary EB-GII is associated with other biomarkers of exposure to tobacco smoke. Specifically, urinary EB-GII was strongly associated with tobacco specific biomarkers total nicotine equivalents (TNE) and 4-(methylnitrosamino)-1-(3-pyridyl)-1-butanol

(NNAL). TNE is the sum of nicotine and its metabolites and is utilized as a biomarker of smoking dose and nicotine exposure[308]. NNAL is a metabolite of tobacco specific carcinogen 4-(methylnitrosamino)-1-(3-pyridyl)-1-butanone (NNK) and is associated with racial/ethnic differences in lung cancer risk[309]. Urinary EB-GII was additionally strongly associated with CEMA, a biomarker of exposure to acrylonitrile that is elevated in smokers as compared to non-smokers[310] and 8-iso-PGF2a, a biomarker of inflammation that is elevated in smokers[311]. EB-GII was moderately associated with CYP2A6 activity. CYP2A6 is responsible for the metabolism of nicotine to cotinine and further to *trans*-3′-hydroxycotinine (3-HCOT). Activity of CYP2A6 in smokers is measured by quantifying the ratio of 3-HCOT to cotinine and is a biomarker of lung cancer risk in smokers[297]. EB-GII was additionally moderately associated with 3-HPMA, a biomarker of acrolein that is increased in smokers[312]. Finally, we observed a weak association between urinary EB-GII and 2-HPMA, a metabolite of propylene oxide that is increased in smokers[313]. Similarly, BD-mercapturic acids MHBMA and DHBMA were associated with other biomarkers of tobacco smoke. The observed associations between BD-derived biomarkers and other independently measured biomarkers of tobacco smoke are consistent with smoking being a major source of human exposure to 1,3-butadiene.

In summary, this study suggests that urinary BD biomarkers EB-GII, MHBMA, and DHBMA are associated with incidence of lung cancer, with higher odds ratios and significantly increased urinary EB-GII levels observed in African American subjects. These results suggest that this population of smokers is more susceptible to BD-induced lung cancer. In agreement with our results, previous studies in the Multiethnic Cohort Study show that African Americans are at a higher risk of smoking induced lung cancer[264, 265]. Additionally, BD-derived biomarkers were associated with other measures of exposure to tobacco smoke and no longer predicted lung cancer

risk if adjusted for smoking dose. This is consistent with smoking representing a major source of human exposure to 1,3-butadiene and indicates that the risk for lung cancer is directly related to the amounts smoked. Previous studies have shown that biomarkers of smoking dose, such as TNE and cigarettes per day, are associated with lung cancer incidence[297, 314]. Tobacco smoke carcinogen metabolites, including MHBMA, are additionally associated with lung cancer incidence[185]. Our results in the present study confirm this association between smoking amount and lung cancer incidence.

5. Stable Isotope Labeling to Quantify Endogenous and Exogenous Sources of N7-(1-hydroxy-3-buten-1-yl) Guanine Adducts In Vivo

This work was conducted in collaboration with Erik Moran, Amanda Degner, Dominic Najjar, and Katelyn M. Tessier under the guidance of Natalia Tretyakova. Amanda Degner, Dominic Najjar and Caitlin C. Jokipii Krueger optimized the genomic DNA extraction methodology. Erik Moran extracted genomic DNA from tissues and quantified genomic EB-GII. Katelyn M. Tessier conducted statistical analysis. Caitlin C. Jokipii Krueger optimized existing analytical methodologies for the stable isotope labeling and quantified urinary adducts and metabolites.

5.1 Introduction

Over the course of a lifetime, humans are exposed to a wide variety of electrophilic chemicals. These exposures do not only occur through external/environmental sources, but also include endogenous molecules formed through normal metabolism, inflammation, oxidative stress, and other biological processes[4, 100]. The collective exposure to both exogenous and endogenous electrophiles is known as the exposome[4, 99], where the endogenous exposome focuses on the DNA damage arising from exposure to physiologically generated molecules[100]. Endogenous DNA damage is prevalent in mammalian cells, with total numbers of spontaneously produced DNA lesions estimated to be greater than 40,000 per cell[100].

Because of their ability to induce cancer-causing mutations, carcinogen-DNA adducts are commonly used as mechanism-based biomarkers in risk assessment. DNA adducts represent the biologically relevant dose of carcinogen that is available for binding to DNA and other cellular biomolecules. However, in some cases, endogenous and exogenous DNA adducts are structurally identical, making it challenging to distinguish between internal and external exposures. For example, N7-methylguanine adducts can form both endogenously via reactions of guanine bases of DNA with endogenous cofactor, S-adenosylmethionine (SAM), and upon exposure to exogenous methylating agents such as anticancer agent temozolomide[315] and environmental agent methyl chloride[316]. Stable isotope labeling in combination with mass spectrometry is a powerful tool that can be used to accurately quantify exogenous and endogenous DNA adducts.[79, 102, 106-108, 113-116, 122, 317]. In this approach, cultured cells or animals are treated with a stable isotope labeled carcinogen. DNA adducts originating from this treatment will contain the isotope label, while any endogenously forming adducts will be unlabeled and can be readily distinguished by mass spectrometry. Using this approach, the Swenberg laboratory evaluated exogenous and endogenous

formaldehyde adducts in laboratory animals[79, 106, 107, 113-116]. Formaldehyde is a known human carcinogen formed endogenously and present in environmental sources such as tobacco smoke and automobile exhaust. In the nasal epithelium of F344 rats exposed to [$^{13}CD_2$]-formaldehyde, endogenous N^2-hydroxymethyl-dG adducts were more prevalent than the exogenous adducts until exposure concentrations reached 10 ppm[113]. In the nose, peripheral blood mononuclear cells, bone marrow, and livers of non-human primates exposed to 1 or 6 ppm of [$^{13}CD_2$]-formaldehyde, endogenous dG-Me-Cys DNA protein crosslink adducts were more prevalent than those forming from the exogenous exposures[79]. In F344 rats exposed to low levels of [^{14}C]-ethylene oxide (0.0001-0.1 mg/kg), endogenous N7-(2-hydroxyethyl)guanine adducts were far more prevalent than any forming from the exogenous exposure[103]. In contrast, liver DNA of laboratory rats exposed to 1100 ppm [$^{13}C_2$]-vinyl chloride contained greater amounts of exogenous 7-(2-oxyethyl)guanine than the corresponding endogenous adducts[102, 122]. Acetaldehyde derived N^2-ethylidene-dG adducts were produced mostly from exogenous exposure to [$^{13}C_2$]-acetaldehyde when human lymphoblastoid cells were treated with > 50 μM levels of the electrophile[108] .

As discussed in Chapter 1.4 of this Thesis, human carcinogen 1,3-butadiene (butadiene, BD) is metabolically activated to 3,4-epoxy-1-butene (EB, Figure 1.7)[318], which can be detoxified via conjugation with glutathione to form mercapturic acids MHBMA and DHBMA (Figure 1.8)[164, 167, 168, 272]. BD-mercapturic acids are considered detoxification metabolites and are excreted in urine. If not detoxified, EB can react at nucleophilic sites in DNA to form DNA adducts such as EB-GII (Figure 1.10) [195, 214]. Due to the destabilization of the glycosidic bond resulting from N7-alkylation, these adducts are spontaneously released from the DNA backbone ($t_{1/2}$ = 2.20 ± 0.12 days) and excreted in urine[13, 23, 280]. EB-GII adducts are not thought to be responsible for the carcinogenic

effects of BD due to their instability and the ability to pair with the correct base (cytosine) but are highly abundant and can be used as biomarkers of risk associated with exposure to BD[13, 214, 280].

Urinary MHBMA, DHBMA, and EB-GII have each been previously evaluated as human biomarkers of exposure to 1,3-butadiene. Urinary levels of all three urinary biomarkers are higher in smokers as compared to non-smokers[178, 305]. The concentrations of MHBMA and EB-GII in urine significantly decreased upon smoking cessation[181, 286]. In contrast, the concentrations of DHBMA were unaffected by smoking status, suggesting that it can be formed from another source[181, 286]. In epidemiological studies conducted in a multiethnic cohort of smokers, DHBMA levels differed between ethnic groups[163] and were positively associated with daily alcohol consumption[183]. Importantly, EB-GII [0.19 (95% CI: 0.15-0.22) fmol/mL urine], MHBMA (<2 μg/L urine), and DHBMA (289 (Range: 19.4-2500) μg/L urine) have been observed in the urine of non-smokers with no known exposures to BD[180, 286].

Urinary excretion of endogenous adducts and metabolites of BD by unexposed individuals can complicate the use of these biomarkers in risk assessment, as they can no longer be specifically linked to exogenous exposure to the carcinogen. If endogenous concentrations of these species are comparable to exogenous values, the observed inter-individual differences in biomarker levels could be due to differences in endogenous formation, rather than exogenous exposure and metabolism. In this situation, the biomarker may still represent risk, but not risk specific to the exogenous exposure. Therefore, it is important to quantify the relative contributions of endogenous and exogenous EB-GII, MHBMA, and DHBMA to total biomarker amounts.

Our laboratory has previously developed high-throughput mass spectrometry-based methodologies for accurate quantification of MHBMA, DHBMA, and EB-GII in human urine[206, 286] and EB-GII in genomic DNA[92]. In the present study, stable isotope labeling in combination with

high resolution mass spectrometry methods were employed to quantify endogenous and exogenous urinary BD-metabolites and BD-DNA adducts in urine and tissues of laboratory rats exposed to BD-d_6. Using these methodologies, endogenous and exogenous metabolites and adducts were readily distinguishable due to the presence of an isotope label, affording accurate quantification of background and induced levels of BD-DNA adducts and metabolites.

5.2 Materials and Methods

Chemicals and materials

LC-MS grade water and acetonitrile were purchased from Fisher Scientific (Pittsburg, PA). Strata X polymeric reversed phase SPE cartridges (30 mg/1 mL) were purchased from Phenomenex (Torrance, CA). Oasis HLB reversed-phase cartridges (30 mg) were purchased from Waters (Milford, MA). MHBMA, DHBMA, and d_7-DHBMA standards were purchased from Toronto Research Chemicals (Toronto, ON, Canada). EB-GII and $^{15}N_5$-EB-GII standards were synthesized as previously reported[211, 281]. All other chemicals and solvents were purchased from Sigma-Aldrich (St. Louis, MO) unless otherwise specified.

Animal treatments with d_6-BD and sample collection

All animal treatments were conducted at the Lovelace Biomedical Research Institute (Albuquerque, NM). Forty Sprague-Dawley rats (aged 23-78 weeks) were used in this study. The rats were selected at random and matched by body weight into 4 groups of 10 animals (5 male and 5 female) per group (Table 5.1). Animals of different ages were included to investigate the effects of age on the biomarkers measured in this study, as age could affect the formation of both endogenous and exogenous DNA adducts and metabolites[319, 320]. Prior to exposure, animals were conditioned in metabolism cages for 24 h. Animals were exposed to BD-d_6 gas using a flow past nose-only inhalation chamber for 6 h/day for 7 days. The exposure concentrations were 0.3, 0.5,

and 3 ppm. The control group was exposed to filtered air for 6 h/day for 7 days using a flow past exposure chamber. At the conclusion of exposures on day 7, animals were placed into metabolism cages for 18 h. Urine was collected and stored at -80 °C prior to analysis. Animals were euthanized by intraperitoneal injection of barbiturate based sedative Euthasol, and euthanasia was confirmed by pneumothorax. Following confirmation of death, necropsy was performed to collect liver, pancreas, mammary glands (female only), heart, lungs, and blood samples. These tissues were selected as they are sites for tumor formation upon butadiene exposure of rats[147]. Tissue samples were flash frozen in liquid nitrogen and stored at -80 °C until DNA extraction.

Table 5.1 Design of the animal study and characteristics of study animals

Variable	All mice (N=40)	Controls (N=10)	0.3 ppm (N=10)	0.5 ppm (N=10)	3.0 ppm (N=10)	P-value[1]
Age (weeks)						
Mean (SD)	38.42 (17.77)	40.79 (19.90)	36.06 (16.60)	35.29 (15.49)	41.56 (20.54)	0.788
Median (Range)	23.36 (23.29, 78.29)	38.29 (23.29, 78.29)	23.36 (23.29, 60.86)	23.29 (23.29, 53.29)	38.36 (23.29, 78.29)	
Gender, n (%)						
Female	20 (50.0%)	5 (50.0%)	5 (50.0%)	5 (50.0%)	5 (50.0%)	>0.999
Male	20 (50.0%)	5 (50.0%)	5 (50.0%)	5 (50.0%)	5 (50.0%)	
Weight (grams)						
Mean (SD)	508.33 (173.50)	508.97 (188.34)	521.47 (203.57)	500.92 (165.21)	501.95 (161.03)	0.994
Median (Range)	501.35 (263.10, 957.20)	481.70 (305.70, 852.70)	546.95 (300.90, 957.20)	489.25 (263.10, 768.50)	512.25 (291.90, 768.20)	

[1]Student's t-tests or Kruskal Wallis tests were used for continuous variables, and Chi-square tests were used for categorical variables.

HPLC-ESI$^-$-HRMS/MS analysis of urinary MHBMA and DHBMA

Urine samples were processed as previously described[206], with the exception that MHBMA-d_0 (27 ng) was used as an internal for quantification of MHBMA-d_6. The previously described HPLC-ESI$^-$-MS/MS method[206] was adapted for use with a Dionex UlitMate 3000 RSLCnano HPLC system (Thermo Fisher Scientific Corp., Waltham, MA) fitted with a 5 µL injection loop and interfaced to a Q Exactive Orbitrap instrument (Thermo Fisher Scientific Corp., Waltham, MA). DHBMA eluted as a sharp peak at 7.2 min, while MHBMA eluted as two peaks at 10.7 and 11.5 minutes corresponding to MHBMA-1 and MHBMA-2 (Figure 1.8).

Tandem mass spectrometry analyses were conducted by fragmenting [M-H]$^-$ ions of MHBMA-d_0 (*m/z* 232.1) in the high collision dissociation (HCD) cell of the instrument using the normalized collision energy (NCE) of 25 and isolation width (IW) of 1.0 amu. The resulting fragment ions [M-NaC-H]$^-$ (*m/z* 103.0223) were detected in the mass range of *m/z* 50-270 using an Orbitrap Q Exactive mass analyzer (HRMS) operated at a resolution of 70,000. MHBMA-d_6 was detected using an analogous scan event consisting of fragmentation of *m/z* 238.1 →109.0600. DHBMA was detected by fragmenting the ions at *m/z* 250.1 ([M-H]$^-$) to *m/z* 121.0329 with normalized collision energy (NCE) of 35. DHBMA-d_5 and DHBMA-d_7 were detected through analogous scan events consisting of fragmentation of *m/z* 255.1 → 126.0643 and m/z 257.1194 →128.0768, respectively.

Internal QC samples (pooled rat urine) were included after every 10 samples on 96-well plates. Statistical analyses were conducted to determine coefficient of variation (CV). The %CV of urinary MHBMA-d_6 (ng/mL urine) and DHBMA-d_5 (ng/mL urine) were 4.4% and 6.4%, respectively. Method LOD and LOQ were estimated as $3.3\sigma/S$ and $10\sigma/S$, where S is the slope of the validation curve in synthetic urine and σ is the standard deviation of the slope[307]. Method LOD was 0.11

ng/mL urine and 0.04 ng/mL urine and method LOQ was 0.32 ng/mL urine and 0.13 ng/mL urine for MHBMA and DHBMA, respectively.

NanoLC-ESI$^+$-HRMS/MS analysis of urinary EB-GII

Urine samples were processed as previously described[23, 286, 305]. The previously described nanoLC-ESI$^+$-HRMS[3] method was adapted for use with a Dionex UlitMate 3000 RSLCnano HPLC system (Thermo Fisher Scientific Corp., Waltham, MA) fitted with a 5 µL injection loop and interfaced to a Q Exactive Orbitrap (Thermo Fisher Scientific Corp., Waltham, MA) equipped with a nanospray source. EB-GII (Figure 1.10) eluted as a sharp peak at 17 min.

Tandem mass spectrometry analysis was conducted by fragmenting $[M+H]^+$ ions of EB-GII (*m/z* 222.1) in the HCD cell of the instrument using the NCE of 30 and IW of 1.0 amu. The resulting fragment ion $[Gua+H]^+$ (*m/z* 152.0565) was detected in the mass range of *m/z* 50-270 using the Orbitrap mass analyzer (HRMS) at a resolution of 70,000. The d_6-labeled adducts originating from BD-d_6 treatment were detected using a second MS/MS scan event consisting of fragmentation of *m/z* =228.1 ($[M+H]^+$) to *m/z* 152.0565 ($[Gua+H]^+$). The $^{15}N_5$ labeled internal standard was detected using an third MS/MS scan event consisting of fragmentation of *m/z* 227.1 ($[M+H]^+$) to *m/z* 157.0418 ($[^{15}N_5\text{-Gua}+H]^+$). EB-GII and EB-GII-$d_6$ amounts were determined by comparing the peak areas of extracted ion chromatograms corresponding to the analyte and internal standard using standard curves generated by analyzing known analyte amounts.

Internal QC samples (pooled rat urine) were included after every 10 samples on 96 well plates. Statistical analyses were conducted to determine coefficient of variation (CV). The %CV of urinary EB-GII-d_6 (fmol/mL urine) was 8.5%. Method LOD and LOQ were estimated as $3.3\sigma/S$ and $10\sigma/S$, where S is the slope of the validation curve in synthetic urine and σ is the

standard deviation of the slope[307]. Method LOD was 0.32 fmol/mL urine and method LOQ was 0.96 fmol/mL urine.

NanoLC-ESI$^+$-HRMS/MS analysis of genomic EB-GII

DNA was isolated from frozen rat tissues based on a previously described method[92], with the following modifications to enhance purity. Briefly, 200 mg of tissue was homogenized into 6 mL of cell lysis solution using a TissueRuptor II (Qiagen, Hilden, Germany), followed by the addition of 30 µL of Puregene Proteinase K solution (Qiagen, Hilden, Germany). Samples were incubated overnight to achieve cell lysis, followed by incubation with 30 µL of Puregene RNase A solution (Qiagen, Hilden, Germany) for 2 h for RNA digestion. Proteins were precipitated with 2 mL of Protein Precipitation Solution (Qiagen, Hilden, Germany), followed by centrifugation at 2000 x g for 15 min. DNA was precipitated with 10 mL of isopropyl alcohol and stored at -20 °C overnight, followed by centrifugation at 2000 g to pellet DNA. DNA was reconstituted in 1 mL of 10 mM Tris-HCl, pH 7.5 and subjected to a second incubation with 30 µL of RNase A solution (Qiagen, Hilden, Germany) for 2 h. RNase A was precipitated via the addition of 750 µL of Protein Precipitation Solution (Qiagen, Hilden, Germany), followed by centrifugation at 2000 x g for 15 minutes. 1.75 mL of 24:1 chloroform/isoamyl alcohol (Sigma Aldrich, St. Louis, MO, USA) was added to each sample, vortexed for 20 seconds, and centrifuged at 3100 x g for 15 minutes. The upper layer containing DNA was removed, and DNA was precipitated with the addition of isopropyl alcohol (4 mL). DNA was washed with 70% ethanol in water (1 mL) and 100% ethanol (1 mL).

DNA samples (250 µg) were concentrated under reduced pressure, spiked with 5 fmol of $^{15}N_5$-EB-GII (internal standard for mass spectrometry), and brought to final volume of 100 µL with water. The sample solution was heated at 70 °C for 1 h and filtered through 10K Nanosep spin filter

(Pall, Port Washington, NY, USA). The filtrates were combined with 5 µL of a 0.1 mg/mL solution of dA (HPLC retention time marker) and subjected to offline HPLC cleanup on an Agilent 1260 series HPLC system equipped with a fraction collector and UV detector (Agilent Technologies, Santa Clara, CA, USA). A Supelcosil LC-18-DB column (250 mm x 4.6 mm, 5 µm, Phenomenex, Torrance, CA, USA) was eluted at a flow rate of 1 mL/min with a gradient of 0.4% formic acid in water (A) and acetonitrile (B). Solvent composition began at 0% B and was linearly increased to 10% B over 6 min, 12% B over 6 min, and 60% B over 18 min. The solvent composition was held at 60% B for 1 min, returned to 0% B over 1 min, and maintained at 0% B for 8 min. Under these conditions, dA eluted at 8 min, and the fraction containing EB-GII and its internal standard was collected between 8.9 and 10 min (1.1 mL). Samples were dried under reduced pressure and subjected to a second offline HPLC cleanup step as previously described[286]. Fractions containing EB-GII and its internal standard were dried under nitrogen, reconstituted in 15 µL of 0.01% acetic acid in water, and subjected to nanoLC-ESI$^+$-HRMS/MS analysis as described above for urinary EB-GII.

Statistical Methods

Baseline characteristics and biomarker levels were summarized for all rats and by dose level using descriptive statistics. To investigate the association between exposure levels and baseline characteristics, Student's t-tests or Kruskal Wallis tests were used for continuous variables; Chi-square tests were used for categorical variables. Lab values that were less than the limit of detection (LOD) were imputed with the LOD. To investigate the effect of various covariates on lab outcomes, left-censored linear regression models using maximum likelihood estimation method and linear regression models using least squares estimation method were used. If results were similar, linear regression models using least squares estimation method were presented. Lab outcomes were log

transformed and presented as ratios of geometric means (GM) and 95% confidence intervals (CI). All reported p-values are two-sided and a significance level of 0.05 was used. Statistical analyses were performed using R (version 4.1.2, R Core Team) and SAS (version 9.4, SAS Institute Inc., Cary, North Carolina).

5.3 Results

5.3.1 Urinary excretion of endogenous and exogenous MHBMA and DHBMA

To compare the levels of endogenous and exogenous urinary BD metabolites, MHBMA, MHBMA-d_6, DHBMA, and DHBMA-d_5 were quantified in rats exposed to 0-3 ppm BD-d_6. DHBMA-d_5, rather than DHBMA-d_6, was observed due to the loss of one deuterium upon alcohol dehydrogenase mediated oxidation of EB-diol to HMVK during the formation of DHBMA from BD-d_6 (Figure 1.8). Endogenous and exogenous biomarkers were distinguished based on their molecular weight, as the addition of each deuterium adds 1.0063 mass units (Table 5.2). Figure 2 shows representative chromatograms from control animals exposed to filtered air and animals exposed to 0.5 ppm BD-d_6. In control animals, only the endogenous DHBMA peak was observed (Figure 5.1a). In BD treated animals, both endogenous and exogenous DHBMA and exogenous MHBMA were detected (Figures 5.1b and 5.1d). As expected, deuterated metabolites were not observed in unexposed animals.

Urinary concentrations of MHBMA-d_6 increased upon increasing BD-d_6 exposure levels (0.13 ± 1.70, 138.39 ± 1.44, 101.74 ± 1.98, and 904.61 ± 1.58 ng/mL urine at 0, 0.3, 0.5, and 3 ppm BD respectively, Table 5.3). A similar trend was observed with DHBMA-d_5 (0.04 ± 1.00, 155.11 ± 1.42, 125.90 ± 2.02, and 1188.50 ± 1.40 ng/mL urine at 0, 0.3, 0.5, and 3 ppm BD respectively, Table 5.3). These results indicate that at low ppm exposures (3 ppm), BD derived mercapturic acid

levels correlate with exposure level. However, at sub ppm exposures, urinary concentrations of BD derived mercapturic acids do not correlate with exposure level, with higher metabolite levels at 0.3 ppm as compared to 0.5 ppm (Table 5.3), although this difference is not statistically significant. This lack of association with dose at these low exposures could be explained by differences in urine concentrations among the animals.

The levels of endogenous DHBMA were 566.76 ± 1.58 ng/mL urine (Table 5.3). There were no statistically significant differences in endogenous DHBMA concentrations between the treatment groups ($p = 0.48$, Table 5.4), indicating that endogenous DHBMA formation is unaffected by BD exposure. Additionally, endogenous DHBMA was not associated with age ($p = 0.19$), gender ($p = 0.89$), or weight ($p = 0.85$, Table 5.4). In the two lower treatment groups (0.3 and 0.5 ppm), the concentrations of endogenous DHBMA were 4.3-fold greater than exogenous DHBMA-d_5 originating from BD-d_6. In the highest treatment group (3 ppm), exogenous DHBMA-d_5 was 2.4-fold more abundant than endogenous DHBMA. This provides further evidence for endogenous sources contributing significantly to the overall level of urinary DHBMA, providing possible explanation for the poor association of this biomarker with smoking status[181, 286].

Table 5.2. PRM transitions employed for nanoLC-ESI$^+$-HRMS/MS analysis of endogenous (d_0) and exogenous metabolites and DNA adducts of 1,3-butadiene (d_6)

Analyte	Precursor Ion	Fragment Ion
EB-GII	222.1	152.0565
EB-GII-d_6	228.1	152.0565
MHBMA	232.1	103.0223
MHBMA-d_6	238.1	109.0600
DHBMA	250.1	121.0329
DHBMA-d_5	255.1	126.0643

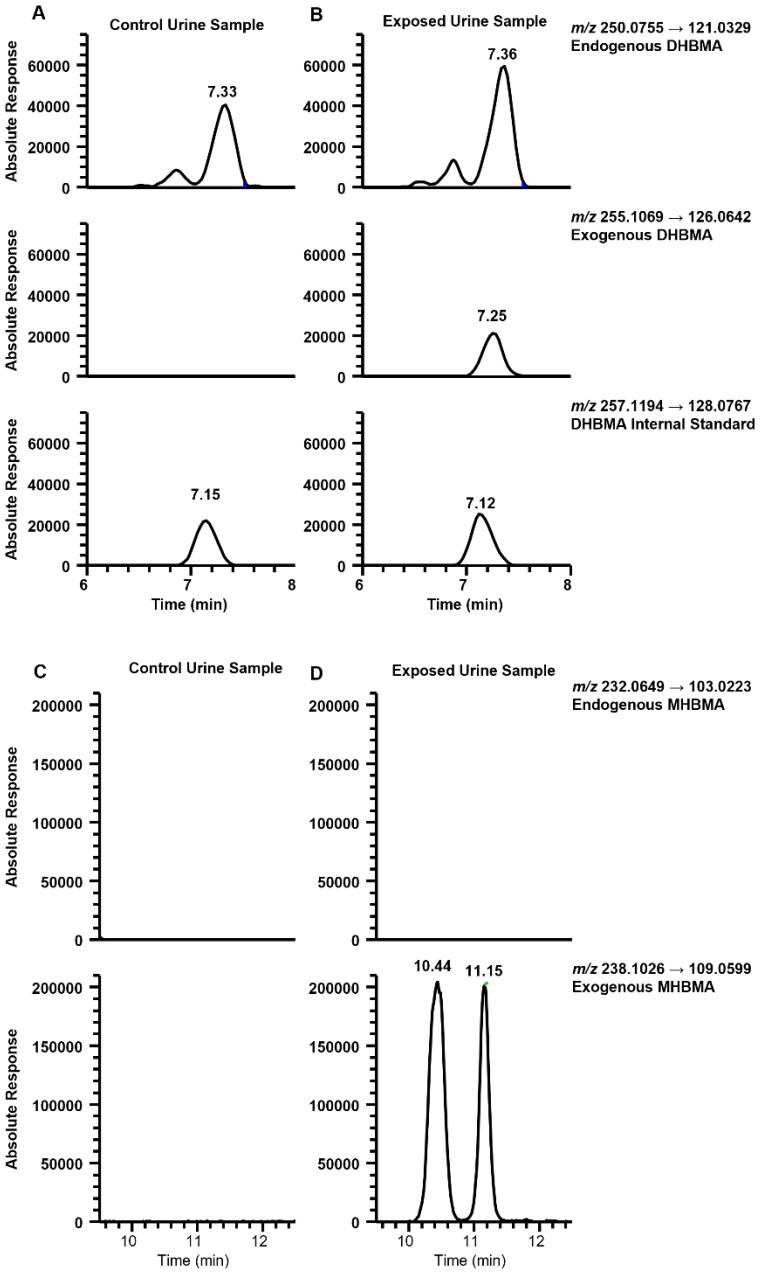

Figure 5.1. Representative nanoLC-ESI^{+}-HRMS/MS traces of BD-mercapturic acid. (a) DHBMA in control urine (b) DHBMA in exposed urine (c) MHBMA in control urine and (d) MHBMA in exposed urine

Table 5.3. Quantitative results for nanoLC-ESI$^+$-HRMS/MS quantification of urinary metabolites and DNA adducts of 1,3-butadiene. Results are shown as geometric means (geometric standard deviation, GSD).

Biomarker		Exposure Level, ppm BD-d_6				
		All	0	0.3	0.5	3
MHBMA (ng/mL urine)	Exogenous	40.33 (28.19)	0.13 (1.70)	138.39 (1.44)	101.74 (1.98)	904.61 (1.58)
	Endogenous	0.00 (NA)	0.00 (NA)	0.00 (NA)	0.00 (NA)	0.00 (NA)
DHBMA (ng/mL urine)	Exogenous	35.45 (49.87)	0.04 (1.00)	155.11 (1.42)	125.90 (2.02)	1188.50 (1.40)
	Endogenous	566.76 (1.58)	591.58 (1.90)	671.43 (1.34)	541.32 (1.56)	490.17 (1.34)
	Ratio	0.06 (52.21)	0.00 (1.90)	0.23 (1.50)	0.23 (1.67)	2.42 (1.24)
EB-GII (fmol/mL urine)	Exogenous	51.37 (20.89)	0.25 (1.00)	124.60 (1.46)	143.86 (1.51)	912.17 (1.29)
	Endogenous	0.56 (2.03)	0.50 (1.64)	0.76 (2.57)	0.41 (1.70)	0.63 (1.80)
	Ratio	91.57 (20.85)	0.50 (1.64)	163.83 (2.40)	354.05 (1.89)	1450.62 (1.71)

Table 5.4. Associations of endogenous urinary DHBMA and EB-GII with exposure concentration and animal age, gender, and weight.

	DHBMA		EB-GII	
	Ratio of GMs (95% CI)	**P-value**	**Ratio of GMs (95% CI)**	**P-value**
Dose				
0	Reference	0.478	Reference	0.224
0.3	1.13 (0.72, 1.78)		1.49 (0.76, 2.92)	
0.5	0.94 (0.61, 1.45)		0.79 (0.40, 1.54)	
3.0	0.81 (0.53, 1.25)		1.29 (0.66, 2.51)	
Age	1.01 (0.996, 1.02)	0.186	0.99 (0.97, 1.01)	0.338
Gender		0.890		0.659
Female	0.96 (0.50, 1.83)		1.24 (0.46, 3.38)	
Male	Reference		Reference	
Starting weight	1.00 (0.998, 1.002)	0.849	1.00 (0.997, 1.003)	0.981

[1]Linear regression was used to investigate the effect of covariates on outcomes. Outcomes were log transformed and presented as ratio of geometric means and 95% CIs.

5.3.2 Urinary excretion of endogenous and exogenous urinary EB-GII

In order to determine the relative contributions of endogenous and exogenous sources to total urinary BD-DNA adduct levels, EB-GII (endogenous adducts) and EB-GII-d_6 (exogenous adducts) were quantified in animals exposed to BD-d_6. Figure 5.2a shows a representative chromatogram for EB-GII quantification in control animals exposed to filtered air. Only endogenously formed unlabeled EB-GII adducts were observed in unexposed animals. Figure 5.2b shows a representative chromatogram from an animal in the 0.5 ppm BD treatment group, revealing a distinct peak corresponding to exogenously formed EB-GII carrying the d_6 isotope label.

The concentrations of endogenous EB-GII were 0.56 ± 2.03 fmol/mL urine (Table 5.3), and there were no statistically significant differences between the treatment groups (p = 0.22, Table 5.4). Additionally, endogenous EB-GII levels were not associated with age, gender, or weight (Table 5.4). In contrast, exogenous EB-GII-d_6 increased in a dose dependent manner (0.25 ± 1.00, 124.60 ± 1.46, 143.86 ± 1.51, and 912.17 ± 1.29 fmol/mL urine at 0, 0.3, 0.5, and 3 ppm BD respectively, Table 5.3). At each treatment level, the concentrations of exogenous adducts were over 160-fold higher than the levels of endogenously formed EB-GII adducts (Table 5.3). These results indicate that while endogenous EB-GII adducts are present in urine, their quantities are small enough to be unlikely to affect risk assessment based on urinary EB-GII quantification. Therefore, urinary EB-GII can be considered a specific biomarker of exposure to butadiene.

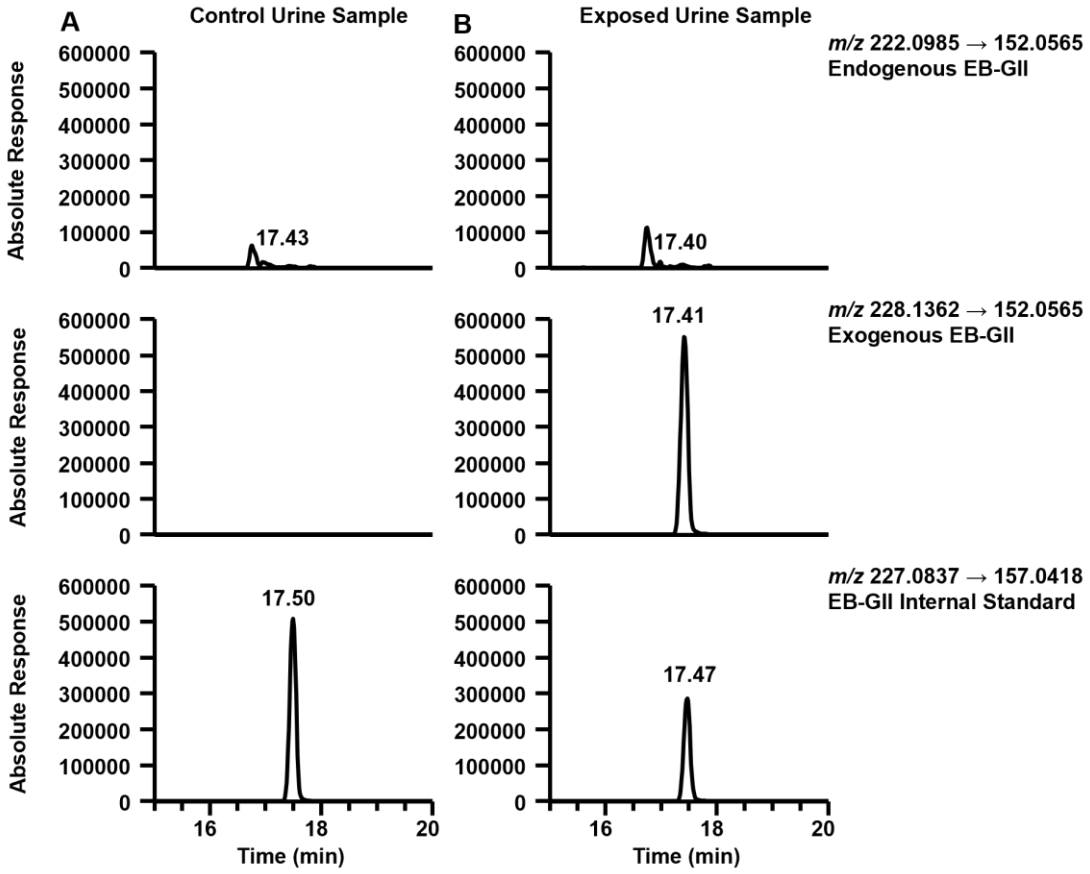

Figure 5.2. Example EB-GII chromatograms. (a) control rat urine and (b) exposed rat urine

5.3.3 Quantification of genomic endogenous and exogenous EB-GII

Genomic EB-GII and EB-GII-d_6 were also quantified in DNA isolated from tissues of BD-d_6 exposed animals (liver, lung, heart, and pancreas). Endogenous EB-GII adducts were observed in each tissue, and their levels were unaffected by BD-d_6 treatment in the lung, heart, and pancreas. (Table 5.5, Table 5.6). Endogenous EB-GII adduct levels in the liver were affected by BD-d_6 treatment, decreasing with increasing levels of BD-d_6 treatment (Table 5.6, $p = 0.04$). This is likely due to the low levels and variable formation of endogenous EB-GII (Table 5.5). In the heart, endogenous adduct levels were associated with age ($p = 0.02$) and weight ($p = 0.02$). Endogenous adduct levels in the pancreas were associated with age ($p = 0.03$) (Table 5.6). Endogenous adduct levels were highest in the heart (0.13 ± 2.07 adducts/10^9 nucleotides) followed by the liver (0.06 ± 2.18 adducts/10^9 nucleotides), pancreas (0.05 ± 6.33 adducts/10^9 nucleotides), and lung (0.03 ± 1.44 adducts/10^9 nucleotides) (Table 5.5).

Exogenous EB-GII-d_6 adducts were absent in genomic DNA of control animals (Table 5.5) and were formed in a dose-dependent manner in each tissue type investigated. In the liver, adduct levels were 0.27 ± 2.85 (0.3 ppm BD-d_6), 0.28 ± 2.21 (0.5 ppm BD-d_6), and 1.02 ± 2.69 adducts/10^9 nucleotides (3 ppm BD-d_6). In the lung, adduct levels were 0.09 ± 1.27 (0.3 ppm BD-d_6), 0.18 ± 1.18 (0.5 ppm BD-d_6), and 1.24 ± 1.21 adducts/10^9 nucleotides (3 ppm BD-d_6). In the heart, adduct levels were 0.16 ± 1.40 (0.3 ppm BD-d_6), 0.28 ± 1.16 (0.5 ppm BD-d_6), and 1.75 ± 1.26 adducts/10^9 nucleotides (3 ppm BD-d_6). In the pancreas, adduct levels were 0.69 ± 1.69 (0.3 ppm BD-d_6), 0.92 ± 1.57 (0.5 ppm BD-d_6), and 7.37 ± 2.08 adducts/10^9 nucleotides (3 ppm BD-d_6).

Table 5.5. Quantitative analysis of genomic EB-GII adducts in tissues of rats treated with BD-d_6. Results are shown as geometric means (GSD).

Tissue		Exposure Level (ppm BD-d_6)				
		All	0	0.3	0.5	3
Liver	Exogenous	0.00 (NA)	0.00 (NA)	0.27 (2.85)	0.28 (2.21)	1.02 (2.69)
	Endogenous	0.06 (2.18)	0.06 (1.91)	0.10 (2.07)	0.06 (1.41)	0.04 (2.47)
	Ratio	0.00 (NA)	0.00 (NA)	2.67 (2.10)	4.77 (2.11)	28.81 (3.08)
Lung	Exogenous	0.00 (NA)	0.00 (NA)	0.09 (1.27)	0.18 (1.18)	1.24 (1.21)
	Endogenous	0.03 (1.44)	0.03 (1.65)	0.03 (1.40)	0.03 (1.27)	0.03 (1.41)
	Ratio	0.00 (NA)	0.00 (NA)	2.91 (1.48)	5.30 (1.35)	38.03 (1.51)
Heart	Exogenous	0.00 (NA)	0.00 (NA)	0.16 (1.40)	0.28 (1.16)	1.75 (1.26)
	Endogenous	0.13 (2.07)	0.13 (1.46)	0.12 (2.74)	0.15 (2.47)	0.11 (1.35)
	Ratio	0.00 (NA)	0.00 (NA)	1.30 (3.40)	1.88 (2.69)	15.63 (1.48)
Pancreas	Exogenous	0.00 (NA)	0.00 (NA)	0.69 (1.69)	0.92 (1.57)	7.37 (2.08)
	Endogenous	0.05 (6.33)	0.04 (31.83)	0.06 (1.85)	0.05 (1.97)	0.05 (2.40)
	Ratio	0.00 (NA)	0.00 (NA)	12.37 (2.25)	19.84 (2.33)	157.51 (3.16)

Table 5.6. Associations of endogenous genomic EB-GII with exposure concentration and animal age, gender, and weight.

Tissue	**Liver**		**Lung**		**Heart**		**Pancreas**	
	Ratio of GMs (95% CI)	**P-value**	**Ratio of GMs (95% CI)**	**P-value**	**Ratio of GMs (95% CI)**	**P-value**	**Ratio of GMs (95% CI)**	**P-value**
Dose		0.043		0.974		0.843		0.981
0	Reference		Reference		Reference		Reference	
0.3	1.70 (0.85, 3.40)		1.00 (0.70, 1.44)		0.81 (0.43, 1.56)		0.93 (0.17, 5.03)	
0.5	1.00 (0.50, 1.99)		1.07 (0.75, 1.54)		1.05 (0.55, 2.00)		0.83 (0.15, 4.43)	
3.0	0.60 (0.31, 1.20)		1.03 (0.72, 1.47)		0.88 (0.47, 1.67)		1.16 (0.22, 6.16)	
Age	1.00 (0.98, 1.02)	0.930	1.00 (0.99, 1.01)	0.410	0.98 (0.96, 0.997)	0.024	0.95 (0.91, 0.99)	0.026
Gender		0.778		0.900		0.095		0.436
Female	1.16 (0.40, 3.31)		0.97 (0.56, 1.68)		2.29 (0.86, 6.12)		2.71 (0.21, 35.19)	
Male	Reference		Reference		Reference		Reference	
Starting weight	1.00 (0.997, 1.003)	0.950	1.00 (0.998, 1.002)	0.919	1.004 (1.001, 1.007)	0.016	1.01 (1.00, 1.013)	0.153

[1]Linear regression was used to investigate the effect of covariates on outcomes. Outcomes were log transformed and presented as ratio of geometric means and 95% CIs.

The ratios of exogenous to endogenous EB-GII adducts varied by butadiene dose and tissue type. Exogenous adducts amounts were greater than the endogenous adducts in the liver (2.67, 4.77, and 28.81 fold), lung (2.91, 5.30, and 38.03 fold), heart (1.30, 1.88, and 15.63 fold), and pancreas (12.37, 19.84, and 157.51 fold) at 0.3, 0.5, and 3 ppm BD-d_6 exposure, respectively (Table 5.5). These results indicate that at sub ppm exposure levels (0.3 and 0.5 ppm), endogenous EB-GII represents a substantial contribution to the overall adduct load in the liver, lung, and heart. In contrast, endogenous EB-GII do not substantially contribute to the overall adduct levels in the pancreas.

5.3.4 Associations between urinary metabolites and DNA adducts of 1,3-butadiene

In order to examine the correlations between various urinary biomarkers of exposure to BD, linear regression analyses were conducted for each metabolite and urinary EB-GII-d_6. Urinary MHBMA-d_6 and DHBMA-d_5 were significantly associated with urinary EB-GII-d_6 ($p < 0.001$, Table 5.7). We did not observe associations between any of the exogenous biomarkers and the age, gender or weight of the animals (Table 5.7). These results indicate that, in laboratory animals, urinary MHBMA, DHBMA, and EB-GII provide similar information.

5.3.5 Associations between urinary and genomic DNA adducts

EB-GII adducts initially form in genomic DNA and are excreted in urine following spontaneous hydrolysis or DNA repair. To determine whether urinary EB-GII adducts can be used as a non-invasive biomarker for genomic EB-GII, we conducted linear regression analyses for urinary and genomic EB-GII-d_6 quantified in various tissues. Urinary EB-GII-d_6 was significantly associated with genomic EB-GII-d_6 in the liver, lung, heart and pancreas ($p < 0.001$, Table 5.8).

These results indicate that urinary EB-GII measurements can be used to estimate the levels of exogenous genomic EB-GII in studies where invasive tissue collections are not feasible.

Table 5.7. Linear regression analyses for urinary biomarkers of exposure to 1,3-butadiene

	MHBMA-d_6		**DHBMA-d_5**		**EB-GII-d_6**	
	Ratio of GMs (95% CI)	**P-value**	**Ratio of GMs (95% CI)**	**P-value**	**Ratio of GMs (95% CI)**	**P-value**
Model with dose						
Dose		<0.001		<0.001		<0.001
0	Reference		Reference		Reference	
0.3	1043.58 (613.38, 1775.49)		3877.72 (2495.25, 6026.13)		498.41 (367.11, 676.67)	
0.5	767.23 (457.06, 1287.89)		3147.56 (2048.14, 4837.13)		575.44 (423.85, 781.26)	
3.0	6821.66 (4063.87, 11450.92)		29712.48 (19334.14, 45661.79)		3648.68 (2687.46, 4953.69)	
Model with dose, age, gender and starting weight						
Dose		<0.001		<0.001		<0.001
0	Reference		Reference		Reference	
0.3	1070.54 (609.27, 1881.05)		3887.46 (2490.70, 6067.53)		507.97 (368.36, 700.49)	
0.5	783.40 (454.67, 1349.79)		3172.53 (2064.35, 4875.61)		583.63 (424.31, 802.76)	
3.0	6763.13 (3934.21, 11626.21)		28999.16 (18903.72, 44486.03)		3614.60 (2631.52, 4964.94)	
Age	1.00 (0.99, 1.02)	0.513	1.01 (0.99, 1.02)	0.364	1.00 (0.995, 1.01)	0.373
Gender		0.720		0.136		0.524
Female	0.87 (0.38, 1.95)		0.62 (0.33, 1.17)		0.86 (0.54, 1.38)	
Male	Reference		Reference		Reference	
Starting weight	0.995 (0.997, 1.002)	0.668	0.999 (0.997, 1.001)	0.442	0.9996 (0.998, 1.001)	0.588
Model with exogenous urinary EB-GII-d_6						
Urinary EB-GII-d_6	1.01 (1.003, 1.008)	<0.001	1.01 (1.004, 1.009)	<0.001		

[1]Left-censored linear regression models using maximum likelihood estimation method and linear regression models using least squares estimation method were used to investigate the effect of covariates on outcomes. Results were similar between the two methods, so linear regression results using least squares estimation are presented. Outcomes were log transformed and presented as ratios of geometric means and 95% CIs.

Table 5.8. Linear regression of log transformed biomarkers with log transformed urinary EB-GII-d_6

Biomarker	Tissue	R	p-value[1]
MHBMA-d_6	Urine	0.99	<0.001
DHBMA-d_5		0.99	<0.001
EB-GII-d_6	Liver	0.72	<0.001
	Lung	0.73	<0.001
	Heart	0.83	<0.001
	Pancreas	0.91	<0.001

[1]Linear regression was used to investigate the associations between urinary EB-GII-d_6 and other exogenous biomarkers. Results are presented as correlation coefficients (R)

5.4 Discussion

While disease risk is often attributed to genetics, environmental factors represent a much larger contribution to risk of disease development[98]. The exposome, a term first described in 2005 to describe the life-course environmental exposures, has been characterized as general external exposures, specific external exposures, and internal exposure[99]. Low level environmental exposures to BD occur through inhalation of automobile exhaust, urban air, and wood burning smoke. Higher specific external exposures are observed in smokers and workers in the polymer industry[189, 269]. Low levels of EB-GII adducts have been detected in unexposed laboratory animals (14.5-87.0 pg/mL urine)[23] and non-smokers with no known external exposures to BD (0.19 (95% CI: 0.15-0.22) fmol/mL urine, Chapter 3)[305]. The presence of BD-DNA adducts originating from internal exposures in humans complicates risk assessment and raises questions about the relative contributions of environmental, dietary, and endogenous sources of DNA damage to cancer development.

Our study is the first to accurately quantify endogenous and exogenous metabolites and adducts commonly used as biomarkers of exposure to BD. We employed animals treated with isotopically labeled BD-d_6 and high resolution mass spectrometry to accurately quantify the contribution of endogenous and exogenous MHBMA, DHBMA, and EB-GII to the overall biomarker levels in biological samples. Previous studies have utilized these metabolites and adducts as biomarkers of tobacco smoke exposure to BD and BD associated cancer risk in humans[23, 163, 178, 181, 183, 286, 305]. These studies attribute these biomarkers as arising from BD exposure and metabolism. However, the presence of endogenous sources of these biomarkers may complicate data interpretation as the biomarkers are not only representative of the metabolism of exogenous exposure.

Our isotope labeling study indicates that DHBMA and, to a smaller extent, EB-GII can form endogenously and are excreted in urine, while the only source of MHBMA is inhalation exposure to 1,3-butadiene. This explains why urinary MHBMA is strongly affected by smoking status while DHBMA is unaffected by smoking cessation[181]. As mentioned above, BD is present in cigarette smoke (16-75 µg/cigarette in mainstream smoke, 205-361 µg/cigarette in sidestream smoke)[269], therefore smoking represents a major source of human exposure to this carcinogen. Our results indicate that urinary MHBMA can be used as an accurate biomarker of exposure to BD.

The ratio of exogenous to endogenous DHBMA varied between 0.23 and 2.42 depending on BD exposure concentration. The endogenous metabolite was more prevalent at the low exposure levels (0.3 and 0.5 ppm) while the exogenous metabolite only become more prevalent at the highest exposure level (3 ppm) (Table 5.3). This indicates that at human exposure levels to BD (~1 ppm for occupationally exposed workers, 16-361 µg/cigarette), endogenous DHBMA represents a significant contribution to measured DHBMA. This helps explain previous reports that DHBMA levels in smokers were unaffected by smoking cessation and did not vary among groups with different risks of lung cancer development[163, 181, 183]. Overall, our results indicate that DHBMA is not an appropriate biomarker for use in assessing risk from exposure to BD.

EB-diol is a metabolic precursor of DHBMA (Figure 1.8). EB-Diol can be further metabolized to 3,4-epoxy-1,2-butanediol (EBD) by cytochromes P450 2E1 and 2A6. Previous studies have quantified the mercapturic acid metabolite of EBD, trihydroxybutyl mercapturic acid (THBMA), and the EBD-DNA adduct N7-2,3,4-trihydroxybutyl guanine (THBG) in smokers and non-smokers[22, 167]. THBMA concentrations were significantly higher in smokers (21.6 ± 10.2 ng/mg creatinine) as compared to non-smokers (13.7 ± 7.9 ng/mg creatinine, $P < 0.01$) and decreased by 25-50% post-smoking cessation. THBG levels were not statistically different between smokers

(8.20 ± 5.12 adducts/10^9 nucleotides) and non-smokers (7.08 ± 5.29 adducts/10^9 nucleotides), and smoking cessation did not result in decreased THBG adducts[22]. THBMA and THBG detected in non-smokers and after smoking cessation in these studies, along with substantial levels of endogenous DHBMA observed in the present work, suggest endogenous sources for EB-diol[164, 167]. Carbohydrate catabolism is a possible endogenous source of EB-diol[22, 162, 167], and therefore DHBMA.

We did not observe any associations between endogenous DHBMA and age, gender, or weight in this study (Table 5.4). This indicates that other factors, such as dietary sources, may be more likely to influence endogenous formation EB-Diol and DHBMA. However, endogenous EB-GII was associated with age in the heart and pancreas and with weight in the heart. This suggests that metabolic processes that are associated with weight and aging may be involved in the formation of endogenous genomic EB-GII DNA adducts. Further studies are underway to identify potential metabolic and dietary precursors of butadiene DNA adducts in cultured human cells.

The contributions of endogenous EB-GII to total urinary adduct levels were low to negligible. Even in the lowest treatment group (0.3 ppm), exogenous EB-GII were over 160-fold more prevalent than the endogenous adducts (Table 5.4). This is in contrast to our results in Chapter 3, showing 5-fold greater levels of urinary EB-GII in smokers as compared to non-smokers[305] and in Chapter 2, showing a 34% decrease in urinary EB-GII following smoking cessation[286]. One possible explanation for this discrepancy is that non-smokers could be exposed to BD in secondhand tobacco smoke, wood burning smoke, and automobile exhaust, as the laboratory animals are not exposed to any of these environmental sources of BD. While endogenous adducts are formed in animals, they represent a very small portion of the adduct load and are unlikely to affect risk assessment using

urinary EB-GII. Therefore, urinary EB-GII can be considered an accurate biomarker of external exposure to BD.

Urinary MHBMA-d_6 and DHBMA-d_5 were highly correlated with urinary EB-GII-d_6 (Table 5.7). These results indicate that urinary DNA adducts and metabolites of EB-GII represent similar BD exposure information, when uncomplicated by the presence of the endogenous biomarkers. This is consistent with our previous studies in smokers, where we observed that MHBMA and DHBMA were associated with EB-GII. However, upon further adjustment for nicotine equivalents as a measure of smoking dose, only the correlation with DHBMA remained[305].

Previous reports[321, 322] and reviews[323, 324] have questioned the use of urinary DNA adducts in risk assessment because they can potentially originate from free nucleotides and RNA rather than genomic DNA. However, our results indicate that urinary and genomic DNA adducts are highly correlated. Urinary EB-GII-d_6 was strongly associated with genomic EB-GII-d_6 in the liver, lung, heart, and pancreas (Table 5.8). Previous studies in our laboratory have utilized urinary EB-GII as a biomarker of BD exposure in smokers and occupationally exposed workers[23, 286, 305]. In such large-scale epidemiological studies, urine is more readily available than genomic DNA. The strong correlation between urinary and genomic EB-GII adducts in rats reported here could be extrapolated to suggest that urinary EB-GII measured in humans is a non-invasive surrogate for genomic EB-GII, further validating the use of urinary EB-GII as a sensitive and specific biomarker of BD exposure in humans. This association should be investigated in future studies in humans where sufficient quantities of urine and genomic DNA are available for the same subjects.

In summary, this study for the first time accurately measured endogenous and exogenous BD-DNA adducts and metabolites in laboratory rats exposed to isotopically labeled BD. We quantified the contribution of endogenous adducts and metabolites to the overall load, showing that MHBMA

and EB-GII are sensitive and specific biomarkers of BD exposure, while DHBMA cannot be used as a biomarker of exogenous BD exposure due to the high endogenous levels of the metabolite. Our results reveal a strong association between urinary and genomic DNA adducts, validating urinary EB-GII as a non-invasive surrogate biomarker for genomic BD DNA damage. These findings support future use of urinary EB-GII and MHBMA as biomarkers of BD exposure and warrant further investigation to identify the sources of endogenous formation of DHBMA and EB-GII.

6. DEB-FAPy-dG Adducts of 1,3-Butadiene: Formation in Diepoxybutane Treated DNA

Adapted with permission from:

Suresh S. Pujari, Caitlin C. Jokipii Krueger, Christopher Chao, Spencer Hutchins, Alexander K. Hurben, Gunnar Boysen, and Natalia Tretyakova. Chem. Eur. J. 2022, 28, e2021032.

Dr. Suresh S. Pujari, with the assistance of Christopher Chao and Alexander Hurben, synthesized and characterized the authentic standards of DEB-FAPy-dG. Gunnar Boysen conducted preliminary cell treatments and quantification of DEB-FAPy-dG. Caitlin Jokipii Krueger developed and validated the mass spectrometry method, treated CT DNA with DEB, and quantified the adducts by mass spectrometry. Spencer Hutchins assisted with CT DNA treatments and adduct quantification.

Additional data included in this chapter generated by Caitlin Jokipii Krueger includes the treatment of MEF cells and nuclei with DEB, preparation of the nuclear protein extract, development of the DEB-FAPy-dG repair assay, and quantification of the adducts in cells, nuclei, and repair assay samples by mass spectrometry. Cell treatments and sample preparation was assisted by Spencer Hutchins and Danielle Chew-Martinez.

6.1 Introduction

1,3-Butadiene (BD) is a known human carcinogen commonly found in automobile exhaust[136], wood burning smoke[135], and is widely used in the rubber and plastic industries[127]. BD is one of the most abundant carcinogens present in cigarette smoke[134]. It induces leukemia and lymphoma, as well as tumors of the lung, ovary, liver, and mammary gland, in laboratory animals[270]. Furthermore, BD causes chromosomal abnormalities and increases the risk of lymphatic and hematopoietic cancer in occupationally exposed workers[125, 126, 149].

BD is metabolically activated by cytochrome 450 monooxygenases CYP2E1 and 2A6 to a reactive epoxide 3,4-epoxy-1-butene (EB)[149, 271]. EB can be further epoxidized to form 1,2,3,4-diepoxybutane (DEB) or hydrolyzed by epoxide hydrolase (EH) to form 1-butene-3,4-diol (EB-diol)[149, 271]. 1,2-dihydroxy-3,4-epoxybutane (EBD) can be formed via two alternative pathways: oxidation of EB-diol and hydrolysis of DEB, with the former pathway predominating (Figure 1.7)[149, 271]. EB, DEB, and EBD are genotoxic and can induce point mutations and deletions; among the three, DEB is by far the most genotoxic and mutagenic[153, 157]. BD-derived epoxides can enter cell nuclei and react with genomic DNA to form covalent DNA adducts at guanine and adenine bases[233]. BD-DNA adducts can cause polymerase errors during DNA replication, potentially leading to mutations and cancer[152, 279, 303, 325].

The N7-position of guanine in DNA is the favored reactive site for simple alkylating agents such as BD-derived epoxides[86, 280, 326, 327]. N7-guanine adducts retain the ability to pair with cytosine[86, 280, 327], but are hydrolytically labile due to the presence of a positive charge on the alkylated base[13, 280, 326, 328]. These adducts undergo two competing reactions: spontaneous depurination to release N7-alkylguanine bases (favored under acidic conditions) and imidazole ring opening to give the formamidopyrimidine (FAPy) lesions (preferred under basic conditions, Figure

6.1)[327]. Imidazole ring scission and alkyl-FAPy formation alters the molecular shape and base pairing preferences of the parent nucleobase, leading to mispairing during DNA replication[329-332]. Alkyl-FAPy lesions are relatively stable and can accumulate in cells over time[326, 327, 333] and have been shown to play a major role in genotoxicity of the liver carcinogen aflatoxin B1[334]. Structurally related unsubstituted FAPy adducts can be formed by a free radical mechanism upon exposure to reactive oxygen species (ROS)[333, 335, 336]. FAPy adducts can be repaired through base excision repair mechanism mediated by 8-oxoguanine glycosylase (OGG1), endonuclease III-like protein (NTHL1), and endonuclease 8-like protein (NEIL1)[337].

Previously, we reported the synthesis and structural characterization of N^6-(2-deoxy-D-*erythro*-pentofuranosyl)-2,6-diamino-3,4-dihydro-4-oxo-5-*N*-(2-hydroxy-3-buten-1-yl)-formamidopyrimidine (EB-FAPy-dG) adducts in DNA exposed to butadiene monoepoxide[86]. EB-FAPy-dG lesions were detected in EB-treated calf thymus DNA and in murine cells in culture (MEF), with higher adduct numbers observed in cells deficient in NEIL1, a DNA repair gene involved in base excision repair[38, 39, 338]. In the present work, we describe the first structural characterization of the corresponding adducts of butadiene derived diepoxide (DEB), N^6-[2-deoxy-D-*erythro*-pentofuranosyl]-2,6-diamino-3,4-dihydro-4-oxo-5-*N*-1-(oxiran-2-yl)propan-1-ol-formamidopyrimidine (DEB-FAPy-dG) (Figure 6.2). DEB-FAPy-dG adducts were detected in DEB-treated calf thymus DNA (CT DNA) using isotope dilution liquid chromatography-high resolution tandem mass spectrometry. To our knowledge, this is the first report of DEB-derived FAPy adducts, which are hypothesized to play a role in genotoxicity of DEB.

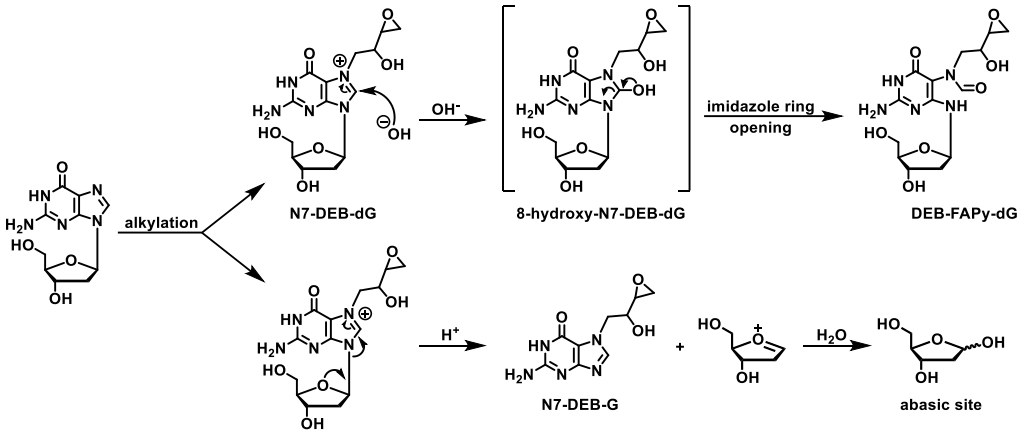

Figure 6.1. Mechanism of apurinic site and formamidopyrimidine formation upon alkylation of deoxyguanosine by DEB.

6.2 Materials and Methods

Synthesis of N^6-[2-deoxy-D-erythro-pentofuranosyl]-2,6-diamino-3,4-dihydro-4-oxo-5-N-1-(oxiran-2-yl)propan-1-ol-formamidopyrimidine (DEB-FAPy-dG)

2-amino-7-(2-hydroxy-2-(oxiran-2-yl)ethyl)-9-((2R,4S,5R)-4-hydroxy-5-(hydroxymethyl)tetrahydrofuran-2-yl)-6-oxo-6,9-dihydro-1H-purin-7-ium (3)

2′-Deoxyguanosine (1 g, 3.74 mmol) was suspended in freshly prepared 10 mM Tris-HCl buffer (30 mL, pH 7.2) and 1,2,3,4-diepoxybutane (DEB) (643 mg, 584 µL, 7.48 mmol) was added dropwise over 10 min. The resulting emulsion was stirred overnight at 37°C. The reaction mixture was filtered to remove the unreacted 2′-deoxyguanosine, and the mother liquor was concentrated and diluted with water (10 ml). The mixture was further chilled at -80°C for overnight and the formed precipitate (unreacted started material) was filtered out. Further, the reaction mixture was purified by preparative HPLC using Sunfire C-18 OBD Prep column, (250 x 19 mm, 14 ml/min flow rate) on an Agilent 1100 HPLC system by the following method. Buffer A: Water, Buffer B: ACN. The solvent composition was changed linearly from 3 to 7% B in 8 min, further to 8% B in 3 min, and held at 8% B for 9 min. Under these conditions, N^7-(2-hydroxy-2-(oxiran-2-yl)ethyl)-dG (**3**) eluted as a broad peak at 8.2 min (130 mg, 10%). It should be noted that under our reaction conditions, the 3,4- epoxy ring of DEB-FAPy-dG remained intact. The epoxide ring could be opened upon extended treatment of adduct **3** with 1 M NaOH to give trihydroxybutyl-FAPy-dG (compound **6**) (Figure 6.2). ESI$^+$MS/MS: *m/z* 354.25 $[M]^+ \rightarrow$ 238.25 $[M\text{-}dR+H]^+$. The UV spectrum of dG monoepoxide (λmax) 274 nm at pH 7.0) is reminiscent of other N7-alkylguanosines, including N7-EB-dG. ^{1}H-NMR (D_2O, 500 MHz) δ 6.30-6.33 (m, 1H, C1′-H), 4.71-4.75 (m, 1H, CH_2), 4.51-4.54 (m, 1H, CH_2), 4.42-4.47 (m, 1H, C3′-H), 4.11-4.13 (m, 1H, CH), 4.01-4.05 (m, 1H, C4′-H), 3.77-3.81 (m, 1H, C5′-H), 3.71-3.72 (m, 1H, C5′-H), 3.21-3.23 (m, 1H, CH_2), 2.86-2.88

(m, 1H, CH), 2.80-2.81 (m, 1H, CH_2), 2.66-2.71 (m, 1H, CH_2-α), 2.54-2.59 (m, 1H, CH_2-β). ^{13}C-NMR (D_2O, 500 MHz) 163.88, 162.66, 149.41, 108.88, 87.88, 86.14, 86.05, 70.37, 68.47, 61.88, 61.05, 61.01, 53.17, 51.64, 44.43, 39.39.

N^6-[2-deoxy-D-erythro-pentofuranosyl]-2,6-diamino-3,4-dihydro-4-oxo-5-N-1-(oxiran-2-yl)propan-1-ol-formamidopyrimidine (4)

N7-alkylated-dG monoepoxide (3, 27 mg) was dissolved in 1M NaOH (3ml) and stirred at room temperature for 1hr. The reaction mixture was further cooled in ice bath for 5 min and immediately neutralized with 20% AcOH to pH 7.0. The reaction mixture was concentrated under reduced pressure and purified by preparative HPLC using Sunfire C-18 OBD Prep column, (250 x 19 mm, 14 ml/min flow rate) on an Agilent 1100 HPLC system by the following method. Buffer A: Water, Buffer B: ACN. The solvent composition was changed linearly from 3 to 7% B in 8 min, further to 8% B in 3 min, and held at 8% B for 9 min. Under these conditions, DEB-FAPy-dG (4) eluted as multiple peaks at 7.02, 8.11 and 8.5 min (130 mg, 10%). UV-Vis λ_{max}: 272 nm (pH = 7.0), 271 nm (pH = 1.0), and 265 nm (pH = 12.0). ESI+MS/MS: m/z 372.26 $[M+H]^+ \rightarrow$ m/z 256.08 [M-dR+H]+ and m/z 372.26 $[M+H]^+ \rightarrow$ m/z 238.17 $[M\text{-}dR\text{-}H_2O+H]^+$. 1H-NMR ($D_2O$, 500 MHz) δ 8.06-8.12 (m, 2H), 7.79-7.84 (m, 2H), 5.13-5.19 (m, 2H), 4.63-4.66 (m, 1H), 4.54-4.59 (m, 1H), 4.44-4.46 (m, 1H), 4.36-4.39 (m, 1H), 4.17-4.22 (1H, m), 3.99-4.06 (m, 1H), 3.95-3.97 (m, 1H), 3.79-3.88 (m, 4H), 3.68-3.74 (m, 3H), 3.63-3.68 (m, 3H), 3.56-3.62 (m, 1H), 3.52-3.56 (m, 3H), 3.47-3.52 (m, 4H), 3.40-3.47 (m, 3H), 3.34-3.40 (m, 1H), 3.07-3.10 (m, 1H), 2.98-3.06 (m, 2H), 2.73-2.79 (m, 3H), 2.64-2.72 (m, 3H), 2.29-2.38 (m, 1H). ^{13}C-NMR (D_2O, 500 MHz) 169.12, 168.81, 167.58, 166.99, 162.85, 160.98, 154.80, 95.08, 91.46, 83.68, 77.26, 68.19, 68.10, 67.94, 67.69, 67.68, 67.63, 67.60, 67.59, 67.53, 67.38, 67.01, 54.34, 53.90, 53.73, 53.33, 47.76, 44.97, 44.79, 44.65, 44.52.

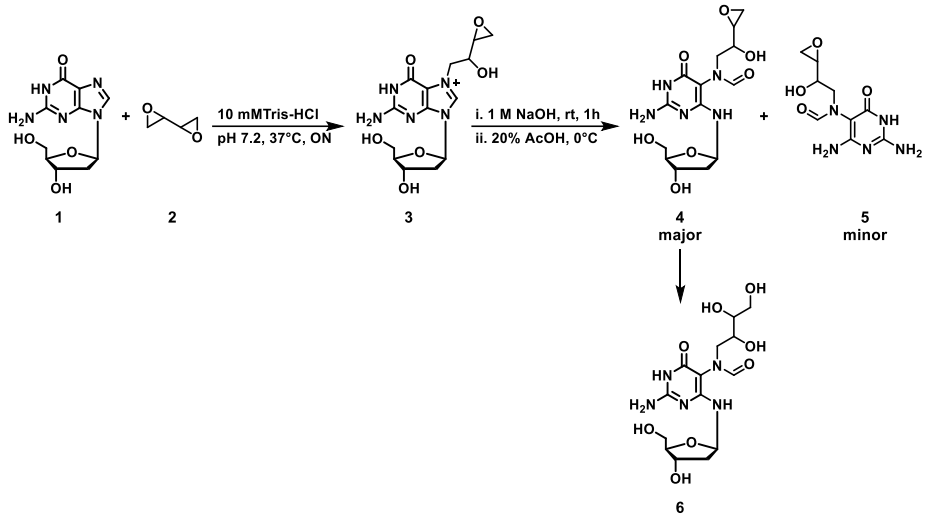

Figure 6.2. Synthesis of DEB-FAPy-dG (6) from 2′-deoxyguanosine (1).

Treatment of Calf Thymus DNA with DEB

To determine dose-dependence of DEB-FAPy-dG at high pH, calf thymus DNA (1 mg in 1 mL of 10 mM Tris-HCl buffer, pH 7.5) was treated with 10 μM, 50 μM, 100 μM, 250 μM, 500 μM, 1mM, 5 mM, or 10 mM DEB at 37 °C for 24 h. The unreacted DEB was extracted with diethyl ether (1 mL) and the DNA was precipitated with cold ethanol (2 mL). The DNA was washed with cold 70% EtOH (1 mL) and cold 100% EtOH (1 mL). DNA was reconstituted in 1 mL of 1N NaOH (pH 12) and incubated for 1 h at room temperature. The solution was neutralized with 1M HCl, followed by ethanol precipitation and washed as described above. DNA was reconstituted in 200 μL of 10 mM Tris-HCl, pH 7.5.

To determine dose-dependence of DEB-FAPy-dG at physiological pH, calf thymus DNA was treated with 500 μM, 1 mM, 5 mM, or 10 mM DEB at 37 °C for 24 h. The unreacted DEB was extracted with diethyl ether, and the DNA was precipitated and washed as described above. DNA was reconstituted in 500 μL of 10 mM Tris-HCl, pH 7.5 and incubated at 37 °C for 72 h.

To determine pH dependence of DEB-FAPy-dG formation, calf thymus DNA was treated with 5 mM DEB at 37 °C for 24 h. The unreacted DEB was extracted with diethyl ether, and the DNA was precipitated and washed as described above. DNA was resuspended in 200 μL Tris-HCl adjusted to pH 7.5, 10, 11, or 12 and incubated at room temperature for 1 h. DNA was precipitated and washed as described above, reconstituted in 500 μL of 10 mM Tris-HCl, pH 7.5 and incubated at 37 °C for 72 h.

Treatment of MEF Cells with DEB

NEIL1$^{-/-}$ and wild type (NEIL1$^{+/+}$) MEF cells were grown in 150 mm tissue culture dishes with DMEM media supplemented with 10% fetal bovine serum in an atmosphere of 5% carbon dioxide, 95% air at 37 °C until approximately 80% confluent. Cells were treated with 0 μM, 100 μM, or 250

μM DEB for 24 h at 37 °C. Cells were washed twice with phosphate buffered saline (PBS) to remove DEB. Cells were treated with trypsin to release from the plate, harvested, and washed twice with PBS. DNA was extracted from cells as previously described[22]. Extracted DNA was incubated at 37 °C for 72 h to allow for formamidopyrimidine formation and processed for analysis as described below.

Treatment of MEF Nuclei with DEB

NEIL1$^{-/-}$ and wild type (NEIL1$^{+/+}$) MEF cells were cultured as described above. Cells were harvested via trypsinization, washed twice with PBS, and re-suspended in 1 mL ice-cold cell lysis buffer (25 mM Tris-HCl (pH 7.5), 0.1% (vol/vol) Triton X-100, 85 mM KCl). The samples were centrifuged at 2,300 g for 5 min at 4 °C. The resulting pellet containing the nuclei was treated with 250 μM DEB in cell lysis buffer for 1 h at 37 °C. Following the treatment, the samples were centrifuged at 2,300 g for 5 min at 4 °C, and the DEB containing supernatant was removed. Nuclei were washed once with cell lysis buffer to remove any remaining DEB. Nuclei were lysed with 0.5 mL of 2% SDS in 20 mM Tris-HCl (pH 7.5), and DNA was extracted as previously described[22]. Extracted DNA was incubated at 37 °C for 72 h to allow for formamidopyrimidine formation and processed for analysis as described below.

Preparation of Nuclear Protein Extract

Nuclear protein extracts were prepared as previously described[339]. In brief, human fibrosarcoma cells (HT1080) were grown in DMEM media supplemented with 10% fetal bovine serum in 150 mm tissue culture dishes in an atmosphere of 5% carbon dioxide, 95% air at 37 °C until confluent. Cells were collected from 15 confluent dishes, washed three times with ice-cold phosphate-buffered saline, and resuspended in 2 mL of buffer A [10 mM Tris (pH 7.4) containing 10 mM KCl, 10 mM MgCl2, 1 mM DTT]. Cells were incubated on ice for 15 min, after which

phenylmethanesulfonyl fluoride (PMSF) was added to a final concentration of 1 mM. Cells were transferred to a Dounce homogenizer and mechanically disrupted by 20 strokes. The mixture was centrifuged at 1500 g for 8 min to collect the nuclei. The nuclei were resuspended in 2 mL of buffer B (buffer A supplemented with 350 mM NaCl, 1 mM PMSF, and cOmplete Mini protease inhibitor cocktail (Roche Diagnostics GmbH, Mannheim, Germany) and incubated on ice for 60 min. The lysed nuclei were then centrifuged at 21,000 g for 30 min at 4 °C. Glycerol was added to 10% of the final concentration of the supernatant, and a 20 μL aliquot was removed for protein quantitation. β-mercaptoethanol was added to a concentration of 10 mM, the nuclear extract was snap-frozen in a dry ice/ethanol bath, and stored at -80 °C. The total protein concentration was measured using the Bradford assay (3.23 mg/mL). Frozen HEK293T extracts were kindly supplied by Dr. Colin Campbell at the University of Minnesota.

Base Excision Repair Assays with Human Fibrosarcoma Nuclear Extracts

CT DNA was treated with 5 mM DEB for 24 h, followed by incubation at pH 12 for 1 h as described above to generate DEB-FAPy-dG containing DNA. Repair assays were performed with 15 μg of DEB-FAPy-dG containing CT DNA in 10 mM HEPES (pH 7.4) buffer containing 100 mM KCl, 1 mM EDTA, 1 mM EGTA, and 0.1 mM DTT in a total volume of 200 μL. Following the addition of nuclear protein extract (50 μg), repair mixtures were incubated at 37 °C for 15, 30, 75, 120, or 180 min. Control samples were incubated without nuclear protein extract added. Heat inactivated controls contained 50 ug of nuclear protein extract that had been heated to 100 °C for 1 h. Following incubation, DNA was precipitated via the addition of 600 μL ice-cold isopropyl alcohol and centrifuged at 15,000 g at 4 °C for 15 min to pellet the precipitated DNA. The supernatant was removed, the DNA was resuspended in 100 μL of 10 mM Tris-HCl (pH = 7.5). 75 μL of Protein Precipitation Solution (Qiagen) was added, samples were vortexed for 30 seconds,

and centrifuged at 2000 g for 15 min to remove remaining nuclear protein extract. The DNA containing supernatant was further subjected to chloroform/isoamyl alcohol extraction. 175 µL of 24:1 chloroform:isoamyl alcohol (Sigma Aldrich) was added to each sample, vortexed for 30 seconds, and centrifuged at 2000 g for 15 min to separate the liquid layers. DNA was precipitated by the addition of 600 µL ice-cold isopropyl alcohol and centrifuged at 15,000 g at 4 °C for 15 min to pellet the precipitated DNA. DNA was processed for nanoLC-ESI$^+$-HRMS/MS analysis detection of DEB-FAPy-dG as described below.

Enzymatic Hydrolysis of DNA and Sample Preparation

DNA (100 µg) was spiked with 350 fmol of $^{15}N_3$-DEB-FAPy-dG as an internal standard for mass spectrometry and enzymatically digested in the presence of 120 mU phosphodiesterase I, 105 mU phosphodiesterase II, 35 U DNase, and 22 U alkaline phosphatase in 200 µL of 10 mM Tris-HCl/15 mM $MgCl_2$ at 37°C for 18 h.

DNA digests were subjected to ultrafiltration through Nanosep 10K filters to remove the enzymes and purified by solid-phase extraction on Hypercarb Hypersep SPE cartridges (100 mg/1 mL). SPE cartridges were conditioned with 2 mL of methanol, followed by 2 mL of water. DNA samples (200 µL) were loaded under neutral pH, washed with 1 mL of water and 1 mL of 30% methanol, and then eluted with 70% methanol in water. SPE fractions were dried under vacuum and reconstituted in 15 µL of 0.05% formic acid in water for nanoLC-ESI$^+$-HRMS/MS analysis.

nanoLC-ESI$^+$-HRMS/MS Analysis of DEB-FAPy-dG

Quantitative analyses of DEB-FAPy-dG were conducted by nanoLC-ESI$^+$-HRMS/MS using a Q Exactive Orbitrap mass spectrometer (Thermo Scientific, Waltham, MA) interfaced with a Dionex Ulitmate 3000 RSLC nanoHPLC system (Thermo Scientific, Waltham, MA). Samples were loaded onto a nanoLC column (0.075 mm x 200 mm) manually packed with Synergi Hydro

RP 80Å (4 μm) chromatographic packing (Phenomenex, Torrance, CA). Gradient elution was achieved using LC/MS-grade water containing 0.05% formic acid (A) and LC/MS grade acetonitrile (B). The initial solvent composition was maintained at 0% B (at 300 nL/min) for 7.5 minutes. The percentage of solvent B was linearly increased to 80% over 9.5 minutes and held at 80% B for 5.5 minutes. Solvent B was returned to 0% over 0.5 minutes, followed by an 11 min column equilibration. Under these conditions, DEB-FAPy-dG and its internal standard eluted at 14.5 minutes.

Electrospray ionization was achieved at a spray voltage of 4000 V and a capillary temperature of 275 °C. Tandem mass spectrometry analysis was performed in the parallel reaction monitoring mode by fragmenting $[M+H]^+$ ions of DEB-FAPy-dG (*m/z* 372.1) in the high collision dissociation (HCD) cell of the instrument using the collision energy (CE) of 20 and an isolation width of 1.0 amu. The resulting fragment ions at *m/z* 238.0935 were detected using the Orbitrap mass analyzer (HRMS) at a mass resolution of 70,000. The $^{15}N_3$ labeled internal standard was detected using an analogous MS/MS scan event consisting of fragmentation of *m/z* 375.1 ($[M+H]^+$). Extracted ion chromatograms corresponding to *m/z* 238.0935 ($[M - dR - H_2O]^+$) were used for quantitation of DEB-FAPy-dG, whereas fragment ions at *m/z* 241.0846 ($[^{15}N_3–M - dR - H_2O]^+$) were used for quantitation of the $^{15}N_3$ labeled internal standard. DEB-FAPy-dG amounts were determined by comparing the areas of the nanoLC/ESI^+-HRMS/MS peaks corresponding to the analyte and its internal standard.

Optimized sample preparation and nanoLC-ESI$^+$-HRMS/MS for simultaneous analysis of DEB-FAPy-dG and THB-FAPy-dG

The nanoLC-ESI$^+$-HRMS/MS method described above was modified in order to enable simultaneous quantification of both DEB-FAPy-dG and THB-FAPy-dG. DNA samples were digested and processed as discussed above, with minor changes to the SPE protocol to better retain THB-FAPy-dG. The second SPE wash step was changed from 30% MeOH to 10% MeOH, as significant amounts of THB-FAPy-dG eluted from the cartridges at 30% MeOH. The HPLC method was modified to improve THB-FAPy-dG peak shape as follows. HPLC solvents were LC/MS-grade water containing 0.05% formic acid (A) and LC/MS grade acetonitrile containing 0.05% formic acid (B). The initial solvent composition was maintained at 0% B and 800 nL/min for 7 minutes. The flow rate was dropped to 300 nL/min over 0.5 min. The percentage of solvent B was linearly increased to 50% over 6.5 min and held at 50% B for 2 minutes. Solvent B was further increased to 80% over 1 min and held for 5.5 min. Solvent B was returned to 0% and the flow increased to 800 nL/min over 0.5 minutes, followed by an 11 min column equilibration. Under these conditions, DEB-FAPy-dG and THB-FAPy-dG eluted between 14.5-15.0 min. The electrospray voltage was lowered from 4000 V to 3000 V, and the capillary temperature was decreased from 275 °C to 250 °C. Tandem mass spectrometry analysis was performed as discussed above for DEB-FAPy-dG. THB-FAPy-dG was detected using an analogous MS/MS scan event consisting of fragmentation of *m/z* 390.1 ($[M+H]^+$) to *m/z* 256.1040 ($[M - dR - H_2O]^+$)

6.3 Results

6.3.1 Development and validation of nanoLC-ESI$^+$-HRMS/MS method for the detection and quantification of DEB-FAPy-dG

Synthetic standards of DEB-FAPy-dG and $^{15}N_3$-DEB-FAPy-dG were used to develop a nanoLC-ESI$^+$-HRMS/MS method for the detection and quantification of DEB-FAPy-dG in CT DNA, cells, and nuclei treated with DEB. 100 μg of DNA was spiked with 350 fmol of $^{15}N_3$-DEB-FAPy-dG, subjected to enzymatic hydrolysis, and enriched via SPE. We investigated DEB-FAPy-dG retention on multiple SPE cartridges (Isolute ENV$^+$ (40 mg/1 mL, Biotage, Charlotte, NC), Strata X polymeric C18 (30 mg/1 mL, Phenomenex, Torrance, CA) and Hypercarb Hypersep (100 mg/1 mL, Thermo Scientific, Waltham, MA) and found that Hypercarb Hypersep was the only stationary phase that retained DEB-FAPy-dG (SPE recovery 58%). SPE fractions containing DEB-FAPy-dG and $^{15}N_3$-DEB-FAPy-dG were concentrated under vacuum and reconstituted in water for nanoLC-ESI$^+$-HRMS/MS analysis.

During nanoLC-ESI$^+$-HRMS/MS method development for DEB-FAPy-dG, several HPLC stationary phases including Hypercarb (Thermo Scientific, Waltham, MA), Synergi Polar RP (Phenomenex, Torrance, CA) and Synergi Hydro RP (Phenomenex, Torrance, CA) were tested with a variety of solvent systems (5 mM ammonium formate, 0.1% formic acid, and 0.05% formic acid with acetonitrile) and various solvent gradients. The best HPLC peak shape and retention were achieved on a Synergi Hydro RP column with a gradient of 0.05% formic acid and acetonitrile. With this method, DEB-FAPy-dG eluted as a complex peak at 14.87 min (Figure 6.3).

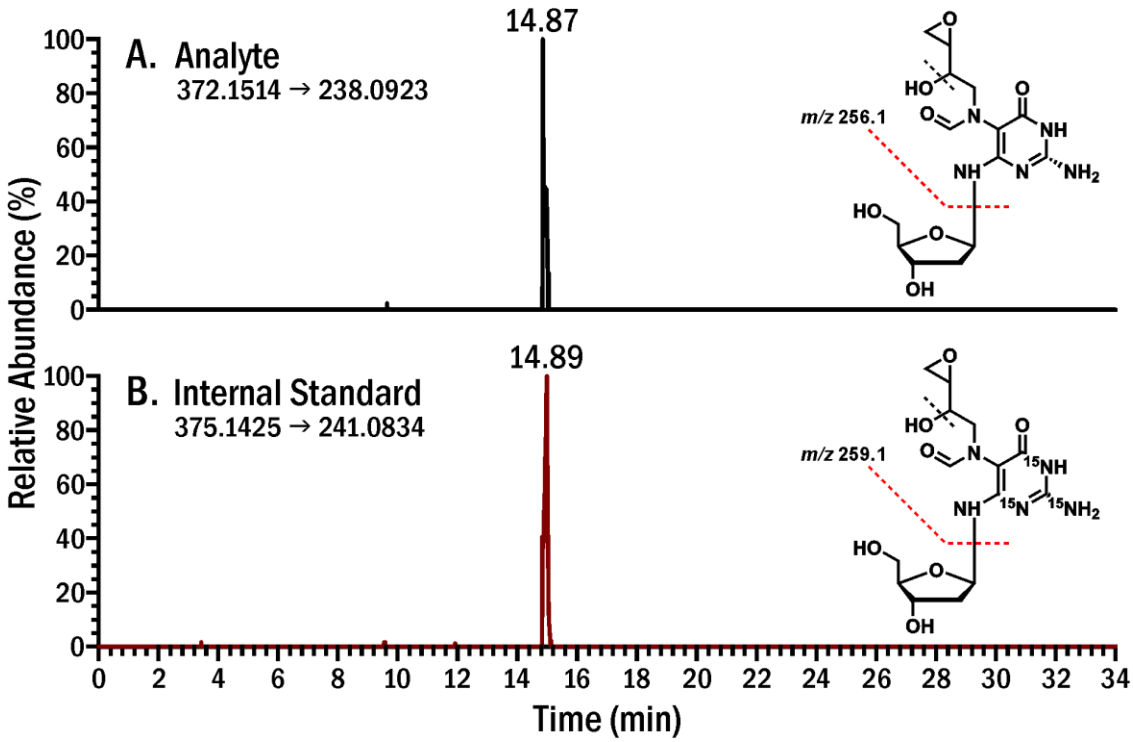

Figure 6.3. Representative nanoLC-ESI^{+}-HRMS/MS traces of DEB-FAPy-dG in CT DNA treated with 50 μM DEB.

NanoLC-ESI$^+$-HRMS/MS analyses were conducted on an Orbitrap Q Exactive mass spectrometer interfaced with a Dionex Ultimate 3000 nano LC system (Thermo Fisher Scientific, Waltham, MA, USA). Instrument resolution was set for 70,000 to allow for excellent selectivity. Quantitative analysis of DEB-FAPy-dG was conducted in the parallel reaction monitoring mode using mass transitions corresponding to the loss of deoxyribose sugar (*m/z* 372.1509 $[M+H]^+ \rightarrow$ 256.1037 $[M-dR+H]^+$) and a loss of 2′-deoxyribose and water (*m/z* 372.1509 $[M+H]^+ \rightarrow$ 238.0923 $[M+H-dR-H_2O]^+$) (Figure 6.3). The $^{15}N_3$-labeled internal standard was monitored using the corresponding signals at *m/z* 375.2349 $[M+H]^+ \rightarrow$ 241.0845 $[M+H-dR-H_2O]^+$ and *m/z* 375.2349 $[M+H]^+ \rightarrow$ 259.0952 $[M+H- dR]^+$ (Figure 6.3). The MS/MS transition corresponding to the neutral loss of both deoxyribose and water provided greater sensitivity and was thus chosen for quantitative analyses, while the second transition was used for confirmation purposes.

The quantitative nanoLC-ESI$^+$-HRMS/MS method for DEB-FAPy-dG was validated by spiking known amounts of analyte (12.5-500 fmol) and internal standard (350 fmol) into calf thymus DNA. A linear correlation was observed between the spiked and calculated amounts of analyte, with an R^2 value of 0.9992 (Figure 6.4).

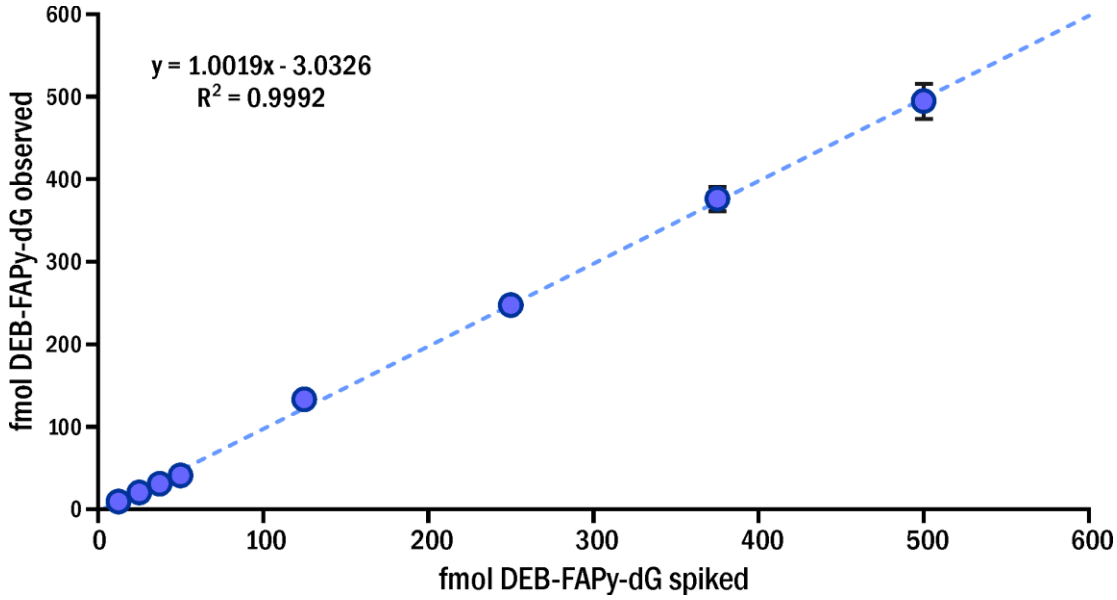

Figure 6.4. Method validation curve for DEB-FAPy-dG

6.3.2 Formation of DEB-FAPy-dG in DEB treated CT DNA

To determine whether DEB-FAPy-dG adducts can form in DNA, calf thymus DNA was treated with increasing amounts of DEB (10 µM to 10 mM). High diepoxide concentrations were chosen in order to facilitate adduct detection. DEB-treated DNA was subjected to enzymatic hydrolysis to 2′-deoxynucleosides, followed by enrichment by solid phase extraction on Hypercarb Hypersep cartridges (Thermo Scientific).

DEB-FAPy-dG formation was investigated at different pH. Aliquots of treated CT DNA were taken and either analyzed directly (physiological pH) or treated with NaOH (pH 12) to induce imidazole ring opening. Samples treated at high pH to induce ring opening exhibited a concentration dependent formation of DEB-FAPy-dG, with adduct numbers ranging from 0.7 to 428.0 DEB-FAPy-dG adducts per 10^6 nucleotides (Figure 6.5a). However, DEB-FAPy-dG lesions were also observed at physiological pH, with amounts approximately 1300-lower than at pH 12 (Figure 6.5b).

In order to establish pH dependence for DEB-FAPy-dG adduct formation, CT DNA was treated with 5 mM DEB at 37 °C for 24 h and subsequently incubated at pH 7.5, 10, 11, and 12 at room temperature for 1 h. DEB-FAPy-dG adducts were observed in all samples, although the amounts were much greater in samples incubated at higher pH (pH 12) (Figure 6.6). This indicates that while DEB-FAPy-dG adducts can form at lower pH, the higher abundance only at pH 12 is consistent with their preferred formation under basic conditions.

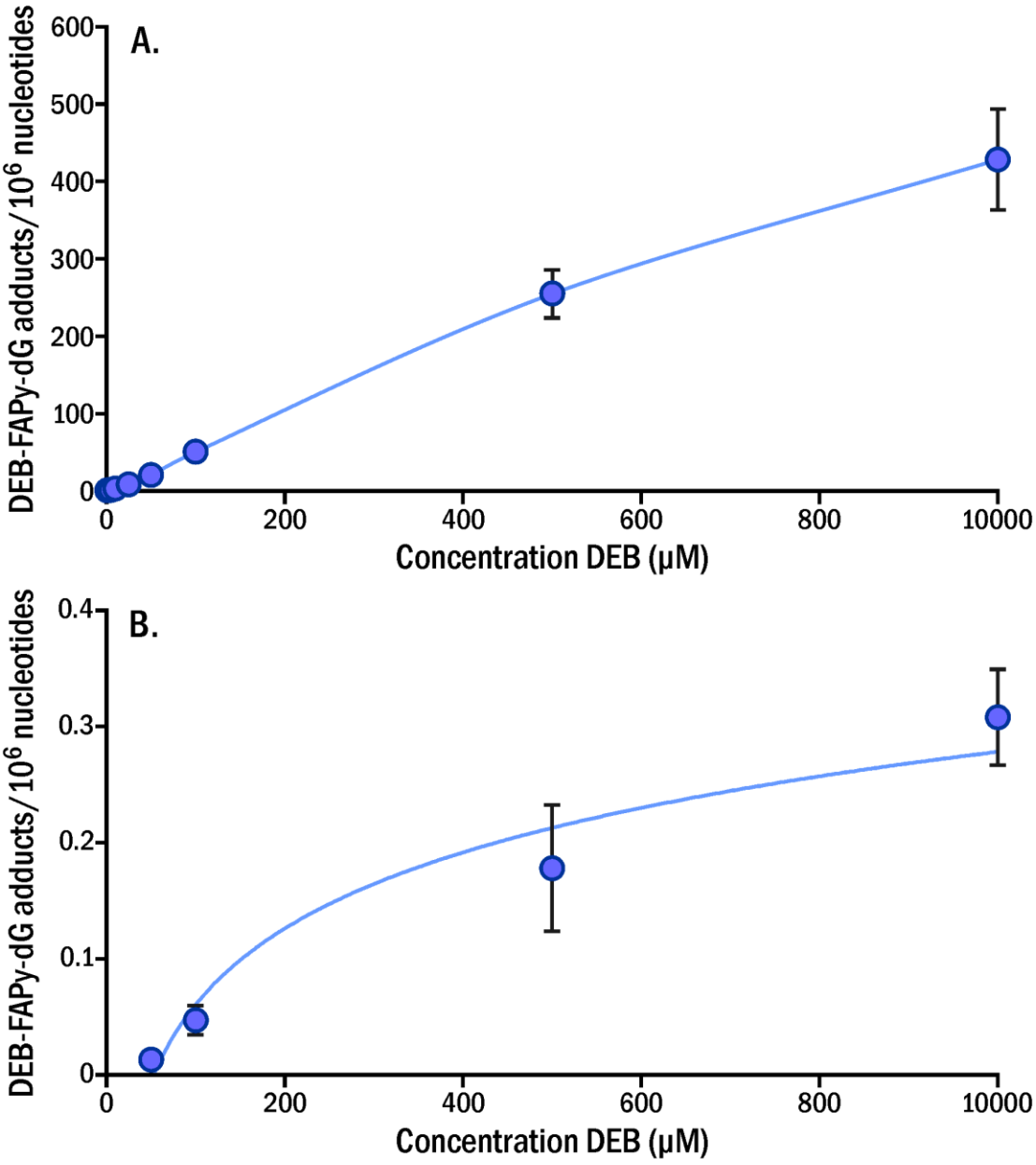

Figure 6.5. Dose-dependent formation of DEB-FAPy-dG under (a) basic (pH 12) and (b) physiological (pH 7.5) conditions.

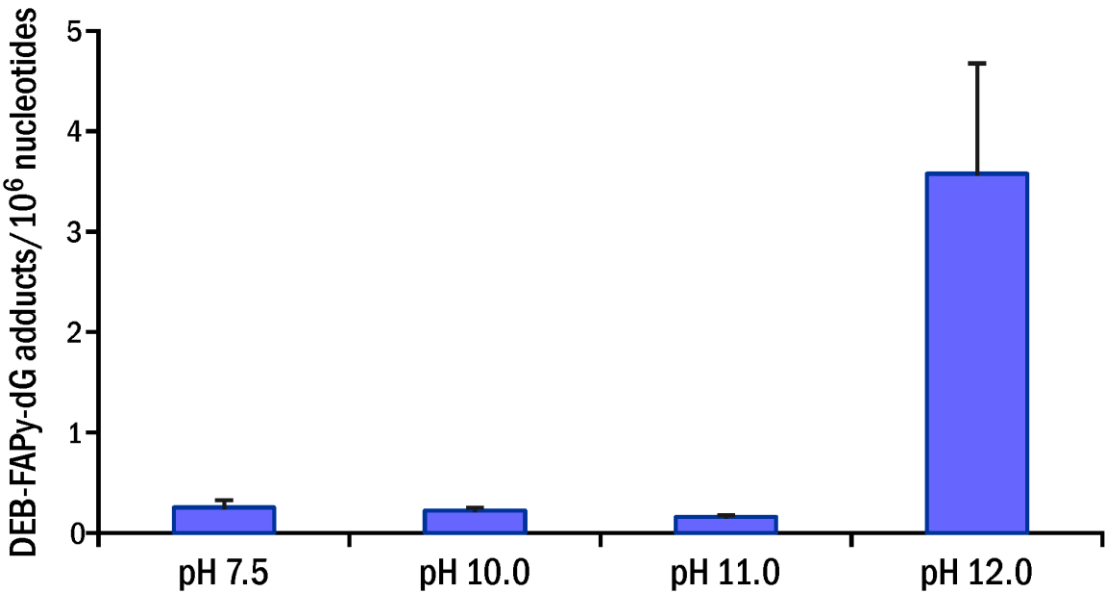

Figure 6.6. pH-dependent formation of DEB-FAPy-dG in CT DNA treated with 5 mM DEB.

6.3.3 Attempted quantitation of DEB-FAPy-dG adducts in DEB treated cells and nuclei

To test the ability of the newly developed method to detect DEB-FAPy-dG adducts in cells, mouse embryonic fibroblast cells were treated for 24 h with 0-250 μM DEB. In a separate experiment, nuclei were treated with 0-250 μM DEB for 1 h. DNA extracted from treated cells and nuclei was incubated for 72 hours at 37 °C following the treatment to facilitate the formation of formamidopyrimidine adducts. We were unable to detect the formation of DEB-FAPy-dG adducts in either the treated cells or nuclei. We additionally investigated the presence of the epoxide ring opened adduct, THB-FAPy-dG (Figure 6.2, **6**), but failed to detect it in any samples.

6.3.4 Investigation of DEB-FAPy-dG repair by human fibrosarcoma nuclear extract

To investigate the ability of nuclear protein extracts to repair DEB-FAPy-dG adducts in DNA, CT DNA was treated with DEB to generate DEB-FAPy-dG adducts and incubated with nuclear protein extract to facilitate repair. DEB-FAPy-dG adduct levels were quantified by our mass spectrometry method. We saw no significant differences in the level of DNA adducts in the DEB control and heat inactivated control samples as compared to any of the nuclear protein extract incubation timepoints (Figure 6.7a). We additionally investigated nuclear protein extracts from different sources and varied extract amounts. DEB containing CT DNA was incubated with varying concentrations of extracts from different sources for 3 h. There was no difference in DEB-FAPy-dG adducts levels among samples treated with fresh or frozen nuclear extract from HT1080 cells, or frozen extract from HEK293T cells (Figure 6.7b).

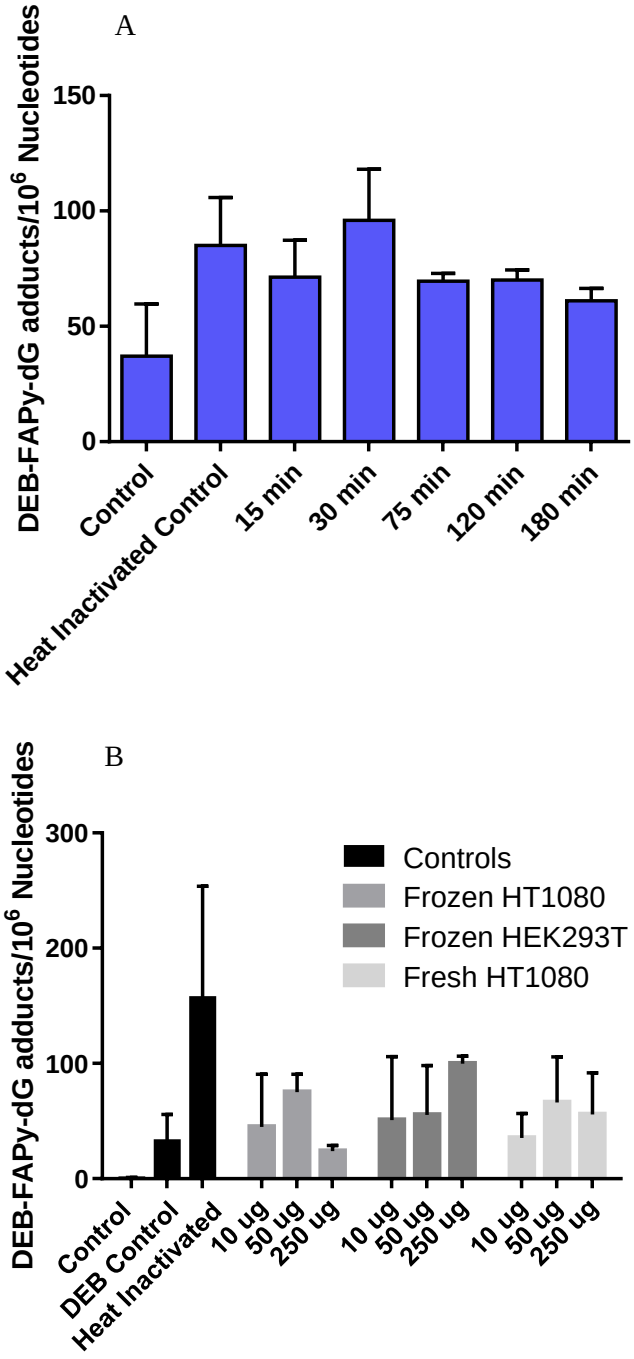

Figure 6.7. (a) Time dependent repair of DEB-FAPy-dG adducts by nuclear protein extract and (b) extract source dependent repair of DEB-FAPy-dG adducts by nuclear protein extract.

6.4 Discussion

1,3-butadiene is a known human carcinogen, inducing lymphatic and hematopoietic cancer in occupationally exposed workers[125-127]. Metabolic activation of BD produces reactive epoxides EB, EBD, and DEB which can alkylate nucleophilic sites in DNA, specifically N7-guanine[149, 233, 271]. While N7-guanine adducts are not expected to be mutagenic, they can be converted to the stable imidazole ring opened formamidopyrimidine adducts, resulting in mispairing during DNA replication[329-332]. Our group has previously reported the synthesis and detection of EB-FAPy-dG adducts in CT DNA and mouse embryonic fibroblast cells[86]. We observed that NEIL1$^{-/-}$ MEF cells were more sensitive to treatment with EB and contained higher levels of EB-FAPy-dG adducts, suggesting EB-FAPy-dG as a substrate for NEIL1[86].

In the present study, we report the first synthesis of N^6-[2-deoxy-D-*erythro*-pentofuranosyl]-2,6-diamino-3,4-dihydro-4-oxo-5-*N*-1-(oxiran-2-yl)propan-1-ol-formamidopyrimidine (DEB-FAPy-dG). Collectively, our mass spectrometry, NMR, and UV spectroscopy results for synthetic DEB-FAPy-dG are consistent with the structure of DEB-FAPy-dG shown in Figure 6.1. Although the molecule was isolated as a mixture of isomers which were difficult or impossible to separate, this represents the structural complexity of DEB-FAPy-dG adducts hypothesized to form in cells. All three stereoisomers of DEB (*S,S, R,R* and *meso*) are produced metabolically upon oxidation of 1,3-butadiene by liver enzymes such as P450 2E1[149, 271].

DEB-FAPy-dG formation was significantly elevated at high pH. While adduct formation was observed in a dose-dependent manner at physiological pH, the amounts were approximately 1300-fold lower than at pH 12 (Figure 6.5). When investigating pH dependence of adduct formation, only at pH 12 does the level of DEB-FAPy-dG adducts observed increase relative to the adduct levels at pH 7.5 (Figure 6.6). This is consistent with the mechanism of DEB-FAPy-dG adduct

formation presented in Figure 6.1, where basic conditions are required for imidazole ring opening to generate the formamidopyrimidine.

We additionally evaluated the formation of DEB-FAPy-dG adducts in NEIL1$^{-/-}$ and wild type (NEIL1$^{+/+}$) mouse embryonic fibroblast cells treated with 0-250 μM DEB. We were unable to detect the formation of DEB-FAPy-dG adducts in these systems. We initially hypothesized that the second epoxide ring opens up to form a triol. However, we were additionally unable to detect the corresponding THB-FAPy-dG adduct that would form from the epoxide opening. We then extracted nuclei from the cells to treat the nuclei directly with DEB, ensuring the DEB was reaching the nucleus. Unfortunately, we again did not detect any DEB-FAPy-dG or THB-FAPy-dG adducts in treated nuclei. It is likely that these adducts form in quantities below our method's limit of detection (12.5 fmol in 100 μg of DNA (0.04 adducts/10^6 nucleotides)), and improvements in the analytical methods sensitivity would allow for adduct detection in cells.

Since NEIL1 is known to repair many alkyl-FAPy adducts, we hypothesized that DEB-FAPy-dG could be a substrate for this repair pathway. To test this hypothesis, we investigated the repair of DEB-FAPy-dG by human fibrosarcoma nuclear extracts that have active base excision repair based on our previous work with other DNA adducts[339]. However, we were unable to detect any repair in calf thymus DNA containing DEB-FAPy-dG, as the levels of DEB-FAPy-dG adducts remained unchanged upon incubation with nuclear protein extract for 15 - 180 min. The use of fresh or frozen nuclear protein extracts from different cell lines (HT1080 or HEK293T) did not impact the levels of DEB-FAPy-dG detected in repair assay samples. It is possible that our failure to detect DEB-FAPy-dG repair is a result of continued formation of these adducts from N7-DEB-dG during the incubation period (Figure 6.1). Our future efforts are to synthesize the

phosphoramidite of DEB-FAPy-dG, incorporate it into an oligonucleotide, and investigate the effects of DEB-FAPy-dG on repair, replication, and transcription.

In terms of their biological effects, ring open alkyl-FAPy adducts are expected to hinder DNA synthesis and/or to mispair during DNA replication[329, 340-343]. For instance, Me-FAPy-dG adducts block DNA polymerases α, β, and hPol δ/PCNA[332]. However, Me-FAPy-dG adducts were bypassed by TLS polymerases η, κ, hRev1/Pol ζ and polymerases η, κ, leading to misinsertion and -1 deletion products[332]. AFB1-FAPy adducts have been shown to be a potent block to DNA synthesis, even when DNA polymerase of lowered replication fidelity was used (MucAB)[334]. AFB1-FAPy-G adducts caused G → T transversions along with G → T mutations in the *ras* oncogene, making them the ultimate lesions responsible for mutagenesis and genotoxicity of aflatoxin[344-347]. In light of these findings, we expect the newly discovered DEB-FAPy-dG lesions, despite their low abundance in cells, will exhibit potent mutagenetic and cytotoxic properties.

In summary, we have successfully synthesized and structurally characterized novel DEB-FAPy-dG and $^{15}N_3$-DEB-FAPy-dG adducts. A sensitive isotope dilution nanoLC-ESI$^+$-MS/MS methodology was developed for the detection and quantitation of DEB-FAPy-dG lesions in DNA. We investigated the formation of DEB-FAPy-dG lesions in CT-DNA treated with DEB, the most genotoxic and carcinogenic metabolite of 1,3-butadiene, and observed concentration dependent adduct formation, which was enhanced at high pH. However, DEB-FAPy-dG adducts could not be detected in cultured human cells treated with DEB, suggesting that they are either formed in low amounts or are rapidly repaired. Further studies are underway to construct DNA strands containing site specific DEB-FAPy-dG adducts in order to establish their effects on DNA replication, transcription, and repair. These future studies will establish whether DEB-FAPy-dG and THB-FAPy-dG could contribute to genotoxicity and mutagenicity of BD.

7. Summary and Conclusions

Lung cancer is the leading cause of cancer related deaths in the United States, with an estimated 236,740 new cases and 130,180 deaths in 2022[256]. About 82% of lung cancer cases are attributable to cigarette smoking[257] and 11-24% of smokers will develop lung cancer in their lifetime[258]. This risk additionally differs by ethnic group; Japanese Americans and Latinos have a lower risk of lung cancer development as compared to whites, and Native Hawaiians and African Americans have a greater risk as compared to whites[265]. Among the 70 carcinogens in tobacco smoke, 1,3-butadiene is one of the most abundant and has the highest cancer risk index[259].

BD is metabolically activated by cytochrome P450s to three reactive epoxides: EB, EBD, and DEB (Figure 1.7). These epoxides can be detoxified through glutathione conjugation to form mercapturic acid metabolites MHBMA, DHBMA, THBMA, and *bis*-BDMA (Figure 1.8). These urinary metabolites have been used as biomarkers of exposure to BD[163, 167, 168, 183, 195, 206]. However, as they are detoxification products, they provide information on carcinogen exposure, not risk associated with exposure. If not detoxified, BD epoxides can form covalent adducts at nucleophilic sites in DNA, leading to mutations and carcinogenesis (Figure 1.10). These DNA adducts represent the biologically relevant dose of BD and are therefore the focus of this dissertation.

In Chapter 2 of this thesis, urinary BD-DNA adduct EB-GII was validated as a non-invasive biomarker of exposure to BD. A highly sensitive and specific nanoLC-ESI$^+$-HRMS^3 methodology previously reported by our group for the detection and quantitation of EB-GII in human urine[23] was updated to utilize 96-well plate sample processing for high-throughput analysis. EB-GII adducts were quantified every two months in 19 smokers over the course of one year. We found that the intraclass correlation coefficient for EB-GII (fmol/mL urine) was 59%, indicating that EB-GII adducts are more variable between individuals than within a single individual, validating the use of

a single measurement as representative of the overall EB-GII levels in an individual. EB-GII adducts were additionally quantified in 17 smoking cessation study participants. We observed a 34% reduction in EB-GII levels within three days post-smoking cessation (Figure 2.4), suggesting smoking as a major source of exposure to 1,3-butadiene and EB-GII adduct formation.

In Chapter 3, we utilized the new high-throughput method developed in Chapter 2 to investigate racial/ethnic differences in urinary EB-GII. We found that EB-GII adducts levels were significantly higher in urine of smokers than non-smokers (0.98 [95%CI: 0.84-1.12] fmol/mL vs 0.19 [95%CI: 0.15-0.22] fmol/mL, $p = 5.8x10^{-34}$, Table 3.2), confirming their association with smoking status. We additionally observed racial/ethnic differences, with Japanese American smokers excreting significantly higher levels of urinary EB-GII as compared to white and Native Hawaiian smokers (Table 3.2). Considering the relatively lower risk for lung cancer in Japanese Americans, the higher level of urinary EB-GII in this group could be explained by more efficient repair of genomic butadiene-DNA adducts. Urinary EB-GII adduct levels were not associated with *GSTT1* gene deletion or CYP2A6 activity variation (Tables 3.3 and 3.4). This lack of association with genetic factors involved in the bioactivation and detoxification of BD further suggests that differences in urinary EB-GII are influenced by other genetic factors such as DNA repair. Our group has previously shown that EB-GII adduct levels are significantly increased in mouse embryonic fibroblasts deficient in base excision repair protein NEIL1$^{-/-}$, as compared to the isogenic strain (NEIL1$^{+/+}$) [86]. We also observed a lack of correlation between urinary DNA adducts and metabolites of BD, indicating that they provide distinct information in epidemiological studies.

We expanded our studies in Chapters 2 and 3 to investigate associations between urinary EB-GII and lung cancer incidence in Chapter 4. We found that urinary EB-GII levels were significantly elevated in lung cancer cases [2.59 (95% CI: 2.24-3.00) fmol/mL urine] as compared to matched

smoker controls [1.65 (95% CI: 1.43-1.91) fmol/mL urine, p = 1.22E-09, Table 4.2]. The odds ratio for urinary EB-GII and lung cancer incidence was 1.91 (Table 4.3), indicating a nearly 2-fold increase in lung cancer risk upon a 1-log unit increase in urinary EB-GII. We additionally observed racial/ethnic differences in the lung cancer risk upon exposure to BD, with a higher OR in African Americans (2.60) than in whites (1.49). Urinary MHBMA and DHBMA were significantly elevated in lung cancer cases as compared to controls. The associations between butadiene biomarkers and lung cancer incidence were no longer significant after adjusting for smoking dose (TNE), suggesting that EB-GII, MHBMA, and DHBMA are biomarkers of lung cancer risk upon exposure to 1,3-butadiene in tobacco smoke.

In Chapters 2 and 3, we observed low but detectable amounts of urinary EB-GII in non-smokers, suggesting the potential of endogenous formation. In Chapter 5, we utilized stable isotope labeling to quantify endogenous and exogenous EB-GII, MHBMA, and DHBMA levels in laboratory rats treated with low ppm levels (0, 0.3, 0.5, 3.0 ppm) of butadiene-d_6. Exogenous urinary EB-GII-d_6 increased in a dose dependent manner (0.25 ± 1.00, 124.60 ± 1.46, 143.86 ± 1.51, and 912.17 ± 1.29 fmol/mL urine at 0, 0.3, 0.5, and 3 ppm BD-d_6 respectively, Table 5.3). Similar trends were observed for exogenous MHBMA-d_6 (0.13 ± 1.70, 138.39 ± 1.44, 101.74 ± 1.98, and 904.61 ± 1.58 ng/mL urine) and exogenous DHBMA-d_5 (0.04 ± 1.00, 155.11 ± 1.42, 125.90 ± 2.02, and 1188.50 ± 1.40 ng/mL urine at 0, 0.3, 0.5, and 3 ppm BD-d_6 respectively, Table 5.3). Endogenous urinary EB-GII (0.56 ± 2.03 fmol/mL urine) and DHBMA (566.76 ± 1.58 ng/mL urine) were unaffected by BD-d_6 dose, while endogenous MHBMA was not detected in any samples. Due to their extremely low levels of endogenous formation, urinary EB-GII and MHBMA were highly specific biomarkers of exogenous exposure to butadiene. However, high levels of DHBMA are formed endogenously, therefore it cannot be considered as a specific biomarker of

exposure to butadiene. Additionally, we observed associations between urinary exogenous EB-GII and genomic exogenous EB-GII (Table 5.8), indicating that urinary adducts can be used as a non-invasive surrogate biomarker of genomic EB-GII DNA damage.

Finally, in Chapter 6, we developed an isotope dilution mass spectrometry-based methodology for the detection and quantification of a novel BD-DNA adduct, DEB-FAPy-dG. Unlike the N7-guanine adducts discussed in the previous chapters of this thesis, alkyl-FAPy adducts are hydrolytically stable and are hypothesized to exhibit mutagenic and cytotoxic properties due to their interference with DNA replication. Using the newly developed methodology, DEB-FAPy-dG was quantified in calf thymus DNA treated with 10 μM to 10 mM DEB. At high pH, adduct levels increased from 0.7 to 428.0 DEB-FAPy-dG adducts per 10^6 nucleotides. At physiological pH, DEB-FAPy-dG adducts were detected in much lower quantities (Figure 6.5). However, our attempts to detect the formation of DEB-FAPy-dG in DEB treated cells and nuclei or to observe repair of DEB-FAPy-dG in calf thymus DNA were unsuccessful.

In summary, the research in this thesis utilized urinary EB-GII as a biomarker of smoking exposure and lung cancer risk in humans. We observed racial/ethnic differences in urinary EB-GII among groups with differing risks of lung cancer development and increased urinary EB-GII in smokers who subsequently developed lung cancer. This work was the first to show the association between urinary butadiene biomarkers and lung cancer incidence. Stable isotope labeling in laboratory rats revealed MHBMA and EB-GII to be sensitive and specific biomarkers of exogenous butadiene exposure, while DHBMA was strongly affected by endogenous exposure and is not a suitable biomarker of butadiene exposure. Finally, a novel isotope dilution mass spectrometry method was developed and validated for BD-DNA adduct DEB-FAPy-dG. This new methodology can be further applied to investigate formation of this adduct in cultured cells and animals.

8. Future Directions

8.1 Quantification of EB-GII adducts in genomic DNA of smokers

In Chapter 3 of this thesis, we quantified urinary EB-GII adducts in smokers belonging to three ethnic groups with varying risks of lung cancer development: Japanese Americans, whites, and Native Hawaiians. We observed significantly higher levels of EB-GII in urine of Japanese American smokers (1.35 [95%CI: 1.04-1.72] fmol/mL) as compared to whites (0.73 [95%CI: 0.56-0.91] fmol/mL, $p = 4.8 \times 10^{-5}$, Table 3.2). The higher levels of urinary adduct excretion among Japanese Americans which does not correlate with their lower lung cancer risk may be representative of more efficient DNA adduct repair. Previous studies from our laboratory have demonstrated the involvement of base excision repair glycosylase NEIL1 in the repair of EB-GII adducts in cells[86]. In the most studied NEIL1 SNP, r4462560, the C/G genotype has been associated with survival in glioma[348] and lower risk of radiation-induced esophageal toxicity and radiation pneumonitis in cancer patients receiving radiation therapy[349]. The C/G genotype is the most prevalent genotype in Japanese (53%) but is less prevalent in Europeans (37%)[350].

We hypothesize that genetic variation in DNA repair, specifically NEIL1, is involved in the racial/ethnic differences observed in urinary EB-GII. We propose to quantify EB-GII in urine and genomic DNA from the same smokers to investigate the relationship between the excreted and persistent adducts. Genomic DNA from smokers can be obtained non-invasively through the collection of saliva samples. We have developed a method for DNA extraction from saliva samples which yields an average of 40 µg of DNA per 2 mL saliva sample. In a preliminary study involving saliva samples from 11 non-smokers and 8 smokers, genomic EB-GII was detected in 3 smokers and not detected in non-smokers. Future studies utilizing greater amounts of genomic DNA from

saliva should be employed to quantify genomic EB-GII adducts in smokers. In the same smokers, urinary EB-GII should be quantified (Figure 8.2). The associations between urinary and genomic DNA adducts in humans will reveal whether more efficient genomic DNA adduct repair results in increased levels of urinary adducts (negative correlation) or if urinary adducts are representative of genomic DNA damage, as we observed in BD exposed rats in Chapter 5 (positive correlation).

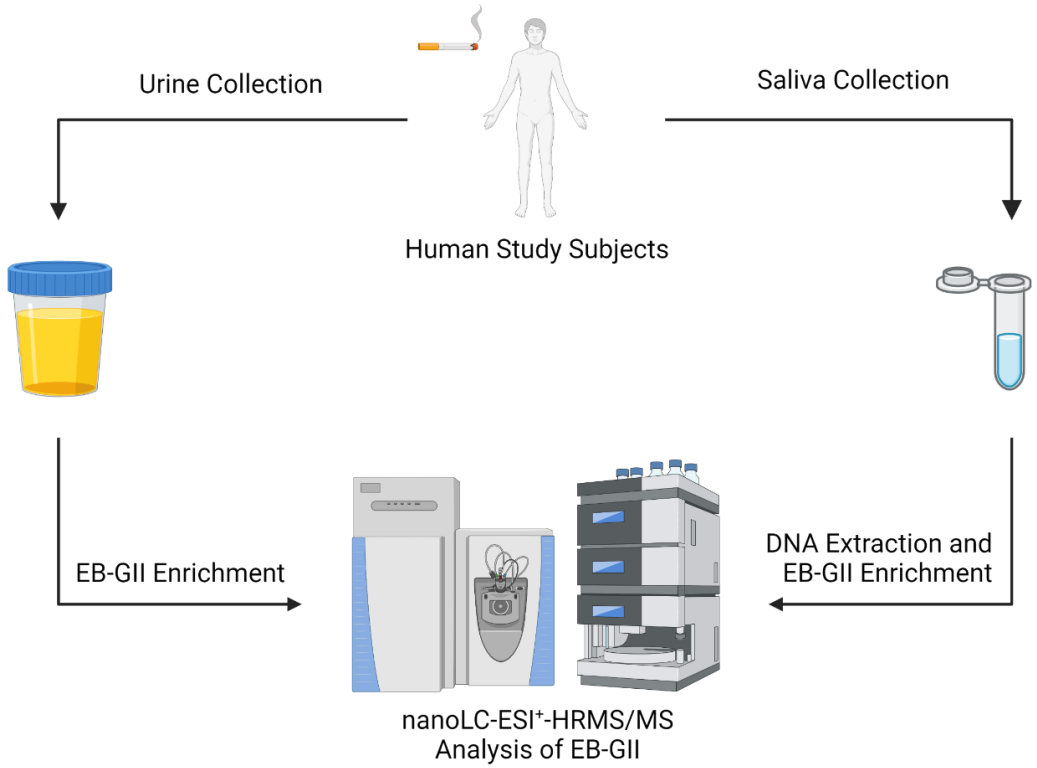

Figure 8.1. Proposed study design quantifying urinary and genomic EB-GII DNA adducts in the same subjects.

Created with Biorender.com

8.2 Identify genetic determinants of EB-GII adduct formation and excretion

In addition to the studies proposed in Chapter 8.1, we recommend the use of a genome wide association study to identify genetic polymorphisms that contribute to urinary EB-GII adduct levels and the observed ethnic/racial differences. In Chapter 3, the subjects were genotyped for selected polymorphisms and we found that urinary EB-GII was not associated with CYP2A6 activity level or GSTT1 copy number. Full genome sequencing for these subjects is currently underway and we hypothesize that a genome wide association study (GWAS) will reveal genetic factors influencing the level of urinary EB-GII in smokers. In addition, the study population should be extended to additional groups (African American and Latino) and larger sample sizes (N=450 per group) to have a high enough frequency of genetic polymorphisms in the study population to identify significant polymorphisms. This study will provide insight on genetic factors responsible for differences in lung cancer risk among racial/ethnic groups. We hypothesize that single nucleotide polymorphisms in DNA repair genes, such as NEIL1, will have significant effects on the levels of urinary EB-GII.

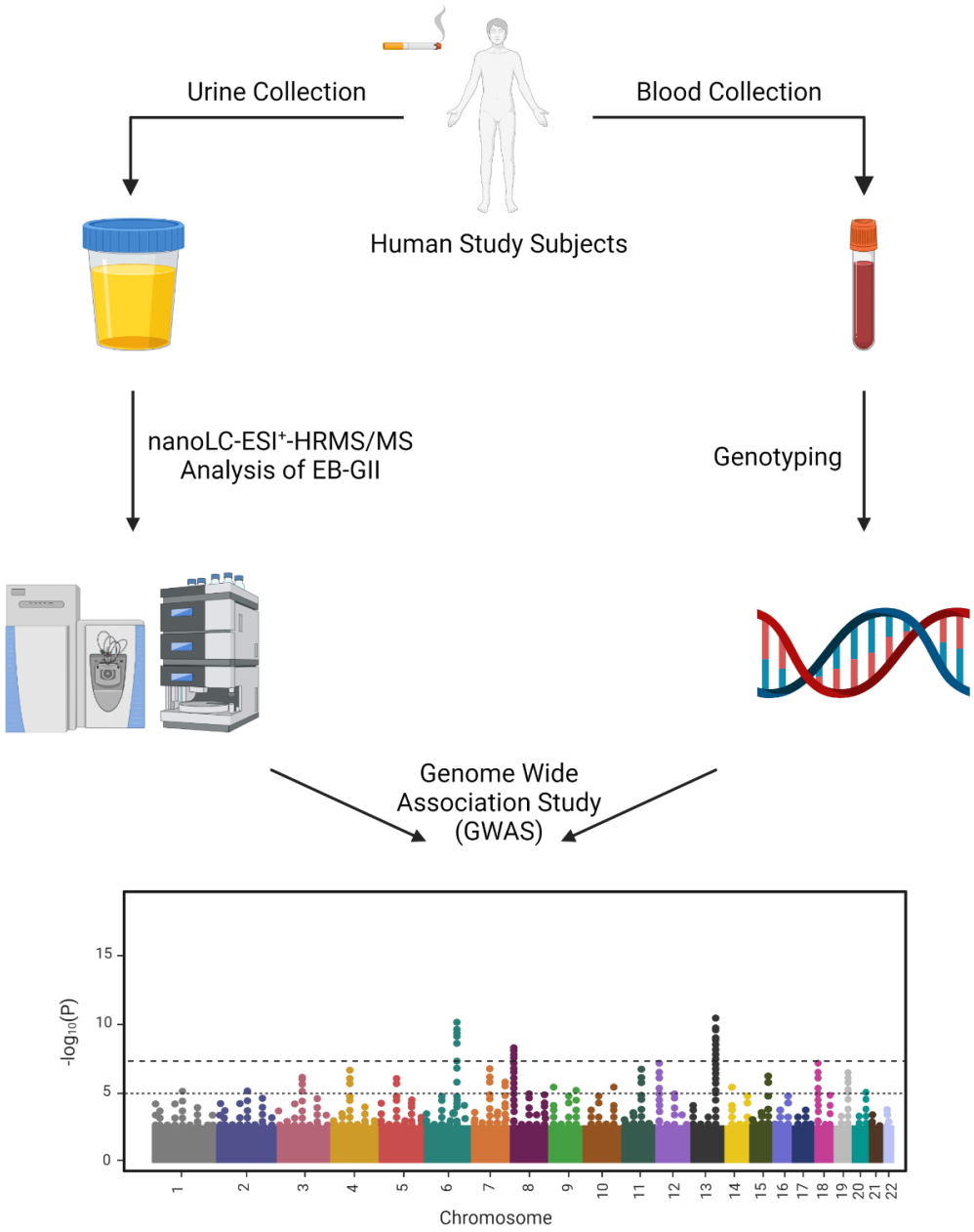

Figure 8.2. Proposed genome wide association study for urinary EB-GII.

Created with Biorender.com

8.3 Quantification of urinary EB-GII in lung cancer cases and controls from additional ethnic groups

In Chapter 4, we quantified urinary EB-GII adducts in lung cancer cases and smoker controls belonging to two racial/ethnic groups: African Americans and whites. We found that urinary EB-GII was associated with lung cancer (OR = 1.91). However, the risk of lung cancer incidence with increased urinary EB-GII levels was different in the two groups, with an OR of 2.60 in African Americans and 1.49 in whites. This association of urinary EB-GII with lung cancer risk should be further explored in additional ethnic groups (Japanese Americans, Latinos, Native Hawaiians) with different risks of cancer development to further investigate the role of 1,3-butadiene in lung cancer risk.

8.4 Characterize the exposome of smokers and investigate associations with race/ethnicity and lung cancer

The studies in Chapters 2-4 focused on one of the most abundant tobacco smoke carcinogens, 1,3-butadiene, and its role in tobacco smoke induced lung carcinogenesis. In Chapter 3, we showed that among racial/ethnic groups with differing risk of cancer development, the excretion of urinary BD-DNA adduct EB-GII is significantly different between groups. Interestingly in this study, we observed significant levels of EB-GII in non-smokers that did not differ by racial/ethnic group, suggesting endogenous sources of formation of this DNA adduct. In Chapter 4, our studies revealed that urinary EB-GII adducts are associated with lung cancer development in smokers. In addition to the targeted quantification of BD biomarkers in smokers reported in this thesis, we propose the use of adductomics methodologies to further characterize the exposome of smokers and to elucidate the mechanisms responsible for the racial/ethnic differences in cancer risk.

Electrophiles are known to react with nucleophilic sites in biomolecules, such as the N-terminal valine in hemoglobin. Hemoglobin adducts provide a unique insight into the exposome, due to the high abundance of hemoglobin in the blood, the lack of repair leading to accumulation of adducts over time, and well-established mass spectrometry methods for their quantification. A modified Edman degradation protocol for the detection and quantification of N-terminal valine adducts has been developed by the Törnqvist group and applied to smokers and non-smokers, identifying seven known and nineteen unknown adducts[351]. We propose the use of this adductomics methodology to characterize the exposome of smokers and identify exposures leading to an increased risk of lung cancer incidence.

8.5 Sources of endogenous BD-DNA adducts

In Chapter 5, we reported the identification and quantification of endogenously forming urinary BD metabolite DHBMA and BD-DNA adduct EB-GII. However, to our knowledge, there are no known endogenous sources of BD. Therefore, further studies are required to identify the sources of trihydroxybutyl and hydroxybutenyl adducts in cells and tissues. Identifying sources of endogenous adducts is vital for identifying potential metabolic, dietary, and lifestyle risk factors for disease development.

Our group has previously reported the formation of BD-DNA adduct THBG at concentrations of 20 adducts/10^9 nucleotides in untreated HT1080 cells[22]. Additionally, THBG adduct levels in humans were not associated with smoking and did not decrease upon smoking cessation[22]. Genomic levels of THBG should be quantified in tissues from the animal study in Chapter 5 to investigate the endogenous formation of THBG. In a preliminary study to identify endogenous sources, we treated HT1080 cells with increasing concentrations of erythrose and erythritol. Erythrose-4-phosphate is a metabolite in the pentose phosphate pathway and erythritol is a zero-calorie sweetener. We did not observe any significant differences in the levels of endogenous adduct formation upon treatment with these potential metabolic and dietary precursors of THBG, indicating that they are not sources of the endogenous THBG formation.

To identify potential metabolic sources of THBG adducts, we propose to treat human cells in culture with stable isotope labeled carbon sources, followed by quantification of isotopically tagged THBG adducts. Treatments with stable isotope labeled cellular metabolites such as glucose and glutamine and detection of any labeled THBG adducts will identify the pathway through which these endogenous adducts are forming and provide further insight into metabolic factors influencing disease.

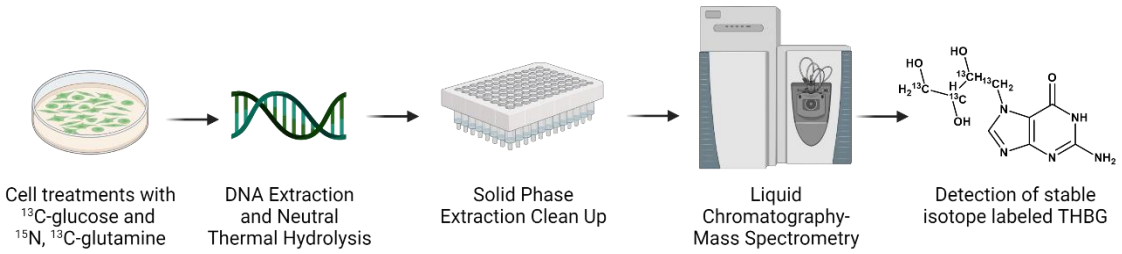

Figure 8.3. Proposed study to identify metabolic pathways of endogenous THBG formation. Created with Biorender.com

8.6 Repair of formamidopyrimidine adducts of 1,3-butadiene

In Chapter 6, we developed and validated a high-resolution mass spectrometry-based methodology for the detection and quantification of DEB-FAPy-dG adducts. Utilizing this novel methodology, DEB-FAPy-dG adducts were detected in a dose dependent formation in CT DNA treated with DEB. Additionally, the formation of DEB-FAPy-dG was investigated in mouse embryonic fibroblast cells treated with DEB, however, we were unable to detect any adducts in DEB treated cells or nuclei. We propose further studies to detect and quantify DEB-FAPy-dG adducts in cells. First, treatments of nuclei with higher concentrations of DEB (500 μM – 1 mM) and for longer times (3 – 6 hours) should be conducted to investigate formation of DEB-FAPy-dG in cellular DNA under stronger treatment conditions.

Additionally, we propose to further investigate the repair of DEB-FAPy-dG adducts in future studies. In the repair studies discussed in Chapter 6, we hypothesized that the lack of observed repair is due to the continued formation of DEB-FAPy-dG adducts from N7-DEB-dG adducts remaining in the DEB treated CT DNA. To remove these N7-DEB-dG adducts, the CT DNA can be heated at 70 °C for 1 hour prior to the incubation with nuclear protein extract. Additionally, the synthesis of the DEB-FAPy-dG phosphoramidite and preparation of DNA oligodeoxynucleotides containing site specific DEB-FAPy-dG adducts is currently underway. Our group has previously reported base excision repair of N^6-deoxyadenosine adducts of BD in short oligodeoxynucleotides by nuclear protein extracts[339]. The availability of DEB-FAPy-dG containing oligonucleotides will allow for similar investigations of DEB-FAPy-dG repair. Upon synthesis of site specifically modified oligodeoxynucleotides, DEB-FAPy-dG repair by recombinant NEIL1 and human fibrosarcoma nuclear protein extracts will be investigated.

Bibliography

1. Lewtas, J., Airborne Carcinogens. *Pharmacology Toxicology* **1993,** *72*, S55-S63.

2. Dayan, A. D., Carcinogenicity and Drinking Water. *Pharmacology Toxicology* **1993,** *72*, 108-115.

3. Abnet, C. C., Carcinogenic food contaminants. *Cancer Invest.* **2007,** *25* (3), 189-96.

4. Wild, C. P., The exposome: from concept to utility. *Int. J. Epidemiol.* **2012,** *41* (1), 24-32.

5. Hwa Yun, B.; Guo, J.; Bellamri, M.; Turesky, R. J., DNA adducts: Formation, biological effects, and new biospecimens for mass spectrometric measurements in humans. *Mass Spec. Rev.* **2020,** *39* (1-2), 55-82.

6. Hemminki, K., DNA adducts, mutations and cancer. *Carcinogenesis* **1993,** *14* (10), 2007-12.

7. Guengerich, F. P., Metabolism of chemcial carcinogens. *Carcinogenesis* **2000,** *21* (3), 345-351.

8. Zhao, M.; Ma, J.; Li, M.; Zhang, Y.; Jiang, B.; Zhao, X.; Huai, C.; Shen, L.; Zhang, N.; He, L.; Qin, S., Cytochrome P450 Enzymes and Drug Metabolism in Humans. *Int. J. Mol. Sci.* **2021,** *22* (23).

9. Medeiros, M., DNA Damage by Endogenous and Exogenous Aldehydes. *J. Braz. Chem. Soc.* **2019**.

10. Rajski, S. R.; Williams, R. M., DNA Cross-Linking Agents as Antitumor Drugs. *Chem. Rev.* **1998,** *98*, 2723-2795.

11. Rendic, S.; Guengerich, F. P., Contributions of human enzymes in carcinogen metabolism. *Chem. Res. Toxicol.* **2012,** *25* (7), 1316-83.

12. van Welie, R. T. H.; van Dijck, R. G. J. M.; Vermeulen, N. P. E.; Van Sittert, N. J., Mercapturic Acids, Protein Adducts, and DNA Adducts as Biomarkers of Electrophilic Chemicals. *Crit. Rev. Toxicol.* **1992,** *22* (5-6), 271-306.

13. Boysen, G.; Pachkowski, B. F.; Nakamura, J.; Swenberg, J. A., The formation and biological significance of N7-guanine adducts. *Mutat. Res.* **2009,** *678* (2), 76-94.

14. Reiner, B.; Zamenhof, S., Studies on the Chemically Reactive Groups of Deoxyribonucleic Acids. *J. Biol. Chem.* **1957,** *228* (1), 475-486.

15. Sancar, A.; Lindsey-Boltz, L. A.; Unsal-Kacmaz, K.; Linn, S., Molecular mechanisms of mammalian DNA repair and the DNA damage checkpoints. *Annu. Rev. Biochem.* **2004,** *73*, 39-85.

16. Minca, E. C.; Kowalski, D., Replication fork stalling by bulky DNA damage: localization at active origins and checkpoint modulation. *Nucleic Acids Res.* **2011,** *39* (7), 2610-23.

17. Hecht, S. S., Lung carcinogenesis by tobacco smoke. *Int. J. Cancer* **2012,** *131* (12), 2724-32.

18. Hecht, S. S., DNA adduct formation from tobacco-specific *N*-nitrosamines. *Mutat. Res.* **1999,** *424*, 127-142.

19. Villalta, P. W.; Hochalter, J. B.; Hecht, S. S., Ultrasensitive High-Resolution Mass Spectrometric Analysis of a DNA Adduct of the Carcinogen Benzo[a]pyrene in Human Lung. *Anal. Chem.* **2017,** *89* (23), 12735-12742.

20. Hecht, S. S., Biochemistry, Biology, and Carcinogenicity of Tobacco-Specific *N*-Nitrosamines. *Chem. Res. Toxicol.* **1998,** *11* (6), 559-603.

21. Goggin, M.; Loeber, R.; Park, S.; Walker, V.; Wickliffe, J.; Tretyakova, N., HPLC-ESI+-MS/MS Analysis of *N*7-Guanine-*N*7-Guanine DNA Cross-Links in Tissues of Mice Exposed to 1,3-Butadiene. *Chem. Res. Toxicol.* **2007,** *20*, 839-847.

22. Sangaraju, D.; Villalta, P.; Goggin, M.; Agunsoye, M. O.; Campbell, C.; Tretyakova, N., Capillary HPLC-accurate mass MS/MS quantitation of N7-(2,3,4-trihydroxybut-1-yl)-guanine adducts of 1,3-butadiene in human leukocyte DNA. *Chem. Res. Toxicol.* **2013,** *26* (10), 1486-97.

23. Sangaraju, D.; Boldry, E. J.; Patel, Y. M.; Walker, V.; Stepanov, I.; Stram, D.; Hatsukami, D.; Tretyakova, N., Isotope Dilution nanoLC/ESI(+)-HRMS(3) Quantitation of Urinary N7-(1-Hydroxy-3-buten-2-yl) Guanine Adducts in Humans and Their Use as Biomarkers of Exposure to 1,3-Butadiene. *Chem. Res. Toxicol.* **2017,** *30* (2), 678-688.

24. Zhang, S.; Balbo, S.; Wang, M.; Hecht, S. S., Analysis of acrolein-derived 1,N2-propanodeoxyguanosine adducts in human leukocyte DNA from smokers and nonsmokers. *Chem. Res. Toxicol.* **2011,** *24*, 119-124.

25. Gorini, F.; Scala, G.; Cooke, M. S.; Majello, B.; Amente, S., Towards a comprehensive view of 8-oxo-7,8-dihydro-2'-deoxyguanosine: Highlighting the intertwined roles of DNA damage and epigenetics in genomic instability. *DNA Repair* **2021,** *97*, 103027.

26. Hemminki, K., DNA-Binding Products of Nornitrogen Mustard, A Metabolite of Cyclophosphamide. *Chem. Biol. Interact.* **1987,** *61*, 75-88.

27. Blommaert, F. A.; Floot, B. G. J.; van Dijk-Knijnenburg, H. C. M.; Berends, F.; Baan, R. A.; Schornagel, J. H.; den Engelse, L.; Fichtinger-Schepman, A. M., The formation and repair of cisplatin-DNA adducts in wild-type and cisplatin-resistant L1210 cells: comparison of immunocytochemical determination with detection in isolated DNA. *Chem. Biol. Interact.* **1998,** *108*, 209-225.

28. Romanski, M.; Rotecki, K.; Nowicki, B.; Tezyk, A.; Glowka, F. K., Liquid chromatography-tandem mass spectrometry method for simultaneous determination of three N-7-guanine adducts of the active epoxides of prodrug treosulfan in DNA in vitro. *Talanta* **2019,** *198*, 464-471.

29. Stornetta, A.; Zimmermann, M.; Cimino, G. D.; Henderson, P. T.; Sturla, S. J., DNA Adducts from Anticancer Drugs as Candidate Predictive Markers for Precision Medicine. *Chem. Res. Toxicol.* **2017,** *30* (1), 388-409.

30. Iyama, T.; Wilson, D. M., 3rd, DNA repair mechanisms in dividing and non-dividing cells. *DNA Repair* **2013,** *12* (8), 620-36.

31. Kaina, B.; Christmann, M.; Naumann, S.; Roos, W. P., MGMT: key node in the battle against genotoxicity, carcinogenicity and apoptosis induced by alkylating agents. *DNA Repair* **2007,** *6* (8), 1079-99.

32. Verbeek, B.; Southgate, T. D.; Gilham, D. E.; Margison, G. P., O6-Methylguanine-DNA methyltransferase inactivation and chemotherapy. *Br. Med. Bull.* **2008,** *85*, 17-33.

33. Duncan, T.; Trewick, S. C.; Koivisto, P.; Bates, P. A.; Lindahl, T.; Sedgwick, B., Reversal of DNA alkylation damage by two human dioxygenases. *Proc. Natl. Acad. Sci. USA* **2002,** *99* (26), 16660-16665.

34. Wei, Y.; Carter, K. C.; Wang, R.; Shell, B., Molecular cloning and functional analysis of a human cDNA encoding an *Escherichia coli* AlkB homolog, a protein involved in DNA alkylation damage repair. *Nucleic Acids Res.* **1996,** *24* (5), 931-937.

35. Sedgwick, B.; Robins, P.; Lindahl, T., Direct Removal of Alkylation Damage from DNA by AlkB and Related DNA Dioxygenases. In *DNA Repair, Part A*, 2006; pp 108-120.

36. D'Augustin, O.; Huet, S.; Campalans, A.; Radicella, J. P., Lost in the Crowd: How Does Human 8-Oxoguanine DNA Glycosylase 1 (OGG1) Find 8-Oxoguanine in the Genome? *Int. J. Mol. Sci.* **2020,** *21* (21).

37. Banda, D. M.; Nunez, N. N.; Burnside, M. A.; Bradshaw, K. M.; David, S. S., Repair of 8-oxoG:A mismatches by the MUTYH glycosylase: Mechanism, metals and medicine. *Free Radic. Biol. Med.* **2017,** *107*, 202-215.

38. Hazra, T. K.; Izumi, T.; Boldogh, I.; Imhoff, B.; Kow, Y. W.; Jaruga, P.; Dizdaroglu, M.; Mitra, S., Identification and characterization of a human DNA glycosylase for repair

of modified bases in oxidatively damaged DNA. *Proc. Natl. Acad. Sci. USA* **2002,** *99* (6), 3523-3528.

39. Hazra, T. K.; Kow, Y. W.; Hatahet, Z.; Imhoff, B.; Boldogh, I.; Mokkapati, S. K.; Mitra, S.; Izumi, T., Identification and characterization of a novel human DNA glycosylase for repair of cytosine-derived lesions. *J. Biol. Chem.* **2002,** *277* (34), 30417-20.

40. Bandaru, V.; Sunkara, S.; Wallace, S. S.; Bond, J. P., A novel human DNA glycosylase that removes oxidative DNA damage and is homologous to *Escherichia coli* endonuclease VIII. *DNA Repair* **2002,** *1*, 517-529.

41. Pearl, L. H., Structure and function in the uracil-DNA glycosylase superfamily. *Mutat. Res.* **2000,** *460*, 165-181.

42. Thompson, P. S.; Cortez, D., New insights into abasic site repair and tolerance. *DNA Repair* **2020,** *90*, 102866.

43. Wilson, D. M., 3rd; Barsky, D., The major human abasic endonuclease: formation, consequences and repair of abasic lesions in DNA. *Mutat. Res.* **2001,** *485*, 283-307.

44. Beard, W. A.; Wilson, S. H., Structure and Mechanism of DNA Polymerase β. *Biochemistry* **2017,** *53* (17), 2768-2780.

45. Sallmyr, A.; Rashid, I.; Bhandari, S. K.; Naila, T.; Tomkinson, A. E., Human DNA ligases in replication and repair. *DNA Repair* **2020,** *93*, 102908.

46. Wilson, D. M., 3rd; Bohr, V. A., The mechanics of base excision repair, and its relationship to aging and disease. *DNA Repair* **2007,** *6* (4), 544-59.

47. You, J. S.; Wang, M.; Lee, S. H., Biochemical analysis of the damage recognition process in nucleotide excision repair. *J. Biol. Chem.* **2003,** *278* (9), 7476-85.

48. Spivak, G., Nucleotide excision repair in humans. *DNA Repair* **2015,** *36*, 13-18.

49. Gillet, L. C. J.; Scharer, O. D., Molecular Mechanisms of Mammalian Global Genome Nucleotide Excision Repair. *Chem. Rev.* **2006,** *106* (2), 253-276.

50. Li, X.; Heyer, W. D., Homologous recombination in DNA repair and DNA damage tolerance. *Cell Res.* **2008,** *18* (1), 99-113.

51. Chang, H. H. Y.; Pannunzio, N. R.; Adachi, N.; Lieber, M. R., Non-homologous DNA end joining and alternative pathways to double-strand break repair. *Nat. Rev. Mol. Cell Biol.* **2017,** *18* (8), 495-506.

52. Jiricny, J., The multifaceted mismatch-repair system. *Nat. Rev. Mol. Cell Biol.* **2006,** *7* (5), 335-46.

53. Haufroid, V.; Lison, D., Mercapturic acids revisited as biomarkers of exposure to reactive chemicals in occupational toxicology: a minireview. *Int. Arch. Occup. Environ. Health* **2005,** *78* (5), 343-54.

54. Mathias, P. I.; B'Hymer, C., Mercapturic acids: recent advances in their determination by liquid chromatography/mass spectrometry and their use in toxicant metabolism studies and in occupational and environmental exposure studies. *Biomarkers* **2016,** *21* (4), 293-315.

55. Törnqvist, M.; Fred, C.; Haglund, J.; Helleberg, H.; Paulsson, B.; Rydberg, P., Protein adducts: quantitative and qualitative aspects of their formation, analysis and applications. *J. Chromatogr. B* **2002,** *778*, 279-308.

56. Carlsson, H.; Tornqvist, M., An Adductomic Approach to Identify Electrophiles In Vivo. *Basic. Clin. Pharmacol. Toxicol.* **2017,** *121 Suppl 3*, 44-54.

57. Preston, G. W.; Phillips, D. H., Protein Adductomics: Analytical Developments and Applications in Human Biomonitoring. *Toxics* **2019,** *7* (2).

58. Rundle, A., Carcinogen-DNA adducts as a biomarker for cancer risk. *Mutat. Res.* **2006,** *600* (1-2), 23-36.

59. Paiano, V.; Maertens, L.; Guidolin, V.; Yang, J.; Balbo, S.; Hecht, S. S., Quantitative Liquid Chromatography-Nanoelectrospray Ionization-High-Resolution Tandem Mass Spectrometry Analysis of Acrolein-DNA Adducts and Etheno-DNA Adducts in Oral Cells from Cigarette Smokers and Nonsmokers. *Chem. Res. Toxicol.* **2020,** *33* (8), 2197-2207.

60. Cheng, G.; Guo, J.; Carmella, S. G.; Lindgren, B.; Ikuemonisan, J.; Jensen, J.; Hatsukami, D. K.; Balbo, S.; Hecht, S. S., Increased Acrolein-DNA Adducts in Buccal Brushings of e-Cigarette Users. *Carcinogenesis* **2022**.

61. Magagnotti, C.; Pastorelli, R.; Pozzi, S.; Andreoni, B.; Fanelli, R.; Airoldi, L., Genetic polymorphisms and modulation of 2-amino-1-methyl-6-phenylimidazo[4,5-b]pyridine (PhIP)-DNA adducts in human lymphocytes. *Int. J. Cancer* **2003,** *107* (6), 878-84.

62. Jones, D. J. L.; Singh, R.; Emms, V.; Farmer, P. B.; Grant, D.; Quinn, P.; Maxwell, C.; Mina, A.; Ng, L. L.; Schumacher, S.; Britton, R. G., Determination of N7-glycidamide guanine adducts in human blood DNA following exposure to dietary acrylamide using liquid chromatography/tandem mass spectrometry. *Rapid Commun. Mass Spectrom.* **2022,** *36* (6), e9245.

63. Souliotis, V. L.; Dimopoulos, M. A.; Sfikakis, P. P., Gene-specific Formation and Repair of DNA Monoadducts and Interstrand Cross-links after the Therapeutic Exposure to Nitrogen Mustards. *Clin. Cancer Res.* **2003,** *9*, 4465-4474.

64. Welters, M. J.; Braakhuis, B. J.; Jacobs-Bergmans, A. J.; Kegel, A.; Baan, R. A.; van der Vijgh, W. J.; Fichtinger-Schepman, A. M., The potential of plantinum-DNA adduct

determination in ex vivo treated tumor fragments for the prediction of sensitivity to cisplatin chemotherapy. *Ann. Oncol.* **1999,** *10* (1), 97-103.

65. Malayappan, B.; Johnson, L.; Nie, B.; Panchal, D.; Matter, B.; Jacobson, P. A.; Tretyakova, N., Quantitative High-Performance Liquid Chromatography-Electrospray Ionization Tandem Mass Spectrometry Analysis of Bis-N7-Guanine DNA-DNA Cross-Links in White Blood Cells of Cancer Patients Recieving Cyclophosphamide Therapy. *Anal. Chem.* **2010,** *82*, 3650-3658.

66. Johnson, L. A.; Malayappan, B.; Tretyakova, N.; Campbell, C.; MacMillan, M. L.; Wagner, J. E.; Jacobson, P. A., Formation of cyclophosphamide specific DNA adducts in hematological diseases. *Pediatr. Blood Cancer* **2012,** *58* (5), 708-14.

67. Johnson, L.; Tretyakova, N.; Jacobson, P. A., Obesity Effects on Cyclophosphamide-induced DNA Damage in Hematopoietic Cell Transplant Recipients. *In Vivo* **2012,** *26*, 853-858.

68. Stornetta, A.; Villalta, P. W.; Gossner, F.; Wilson, W. R.; Balbo, S.; Sturla, S. J., DNA Adduct Profiles Predict in Vitro Cell Viability after Treatment with the Experimental Anticancer Prodrug PR104A. *Chem. Res. Toxicol.* **2017,** *30* (3), 830-839.

69. Shuker, D. E.; Farmer, P. B., Relevance of Urinary DNA Adducts as Markers of Carcinogen Exposure. *Chem. Res. Toxicol.* **1992,** *5*, 450-460.

70. Lee, C.-S.; Gibson, N. W., DNA interstrand cross-links induced by the cyclopropylpyrroloindole antitumor agent bizelesin are reversible upon exposure to alkali. *Biochemistry* **1993,** *32* (35), 9108-9114.

71. Prakash, A. S.; Pereira, T. N.; Smith, B. L.; Shaw, G.; Seawright, A. A., Mechanism of bracken fern carcinogenesis: evidence for H-ras activation via initial adenine alkylation by ptaquiloside. *Natural Toxins* **1996,** *4*, 221-227.

72. Saeed, M.; Higginbotham, S.; Rogan, E.; Cavalieri, E., Formation of depurinating N3adenine and N7guanine adducts after reaction of 1,2-naphthoquinone or enzyme-activated 1,2-dihydroxynaphthalene with DNA. Implications for the mechanism of tumor initiation by naphthalene. *Chem. Biol. Interact.* **2007,** *165* (3), 175-88.

73. Walton, M.; Egner, P.; Scholl, P. F.; Walker, J.; Kensler, T. W.; Groopman, J. D., Liquid Chromatography Electrospray-Mass Spectrometery of Urinary Aflatoxin Biomarkers: Characterization and Application to Dosimetry and Chemoprevention in Rats. *Chem. Res. Toxicol.* **2001,** *14*, 919-926.

74. Mikes, P.; Korinek, M.; Linhart, I.; Krouzelka, J.; Frantik, E.; Vodickova, L.; Neufussova, L., Excretion of urinary N7 guanine and N3 adenine DNA adducts in mice after inhalation of styrene. *Toxicol. Lett.* **2009,** *184* (1), 33-7.

75. Rogan, E. G.; RamaKrishna, N. V. S.; Higginbotham, S.; Cavalieri, E. L.; Jeong, H.; Jankowiak, R.; Small, G. J., Identification and Quantification of 7-(Benzo[*a*]pyren-6-yl)guanine in the Urine and Feces of Rats Treated with Benzo[*a*]pyrene. *Chem. Res. Toxicol.* **1990,** *3*, 441-444.

76. Tang, H.; Zhang, J., Recent developments in DNA adduct analysis using liquid chromatography coupled with mass spectrometry. *J. Sep. Sci.* **2020,** *43* (1), 31-55.

77. Tretyakova, N.; Goggin, M.; Sangaraju, D.; Janis, G., Quantitation of DNA adducts by stable isotope dilution mass spectrometry. *Chem. Res. Toxicol.* **2012,** *25* (10), 2007-35.

78. Goggin, M.; Swenberg, J. A.; Walker, V. E.; Tretyakova, N., Molecular dosimetry of 1,2,3,4-diepoxybutane-induced DNA-DNA cross-links in B6C3F1 mice and F344 rats exposed to 1,3-butadiene by inhalation. *Cancer Res.* **2009,** *69* (6), 2479-86.

79. Lai, Y.; Yu, R.; Hartwell, H. J.; Moeller, B. C.; Bodnar, W. M.; Swenberg, J. A., Measurement of Endogenous versus Exogenous Formaldehyde-Induced DNA-Protein Crosslinks in Animal Tissues by Stable Isotope Labeling and Ultrasensitive Mass Spectrometry. *Cancer Res.* **2016,** *76* (9), 2652-61.

80. Hecht, S. S., Oral Cell DNA Adducts as Potential Biomarkers for Lung Cancer Susceptibility in Cigarette Smokers. *Chem. Res. Toxicol.* **2017,** *30* (1), 367-375.

81. Bessette, E. E.; Spivack, S. D.; Goodenough, A. K.; Wang, T.; Pinto, S.; Kadlubar, F. F.; Turesky, R. J., Identification of Carcinogen DNA Adducts in Human Saliva by Linear Quadrupole Ion Trap/Multistage Tandem Mass Spectrometry. *Chem. Res. Toxicol.* **2010,** *23*, 1234-1244.

82. Chen, H. J.; Lin, W. P., Quantitative analysis of multiple exocyclic DNA adducts in human salivary DNA by stable isotope dilution nanoflow liquid chromatography-nanospray ionization tandem mass spectrometry. *Anal. Chem.* **2011,** *83* (22), 8543-51.

83. Li, X.; Liu, L.; Wang, H.; Chen, J.; Zhu, B.; Chen, H.; Hou, H.; Hu, Q., Simultaneous analysis of six aldehyde-DNA adducts in salivary DNA of nonsmokers and smokers using stable isotope dilution liquid chromatography electrospray ionization-tandem mass spectrometry. *J. Chromatogr. B Analyt. Technol. Biomed. Life Sci.* **2017,** *1060*, 451-459.

84. Talaska, G.; Schamer, M.; Skipper, P.; Tannenbaum, S.; Caporaso, N.; Unruh, L.; Kadlubar, F. F.; Bartsch, H.; Malaveille, C.; Vineis, P., Detection of carcinogen-DNA adducts in exfoliated urothelial cells of cigarette smokers: association with smoking, hemoglobin adducts, and urinary mutagenicity. *Cancer Epidemiol. Biomarkers Prev.* **1991,** *1* (1), 61-66.

85. Guo, L.; Wu, H.; Yue, H.; Lin, S.; Lai, Y.; Cai, Z., A novel and specific method for the determination of aristolochic acid-derived DNA adducts in exfoliated urothelial cells by

using ultra performance liquid chromatography-triple quadrupole mass spectrometry. *J. Chromatogr. B Analyt. Technol. Biomed. Life Sci.* **2011,** *879* (2), 153-8.

86. Groehler, A. S. t.; Najjar, D.; Pujari, S. S.; Sangaraju, D.; Tretyakova, N. Y., N(6)-(2-Deoxy-d- erythro-pentofuranosyl)-2,6-diamino-3,4-dihydro-4-oxo-5- N-(2-hydroxy-3-buten-1-yl)-formamidopyrimidine Adducts of 1,3-Butadiene: Synthesis, Structural Identification, and Detection in Human Cells. *Chem. Res. Toxicol.* **2018,** *31* (9), 885-897.

87. Schumacher, F.; Herrmann, K.; Florian, S.; Engst, W.; Glatt, H., Optimized enzymatic hydrolysis of DNA for LC-MS/MS analyses of adducts of 1-methoxy-3-indolylmethyl glucosinolate and methyleugenol. *Anal. Biochem.* **2013,** *434* (1), 4-11.

88. Ma, B.; Villalta, P. W.; Balbo, S.; Stepanov, I., Analysis of a malondialdehyde-deoxyguanosine adduct in human leukocyte DNA by liquid chromatography nanoelectrospray-high-resolution tandem mass spectrometry. *Chem. Res. Toxicol.* **2014,** *27* (10), 1829-36.

89. Goggin, M.; Anderson, C.; Park, S.; Swenberg, J.; Walker, V.; Tretyakova, N., Quantitative High-Performance Liquid Chromatography-Electrospray Ionization-Tandem Mass Spectrometry Analysis of the Adenine-Guanine Cross-Links of 1,2,3,4-Diepoxybutane in Tissues of Butadiene-Exposed B6C3F1 Mice. *Chem. Res. Toxicol.* **2008,** *21,* 1163-1170.

90. Upadhyaya, P.; Lindgren, B. R.; Hecht, S. S., Comparative levels of O6-methylguanine, pyridyloxobutyl-, and pyridylhydroxybutyl-DNA adducts in lung and liver of rats treated chronically with the tobacco-specific carcinogen 4-(methylnitrosamino)-1-(3-pyridyl)-1-butanone. *Drug Metab. Dispos.* **2009,** *37* (6), 1147-51.

91. Tarun, M.; Rusling, J. F., Measuring DNA nucleobase adducts using neutral hydrolysis and liquid chromatography-mass spectrometry. *Crit. Rev. Eukaryot. Gene Expr.* **2005,** *15* (4), 295-316.

92. Sangaraju, D.; Villalta, P. W.; Wickramaratne, S.; Swenberg, J.; Tretyakova, N., NanoLC/ESI+ HRMS3 quantitation of DNA adducts induced by 1,3-butadiene. *J. Am. Soc. Mass. Spectrom.* **2014,** *25* (7), 1124-35.

93. Sangaraju, D.; Goggin, M.; Walker, V.; Swenberg, J.; Tretyakova, N., NanoHPLC-nanoESI(+)-MS/MS quantitation of bis-N7-guanine DNA-DNA cross-links in tissues of B6C3F1 mice exposed to subppm levels of 1,3-butadiene. *Anal. Chem.* **2012,** *84* (3), 1732-9.

94. Tretyakova, N.; Villalta, P. W.; Kotapati, S., Mass spectrometry of structurally modified DNA. *Chem. Rev.* **2013,** *113* (4), 2395-436.

95. Makarov, A. A., Electrostatic Axially Harmonic Orbital Trapping: A High-Performance Technique of Mass Analysis. *Anal. Chem.* **2000,** *72*, 1156-1162.

96. Balbo, S.; Villalta, P. W.; Hecht, S. S., Quantitation of 7-ethylguanine in leukocyte DNA from smokers and nonsmokers by liquid chromatography-nanoelectrospray-high resolution tandem mass spectrometry. *Chem. Res. Toxicol.* **2011,** *24* (10), 1729-34.

97. Erber, L.; Goodman, S.; Jokipii Krueger, C. C.; Rusyn, I.; Tretyakova, N., Quantitative NanoLC/NSI(+)-HRMS Method for 1,3-Butadiene Induced bis-N7-guanine DNA-DNA Cross-Links in Urine. *Toxics* **2021,** *9* (10).

98. Siegel, R. L.; Miller, K. D.; Fuchs, H. E.; Jemal, A., Cancer Statistics, 2021. *CA: Cancer J. Clin.* **2021**.

99. Wild, C. P., Complementing the genome with an "exposome": the outstanding challenge of environmental exposure measurement in molecular epidemiology. *Cancer Epidemiol. Biomarkers Prev.* **2005,** *14* (8), 1847-50.

100. Nakamura, J.; Mutlu, E.; Sharma, V.; Collins, L.; Bodnar, W.; Yu, R.; Lai, Y.; Moeller, B.; Lu, K.; Swenberg, J., The endogenous exposome. *DNA Repair* **2014,** *19*, 3-13.

101. O'Brien, P. J.; Siraki, A. G.; Shangari, N., Aldehyde sources, metabolism, molecular toxicity mechanisms, and possible effects on human health. *Crit. Rev. Toxicol.* **2005,** *35* (7), 609-62.

102. Mutlu, E.; Jeong, Y. C.; Collins, L. B.; Ham, A. J.; Upton, P. B.; Hatch, G.; Winsett, D.; Evansky, P.; Swenberg, J. A., A new LC-MS/MS method for the quantification of endogenous and vinyl chloride-induced 7-(2-Oxoethyl)guanine in sprague-dawley rats. *Chem. Res. Toxicol.* **2012,** *25* (2), 391-9.

103. Marsden, D. A.; Jones, D. J.; Britton, R. G.; Ognibene, T.; Ubick, E.; Johnson, G. E.; Farmer, P. B.; Brown, K., Dose-response relationships for N7-(2-hydroxyethyl)guanine induced by low-dose [14C]ethylene oxide: evidence for a novel mechanism of endogenous adduct formation. *Cancer Res.* **2009,** *69* (7), 3052-9.

104. IARC, Re-evaluation of some organic chemicals, hydrazine and hydrogen peroxide. *IARC Monographs on the Evaluation of Carcinogenic Risk to Humans* **1999,** *71*, 319-335.

105. IARC, Formaldehyde, 2-Butoxyethanol and 1-*tert*-Butoxypropan-2-ol. *IARC Monographs on the Evaluation of Carcinogenic Risk to Humans* **2006,** *88*, 1-287.

106. Lu, K.; Collins, L. B.; Ru, H.; Bermudez, E.; Swenberg, J. A., Distribution of DNA adducts caused by inhaled formaldehyde is consistent with induction of nasal carcinoma but not leukemia. *Toxicol. Sci.* **2010,** *116* (2), 441-51.

107. Lu, K.; Craft, S.; Nakamura, J.; Moeller, B. C.; Swenberg, J. A., Use of LC-MS/MS and stable isotopes to differentiate hydroxymethyl and methyl DNA adducts from formaldehyde and nitrosodimethylamine. *Chem. Res. Toxicol.* **2012,** *25* (3), 664-75.

108. Moeller, B. C.; Recio, L.; Green, A.; Sun, W.; Wright, F. A.; Bodnar, W. M.; Swenberg, J. A., Biomarkers of exposure and effect in human lymphoblastoid TK6 cells following [13C2]-acetaldehyde exposure. *Toxicol. Sci.* **2013,** *133* (1), 1-12.

109. Balbo, S.; Meng, L.; Bliss, R. L.; Jensen, J. A.; Hatsukami, D. K.; Hecht, S. S., Kinetics of DNA adduct formation in the oral cavity after drinking alcohol. *Cancer Epidemiol. Biomarkers Prev.* **2012,** *21* (4), 601-8.

110. Drablos, F.; Feyzi, E.; Aas, P. A.; Vaagbo, C. B.; Kavli, B.; Bratlie, M. S.; Pena-Diaz, J.; Otterlei, M.; Slupphaug, G.; Krokan, H. E., Alkylation damage in DNA and RNA--repair mechanisms and medical significance. *DNA Repair* **2004,** *3* (11), 1389-407.

111. Mentch, S. J.; Locasale, J. W., One-carbon metabolism and epigenetics: understanding the specificity. *Ann. N. Y. Acad. Sci.* **2016,** *1363*, 91-8.

112. Sharma, V.; Collins, L. B.; Clement, J. M.; Zhang, Z.; Nakamura, J.; Swenberg, J. A., Molecular dosimetry of endogenous and exogenous O(6)-methyl-dG and N7-methyl-G adducts following low dose [D3]-methylnitrosourea exposures in cultured human cells. *Chem. Res. Toxicol.* **2014,** *27* (4), 480-2.

113. Lu, K.; Moeller, B.; Doyle-Eisele, M.; McDonald, J.; Swenberg, J. A., Molecular dosimetry of N2-hydroxymethyl-dG DNA adducts in rats exposed to formaldehyde. *Chem. Res. Toxicol.* **2011,** *24* (2), 159-61.

114. Yu, R.; Lai, Y.; Hartwell, H. J.; Moeller, B. C.; Doyle-Eisele, M.; Kracko, D.; Bodnar, W. M.; Starr, T. B.; Swenberg, J. A., Formation, Accumulation, and Hydrolysis of Endogenous and Exogenous Formaldehyde-Induced DNA Damage. *Toxicol. Sci.* **2015,** *146* (1), 170-82.

115. Moeller, B. C.; Lu, K.; Doyle-Eisele, M.; McDonald, J.; Gigliotti, A.; Swenberg, J. A., Determination of N2-hydroxymethyl-dG adducts in the nasal epithelium and bone marrow of nonhuman primates following 13CD2-formaldehyde inhalation exposure. *Chem. Res. Toxicol.* **2011,** *24* (2), 162-4.

116. Lu, K.; Gul, H.; Upton, P. B.; Moeller, B. C.; Swenberg, J. A., Formation of hydroxymethyl DNA adducts in rats orally exposed to stable isotope labeled methanol. *Toxicol. Sci.* **2012,** *126* (1), 28-38.

117. El Ghissassi, F.; Barbin, A.; Bartsch, H., Metabolic Activation of Vinyl Chloride by Rat Liver Microsomes: Low-Dose Kinetics and Involvement of Cytochrome P450 2E1. *Biochem. Pharmacol.* **1998,** *55*, 1445-1452.

118. Fedtke, N.; Boucheron, J. A.; Walker, V. E.; swenberg, J., Vinyl chloride-induced DNA adducts. II: Formation and persistence of 7-(2'-oxoethyl)guanine and N^2,3-ethenoguanine in rat tissue DNA. *Carcinogenesis* **1990,** *11* (8), 1287-1292.

119. Ham, A. J.; Ranasinghe, A.; Morinello, E.; Nakamura, J.; Upton, P.; Johnson, F.; Swenberg, J., Immunoaffinity/Gas Chromatography/High-Resolution Mass Spectrometry Method for the Detection of N^2,3-Ethenoguanine. *Chem. Res. Toxicol.* **1999,** *12*, 1240-1246.

120. Morinello, E.; Ham, A. J.; Ranasinghe, A.; Sangaiah, R.; Swenberg, J., Simultaneous Quantitation of N^2,3-Ethenoguanine and 1,N^2-Ethenoguanine with an Immunoaffinity/Gas Chromatography/High-Resolution Mass Spectrometry Assay. *Chem. Res. Toxicol.* **2001,** *14*, 327-334.

121. Morinello, E.; Ham, A. J.; Ranasinghe, A.; Nakamura, J.; Upton, P.; Swenberg, J., Molecular Dosimetry and Repair of N^2,3-Ethenoguanine in Rats Exposed to Vinyl Chloride. *Cancer Res.* **2002,** *62*, 5189-5195.

122. Mutlu, E.; Collins, L.; Stout, M.; Upton, P.; Daye, L.; Winsett, D.; Hatch, G.; Evansky, P.; Swenberg, J., Development and Application of an LC-MS/MS Method for the Detection of the Vinyl Chloride-Induced DNA Adduct N^2,3-Ethenoguanine in Tissues of Adult and Weanling Rats Following Exposure to [$^{13}C_2$]-VC. *Chem. Res. Toxicol.* **2010,** *23*, 1485-1491.

123. IARC, Chemical Agents and Related Occupations. *IARC Monographs on the Evaluation of Carcinogenic Risk to Humans* **2012,** *100F*, 379-400.

124. Fajen, J. M.; Roberts, D. R.; Ungers, L. J.; Krishnan, E. R., Occupational exposure of workers to 1,3-butadiene. *Environ. Health Perspect.* **1990,** *86*, 11-8.

125. Delzell, E.; Sathiakumar, N.; Hovinga, M.; Macaluso, M.; Julian, J.; Larson, R.; Cole, P.; Muir, D. C., A follow-up study of synthetic rubber workers. *Toxicology* **1996,** *113* (1-3), 182-9.

126. Sathiakumar, N.; Graff, J.; Macaluso, M.; Maldonado, G.; Matthews, R.; Delzell, E., An updated study of mortality among North American synthetic rubber industry workers. *Occup. Environ. Med.* **2005,** *62* (12), 822-9.

127. Cheng, H.; Sathiakumar, N.; Graff, J.; Matthews, R.; Delzell, E., 1,3-Butadiene and leukemia among synthetic rubber industry workers: exposure-response relationships. *Chem. Biol. Interact.* **2007,** *166* (1-3), 15-24.

128. Sathiakumar, N.; Tipre, M.; Leader, M.; Brill, I.; Delzell, E., Mortality Among Men and Women in the North American Synthetic Rubber Industry, 1943 to 2009. *Occup. Environ. Med.* **2019,** *61* (11), 887-897.

129. Sathiakumar, N.; Bolaji, B. E.; Brill, I.; Chen, L.; Tipre, M.; Leader, M.; Arora, T.; Delzell, E., 1,3-Butadiene, styrene and lymphohaematopoietic cancers among North American synthetic rubber polymer workers: exposure-response analyses. *Occup. Environ. Med.* **2021,** *78* (12), 859-868.

130. Sathiakumar, N.; Brill, I.; Leader, M.; Delzell, E., 1,3-Butadiene, styrene and lymphohematopoietic cancer among male synthetic rubber industry workers--Preliminary exposure-response analyses. *Chem. Biol. Interact.* **2015,** *241*, 40-49.

131. Sathiakumar, N.; Brill, I.; Delzell, E., 1,3-butadiene, styrene and lung cancer among synthetic rubber industry workers. *Occup. Environ. Med.* **2009,** *51* (11), 1326-32.

132. Sathiakumar, N.; Delzell, E., A follow-up study of mortality among women in the North American synthetic rubber industry. *Occup. Environ. Med.* **2009,** *51* (11), 1314-25.

133. Sathiakumar, N.; Bolaji, B.; Brill, I.; Chen, L.; Tipre, M.; Leader, M.; Arora, T.; Delzell, E., 1,3-Butadiene, styrene and selected outcomes among synthetic rubber polymer workers: Updated exposure-response analyses. *Chem. Biol. Interact.* **2021,** *347*, 109600.

134. Hecht, S. S., Tobacco carcinogens, their biomarkers and tobacco-induced cancer. *Nat. Rev. Cancer* **2003,** *3* (10), 733-44.

135. Gustafson, P.; Barregard, L.; Strandberg, B.; Sallsten, G., The impact of domestic wood burning on personal, indoor and outdoor levels of 1,3-butadiene, benzene, formaldehyde and acetaldehyde. *J. Environ. Monit.* **2007,** *9* (1), 23-32.

136. Pelz, N.; Dempster, N. M.; Shore, P. R., Analysis of low molecular weight hydrocarbons including 1,3-butadiene in engine exhaust gases using an aluminum oxide porous-layer open-tubular fused-silica column. *J. Chromatogr. Sci.* **1990,** *28* (5), 230-5.

137. Kocher, G. J.; Sesia, S. B.; Lopez-Hilfiker, F.; Schmid, R. A., Surgical smoke: still an underestimated health hazard in the operating theatre. *Eur. J. Cardiothorac Surg.* **2019,** *55* (4), 626-631.

138. Grant, R. L.; Leopold, V.; McCant, D.; Honeycutt, M., Spatial and temporal trend evaluation of ambient concentrations of 1,3-butadiene and chloroprene in Texas. *Chem. Biol. Interact.* **2007,** *166* (1-3), 44-51.

139. Heck, J. E.; Park, A. S.; Qiu, J.; Cockburn, M.; Ritz, B., Risk of leukemia in relation to exposure to ambient air toxics in pregnancy and early childhood. *Int. J. Hyg. Environ. Health* **2014,** *217* (6), 662-8.

140. Symanski, E.; Tee Lewis, P. G.; Chen, T. Y.; Chan, W.; Lai, D.; Ma, X., Air toxics and early childhood acute lymphocytic leukemia in Texas, a population based case control study. *Environ. Health* **2016,** *15* (1), 70.

141. von Ehrenstein, O. S.; Heck, J. E.; Park, A. S.; Cockburn, M.; Escobedo, L.; Ritz, B., In Utero and Early-Life Exposure to Ambient Air Toxics and Childhood Brain Tumors: A Population-Based Case-Control Study in California, USA. *Environ. Health Perspect.* **2016,** *124* (7), 1093-9.

142. Hall, C.; Heck, J. E.; Ritz, B.; Cockburn, M.; Escobedo, L. A.; von Ehrenstein, O. S., Prenatal Exposure to Air Toxics and Malignant Germ Cell Tumors in Young Children. *Occup. Environ. Med.* **2019,** *61* (6), 529-534.

143. Kuang, H.; Li, Z.; Lv, X.; Wu, P.; Tan, J.; Wu, Q.; Li, Y.; Jiang, W.; Pang, Q.; Wang, Y.; Fan, R., Exposure to volatile organic compounds may be associated with oxidative DNA damage-mediated childhood asthma. *Ecotoxicol. Environ. Saf.* **2021,** *210*, 111864.

144. Cicalese, L.; Raun, L.; Shirafkan, A.; Campos, L.; Zorzi, D.; Montalbano, M.; Rhoads, C.; Gazis, V.; Ensor, K.; Rastellini, C., An Ecological Study of the Association between Air Pollution and Hepatocellular Carcinoma Incidence in Texas. *Liver Cancer* **2017,** *6* (4), 287-296.

145. Melnick, R. L.; Shackelford, C. C.; Huff, J., Carcinogenicity of 1,3-butadiene. *Environ. Health Perspect.* **1993,** *100*, 227-36.

146. Owen, P. E.; Glaister, J. R., Inhalation Toxicity and Carcinogenicity of 1,3-Butadiene in Sprague-Dawley Rats. *Environ. Health Perspect.* **1990,** *86*, 19-25.

147. Owen, P. E.; Glaister, J. R.; Gaunt, I. F.; Pullinger, D. H., Inhalation toxicity studies with 1,3-butadiene. 3. Two year toxicity/carcinogenicity study in rats. *Am. Ind. Hyg. Assoc. J.* **1987,** *48* (5), 407-13.

148. International Agency for Research on Cancer. 1,3-Butadiene, Ethylene Oxide and Vinyl Halides (Vinyl Fluoride, Vinyl Chloride and Vinyl Bromide). *IARC Monographs on the Evaluation of Carcinogenic Risk to Humans* **2008,** *97*, IARC, Lyon, FR.

149. Duescher, R. J.; Elfarra, A. A., Human liver microsomes are efficient catalysts of 1,3-butadiene oxidation: evidence for major roles by cytochromes P450 2A6 and 2E1. *Arch. Biochem. Biophys.* **1994,** *311* (2), 342-9.

150. Krause, R. J.; Sharer, J. E.; Elfarra, A. A., Epoxide Hydrolase-Dependent Metabolism of Butadiene Monoxide to 3-Butene-1,2-diol in Mouse, Rat, and Human Liver. *Drug Metab. Dispos.* **1997,** *25* (8), 1013-1015.

151. Csanády, G.; Guengerich, F. P.; Bond, J. A., Comparison of the biotransformation of 1,3-butadiene and its metabolite, butadiene monoepoxide, by hepatic and pulmonary tissues from humans, rats and mice. *Carcinogenesis* **1993,** *14*, 783-784.

152. Steen, A.; Meyer, K. G.; Recio, L., Analysis of *hprt* mutations occurring in human TK6 lymphoblastoid cells following exposure to 1,2,3,4-diepoxybutane. *Mutagenesis* **1997,** *12* (2), 61-67.

153. Cochrane, J. E.; Skopek, T. R., Mutagenicity of butadiene and its expoxide metabolites: I. Mutagenic potential of 1,2-epoxybutene, 1,2,3,4-diepoxybutane and 3,4-epoxy-1,2-butanediol in cultured human lymphoblasts. *Carcinogenesis* **1994,** *15* (4), 713-717.

154. Recio, L.; Steen, A.; Pluta, L.; Meyer, K. G.; Saranko, C. J., Mutational spectrum of 1,3-butadiene and metabolites 1,2-epoxybutene and 1,2,3,4-diepoxybutane to assess mutagenic mechanisms. *Chem. Biol. Interact.* **2001,** *135-136*, 325-341.

155. Steen, A.; Meyer, K. G.; Recio, L., Characterization of hprt mutations following 1,2-epoxy-3-butene exposure of human TK6 cells. *Mutagenesis* **1997,** *12* (5), 359-364.

156. Lee, D. H.; Kim, T. H.; Lee, S. Y.; Kim, H. J.; Rhee, S. K.; Yoon, B.; Pfeifer, G. P.; Lee, C. S., Mutations Induced by 1,3-Butadiene Metabolites, Butadiene Diolepoxide, and 1,2,3,4-Diepoxybutane at the *Hprt* Locus in CHO-K1 cells. *Mol. Cells* **2002,** *14* (3), 411-419.

157. Cochrane, J. E.; Skopek, T. R., Mutagenicity of butadiene and its epoxide metabolites: II. Mutational spectra of butadiene, 1,2-epoxybutene and diepoxybutane at the hprt locus in splenic T cells from exposed B6C3F1 mice. *Carcinogenesis* **1994,** *15* (4), 719-23.

158. Ma, H.; Wood, T. G.; Ammenheuser, M. M.; Rosenblatt, J. I.; Ward Jr, J. B., Molecular Analysis of *hprt* Mutant Lymphocytes From 1,3-Butadiene-Exposed Workers. *Environ. Mol. Mutagen.* **2000,** *36*, 59-71.

159. Liu, S.; Ao, L.; Du, B.; Zhou, Y.; Yuan, J.; Bai, Y.; Zhou, Z.; Cao, J., HPRT mutations in lymphocytes from 1,3-butadiene-exposed workers in China. *Environ. Health Perspect.* **2008,** *116* (2), 203-8.

160. Hayes, R. B.; Xi, L.; Bechtold, W. E.; Rothman, N.; Yao, M.; Henderson, R.; Zhang, L.; Smith, M. T.; Zhang, D.; Wiemels, J.; Dosemeci, M.; Yin, S.; O'Neil, J. P., *hprt* Mutation frequency among workers exposed to 1,3-butadiene in China. *Toxicology* **1996**, 100-105.

161. Tates, A. D.; van Dam, F. J.; de Zwart, F. A.; Darroudi, F.; Natarajan, A. T.; Rössner, P.; Peterkova, K.; Peltonen, K.; Demopoulos, N. A.; Stephanou, G.; Vlachodimitropoulos, D.; Sram, R. J., Biological effect monitoring in industrial workers from the Czech Republic exposed to low levels of butadiene. *Toxicology* **1996,** *113*, 91-99.

162. Fustinoni, S.; Soleo, L.; Warholm, M.; Begemann, P.; Rannug, A.; Neumann, H. G.; Swenberg, J. A.; Vimercati, L.; Colombi, A., Influence of metabolic genotypes on biomarkers of exposure to 1,3-butadiene in humans. *Cancer Epidemiol. Biomarkers Prev.* **2002,** *11* (10 Pt 1), 1082-90.

163. Boldry, E. J.; Patel, Y. M.; Kotapati, S.; Esades, A.; Park, S. L.; Tiirikainen, M.; Stram, D. O.; Le Marchand, L.; Tretyakova, N., Genetic Determinants of 1,3-Butadiene Metabolism and Detoxification in Three Populations of Smokers with Different Risks of Lung Cancer. *Cancer Epidemiol. Biomarkers Prev.* **2017,** *26* (7), 1034-1042.

164. van Sittert, N. J.; Megens, H. J.; Watson, W. P.; Boogaard, P. J., Biomarkers of exposure to 1,3-butadiene as a basis for cancer risk assessment. *Toxicol. Sci.* **2000,** *56* (1), 189-202.

165. Alwis, K. U.; Blount, B. C.; Britt, A. S.; Patel, D.; Ashley, D. L., Simultaneous analysis of 28 urinary VOC metabolites using ultra high performance liquid chromatography coupled with electrospray ionization tandem mass spectrometry (UPLC-ESI/MSMS). *Anal. Chim. Acta.* **2012,** *750*, 152-60.

166. Elfarra, A. A.; Sharer, J. E.; Duescher, R. J., Synthesis and Characterization of *N*-Acetyl-L-cystein *S*-Conjugates of Butadiene Monoxide and Their Detection and Quantification in Urine of Rats and Mice Given Butadiene Monoxide. *Chem. Res. Toxicol.* **1995,** *8*, 68-76.

167. Kotapati, S.; Matter, B. A.; Grant, A. L.; Tretyakova, N. Y., Quantitative analysis of trihydroxybutyl mercapturic acid, a urinary metabolite of 1,3-butadiene, in humans. *Chem. Res. Toxicol.* **2011,** *24* (9), 1516-26.

168. Kotapati, S.; Sangaraju, D.; Esades, A.; Hallberg, L.; Walker, V. E.; Swenberg, J. A.; Tretyakova, N. Y., Bis-butanediol-mercapturic acid (bis-BDMA) as a urinary biomarker of metabolic activation of butadiene to its ultimate carcinogenic species. *Carcinogenesis* **2014,** *35* (6), 1371-8.

169. Sabourin, P. J.; Burka, L. T.; Bechtold, W. E.; Dahl, A. R.; Hoover, M. D.; Chang, I. Y.; Henderson, R. F., Species differences in urinary butadiene metabolites; identification of 1,2-dihydroxy-4-(*N*-acetylcysteinyl)butane, a novel metabolite of butadiene. *Carcinogenesis* **1992,** *13* (9), 1633-1638.

170. Bechtold, W. E.; Strunk, M. R.; Chang, I. Y.; Ward, J. B., Jr.; Henderson, R. F., Species differences in urinary butadiene metabolites: comparisons of metabolite ratios between mice, rats, and humans. *Toxicol. Appl. Pharmacol.* **1994,** *127* (1), 44-9.

171. Albertini, R. A.; Sram, R. J.; Vacek, P.; Lynch, J.; Wright, M.; Nicklas, J. A.; Boogaard, P. J.; Henderson, R. F.; Swenberg, J.; Tates, A. D.; Ward Jr, J. B., Biomarkers for assessing occupational exposures to 1,3-butadiene. *Chem. Biol. Interact.* **2001,** *135-136*, 429-453.

172. Albertini, R.; Sram, R. J.; Vacek, P.; Lynch, J.; Nicklas, J. A.; Van Sittert, N. J.; Boogaard, P. J.; Henderson, R.; Swenberg, J.; Tates, A. D.; Ward Jr, J. B.; Wright, M.; Ammenheuser, M. M.; Binkova, B.; Blackwell, W. B.; De Zwart, F. A.; Krako, D.; Krone, J. R.; Megens, H. J.; Musilova, P.; Rajska, G.; Ranasinghe, A.; Rosenblatt, J. I.; Rossner, P.; Rubes, J.; Sullivan, L.; Upton, P.; Zwinderman, A. H., Biomarkers in Czech workers exposed to 1,3-butadiene: a transitional epidemiologic study. *Res. Rep. Health. Eff. Inst.* **2003,** *116*, 1-162.

173. Sapkota, A.; Halden, R. U.; Dominici, F.; Groopman, J. D.; Buckley, T. J., Urinary biomarkers of 1,3-butadiene in environmental settings using liquid chromatography isotope dilution tandem mass spectrometry. *Chem. Biol. Interact.* **2006,** *160* (1), 70-9.

174. Ahmadkhaniha, R.; Ghoochani, M.; Rastkari, N., Application of biological monitoring for exposure assessment of 1.3 Butadiene. *J. Environ. Health Sci. Eng.* **2020,** *18* (2), 1265-1269.

175. Arayasiri, M.; Mahidol, C.; Navasumrit, P.; Autrup, H.; Ruchirawat, M., Biomonitoring of benzene and 1,3-butadiene exposure and early biological effects in traffic policemen. *Sci. Total Environ.* **2010,** *408* (20), 4855-62.

176. Borgie, M.; Garat, A.; Cazier, F.; Delbende, A.; Allorge, D.; Ledoux, F.; Courcot, D.; Shirali, P.; Dagher, Z., Traffic-related air pollution. A pilot exposure assessment in Beirut, Lebanon. *Chemosphere* **2014,** *96*, 122-8.

177. Frigerio, G.; Campo, L.; Mercadante, R.; Mielzynska-Svach, D.; Pavanello, S.; Fustinoni, S., Urinary Mercapturic Acids to Assess Exposure to Benzene and Other Volatile Organic Compounds in Coke Oven Workers. *Int. J. Environ. Res. Public Health* **2020,** *17* (5).

178. Roethig, H. J.; Munjal, S.; Feng, S.; Liang, Q.; Sarkar, M.; Walk, R. A.; Mendes, P. E., Population estimates for biomarkers of exposure to cigarette smoke in adult U.S. cigarette smokers. *Nicotine Tob. Res.* **2009,** *11* (10), 1216-25.

179. Urban, M.; Gilch, G.; Schepers, G.; Miert, E. v.; Scherer, G., Determination of the major mercapturic acids of 1,3-butadiene in human and rat urine using liquid chromatography with tandem mass spectrometry. *J. Chromatogr. B* **2003,** *796* (1), 131-140.

180. Schettgen, T.; Musiol, A.; Alt, A.; Ochsmann, E.; Kraus, T., A method for the quantification of biomarkers of exposure to acrylonitrile and 1,3-butadiene in human urine by column-switching liquid chromatography-tandem mass spectrometry. *Anal. Bioanal. Chem.* **2009,** *393* (3), 969-81.

181. Carmella, S. G.; Chen, M.; Han, S.; Briggs, A.; Jensen, J.; Hatsukami, D. K.; Hecht, S. S., Effects of smoking cessation on eight urinary tobacco carcinogen and toxicant biomarkers. *Chem. Res. Toxicol.* **2009,** *22* (4), 734-41.

182. Sarkar, M.; Kapur, S.; Frost-Pineda, K.; Feng, S.; Wang, J.; Liang, Q.; Roethig, H., Evaluation of biomarkers of exposure to selected cigarette smoke constituents in adult smokers switched to carbon-filtered cigarettes in short-term and long-term clinical studies. *Nicotine Tob. Res.* **2008,** *10* (12), 1761-72.

183. Park, S. L.; Kotapati, S.; Wilkens, L. R.; Tiirikainen, M.; Murphy, S. E.; Tretyakova, N.; Le Marchand, L., 1,3-Butadiene exposure and metabolism among Japanese American, Native Hawaiian, and White smokers. *Cancer Epidemiol. Biomarkers Prev.* **2014,** *23* (11), 2240-9.

184. St Helen, G.; Benowitz, N. L.; Ko, J.; Jacob, P.; Gregorich, S. E.; Perez-Stable, E. J.; Murphy, S. E.; Hecht, S. S.; Hatsukami, D. K.; Donny, E. C., Differences in exposure to

toxic and/or carcinogenic volatile organic compounds between Black and White cigarette smokers. *J. Expo. Sci. Environ. Epidemiol.* **2021,** *31* (2), 211-223.

185. Yuan, J. M.; Gao, Y. T.; Wang, R.; Chen, M.; Carmella, S. G.; Hecht, S. S., Urinary levels of volatile organic carcinogen and toxicant biomarkers in relation to lung cancer development in smokers. *Carcinogenesis* **2012,** *33* (4), 804-9.

186. Lorkiewicz, P.; Riggs, D. W.; Keith, R. J.; Conklin, D. J.; Xie, Z.; Sutaria, S.; Lynch, B.; Srivastava, S.; Bhatnagar, A., Comparison of Urinary Biomarkers of Exposure in Humans Using Electronic Cigarettes, Combustible Cigarettes, and Smokeless Tobacco. *Nicotine Tob. Res.* **2019,** *21* (9), 1228-1238.

187. St Helen, G.; Jacob, P., 3rd; Peng, M.; Dempsey, D. A.; Hammond, S. K.; Benowitz, N. L., Intake of toxic and carcinogenic volatile organic compounds from secondhand smoke in motor vehicles. *Cancer Epidemiol. Biomarkers Prev.* **2014,** *23* (12), 2774-82.

188. Richardson, K. A.; Peters, M. M. C. G.; Wong, B. A.; Megens, R. H. J. J. J.; van Elburg, P. A.; Booth, E. D.; Boogaard, P. J.; Bond, J. A.; Medinsky, M. A.; Watson, W. P.; Van Sittert, N. J., Quantitative and Qualitative Differences in the Metabolism of ^{14}C-1,3-Butadiene in Rats and Mice: Relevance to Cancer Susceptibility. *Toxicol. Sci.* **1999,** *49*, 186-201.

189. Occupational Safety and Health Administration Toxic and Hazardous Substances. 1,3-Butadiene. https://www.osha.gov/laws-regs/regulations/standardnumber/1910/1910.1051.

190. Krause, R. J.; Elfarra, A. A., Oxidation of Butadiene Monoxide to *meso*- and (±)-Diepoxybutane by cDNA-Expressed Human Cytochrome P450s and by Mouse, Rat, and Human Liver Microsomes: Evidence for Preferential Hydration of *meso*-Diepoxybutane in Rat and Human Liver Microsomes. *Arch. Biochem. Biophys.* **1997,** *337*, 176-184.

191. Swenberg, J. A.; Bordeerat, N. K.; Boysen, G.; Carro, S.; Georgieva, N. I.; Nakamura, J.; Troutman, J. M.; Upton, P. B.; Albertini, R. J.; Vacek, P. M.; Walker, V. E.; Sram, R. J.; Goggin, M.; Tretyakova, N., 1,3-Butadiene: Biomarkers and application to risk assessment. *Chem. Biol. Interact.* **2011,** *192* (1-2), 150-4.

192. Törnqvist, M.; Mowrer, J.; Jensen, S.; Ehrenberg, L., Monitoring of Environmental Cancer Initiators through Hemoglobin Adducts by a Modified Edman Degradation Method. *Anal. Chem.* **1986,** *154*, 255-266.

193. Osterman-Golkar, S.; Kautiainen, A.; Bergmark, E.; Hakansson, K.; Maki-Paakkanen, J., Hemoglobin Adducts and Urinary Mercapturic Acids in Rats as Biological Indicators of Butadiene Exposure. *Chem. Biol. Interact.* **1991,** *80*, 291-302.

194. Albrecht, O. E.; Filser, J. G.; Neumann, H. G., Biological monitoring of 1,3-butadiene: species differences in haemoglobin binding in rat and mouse. *IARC Sci. Publ.* **1993,** *127*, 135-142.

195. Tretyakova, N.; Lin, Y. P.; Upton, P. B.; Sangaiah, R.; Swenberg, J. A., Macromolecular adducts of butadiene. *Toxicology* **1996,** *113* (1-3), 70-6.

196. Swenberg, J.; Christova-Gueorguieva, N. I.; Upton, P.; Ranasinghe, A.; Scheller, N.; Wu, K. Y.; Yen, T. Y.; Hayes, R. B., 1,3-Butadiene: Cancer, Mutations, and Adducts. Part V: Hemoglobin Adducts as Biomarkers of 1,3-Butadiene Exposure and Metabolism. *Res. Rep. Health. Eff. Inst.* **2000**, 191-210.

197. Osterman-Golkar, S.; Peltonen, K.; Anttinen-Klemetti, T.; Hindso Landin, H.; Zorcec, V.; Sorsa, M., Haemoglobin adducts as biomarkers of occupational exposure to 1,3-butadiene. *Mutagenesis* **1996,** *11* (2), 145-149.

198. Albertini, R., *HPRT* mutations in humans: biomarkers for mechanistic studies. *Mutat. Res.* **2001,** *489*, 1-16.

199. Ahmadkhaniha, R.; Izadpanah, F.; Rastkari, N., Hemoglobin adducts as an important marker of chronic exposure to low concentration of 1, 3-butadiene. *J. Environ. Health Sci. Eng.* **2021,** *19* (2), 1607-1611.

200. Perez, H. L.; Lahdetie, J.; Hindso Landin, H.; Kilpelainen, I.; Koivisto, P.; Peltonen, K.; Osterman-Golkar, S., Haemoglobin adducts of epoxybutanediol from exposure to 1,3-butadiene or butadiene epoxides. *Chem. Biol. Interact.* **1997,** *105*, 181-198.

201. Kautiainen, A.; Fred, C.; Rydberg, P.; Törnqvist, M., A liquid chromatography tandem mass spectrometric method for in vivo dose monitoring of diepoxybutane, a metabolite of butadiene. *Rapid Commun. Mass Spectrom.* **2000,** *14* (19), 1848-1853.

202. Fred, C.; Kautiainen, A.; Athanassiadis, I.; Törnqvist, M., Hemoglobin Adduct Levels in Rat and Mouse Treated with 1,2:3,4-Diepoxybutane. *Chem. Res. Toxicol.* **2004,** *17*, 785-794.

203. Boysen, G.; Georgieva, N.; Upton, P.; Jayaraj, K.; Li, Y.; Walker, V. E.; Swenberg, J. A., Analysis of Diepoxide-Specific Cyclic *N*-Terminal Globin Adducts in Mice and Rats after Inhalation Exposure to 1,3-Butadiene. *Cancer Res.* **2004,** *64*, 8517-8520.

204. Georgieva, N. I.; Boysen, G.; Bordeerat, N.; Walker, V. E.; Swenberg, J. A., Exposure-response of 1,2:3,4-diepoxybutane-specific N-terminal valine adducts in mice and rats after inhalation exposure to 1,3-butadiene. *Toxicol. Sci.* **2010,** *115* (2), 322-9.

205. Boysen, G.; Georgieva, N. I.; Bordeerat, N. K.; Sram, R. J.; Vacek, P.; Albertini, R. J.; Swenberg, J. A., Formation of 1,2:3,4-diepoxybutane-specific hemoglobin adducts in 1,3-butadiene exposed workers. *Toxicol. Sci.* **2012,** *125* (1), 30-40.

206. Kotapati, S.; Esades, A.; Matter, B.; Le, C.; Tretyakova, N., High throughput HPLC-ESI(-)-MS/MS methodology for mercapturic acid metabolites of 1,3-butadiene: Biomarkers of exposure and bioactivation. *Chem. Biol. Interact.* **2015,** *241*, 23-31.

207. Neagu, I.; Koivisto, P.; Neagu, C.; Kostiainen, R.; Stenby, K.; Peltonen, K., Butadiene monoxide and deoxyguanosine alkylation products at the N7-position. *Carcinogenesis* **1995,** *16* (8), 1809-1813.

208. Bolt, H. M.; Jelitto, B., Biological formation of the 1,3-butadiene DNA adducts 7-N-(2-hydroxy-3-buten-1-yl)guanine, 7-N-(1-hydroxy-3-buten-2-yl)guanine and 7-N-(2,3,4-trihydroxy-butyl)guanine. *Toxicology* **1996,** *113*, 328-330.

209. Selzer, R. R.; Elfarra, A. A., Synthesis and Biochemical Characterization of N^1-, N^2-, and N^7-Guanosine Adducts of Butadiene Monoxide. *Chem. Res. Toxicol.* **1996,** *9*, 126-132.

210. Selzer, R. R.; Elfarra, A. A., In vitro reaction of butadiene monoxide with single- and double- stranded DNA: characterization and quantitation of several purine and pyrimidine adducts. *Carcinogenesis* **1999,** *20* (2), 285-292.

211. Tretyakova, N.; Lin, Y.; Sangaiah, R.; Upton, P. B.; Swenberg, J. A., Identification and quantitation of DNA adducts from calf thymus DNA exposed to 3,4-epoxy-1-butene. *Carcinogenesis* **1997,** *18* (1), 137-47.

212. Selzer, R. R.; Elfarra, A. A., Characterization of N^1- and N^6-Adenosine Adducts and N^1-Inosine Adducts Formed by the Reaction of Butadiene Monoxide with Adenosine: Evidence for the N^1-Adenosine Adducts as Major Initial Products. *Chem. Res. Toxicol.* **1996,** *9*, 875-881.

213. Tretyakova, N.; Chaing, S.-Y.; Walker, V.; Swenberg, J., Quantitative Analysis of 1,3-Butadiene-induced DNA Adducts In vivo and In vitro using Liquid Chromatography Electrospray Ionization Tandem Mass Spectrometry. *J. Mass Spectrom.* **1998,** *33*, 363-376.

214. Koc, H.; Tretyakova, N. Y.; Walker, V. E.; Henderson, R. F.; Swenberg, J. A., Molecular Dosimetry of N-7 Guanine Adduct Formation in Mice and Rats Exposed to 1,3-Butadiene. *Chem. Res. Toxicol.* **1999,** *12* (7), 566-574.

215. Zhao, C.; Koskinen, M.; Hemminki, K., ^{32}P-postlabelling analysis of 1,3-butadiene-induced DNA adducts in vivo and in vitro. *Biomarkers* **2000,** *5* (3), 168-181.

216. Seneviratne, U.; Antsypovich, S.; Goggin, M.; Quirk Dorr, D.; Guza, R.; Moser, A.; Thompson, C.; York, D. M.; Tretyakova, N., Exocyclic Deoxyadenosine Adducts of 1,2,3,4-Diepoxybutane: Synthesis, Structural Elucidation, and Mechanistic Studies. *Chem. Res. Toxicol.* **2010,** *23*, 118-133.

217. Park, S.; Tretyakova, N., Structural characterization of the major DNA-DNA cross-link of 1,2,3,4-diepoxybutane. *Chem. Res. Toxicol.* **2004,** *17* (2), 129-36.

218. Park, S.; Hodge, J.; Anderson, C.; Tretyakova, N., Guanine-Adenine DNA Cross-Linking by 1,2,3,4-Diepoxybutane: Potential Basis for Biological Activity. *Chem. Res. Toxicol.* **2004,** *17*, 1638-1651.

219. Koivisto, P.; Adler, I.; Sorsa, M.; Peltonen, K., Inhalation Exposure of Rats and Mice to 1,3-Butadiene Induces N^6-Adenine Adducts of Epoxybutene Detected by ^{32}P-Postlabeling and HPLC. *Environ. Health Perspect.* **1996,** *104*, 655-657.

220. Kumar, R.; Vodicka, P.; Koivisto, P.; Peltonen, K.; Hemminki, K., ^{32}P-Postlabeling of diasteromeric 7-alkylguanine adducts of butadiene monoepoxide. *Carcinogenesis* **1996,** *17* (6), 1297-1303.

221. Leuratti, C.; Jones, N. J.; Marafante, E.; Peltonen, K.; Kostiainen, R.; Waters, R., Biomonitoring of exposure to 1,3-butadiene: detection by high-performance liquid chromatography and 32P-postlabelling of an adenine adduct formed by diepoxybutane. *IARC Sci. Publ.* **1993,** *127*, 143-150.

222. Leuratti, C.; Jones, N. J.; Marafante, E.; Kostiainen, R.; Peltonen, K.; Waters, R., DNA damage induced by the environmental carcinogen butadiene: identification of a diepoxybutane-adenine adduct and its detection by 32P-postlabelling. *Carcinogenesis* **1994,** *15* (9), 1903-1910.

223. Mabon, N.; Randerath, K., ^{32}P-postlabeling of 1,3-butadiene and 4-vinyl-1-cyclohexene metabolite-DNA adducts: in vitro and in vivo applications. *Toxicology* **1996,** *113*, 341-344.

224. Mabon, N.; Moorthy, B.; Randerath, E.; Randerath, K., Monophosphate ^{32}P-postlabeling assay of DNA adducts from 1,2:3,4-diepoxybutane, the most genotoxic metabolite of 1,3-butadiene: in vitro methological studies and in vivo dosimetry. *Mutat. Res.* **1996,** *371*, 87-104.

225. Zhao, C.; Koskinen, M.; Hemminki, K., ^{32}P-postlabelling of N^6-adenine adducts of epoxybutanediol in vivo after 1,3-butadiene exposure. *Toxicol. Lett.* **1998,** *102-103*, 591-594.

226. Koivisto, P.; Adler, I.; Pacchierotti, F.; Peltonen, K., DNA adducts in mouse testis and lung after inhalation exposure to 1,3-butadiene. *Mutat. Res.* **1998,** *397*, 3-10.

227. Koivisto, P.; Kilpeläinen, I.; Rasanen, I.; Adler, I.; Pacchierotti, F.; Peltonen, K., Butadiene diolepoxide- and diepoxybutane-derived DNA adducts at N7-guanine: a high occurrence of diolexpoxide-derived adducts in mouse lung after 1,3-butadiene exposure. *Carcinogenesis* **1999,** *20* (7), 1253-1259.

228. Koivisto, P.; Peltonen, K., N7-guanine adducts of the epoxy metabolites of 1,3-butadiene in mice lung. *Chem. Biol. Interact.* **2001,** *135-136*, 363-372.

229. Koivisto, P.; Adler, I.; Pacchierotti, F.; Peltonen, K., Regio and stereospecific DNA adduct formation in mouse lung at N6 and N7 position of adenine and guanine after 1,3 butadiene inhalation exposure. *Biomarkers* **1998,** *3* (6), 385-397.

230. Zhao, C.; Vodicka, P.; J.Sˇra´m, R.; Hemminki, K., Human DNA adducts of 1,3-butadiene, an important environmental carcinogen. *Carcinogenesis* **2000,** *21* (1), 107-111.

231. Zhao, C.; Vodicka, P.; Sram, R. J.; Hemminki, K., DNA Adducts of 1,3-Butadiene in Humans: Relationships to Exposure, GST Genotypes, Single-Strand Breaks, and Cytogenetic End Points. *Environ. Mol. Mutagen.* **2001,** *37*, 226-230.

232. Oe, T.; Kambouris, S. J.; Walker, V. E.; Meng, Q.; Recio, L.; Wherli, S.; Chaudhary, A. K.; Blair, I. A., Persistence of N7-(2,3,4-Trihydroxybutyl)guanine Adducts in the Livers of Mice and Rats Exposed to 1,3-Butadiene. *Chem. Res. Toxicol.* **1999,** *12* (3), 247-257.

233. Blair, I. A.; Oe, T.; Kambouris, S. J.; Chaudhary, A. K., 1,3-butadiene: cancer, mutations, and adducts. Part IV: Molecular dosimetry of 1,3-butadiene. *Res. Rep. Health. Eff. Inst.* **2000,** *92*, 151-190.

234. Booth, E. D.; Kilgour, J. D.; Robinson, S. A.; Watson, W. P., Dose responses for DNA adduct formation in tissues of rats and mice exposed by inhalation to low concentrations of 1,3-[2,3-[(14)C]-butadiene. *Chem. Biol. Interact.* **2004,** *147* (2), 195-211.

235. Boogaard, P. J.; de Kloe, K. P.; Booth, E. D.; Watson, W. P., DNA adducts in rats and mice following exposure to [4-14C]-1,2-epoxy-3-butene and to [2,3-14C]-1,3-butadiene. *Chem. Biol. Interact.* **2004,** *148* (1-2), 69-92.

236. Chappell, G.; Kobets, T.; O'Brien, B.; Tretyakova, N.; Sangaraju, D.; Kosyk, O.; Sexton, K. G.; Bodnar, W.; Pogribny, I. P.; Rusyn, I., Epigenetic events determine tissue-specific toxicity of inhalational exposure to the genotoxic chemical 1,3-butadiene in male C57BL/6J mice. *Toxicol. Sci.* **2014,** *142* (2), 375-84.

237. Lewis, L.; Borowa-Mazgaj, B.; de Conti, A.; Chappell, G. A.; Luo, Y.-S.; Bodnar, W.; Konganti, K.; Wright, F. A.; Threadgill, D. W.; Chiu, W. A.; Pogribny, I. P.; Rusyn, I., Population-Based Analysis of DNA Damage and Epigenetic Effects of 1,3-Butadiene in the Mouse. *Chem. Res. Toxicol.* **2019,** *32* (5), 887-898.

238. Erber, L.; Goodman, S.; Wright, F. A.; Chiu, W. A.; Tretyakova, N. Y.; Rusyn, I., Intra- and Inter-Species Variability in Urinary N7-(1-Hydroxy-3-buten-2-yl)guanine Adducts Following Inhalation Exposure to 1,3-Butadiene. *Chem. Res. Toxicol.* **2021,** *34* (11), 2375-2383.

239. Chappell, G. A.; Israel, J. W.; Simon, J. M.; Pott, S.; Safi, A.; Eklund, K.; Sexton, K. G.; Bodnar, W.; Lieb, J. D.; Crawford, G. E.; Rusyn, I.; Furey, T. S., Variation in DNA-Damage Responses to an Inhalational Carcinogen (1,3-Butadiene) in Relation to Strain-Specific Differences in Chromatin Accessibility and Gene Transcription Profiles in C57BL/6J and CAST/EiJ Mice. *Environ. Health Perspect.* **2017,** *125* (10), 107006.

240. Melnick, R. L.; Huff, J.; Chou, B. J.; Miller, R. A., Carcinogenicity of 1,3-Butadiene in C57BL/6 x C3H F, Mice at Low Exposure Concentrations. *Cancer Res.* **1990,** *50*, 6592-6599.

241. Lewis, L.; Chappell, G. A.; Kobets, T.; O'Brian, B. E.; Sangaraju, D.; Kosyk, O.; Bodnar, W.; Tretyakova, N. Y.; Pogribny, I. P.; Rusyn, I., Sex-specific differences in genotoxic and epigenetic effects of 1,3-butadiene among mouse tissues. *Arch. Toxicol.* **2019,** *93* (3), 791-800.

242. Goggin, M.; Seneviratne, U.; Swenberg, J.; Walker, V.; Tretyakova, N., Column Switching HPLC-ESI$^+$-MS/MS Methods for Quantitative Analysis of Exocyclic dA Adducts in the DNA of Laboratory Animals Exposed to 1,3-Butadiene. *Chem. Res. Toxicol.* **2010,** *23*, 808-812.

243. Goggin, M.; Sangaraju, D.; Walker, V. E.; Wickliffe, J.; Swenberg, J. A.; Tretyakova, N., Persistence and repair of bifunctional DNA adducts in tissues of laboratory animals exposed to 1,3-butadiene by inhalation. *Chem. Res. Toxicol.* **2011,** *24* (6), 809-17.

244. Seaton, M. J.; Follansbee, M. H.; Bond, J. A., Oxidation of 1,2-epoxy-3-butene to 1,2:3,4-diepoxybutane by cDNA-expressed human cytochromes P450 2E1 and 3A4 and human, mouse and rat liver microsomes. *Carcinogenesis* **1995,** *16* (10), 2287-2293.

245. Csanady, G. A.; Guengerich, F. P.; Bond, J. A., Comparison of the biotransformation of 1,3-butadiene and its metabolite, butadiene monoepoxide, by hepatic and pulmonary tissues from humans, rats and mice. *Carcinogenesis* **1992,** *13* (7), 1143-53.

246. Himmelstein, M. W.; Turner, M. J.; Asgharian, B.; Bond, J. A., Comparison of blood concentrations of 1,3-butadiene and butadiene epoxides in mice and rats exposed to 1,3-butadiene by inhalation. *Carcinogenesis* **1994,** *15* (8), 1479-1486.

247. Thornton-Manning, J. R.; Dahl, A. R.; Bechtold, W. E.; Griffith Jr., W. C.; Henderson, R., Comparison of the disposition of butadiene epoxides in Sprague-Dawley rats and B6C3F1 mice following a single and repeated exposures to 1,3-butadiene via inhalation. *Toxicology* **1997,** *123*, 125-134.

248. Thornton-Manning, J. R.; Dahl, A. R.; Bechtold, W. E.; Henderson, R. F., Gender and species differences in the metabolism of 1,3-butadiene monoepoxide and butadiene diepoxide in rodents following low-level inhalation exposures. *Toxicology* **1996,** *113*, 322-325.

249. Albertini, R. J.; Sram, R. J.; Vacek, P. M.; Lynch, J.; Rossner, P.; Nicklas, J. A.; McDonald, J. D.; Boysen, G.; Georgieva, N.; Swenberg, J. A., Molecular epidemiological studies in 1,3-butadiene exposed Czech workers: female-male comparisons. *Chem. Biol. Interact.* **2007,** *166* (1-3), 63-77.

250. Osterman-Golkar, S.; Bond, J. A.; Ward Jr, J. B.; Legator, M. S., Use of haemoglobin adducts for biomonitoring exposure to 1,3-butadiene. *IARC Sci. Publ.* **1993,** *127*, 127-134.

251. Boysen, G.; Georgieva, N. I.; Upton, P. B.; Walker, V. E.; Swenberg, J. A., N-terminal globin adducts as biomarkers for formation of butadiene derived epoxides. *Chem. Biol. Interact.* **2007,** *166* (1-3), 84-92.

252. Powley, M. W.; Li, Y.; Upton, P. B.; Walker, V. E.; Swenberg, J. A., Quantification of DNA and hemoglobin adducts of 3,4-epoxy-1,2-butanediol in rodents exposed to 3-butene-1,2-diol. *Carcinogenesis* **2005,** *26* (9), 1573-80.

253. Vacek, P. M.; Albertini, R. J.; Sram, R. J.; Upton, P.; Swenberg, J. A., Hemoglobin adducts in 1,3-butadiene exposed Czech workers: female-male comparisons. *Chem. Biol. Interact.* **2010,** *188* (3), 668-76.

254. Walker, V. E.; Meng, Q., 1,3-butadiene: cancer, mutations, and adducts. Part III: In vivo mutation by the endogenous hprt genes of mice and rats by 1,3-butadiene and its metabolites. *Res. Rep. Health. Eff. Inst.* **2000,** *92*, 89-139.

255. Walker, V.; Walker, D. M.; Meng, Q.; McDonald, J. D.; Scott, B. R.; Seilkop, S. K.; Claffey, D. J.; Upton, P. B.; Powley, M. W.; Swenberg, J. A.; Henderson, R., Genotoxicity of 1,3-butadiene and its Epoxy Intermediates. *Res. Rep. Health. Eff. Inst.* **2009,** *144*.

256. Siegel, R. L.; Miller, K. D.; Fuchs, H. E.; Jemal, A., Cancer statistics, 2022. *CA: Cancer J. Clin.* **2022,** *72* (1), 7-33.

257. Islami, F.; Goding Sauer, A.; Miller, K. D.; Siegel, R. L.; Fedewa, S. A.; Jacobs, E. J.; McCullough, M. L.; Patel, A. V.; Ma, J.; Soerjomataram, I.; Flanders, W. D.; Brawley, O. W.; Gapstur, S. M.; Jemal, A., Proportion and number of cancer cases and deaths attributable to potentially modifiable risk factors in the United States. *CA: Cancer J. Clin.* **2018,** *68* (1), 31-54.

258. Ma, B.; Stepanov, I.; Hecht, S. S., Recent Studies on DNA Adducts Resulting from Human Exposure to Tobacco Smoke. *Toxics* **2019,** *7* (1).

259. Fowles, J.; Dybing, E., Application of toxicological risk assessment principles to the chemical constituents of cigarette smoke. *Tob. Control* **2003,** *12* (4), 424-30.

260. Le Marchand, L.; Wilkens, L. R.; Kolonel, L. N., Ethnic Differences in the Lung Cancer Risk Associated with Smoking. *Cancer Epidemiol. Biomarkers Prev.* **1992,** *1*, 103-107.

261. Hinds, M. W.; Stemmermann, G. N.; Yang, H. Y.; Kolonel, L. N.; Lee, J.; Wegner, E., Differences in lung cancer risk from smoking among Japanese, Chinese and Hawaiian women in Hawaii. *Int. J. Cancer* **1981,** *27*, 297-302.

262. Schwartz, A. G.; Swanson, G. M., Lung carcinoma in African Americans and whites. A population-based study in metropolitan Detroit, Michigan. *Cancer* **1997,** *79* (1), 45-52.

263. Kolonel, L. N.; Henderson, B. E.; Hankin, J. H.; Nomura, A. M.; Wilkens, L. R.; Pike, M. C.; Stram, D. O.; Monroe, K. R.; Earle, M. E.; Nagamine, F. S., A multiethnic cohort in Hawaii and Los Angeles: baseline characteristics. *Am. J. Epidemiol.* **2000,** *151* (4), 346-57.

264. Haiman, C. A.; Stram, D. O.; Wilkens, L. R.; Pike, M. C.; Kolonel, L. N.; Henderson, B. E.; Le Marchand, L., Ethnic and racial differences in the smoking-related risk of lung cancer. *N. Engl. J. Med.* **2006,** *354* (4), 333-42.

265. Stram, D. O.; Park, S. L.; Haiman, C. A.; Murphy, S. E.; Patel, Y.; Hecht, S. S.; Le Marchand, L., Racial/Ethnic Differences in Lung Cancer Incidence in the Multiethnic Cohort Study: An Update. *J. Natl. Cancer Inst.* **2019,** *111* (8), 811-819.

266. Siegel, R. L.; Miller, K. D.; Jemal, A., Cancer statistics, 2018. *CA: Cancer J. Clin.* **2018,** *68* (1), 7-30.

267. International Agency for Research on Cancer, Tobacco Smoke and Involuntary Smoking. In *IARC Monographs on the Evaluation of Carcinogenic Risks to Humans, vol. 83*, 2004; pp 33-1187.

268. Church, T. R.; Anderson, K. E.; Le, C.; Zhang, Y.; Kampa, D. M.; Benoit, A. R.; Yoder, A. R.; Carmella, S.; Hecht, S. S., Temporal stability of urinary and plasma biomarkers of tobacco smoke exposure among cigarette smokers. *Biomarkers* **2010,** *15* (4), 345-352.

269. Brunnemann, K. D.; Kagan, M. R.; Cox, J. E.; Hoffmann, D., Analysis of 1,3-butadiene and other selected gas-phase components in cigarette mainstream and sidestream smoke by gas chromatography-mass selective detection. *Carcinogenesis* **1990,** *11* (10), 1863-8.

270. Himmelstein, M. W.; Acquavella, J. F.; Recio, L.; Medinsky, M. A.; Bond, J. A., Toxicology and epidemiology of 1,3-butadiene. *Crit. Rev. Toxicol.* **1997,** *27* (1), 1-108.

271. Elfarra, A. A.; Krause, R. J.; Selzer, R. R., Biochemistry of 1,3-butadiene metabolism and its relevance to 1,3-butadiene-induced carcinogenicity. *Toxicology* **1996,** *113*, 23-30.

272. Boogaard, P. J.; van Sittert, N. J.; Megens, H. J., Urinary metabolites and haemoglobin adducts as biomarkers of exposure to 1,3-butadiene: a basis for 1,3-butadiene cancer risk assessment. *Chem. Biol. Interact.* **2001,** *135-136*, 695-701.

273. Ding, Y. S.; Blount, B. C.; Valentin-Blasini, L.; Applewhite, H. S.; Xia, Y.; Watson, C. H.; Ashley, D. L., Simultaneous determination of six mercapturic acid metabolites of volatile organic compounds in human urine. *Chem. Res. Toxicol.* **2009,** *22* (6), 1018-25.

274. Fustinoni, S.; Perbellini, L.; Soleo, L.; Manno, M.; Foa, V., Biological monitoring in occupational exposure to low levels of 1,3-butadiene. *Toxicol. Lett.* **2004,** *149* (1-3), 353-60.

275. Li, W.; Chen, J.; Jiang, D.; Xin, C.; Cao, Y.; Li, F., Sensitive determination of two major mercapturic acid metabolites of 1,3-butadiene in human urine based on the isotope dilution ultrahigh performance liquid chromatography-tandem mass spectrometry. *Anal. Methods* **2015,** *7* (11), 4691-4698.

276. Zhang, X.; Hou, H.; Chen, H.; Liu, Y.; Wang, A.; Hu, Q., A column-switching LC-MS/MS method for simultaneous quantification of biomarkers for 1,3-butadiene exposure and oxidative damage in human urine. *J. Chromatogr. B Analyt. Technol. Biomed. Life Sci.* **2015,** *1002*, 123-9.

277. Kirman, C. R.; Albertini, R. A.; Gargas, M. L., 1,3-Butadiene: III. Assessing carcinogenic modes of action. *Crit. Rev. Toxicol.* **2010,** *40 Suppl 1*, 74-92.

278. Carmical, J. R.; Kowalczyk, A.; Zou, Y.; Van Houten, B.; Nechev, L. V.; Harris, C. M.; Harris, T. M.; Lloyd, R. S., Butadiene-induced intrastrand DNA cross-links: a possible role in deletion mutagenesis. *J. Biol. Chem.* **2000,** *275* (26), 19482-9.

279. Kotapati, S.; Wickramaratne, S.; Esades, A.; Boldry, E. J.; Quirk Dorr, D.; Pence, M. G.; Guengerich, F. P.; Tretyakova, N. Y., Polymerase Bypass of N(6)-Deoxyadenosine Adducts Derived from Epoxide Metabolites of 1,3-Butadiene. *Chem. Res. Toxicol.* **2015,** *28* (7), 1496-507.

280. Gates, K. S.; Nooner, T.; Dutta, S., Biologically relevant chemical reactions of N7-alkylguanine residues in DNA. *Chem. Res. Toxicol.* **2004,** *17* (7), 839-56.

281. Citti, L.; Gervasi, P. G.; Turchi, G.; Bellucci, G.; Bianchini, R., The reaction of 3,4-epoxy-1-butene with deoxyguanosine and DNA in vitro: synthesis and characterization of the main adducts. *Carcinogenesis* **1984,** *5* (1), 47-52.

282. Tuytten, R.; Lemière, F.; Van Dongen, W.; Esmans, E. L.; Witters, E.; Herrebout, W.; Van Der Veken, B.; Dudley, E.; Newton, R. P., Intriguing Mass Spectrometric Behavior of Guanosine Under Low Energy Collision-Induced Dissociation: H2O Adduct Formation and Gas-Phase Reactions in the Collision Cell. *J. Am. Soc. Mass Spectrom.* **2005,** *16* (8), 1291-1304.

283. National Toxicology Program, 1,3-butadiene. In *Report on Carcinogens, Fourteenth Edition*, U.S. Department of Health and Human Services, Public Health Service: Research Triangle Park, NC, 2016.

284. American Cancer Society, *Cancer Facts & Figures 2020*. American Cancer Society: Atlanta, 2020.

285. Huang, B. Z.; Stram, D. O.; Le Marchand, L.; Haiman, C. A.; Wilkens, L. R.; Pandol, S. J.; Zhang, Z. F.; Monroe, K. R.; Setiawan, V. W., Interethnic differences in pancreatic cancer incidence and risk factors: The Multiethnic Cohort. *Cancer Med.* **2019,** *8* (7), 3592-3603.

286. Jokipii Krueger, C. C.; Madugundu, G.; Degner, A.; Patel, Y.; Stram, D.; Church, T. R.; Tretyakova, N., Urinary N7-(1-hydroxy-3-buten-2-yl) guanine Adducts in Humans: Temporal Stability and Association with Smoking. *Mutagenesis* **2020,** *35*, 19-26.

287. Derby, K. S.; Cuthrell, K.; Caberto, C.; Carmella, S.; Murphy, S. E.; Hecht, S. S.; Le Marchand, L., Exposure to the carcinogen 4-(methylnitrosamino)-1-(3-pyridyl)-1-butanone (NNK) in smokers from 3 populations with different risks of lung cancer. *Int. J. Cancer* **2009,** *125* (10), 2418-24.

288. Derby, K. S.; Cuthrell, K.; Caberto, C.; Carmella, S. G.; Franke, A. A.; Hecht, S. S.; Murphy, S. E.; Le Marchand, L., Nicotine metabolism in three ethnic/racial groups with different risks of lung cancer. *Cancer Epidemiol. Biomarkers Prev.* **2008,** *17* (12), 3526-35.

289. Hecht, S. S.; Carmella, S.; Chen, M.; Koch, J. F. D.; Miller, A. T.; Murphy, S. E.; Jensen, A. J.; Zimmerman, C. L.; Hatsukami, D., Quantitation of Urinary Metabolites of a Tobacco-specific Lung Carcinogen after Smoking Cessation. *Cancer Res.* **1999,** *59*, 590-596.

290. Hecht, S. S.; Carmella, S.; Murphy, S. E., Effects of Watercress Consumption on Urinary Metabolites of Nicotine in Smokers. *Cancer Epidemiol. Biomarkers Prev.* **1999,** *8*, 907-913.

291. Tricker, A. R., Nicotine metabolism, human drug metabolism polymorphisms, and smoking behaviour. *Toxicology* **2003,** *183* (1-3), 151-173.

292. Malaiyandi, V.; Goodz, S. D.; Sellers, E. M.; Tyndale, R. F., CYP2A6 genotype, phenotype, and the use of nicotine metabolites as biomarkers during ad libitum smoking. *Cancer Epidemiol. Biomarkers Prev.* **2006,** *15* (10), 1812-9.

293. Boysen, G.; Arora, R.; Degner, A.; Vevang, K. R.; Chao, C.; Rodriguez, F.; Walmsley, S. J.; Erber, L.; Tretyakova, N. Y.; Peterson, L. A., Effects of GSTT1 Genotype on the Detoxification of 1,3-Butadiene Derived Diepoxide and Formation of Promutagenic DNA-DNA Cross-Links in Human Hapmap Cell Lines. *Chem. Res. Toxicol.* **2021,** *34* (1), 119-131.

294. Degner, A.; Arora, R.; Erber, L.; Chao, C.; Peterson, L. A.; Tretyakova, N. Y., Interindividual Differences in DNA Adduct Formation and Detoxification of 1,3-Butadiene-Derived Epoxide in Human HapMap Cell Lines. *Chem. Res. Toxicol.* **2020**.

295. Boldry, E. J.; Yuan, J. M.; Carmella, S. G.; Wang, R.; Tessier, K.; Hatsukami, D. K.; Hecht, S. S.; Tretyakova, N. Y., Effects of 2-Phenethyl Isothiocyanate on Metabolism of 1,3-Butadiene in Smokers. *Cancer Prev. Res.* **2020,** *13* (1), 91-100.

296. Hang, B., Formation and repair of tobacco carcinogen-derived bulky DNA adducts. *J. Nucleic Acids* **2010,** *2010*, 709521.

297. Park, S. L.; Murphy, S. E.; Wilkens, L. R.; Stram, D. O.; Hecht, S. S.; Le Marchand, L., Association of CYP2A6 activity with lung cancer incidence in smokers: The multiethnic cohort study. *PLoS One* **2017,** *12* (5), e0178435.

298. Park, S. L.; Tiirikainen, M. I.; Patel, Y. M.; Wilkens, L. R.; Stram, D. O.; Le Marchand, L.; Murphy, S. E., Genetic determinants of CYP2A6 activity across racial/ethnic groups with different risks of lung cancer and effect on their smoking intensity. *Carcinogenesis* **2016,** *37* (3), 269-279.

299. Cheng, X.; Zhang, T.; Zhao, J.; Zhou, J.; Shao, H.; Zhou, Z.; Kong, F.; Feng, N.; Sun, Y.; Shan, B.; Xia, Z., The association between genetic damage in peripheral blood lymphocytes and polymorphisms of three glutathione S-transferases in Chinese workers exposed to 1,3-butadiene. *Mutat. Res.* **2013,** *750* (1-2), 139-46.

300. Thun, M. J.; Henley, S. J.; Callie, E. E., Tobacco use and cancer: an epidemiologic perspective for geneticists. *Oncogene* **2002,** *21*, 7307-7325.

301. Sun, Y.; Li, Z.; Li, J.; Li, Z.; Han, J., A Healthy Dietary Pattern Reduces Lung Cancer Risk: A Systematic Review and Meta-Analysis. *Nutrients* **2016,** *8* (3), 134.

302. Jha, P.; Ramasundarahettige, C.; Landsman, V.; Rostron, B.; Thun, M.; Anderson, R. N.; McAfee, T.; Peto, R., 21st-century hazards of smoking and benefits of cessation in the United States. *N. Engl. J. Med.* **2013,** *368* (4), 341-50.

303. Carmical, J. R.; Nechev, L. V.; Harris, C. M.; Harris, T. M.; Lloyd, R. S., Mutagenic potential of adenine N(6) adducts of monoepoxide and diolepoxide derivatives of butadiene. *Environ. Mol. Mutagen.* **2000,** *35* (1), 48-56.

304. Scharer, O. D., DNA interstrand crosslinks: natural and drug-induced DNA adducts that induce unique cellular responses. *ChemBioChem* **2005,** *6* (1), 27-32.

305. Jokipii Krueger, C. C.; Park, S. L.; Madugundu, G.; Patel, Y.; Le Marchand, L.; Stram, D.; Tretyakova, N., Ethnic differences in excretion of butadiene-DNA adducts by current smokers. *Carcinogenesis* **2021**.

306. Signorello, L. B.; Hargreaves, M. K.; Blot, W. J., The Southern Community Cohort Study: investigating health disparities. *J. Health Care Poor Underserved* **2010,** *21* (1 Suppl), 26-37.

307. International Conference on Harmonization Q2(R1) Validation of Analytical Procedure: Text and Methodology. https://www.fda.gov/regulatory-information/search-fda-guidance-documents/q2r1-validation-analytical-procedures-text-and-methodology-guidance-industry.

308. Taghavi, T.; Novalen, M.; Lerman, C.; George, T. P.; Tyndale, R. F., A Comparison of Direct and Indirect Analytical Approaches to Measuring Total Nicotine Equivalents in Urine. *Cancer Epidemiol. Biomarkers Prev.* **2018,** *27* (8), 882-891.

309. Park, S. L.; Carmella, S. G.; Ming, X.; Vielguth, E.; Stram, D. O.; Le Marchand, L.; Hecht, S. S., Variation in levels of the lung carcinogen NNAL and its glucuronides in the urine of cigarette smokers from five ethnic groups with differing risks for lung cancer. *Cancer Epidemiol. Biomarkers Prev.* **2015,** *24* (3), 561-9.

310. Luo, X.; Carmella, S. G.; Chen, M.; Jensen, J. A.; Wilkens, L. R.; Le Marchand, L.; Hatsukami, D. K.; Murphy, S. E.; Hecht, S. S., Urinary Cyanoethyl Mercapturic Acid, a Biomarker of the Smoke Toxicant Acrylonitrile, Clearly Distinguishes Smokers From Nonsmokers. *Nicotine Tob. Res.* **2020,** *22* (10), 1744-1747.

311. van der Plas, A.; Pouly, S.; de La Bourdonnaye, G.; Baker, G.; Ludicke, F., Influence of smoking on levels of urinary 8-iso Prostaglandin F2alpha. *Toxicol. Rep.* **2019,** *6*, 18-25.

312. Carmella, S.; Chen, M.; Zhang, Y.; Zhang, S.; Hatsukami, D.; Hecht, S. S., Quantitation of Acrolein-Derived (3-Hydroxypropyl)mercapturic Acid in Human Urine by Liquid Chromatography−Atmospheric Pressure Chemical Ionization Tandem Mass Spectrometry: Effects of Cigarette Smoking. *Chem. Res. Toxicol.* **2007,** *20*, 986-990.

313. Zarth, A. T.; Carmella, S. G.; Le, C. T.; Hecht, S. S., Effect of cigarette smoking on urinary 2-hydroxypropylmercapturic acid, a metabolite of propylene oxide. *J. Chromatogr. B Analyt. Technol. Biomed. Life Sci.* **2014,** *953-954*, 126-31.

314. Remen, T.; Pintos, J.; Abrahamowicz, M.; Siemiatycki, J., Risk of lung cancer in relation to various metrics of smoking history: a case-control study in Montreal. *BMC Cancer* **2018,** *18* (1), 1275.

315. Strobel, H.; Baisch, T.; Fitzel, R.; Schilberg, K.; Siegelin, M. D.; Karpel-Massler, G.; Debatin, K. M.; Westhoff, M. A., Temozolomide and Other Alkylating Agents in Glioblastoma Therapy. *Biomedicines* **2019,** *7* (3).

316. Sedgwick, B.; Vaughan, P., Widespread adaptive response agains environmental methylating agents in microorganisms. *Mutat. Res.* **1991,** *250*, 211-221.

317. Morinello, E.; Koc, H.; Ranasinghe, A.; Swenberg, J., Differential Induction of N^2,3-Ethenoguanine in Rat Brain and Liver after Exposure to Vinyl Chloride. *Cancer Res.* **2002,** *62*, 5183-5188.

318. *1,3-butadiene*; National Toxicology Program, Department of Health and Human Services: Report on Carcinogens.

319. Maynard, S.; Fang, E. F.; Scheibye-Knudsen, M.; Croteau, D. L.; Bohr, V. A., DNA Damage, DNA Repair, Aging, and Neurodegeneration. *Cold Spring Harb. Perspect. Med.* **2015,** *5* (10).

320. Catic, A., Cellular Metabolism and Aging. *Prog. Mol. Biol. Transl. Sci.* **2018,** *155*, 85-107.

321. Topal, M. D.; Baker, M. S., DNA precursor pool: A significant target for *N*-methyl-*N*-nitrosourea in C3H/10T1/2 clone 8 cells. *Proc. Natl. Acad. Sci. USA* **1982,** *79*, 2211-2215.

322. Evans, M. D.; Mistry, V.; Singh, R.; Gackowski, D.; Rozalski, R.; Siomek-Gorecka, A.; Phillips, D. H.; Zuo, J.; Mullenders, L.; Pines, A.; Nakabeppu, Y.; Sakumi, K.; Sekiguchi, M.; Tsuzuki, T.; Bignami, M.; Olinski, R.; Cooke, M. S., Nucleotide excision repair of oxidised genomic DNA is not a source of urinary 8-oxo-7,8-dihydro-2'-deoxyguanosine. *Free Radic. Biol. Med.* **2016,** *99*, 385-391.

323. Cooke, M. S.; Evans, M. D.; Herbert, K. E.; Lunec, J., Urinary 8-oxo-2'-deoxyguanosine--source, significance and supplements. *Free Radic. Res.* **2000,** *32* (5), 381-97.

324. Evans, M. D.; Saparbaev, M.; Cooke, M. S., DNA repair and the origins of urinary oxidized 2'-deoxyribonucleosides. *Mutagenesis* **2010,** *25* (5), 433-42.

325. Seo, K. Y.; Jelinsky, S. A.; Loechler, E. L., Factors that influence the mutagenic patterns of DNA adducts from chemical carcinogens. *Mutat. Res.* **2000,** *463* (3), 215-246.

326. Gates, K. S., An Overview of Chemical Processes That Damage Cellular DNA: Spontaneous Hydrolysis, Alkylation, and Reactions with Radicals. *Chem. Res. Toxicol.* **2009,** *22* (11), 1747-1760.

327. Pujari, S. S.; Tretyakova, N., Chemical Biology of N(5)-Substituted Formamidopyrimidine DNA Adducts. *Chem. Res. Toxicol.* **2017,** *30* (1), 434-452.

328. Watson, J. D.; Crick, F. H. C., Molecular Structure of Nucleic Acids: A Structure for Deoxyribose Nucleic Acid. *Nature* **1953,** *171* (4356), 737-738.

329. Tudek, B.; Boiteux, S.; Laval, J., Biological properties of imidazole ring-opened N7-methylguanine in M13mp18 phage DNA. *Nucleic Acids Res.* **1992,** *20* (12), 3079-84.

330. Boiteux, S.; Laval, J., Imidazole open ring 7-methylguanine: an inhibitor of DNA synthesis. *Biochem. Biophys. Res. Commun.* **1983,** *110* (2), 552-558.

331. Asagoshi, K.; Terato, H.; Ohyama, Y.; Ide, H., Effects of a guanine-derived formamidopyrimidine lesion on DNA replication: translesion DNA synthesis, nucleotide insertion, and extension kinetics. *J. Biol. Chem.* **2002,** *277* (17), 14589-14597.

332. Christov, P. P.; Yamanaka, K.; Choi, J. Y.; Takata, K.; Wood, R. D.; Guengerich, F. P.; Lloyd, R. S.; Rizzo, C. J., Replication of the 2,6-diamino-4-hydroxy-N(5)-(methyl)-formamidopyrimidine (MeFapy-dGuo) adduct by eukaryotic DNA polymerases. *Chem. Res. Toxicol.* **2012,** *25* (8), 1652-1661.

333. Evans, M. D.; Dizdaroglu, M.; Cooke, M. S., Oxidative DNA damage and disease: induction, repair and significance. *Mutat. Res.* **2004,** *567* (1), 1-61.

334. Smela, M. E.; Hamm, M. L.; Henderson, P. T.; Harris, C. M.; Harris, T. M.; Essigmann, J. M., The aflatoxin B_1 formamidopyrimidine adduct plays a major role in causing the types of mutations observed in human hepatocellular carcinoma. *Proc. Natl. Acad. Sci. USA* **2002,** *99* (10), 6655-6660.

335. Greenberg, M. M., The Formamidopyrimidines: Purine Lesions Formed in Competition With 8-Oxopurines From Oxidative Stress. *Acc. Chem. Res.* **2012,** *45* (4), 588-597.

336. Dizdaroglu, M.; Kirkali, G.; Jaruga, P., Formamidopyrimidines in DNA: Mechanisms of formation, repair, and biological effects. *Free Radic. Biol. Med.* **2008,** *45* (12), 1610-1621.

337. Hu, J.; de Souza-Pinto, N. C.; Haraguchi, K.; Hogue, B. A.; Jaruga, P.; Greenberg, M. M.; Dizdaroglu, M.; Bohr, V. A., Repair of formamidopyrimidines in DNA involves different glycosylases: role of the OGG1, NTH1, and NEIL1 enzymes. *J. Biol. Chem.* **2005,** *280* (49), 40544-51.

338. Vartanian, V.; Minko, I. G.; Chawanthayatham, S.; Egner, P. A.; Lin, Y. C.; Earley, L. F.; Makar, R.; Eng, J. R.; Camp, M. T.; Li, L.; Stone, M. P.; Lasarev, M. R.; Groopman, J. D.; Croy, R. G.; Essigmann, J. M.; McCullough, A. K.; Lloyd, R. S., NEIL1 protects against aflatoxin-induced hepatocellular carcinoma in mice. *Proc. Natl. Acad. Sci. USA* **2017,** *114* (16), 4207-4212.

339. Wickramaratne, S.; Banda, D. M.; Ji, S.; Manlove, A. H.; Malayappan, B.; Nunez, N. N.; Samson, L.; Campbell, C.; David, S. S.; Tretyakova, N., Base Excision Repair of N(6)-Deoxyadenosine Adducts of 1,3-Butadiene. *Biochemistry* **2016,** *55* (43), 6070-6081.

340. Graziewicz, M. A.; Zastawny, T. H.; Oliński, R.; Speina, E.; Siedlecki, J.; Tudek, B., Fapyadenine is a moderately efficient chain terminator for prokaryotic DNA polymerases. *Free Radic. Biol. Med.* **2000,** *28* (1), 75-83.

341. Grąziewicz, M.-A.; Zastawny, T. H.; Oliński, R.; Tudek, B., SOS-dependent A→G transitions induced by hydroxyl radical generating system hypoxanthine/xanthine oxidase/Fe3+/EDTA are accompanied by the increase of Fapy-adenine content in M13 mp18 phage DNA. *Mutat. Res.* **1999,** *434* (1), 41-52.

342. Tudek, B.; Graziewicz, M.; Kazanova, O.; Zastawny, T. H.; Obtułowicz, T.; Laval, J., Mutagenic specificity of imidazole ring-opened 7-methylpurines in M13mp18 phage DNA. *Acta. Biochim. Pol.* **1999,** *46* (3), 785-799.

343. Tudek, B., Imidazole ring-opened DNA purines and their biological significance. *J. Biochem. Mol. Biol.* **2003,** *36* (1), 12-19.

344. McMahon, G.; Davis, E. F.; Huber, L. J.; Kim, Y.; Wogan, G. N., Characterization of c-Ki-ras and N-ras oncogenes in aflatoxin B1-induced rat liver tumors. *Proc. Natl. Acad. Sci. USA* **1990,** *87* (3), 1104-1108.

345. Chang, Y. J.; Mathews, C.; Mangold, K.; Marien, K.; Hendricks, J.; Bailey, G., Analysis of ras gene mutations in rainbow trout liver tumors initiated by aflatoxin B1. *Mol. Carcinog.* **1991,** *4* (2), 112-119.

346. Hsu, I. C.; Metcalf, R. A.; Sun, T.; Welsh, J. A.; Wang, N. J.; Harris, C. C., Mutational hotspot in the p53 gene in human hepatocellular carcinomas. *Nature* **1991,** *350* (6317), 427-248.

347. Bressac, B.; Kew, M.; Wands, J.; Ozturk, M., Selective G to T mutations of p53 gene in hepatocellular carcinoma from southern Africa. *Nature* **1991,** *350* (6317), 429-431.

348. Berntsson, S. G.; Wibom, C.; Sjostrom, S.; Henriksson, R.; Brannstrom, T.; Broholm, H.; Johansson, C.; Fleming, S. J.; McKinney, P. A.; Bethke, L.; Houlston, R.; Smits, A.; Andersson, U.; Melin, B. S., Analysis of DNA repair gene polymorphisms and survival in low-grade and anaplastic gliomas. *J Neurooncol.* **2011,** *105* (3), 531-8.

349. Chen, Y.; Zhu, M.; Zhang, Z.; Jiang, G.; Fu, X.; Fan, M.; Sun, M.; Wei, Q.; Zhao, K., A NEIL1 single nucleotide polymorphism (rs4462560) predicts the risk of radiation-induced toxicities in esophageal cancer patients treated with definitive radiotherapy. *Cancer* **2013,** *119* (23), 4205-11.

350. The 1000 Genomes Project Consortium, A global reference for human genetic variation. *Nature* **2015,** *526* (7571), 68-74.

351. Carlsson, H.; von Stedingk, H.; Nilsson, U.; Tornqvist, M., LC-MS/MS screening strategy for unknown adducts to N-terminal valine in hemoglobin applied to smokers and nonsmokers. *Chem. Res. Toxicol.* **2014,** *27* (12), 2062-70.